Transition Metal Oxides

Crystal Chemistry, Phase Transition and Related Aspects

C. N. R. Rao and G. V. Subba Rao

Department of Chemistry
Indian Institute of Technology
Kanpur-16, India

U.S. DEPARTMENT OF COMMERCE, Frederick B. Dent, *Secretary*
NATIONAL BUREAU OF STANDARDS, Richard W. Roberts, *Director*
Issued June 1974

Library of Congress Catalog Number: 73-600267

NSRDS-NBS 49

Nat. Stand. Ref. Data Ser., Nat. Bur. Stand. (U.S.), 49, 138 pages (June 1974)

CODEN: NSRDAP

U.S. GOVERNMENT PRINTING OFFICE
WASHINGTON: 1974

For sale by the Superintendent of Documents, U.S. Government Printing Office
Washington, D.C. 20402 (Order by SD Catalog No. C13.48:49) Price $1.70
Stock Number 0303-01190

Foreword

The National Standard Reference Data System provides access to the quantitative data of physical science, critically evaluated and compiled for convenience and readily accessible through a variety of distribution channels. The System was established in 1963 by action of the President's Office of Science and Technology and the Federal Council for Science and Technology, and responsibility to administer it was assigned to the National Bureau of Standards.

NSRDS receives advice and planning assistance from a Review Committee of the National Research Council of the National Academy of Sciences-National Academy of Engineering. A number of Advisory Panels, each concerned with a single technical area, meet regularly to examine major portions of the program, assign relative priorities, and identify specific key problems in need of further attention. For selected specific topics, the Advisory Panels sponsor subpanels which make detailed studies of users' needs, the present state of knowledge, and existing data resources as a basis for recommending one or more data compilation activities. This assembly of advisory services contributes greatly to the guidance of NSRDS activities.

The System now includes a complex of data centers and other activities in academic institutions and other laboratories. Components of the NSRDS produce compilations of critically evaluated data, reviews of the state of quantitative knowledge in specialized areas, and computations of useful functions derived from standard reference data. The centers and projects also establish criteria for evaluation and compilation of data and recommend improvements in experimental techniques. They are normally associated with research in the relevant field.

The technical scope of NSRDS is indicated by the categories of projects active or being planned: nuclear properties, atomic and molecular properties, solid state properties, thermodynamic and transport properties, chemical kinetics, and colloid and surface properties.

Reliable data on the properties of matter and materials is a major foundation of scientific and technical progress. Such important activities as basic scientific research, industrial quality control, development of new materials for building and other technologies, measuring and correcting environmental pollution depend on quality reference data. In NSRDS, the Bureau's responsibility to support American science, industry, and commerce is vitally fulfilled.

RICHARD W. ROBERTS, *Director*

Preface

As part of our program in presenting critical reviews of phase transitions of inorganic solids,* we have surveyed the phase equilibria, crystal chemistry, and phase transitions of transition metal oxides in detail. Transition metal oxides form an interesting series of materials for the study of a variety of solid state phenomena, many of which arise from the presence of different *d*-electron configurations. Crystal structure transformations in several of the transition metal oxides are accompanied by significant changes in electrical, magnetic, and other properties and we have, therefore, briefly presented the recent data on the various properties of these oxides. We trust that this monograph will not only serve as a source of valuable information, but also provide a fascinating case history of an important class of solid state materials.

In this paper, we have covered the binary oxides of 3*d*-, 4*d*-, and 5*d*-transition metals with important references to the literature up to 1973.

The authors acknowledge the support by the National Bureau of Standards through their Special International Programs. The authors' thanks are due to G. Rama Rao for his assistance in the preparation of the manuscript.

* The first monograph of this series is on binary halides by C. N. R. Rao and M. Natarajan, NSRDS-NBS-41, 1972. (Supported by NBS Project G-77).

Contents

		Page
	Foreword	iii
	Preface	iv
	Symbols and abbreviations	1
	Introduction	1
I.	Oxides of 3*d* transition elements	
	1. Scandium oxide	7
	2. Titanium oxides	9
	3. Vanadium oxides	31
	4. Chromium oxides	50
	5. Manganese oxides	54
	6. Iron oxides	60
	7. Cobalt oxides	69
	8. Nickel oxides	75
	9. Copper oxides	79
	10. Zinc oxides	81
II.	Oxides of 4*d* transition elements	
	1. Yttrium oxides	83
	2. Zirconium oxides	85
	3. Niobium oxides	92
	4. Molybdenum oxides	99
	5. Technitium oxides	102
	6. Ruthenium oxides	103
	7. Rhodium oxides	104
	8. Palladium oxide	105
	9. Silver oxides	106
	10. Cadmium oxides	107
III.	Oxides of 5*d* transition elements	
	1. Lanthanum oxides	109
	2. Hafnium oxides	111
	3. Tantalum oxides	113
	4. Tungsten oxides	117
	5. Rhenium oxides	123
	6. Osmium oxides	125
	7. Iridium oxides	127
	8. Platinum oxides	127
	9. Gold oxides	128
	10. Mercury oxides	129
IV.	Some recent studies	130

Transition Metal Oxides

Crystal Chemistry, Phase Transitions and Related Aspects

C. N. R. Rao and G. V. Subba Rao

A survey is made of the data describing the thermodynamics of phase equilibria, crystal chemistry and phase transformations of binary oxides of 3*d*, 4*d*, and 5*d* transition metals. Changes in electrical, magnetic, and other properties which accompany phase transitions are discussed. Nearly complete coverage of the literature is provided up to 1973.

Key words: Crystal structure transformations; critical data, transition metal oxides; electronic properties; phase equilibria; phase transitions; magnetic properties.

Symbols and Abbreviations

AFMR—Anti-Ferromagnetic Resonance
APW—Augmented Plane Wave
B—Crystal field Racah parameter
bp—boiling point
C_p—Heat capacity at constant pressure
cal—Thermochemical calorie = 4.1840 Joules
C_v—Heat capacity at constant volume
CS—Crystallographic shear
DTA—Differential Thermal Analysis
d—Density
E_a—Energy of activation
E_F—Fermi level
E_g—Band gap
e—electronic charge
EMF—Electro Motive Force
ESCA—Electron Spectroscopy for Chemical Analysis
ESR—Electron Spin Resonance
ΔG—Gibbs free energy change
H—Enthalpy
ΔH—Enthalpy change
h—hours
k—Knight shift
k—Boltzmann constant
LCAO—Linear Combination of Atomic Orbitals
M_o—Spontaneous magnetization
M_s—Saturation magnetization
min—minutes
m—free electron mass
*m**—Effective electron mass
mp—melting point
m_p*—Effective polaron mass
NMR—Nuclear Magnetic Resonance
n—Refractive index
n_c—number of charge carriers
P—Pressure: 1 atm = 101325 Nm^{-2} = 1013250 dyn cm^{-2}
p_{O_2}—Partial pressure of oxygen
R_H—Hall constant
ΔS—Entropy change
T—Temperature in degrees Kelvin
T_C—Curie temperature
T_N—Néel temperature
T_{sc}—Superconducting transition temperature
T_M—Transition temperature (Morin transition)
T_t—Transition temperature
t—Temperature in °C (degree Celsius)
TEC—Thermal Expansion Coefficient
TGA—Thermo Gravimetric Analysis
ΔV—Volume change
v_L—Longitudinal sound-wave velocity
v_S—Shear sound-wave velocity
UHF—Ultra High Frequency
W—Watt
α—Seebeck coefficient; angle
α_F*—Fröhlich polaron coupling constant
α_{td}—Thermal diffusivity ($\kappa/C_p d$)
β—Angle
γ—Angle
γ_G—Grüneisen constant
ϵ—Dielectric constant
θ_D—Debye temperature
κ—Thermal conductivity
μ_B—Bohr magneton
μ_D—Drift mobility
μ_H—Hall mobility
ρ—Resistivity
$\Delta\rho$—Jump in resistivity
σ—Conductivity
χ—Magnetic susceptibility
χ_M—Molar magnetic susceptibility
Z—Number of molecules per unit cell

Introduction

Transition metal oxides probably form one of the most interesting class of solids, exhibiting a variety of novel properties [1–5].[1] These properties undoubtedly arise from the outer *d* electrons of the transition metal ions. These *d* electrons can neither be described by a collective electron model (as in the case of *s* and *p* electrons) nor by a localized electron model (as in the case of *f* electrons which

[1] Figures in brackets indicate the literature references on page that appear at the end of each section.

are tightly bound to the nuclei). Outer *d* electrons are not screened from the neighboring atoms by the outer core electrons, and the intermediate character of these electrons shows itself in terms of localized electron behavior in some oxides and collective electron behavior in some others; in a few instances, both kinds of *d* electrons can exist simultaneously. In recent years, the field of transition metal oxides has been a subject of intensive study by chemists and others interested in solid state materials. A study of the properties of these oxides not only serves as one of the best introductions to solid state chemistry and materials science, but also provides a wealthy source of fascinating research problems for experimental and theoretical investigations.

Transition metal oxides of the general formulae MO, M_2O_3, MO_2, M_2O_5, MO_3, M_nO_{2n-1}, M_nO_{2n+1} are known to exist. The nature of bonding in these oxides varies from purely ionic (e.g., NiO, CoO) to purely covalent (e.g., OsO_4, RuO_4); metallic bonding is seen in oxides like TiO, NbO, and ReO_3. The crystal structure of transition metal oxides varies from cubic to triclinic symmetry. Simple binary oxides of the composition, MO, generally possess the rock-salt structure, while the dioxides, MO_2, possess fluorite, rutile, distorted rutile or even more complex structures; many sesquioxides, M_2O_3, possess the corundum structure. Transition metals form important ternary oxides like perovskites, spinels, bronzes, and garnets. Many of these oxides show interesting phase transitions from one crystal structure to another accompanied by changes in magnetic, electrical, and other properties.

Many transition metal oxides show a wide range of non-stoichiometry as in the case of oxides of titanium, vanadium, iron, and niobium. Deviations from stoichiometry can be due to cation deficiency (as in Fe_3O_4) or anion deficiency (as in ZnO). Large deviations from stoichiometry cause marked changes in unit cell dimensions or in crystal structure. In many oxides, the defects are so highly ordered that we cannot really consider them as ordinary defect solids (e.g., TiO, NbO). Similarly, many oxide phases which may appear as nonstoichiometric could truly be stoichiometric compositions (with narrow ranges of homogeneity) resulting from different modes of sharing of the metal-oxygen polyhedra (e.g., Ti_nO_{2n-1} and similar Magneli phases) [6, 7]. In oxides where there are wide ranges of homogeneity lattice constants vary with composition; a typical case is that of TiO_x ($0.8 \leqslant x \leqslant 1.2$). In such oxides a comparison of the pyknometric density with the x-ray density will be useful; generally, when compounds deviate from stoichiometry, an increase in density indicates interstitials and a decrease denotes vacancies. Electrical conductivity of oxides is markedly affected by deviations from stoichiometry. Similarly, foreign metal ions, present as impurities or doped intentionally, would also cause marked changes in the properties of metal oxides. There are many instances where foreign impurities stabilize a particular phase. Thus, sulfate ion stabilizes the anatase phase of TiO_2 while Fe^{+3} stabilizes the high temperature pseudobrookite phase of Ti_3O_5.

Transition metal oxides exhibit a wide range of magnetic properties: TiO_2, ZrO_2, V_2O_5, and MoO_3 are diamagnetic; metallic TiO and ReO_3 are Pauli-paramagnetic; VO_2, NbO_2, and Ti_2O_3 are paramagnetic; MnO, CoO, NiO, V_2O_3 and Cr_2O_3 are antiferromagnetic with well-defined Néel temperatures; Mn_3O_4 and Fe_3O_4 are ferrimagnetic; CrO_2 is ferromagnetic. The magnetic properties of binary oxides have been reviewed by Goodenough and others [1, 3, 4, 8].

Transition metal oxides show a spectacular range of values of electrical conductivity. At one extreme we have the insulator behavior as typified by MnO ($\sigma \approx 10^{-15}\Omega^{-1}\text{cm}^{-1}$), and at the other extreme we have oxides like ReO_3, CrO_2, RuO_2, TiO, and NbO with metallic conductivities (fig. 1). In between these extremes we have a large number of oxide semiconductors. The mechanism of conduction in such semiconducting oxides may involve the hopping of char carriers (as in Nb_2O_5) or the excitation from t valence band to the conduction band (as in SrTi(and SnO_2). Of special interest are the transitio metal oxides which exhibit insulator (or semicor

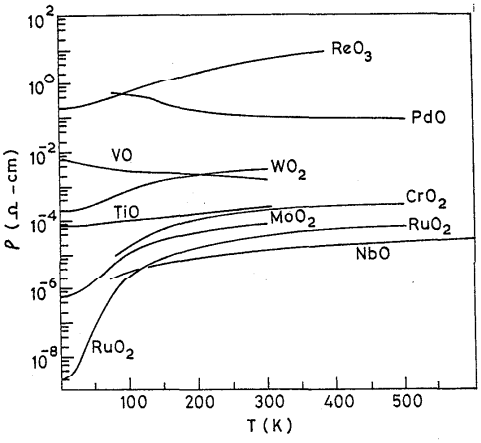

FIGURE 1. *Resistivities of highly conducting (metallic) oxides.*

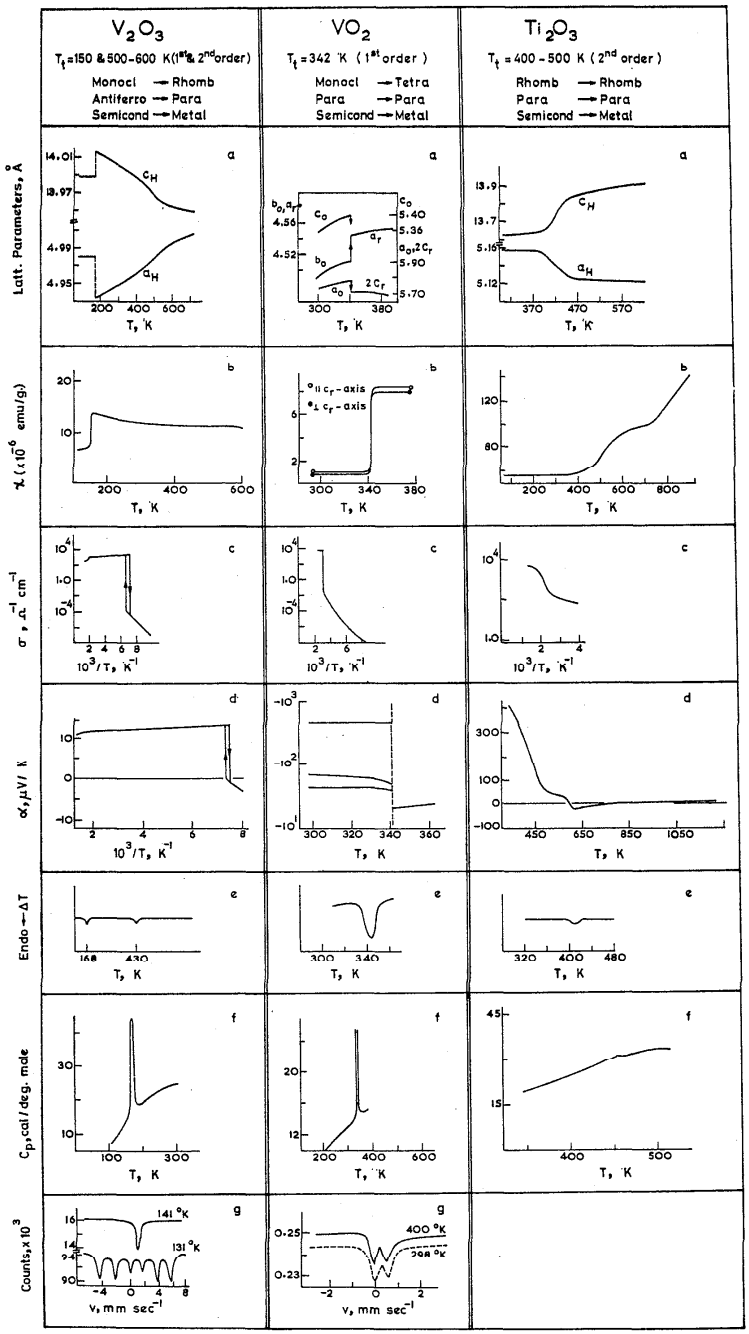

FIGURE 2. *Phase transitions in metal oxides investigated by various techniques.*

ductor)-to-metal transitions; typical of these oxides are V_2O_3, VO_2, and Ti_2O_3 (fig. 2). Conduction in oxides can be electronic or ionic; for example, lithium-doped NiO is a pure electronic conductor while Ca-doped ZrO_2 is a pure ionic conductor.

A number of authors have recently reviewed electron transport and related properties of transition metal oxides [3–5, 9–15]. Of the various attempts to explain these properties, the qualitative approach of Goodenough [5, 16–18] based on principles of chemical bonding has been eminently successful. With empirically derived criteria for the overlap of cation-cation and cation-anion-cation orbitals as determined by the crystal structures, Goodenough has attempted to provide a unified understanding of the magnetic and electrical properties of variety of inorganic materials including simple transition metal oxides, perovskites, spinels, bronzes, sulfides etc. Goodenough distinguishes two classes of oxides, those having large interactions between *d* electrons on neighboring atoms or ions because of large cation-cation interactions via a small cation-cation separation (Class I) and those having large interactions between *d* electrons of neighboring atoms because of large cation-anion-cation interactions via a large covalent mixing of anionic *p* orbitals into the cationic *d* orbitals (Class II); there are also oxides belonging to Class I-II where the two mechanisms coexist.

Our knowledge of the band structures of transition metal oxides is far from satisfactory. A detailed discussion of the theoretical models would be outside the scope of this work and the reader is referred to the various reviews [1–5] and other articles listed at the end of this section. The intuitive approach based on molecular orbital theory provides crude but reasonable approximations. In figure 3 is shown a summary of the over-simplified one-electron energy diagrams for a few crystal structures with the predicted Fermi levels for the various *d* electron configurations. This figure predicts either metallic or semiconducting behavior for any crystal structure depending on the number of *d* electrons in the cation. Such models will undoubtedly provide a basis for further studies which may eventually turn out to be technologically important. We may note here that the properties of highly conducting oxides such as TiO can be satisfactorily explained on the basis of such elementary band structure models. The status of our understanding of the electrical properties of the metal oxides which exhibit electrical transitions is, however, in a constant state of flux; there are many theories, none of which is entirely satisfactory and the field is rapidly developing [4, 10–15]. In figure 2 we have summarized the recent data on the

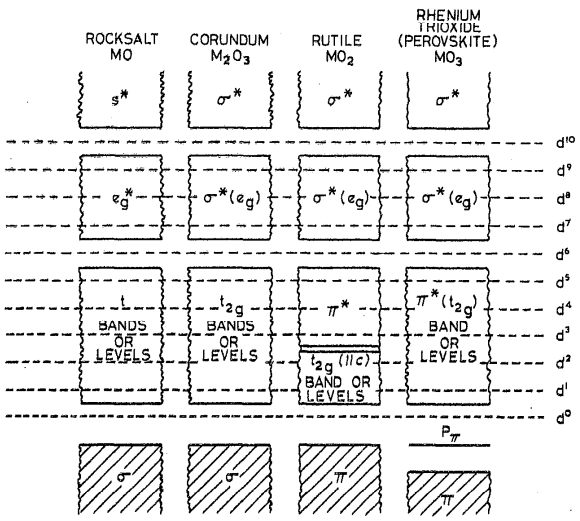

FIGURE 3. *Schematic one-electron energy level diagrams for different cation electronic configurations in various crystal structures (after Vest and Honig).*

Dotted lines show predicted Fermi levels.

electrical transitions of three transition metal oxides (V_2O_3, VO_2, and Ti_2O_2) in order to illustrate the wealth of information available in the literature. There is considerable doubt concerning the mechanism responsible for the observed changes in V_2O_3 and VO_2. Both these transitions are related to the changes in crystal structure that occur simultaneously. The situation is not straight-forward since the structural changes could themselves be determined by the electronic properties of the oxides. Thus, it is possible that distortions occur at the critical temperature in such a way as to create a gap at the Fermi level. This may lower the energy of the occupied electron states or raise the energy of the unoccupied states. If initially the band is half-filled and then split into two (accompanying the crystalline distortion) there will be a transition from metallic behavior of the symmetric phase (rhombohedral in V_2O_3 and rutile in VO_2) to semiconducting properties for the less symmetric phase (monoclinic in V_2O_3 and VO_2).

Several other mechanisms have been proposed to account for the transition in V_2O_3. (i) One of the mechanisms invokes the onset of antiferromagnetism (whose existence has been verified by polarized neutron scattering). Here, the potential of the electrons differs for the spin-up and spin-down alignments of vanadium ions of the antiferromagnetic phase and there is a doubling of the unit cell in the magnetic superlattice. This is accompanied by a

splitting of the band. (ii) A combination of the two preceding mechanisms has also been invoked. The band gap opening up under the combined action of both these effects would be sufficiently large to cause a decrease in the carrier density and account for the increase in resistivity. This would mean that the mobility remains nonactivated and essentially unchanged. On the other hand, if either of the two mechanisms (distortion or antiferromagnetism) were alone to operate, there would be a decrease in carrier density of only two orders of magnitude. In such a case a change in mobility of five orders of magnitude would be necessary to account for the observations. The mobility in the low-temperature monoclinic phase would then be low enough to correspond to an activated process. (iii) The possibility that band overlap may occur in V_2O_3 has been proposed, based on transport measurements. In this event, the transition could be thought of as being driven by the coulomb interaction between the holes and electrons (simultaneously present in the overlapping bands). This would result in a distortion which lifts the band overlap. The insulating phase, according to this mechanism, would be an 'excitonic insulator.' Accordingly, the transition can be entirely suppressed by application of hydrostatic pressure. Resistivity studies of the metallic phase under compression down to liquid helium temperatures indicate the presence of overlapping bands. (iv) It has been suggested that V_2O_3 may be an example of a 'Mott insulator.' This implies that small changes in interatomic distances in the lattice causes sufficient alterations in the band overlap to change the system from itinerant to localized behavior. (v) The effect of electron correlations has also been considered important, since the bands in V_2O_3 are relatively narrow. According to this theory, if the bandwidth is within a certain narrow range and is further reduced (by temperature changes or so) then a splitting into two sub-bands takes place. It should be possible to devise a single, comprehensive theory, in which the possibilities discussed above become special cases. To decide among the various alternatives it is necessary to obtain more detailed experimental data. The case of the VO_2 transition is similar to that of V_2O_3, with the exception that VO_2 does not exhibit magnetic order.

Ti_2O_3 differs from the cases discussed earlier in that, this oxide undergoes a transition over a rather wide temperature range. It does not exhibit either magnetic order or undergo a crystallographic transition. A band broadening model has been suggested to account for the transition of Ti_2O_3. At low temperatures, the completely filled band is separated by a gap of $\sim$0.06 eV from the next higher one. The pure material is, therefore, an intrinsic semiconductor at liquid helium temperatures. With increase in temperature, the distension of the unit cell is in such a direction as to widen the bands and eliminate the gap. The material thus gradually is converted into an overlap material. All these theories of the semiconductor-metal transitions have been discussed in the various references listed at this introduction and they are again referred to in the respective sections in the text.

It was our purpose initially to review phase transitions of transition metal oxides in this monograph. We soon came to the conclusion that such a review would be incomplete unless the relevant information on the crystal chemistry, phase equilibria as well as electrical, magnetic and other important properties are also included. This is because, phase transitions in many of these oxides are associated with interesting changes in various properties (as in fig. 2). In the phase transitions of some of the oxides like TiO_2 and ZrO_2 electronic factors may not be very important, but the transitions themselves are of academic and technological interest. The phase equilibria and crystal chemistry of many of the transition metal-oxygen systems are not fully investigated. As new phases of these oxides get established, there will undoubtedly be further scope for the study of phase transitions and other properties. The Magnéli phases of titanium and vanadium serve to illustrate this point. We have tried to keep the future possibilities in mind in presenting the available information on transition metal oxides.

We have presented the information on the binary oxides of the 3*d*, 4*d*, and 5*d* transition metals by first summarizing the general features of the phase equilibria, phase transitions and physical properties in each metal-oxygen system followed by a detailed tabulation of the data. This tabular presentation of the data is expected to give a brief summary of the present status of knowledge on each oxide system. The material on each oxide system forms a self-contained section by itself and includes the relevant information on all the important properties. Such a review of transition metal oxides is not presently available in the literature and we hope that this present effort will be well-received by chemists, solid state scientists and others.

The various binary oxides discussed in the paper are shown in table 1. We have listed most of the important references to the literature (up to 1973) on each oxide system and we apologize for any omissions due to oversight or errors in judgement. Crystallographic data only from the recent literature

TABLE I.1. *Magnetic and electrical properties of stable oxides of transition metals*[a]

III B	IV B	V B	VI B	VII B	VIII			I B	II B
$^{d}Sc_2O_3$	$^{pp}TiO_x$(s.c.) $(0.70<x<1.25)$	$^{pp}VO_x$ $(0.79<x<1.00)$	$^{af}Cr_2O_3$	^{af}MnO	^{af}FeO	^{af}CoO	^{af}NiO	Cu_2O	ZnO
	Ti_2O $^{p}Ti_6O_{11}$	$^{p}VO_x$ $(1.02<x<1.25)$	$^{f}CrO_2$	$^{fe}Mn_3O_4$	$^{fe}Fe_3O_4$	$^{af}Co_3O_4$	Ni_3O_4(??)	CuO	ZnO_2(??)
	$^{p}Ti_2O_3$ Ti_7O_{13}(?)	$^{af}V_2O_3$ $^{af}V_8O_{15}$	Cr_5O_{12}(?)	$^{af}Mn_2O_3$	$^{af}Fe_2O_3$				
	$^{p}Ti_3O_5$ Ti_8O_{15}	$^{af}V_3O_5$ $^{p}VO_2$	Cr_6O_{15}(?)	$^{af}MnO_2$					
	$^{p}Ti_4O_7$ Ti_9O_{17}(?)	$^{af}V_4O_7$ $^{p}V_6O_{13}$	$^{d}CrO_3$						
	$^{p}Ti_5O_9$ $Ti_{10}O_{19}$(?)	$^{af}V_5O_9$ V_4O_9(?)							
	$^{d}TiO_2$	$^{af}V_6O_{11}$ V_3O_7(?)							
		$^{af}V_7O_{13}$ $^{d}V_2O_5$							
$^{d}Y_2O_3$	ZrO_2	^{pp}NbO(s.c.)	$^{pp}MoO_2$ Mo_8O_{23}(?)	TcO_2(?)	$^{pp}RuO_2$	Rh_2O_3	PdO	Ag_2O	CdO
		$^{p}NbO_2$	Mo_4O_{11} Mo_9O_{26}(?)	Tc_2O_7(?)		$^{pp}RhO_2$		^{d}AgO	CdO_2(??)
		$Nb_{3n+1}O_{8n-2}$ $(5\leq n\leq 8)$(?)	$Mo_{17}O_{47}$ $^{d}MoO_3$						
		$Nb_{12}O_{19}$(?)	Mo_5O_{14}(?)						
		$Nb_{47}O_{116}$							
		$^{d}Nb_2O_5$							
$^{d}La_2O_3$	HfO_2	TaO_2(?)	WO_2 $W_{18}O_{148}$(?)	$^{pp}ReO_2$	$^{pp}OsO_2$	$^{pp}IrO_2$(??)	PtO(??)	Au_2O(??)	
		$^{d}Ta_2O_5$	$W_{18}O_{49}$(?) $W_{20}O_{119}$(?)	Re_2O_5(??)	OsO_4(?)		Pt_3O_4(?)	Au_2O_3(?)	^{d}HgO(?)
			$W_{20}O_{58}$ $^{d}WO_3$	$^{pp}ReO_3$			PtO_2		HgO_2(??)
				Re_2O_7(?)					

[a] Magnetic and electrical properties are shown with the following symbols: *d*, diamagnetic; *f*, ferromagnetic; *af*, antiferromagnetic; *fe*, ferrimagnetic; *p*, paramagnetic; *pp*, Pauli paramagnetic; s.c., superconductor; ——, metal; – – –, semiconductor; ═══, exhibits semiconductor-metal transition; . . . . , degenerate semiconductor.
(?), not investigated in detail; (??), not known or doubtful existence.

have been quoted and well-established data on standard substances found in the papers have not been repeated. Studies on solid solutions of oxides, liquid oxides, oxide hydrates and thin films have not been included and the review pertains only to the bulk properties of oxides in solid state. Effects of impurities have been discussed wherever results are relevant. We must add that the information on the phase transitions of ternary oxides and other systems is very vast, but does not fall within the scope of this monograph. We have not included any general discussion of the theory of phase transitions of inorganic materials as this subject has been adequately reviewed elsewhere [19–21].

References

[1] Goodenough, J. B., Magnetism and the Chemical Bond (John Wiley-Interscience, New York, 1963).
[2] Howe, A. T., and Fensham, P. J., Quart. Rev. (Chem. Soc. London), **21**, 507 (1967).
[3] Adler, D., Solid State Phys., Eds. F. Seitz, D. Turnbull, and H. Ehrenreich **21**, 1 (1968).
[4] Rao, C. N. R., and Subba Rao, G. V., phys. stat. solidi (a) **1**, 597 (1970).
[5] Goodenough, J. B., in Progress in Solid State Chemistry, Vol. 5, Ed. H. Reiss (Pergamon Press, Oxford, 1971).
[6] Anderson, J. S., in Modern Aspects of Solid State Chemistry, Ed. C. N. R. Rao (Plenum Press, New York, 1970).
[7] Chemistry of Extended Defects in Non-Metallic Solids, Eds. L. Eyring and M. O'Keeffe (North Holland Publ. Co., Amsterdam, 1970).
[8] Menyuk, N., in Modern Aspects of Solid State Chemistry, Ed. C. N. R. Rao (Plenum Press, New York, 1970).
[9] Bosman, A. J., and van Daal, H. J., Adv. Phys. **19**, 1 (1970).
[10] Adler, D., Rev. Mod. Phys. **40**, 714 (1968).
[11] (a) Mott, N. F., Phil. Mag. **20**, 1 (1969); Rev. Mod. Phys. **40**, 677 (1968).
(b) Zinamon, Z., and Mott, N. F., Phil. Mag. **21**, 881 (1970).
[12] (a) Honig, J. M., IBM J. Res. Dev. **14**, 232 (1970).
(b) Honig, J. M., in Modern Aspects of Solid State Chemistry, Ed. C. N. R. Rao (Plenum Press, New York, 1970).
[13] Rice, T. M., and McWhan, D. B., IBM J. Res. Dev. **14**, 251 (1970).
[14] Doniach, S., Adv. Phys. **18**, 819 (1969).
[15] Hyland, G. J., J. Solid State Chem. **2**, 318 (1970).
[16] Goodenough, J. B., Bull. Soc. Chim. France **4**, 1200 (1965).
[17] Goodenough, J. B., Czech. J. Phys. **17B**, 304 (1967).
[18] Goodenough, J. B., J. Appl. Phys. **37**, 1415 (1966); **39** 403 (1968).
[19] Rao, C. N. R., and Rao, K. J., in Progress in Solid State Chemistry, Vol. 4, Ed. H. Reiss (Pergamon Press, Oxford, 1967).
[20] Rao, C. N. R., in Modern Aspects of Solid State Chemistry, Ed. C. N. R. Rao (Plenum Press, New York, 1970).
[21] Rao, C. N. R., and Natarajan, M., Crystal Structure Transformations in Binary Halides, Nat. Stand. Ref. Data Ser., Nat. Bur. Stand. (U.S.), 41, 53 pages (July 1972).

I. Oxides of 3*d* Transition Elements

I.1. Scandium Oxide

Scandium apparently forms only one oxide, Sc_2O_3. Petru and Dufek [1] reported a grey-black oxide, which they believed to be a monoxide, ScO, obtained by the hydrogen reduction of Sc_2O_3 at 2170 K; this monoxide has, however, not been characterized. Sc_2O_3 is cubic [2–5] and has the C-type rare-earth oxide structure in which the metal atoms are distributed in the ratio 1:3 into two crystallographically distinct sites each with six-fold coordination. The structure is relatively open and can be described as a defect fluorite form in which one fourth of the anions are absent. No magnetic ordering is known in Sc_2O_3 and heat capacity data [6, 7] do not indicate any phase transformations in the range 53 to 1800 K. Reid and Ringwood [8] found that Sc_2O_3 transforms to the monoclinic B-type rare-earth oxide structure at 130 kbar pressure and 1273 K. The unit cell volume decreases by 7.8 percent (density increases by 8.3 percent) accompanied by an increase in coordination number from six- to seven-fold for two thirds of the metal atoms. No change in the crystal structure is noticed at 30 or 80 kbar pressure at 1273 K (or at 89 kbar at 1573 K) and at 110 kbar at 1273 K, poorly crystallized high pressure phase of Sc_2O_3 is obtained [8, 9].

Sc_2O_3 is a semiconductor at all temperatures [10–13] and considerable ionic contribution to the total conductivity is noticed at and below 1100 K [11, 12].

Sc_2O_3 forms a complete series of solid solutions with In_2O_3 [9, 14], Y_2O_3 [15, 16], Yb_2O_3 [15], and Cr_2O_3 [17] and binary systems of the type MO_2-Sc_2O_3 where M = Ti [18], Zr [18–21], Hf [22, 23], Th [24], and U [24] and CaO-Sc_2O_3 [25] have been investigated in detail in the literature. Generally, solid solution formation occurs up to certain composition and the binary systems exhibit considerable ionic conductivity.

Oxide and description of the study	Data	Remarks and inferences	References
Sc_2O_3			
Crystal structure and melting point.	Ordinary form: Cubic; space group, Ia3; $Z=16$; $a=9.844\pm0.002$ Å. High-pressure form: Monoclinic; space group, C2/m; $Z=6$; $a=13.173\pm0.01$ Å; $b=3.194\pm0.005$ Å; $c=7.976\pm0.01$ Å; $\beta=100.40°\pm0.05°$. Melting point = 2740 K.	This relatively open C-type structure is adopted by many rare-earth oxides and is closely related to the fluorite structure. The high pressure form is denser and is akin to the B-type structure adopted by the rare-earth oxides. The transformation does not involve the intermediate corundum structure.	[4, 8, 26].
Electrical properties.	Semiconductor behavior in the range 370–1870 K; reliable data on pure and single crystal material are not available.	—	[10–13].
Optical properties.	Optical energy gap = 5.4 eV; infrared stretching frequency = 635 cm^{-1}.	—	[27, 28]

References

[1] Petru, F., and Dufek, V., Z. Chem. 6, 345 (1966).
[2] Milligan, W. O., Vernon, L. W., Levy, H. A., and Peterson, S. W., J. Phys. Chem. 57, 535 (1953).
[3] Reid, A. F., and Sienko, M. J., Inorg. Chem. 6, 521 (1967).
[4] Geller, S., Romo, P., and Remeika, J. P., Z. Crystallogr. 124, 136 (1967); 126, 461 (1968).
[5] Norrestam, R., Arkiv för Kemi 29, 343 (1968).
[6] Weller, W. W., and King, E. G., US Bur. Mines Rept. Invest. No. 6245 (1963).
[7] Pankratz, L. B., and Kelley, K. K., US Bur. Mines Rept. Invest. No. 6198 (1963).
[8] Reid, A. F., and Ringwood, A. E., J. Geophys. Res. 74, 3238 (1969).
[9] Prewitt, C. T., Shannon, R. D., Rogers, D. B., and Sleight, A. W., Inorg. Chem. 8, 1985 (1969).
[10] Noddack, W., and Walch, H., Z. Elektrochem. 63, 269 (1959).
[11] Schmalzried, H., Z. Physik. Chem. 38, 87 (1963).
[12] Tripp, W. C., and Tallan, N. M., Bull. Am. Ceram. Soc. 47, 355 (1968).
[13] Zyrin, A. V., Dubok, V. A., and Tresvyatskii, S. G., Khim. Vysokotemp. Mater., Tr. Vses. Soveshch. 2nd Leningrad 59 (1965, Publ. 1967); Chem. Abstr. 69, 62562t (1968).
[14] Schneider, S. J., Roth, R. S., and Waring, J. L., J. Res. Nat. Bur. Stand. (U.S.), 65A (Phys. and Chem.), No. 4, 345–374 (July–Aug. 1961).
[15] Hazek, B., Petru, F., Kalalova, E., and Dolezalova, J., Z. Chem. 6, 268 (1966).
[16] Trzebiatowskii, W., and Horyn, R., Bull. Acad. Polon. Sci., Ser. Sci. Chim. 13, 311 (1965).
[17] Tresvyatskii, S. G., Pavlikov, V. N., and Lopato, L. M., Izv. Akad. Nauk SSSR Neorg. Mater. 2, 269 (1966).
[18] Collongues, M. R., Queyroux, F., Perez, M., Jorba, Y., and Gilles, J.-C., Bull. Soc. Chim. France 4, 1141 (1965).
[19] Lefevre, J., Rev. Hautes Temp. Refract. 1, 229 (1964).
[20] Thornber, M. R., Bevan, D. J. M., and Graham, J., Acta Cryst. 24B, 1183 (1968).
[21] Spiridonov, F. M., Popova, L. N., and Popils'kii, R. Ya., J. Solid State Chem. 2, 430 (1970).
[22] Komissarova, L. N., and Spiridonov, F. M., Dokl. Akad. Nauk SSSR 182, 834 (1968).
[23] Kalinovskaya, C. A., Spiridonov, F. M., and Komissarova, L. N., J. Less-Comm. Metals 17, 151 (1969).
[24] Trezebiatowskii, W., and Horyn, R., Bull. Acad. Polon. Sci., Ser. Sci. Chim. 13, 303 (1965).
[25] Trezebiatowskii, W., and Horyn, R., Bull. Acad. Polon. Sci., Ser. Sci. Chim. 13, 315 (1965).
[26] Noguchi, T., and Mizuno, M., Solar Energy 11, 90 (1967).
[27] Companion, A. L., J. Phys. Chem. Solids 25, 357 (1964).
[28] Petru, F., and Muck, A., Z. Chem. 6, 386 (1966).

I.2. Titanium Oxides

The Ti-O system has been studied exhaustively by various workers over the past several years. DeVries and Roy [1] reviewed the available literature up to 1954 and gave a tentative phase diagram. Since then, different groups of investigators [2–6] have contributed much to the understanding of the various phases in the Ti-O system. The important phases of the systems are the following: Ti_6O (reported by Kornilov and Glazova [7, 8] and characterized by Yamaguchi et al. [9]), Ti_3O (reported by Kornilov and Glazova [7, 8] and characterized by Jostsons and Malin [10]), rhombohedral Ti_2O [3–6, 8, 11], a cubic monoxide, TiO_x, having a wide homogeneity range ($0.75 \leqslant x \leqslant 1.30$) with disordered rock salt structure at high temperatures containing many vacancies [3–6, 12–16], a low temperature ordered monoxide recently characterized by Watanabe et al. [17], an ordered $TiO_{1.25}$ [18–20], a sesquioxide Ti_2O_3 with a narrow homogeneity range, Ti_3O_5, Magnéli phases of the general formula Ti_nO_{2n-1} ($4 \leqslant n \leqslant 10$) and TiO_2. The phase diagram of Porter and Roy [5] is reproduced in figure I.1. Recent studies have revealed the complicated nature of the Ti-O phase diagram; according to Hirabayashi and co-workers [21], below 670 K, there is an almost infinite number of ordered phases in the composition range $0.09 < O/Ti < 0.40$ and also a number of higher Magnéli phases ($n \sim 11$–53; range, $1.90 < O/Ti < 2.00$) (22, 23].

Titanium oxides show a wide variety of interesting electrical, magnetic and optical properties and interesting phase transitions. We shall now critically discuss some important aspects in this section.

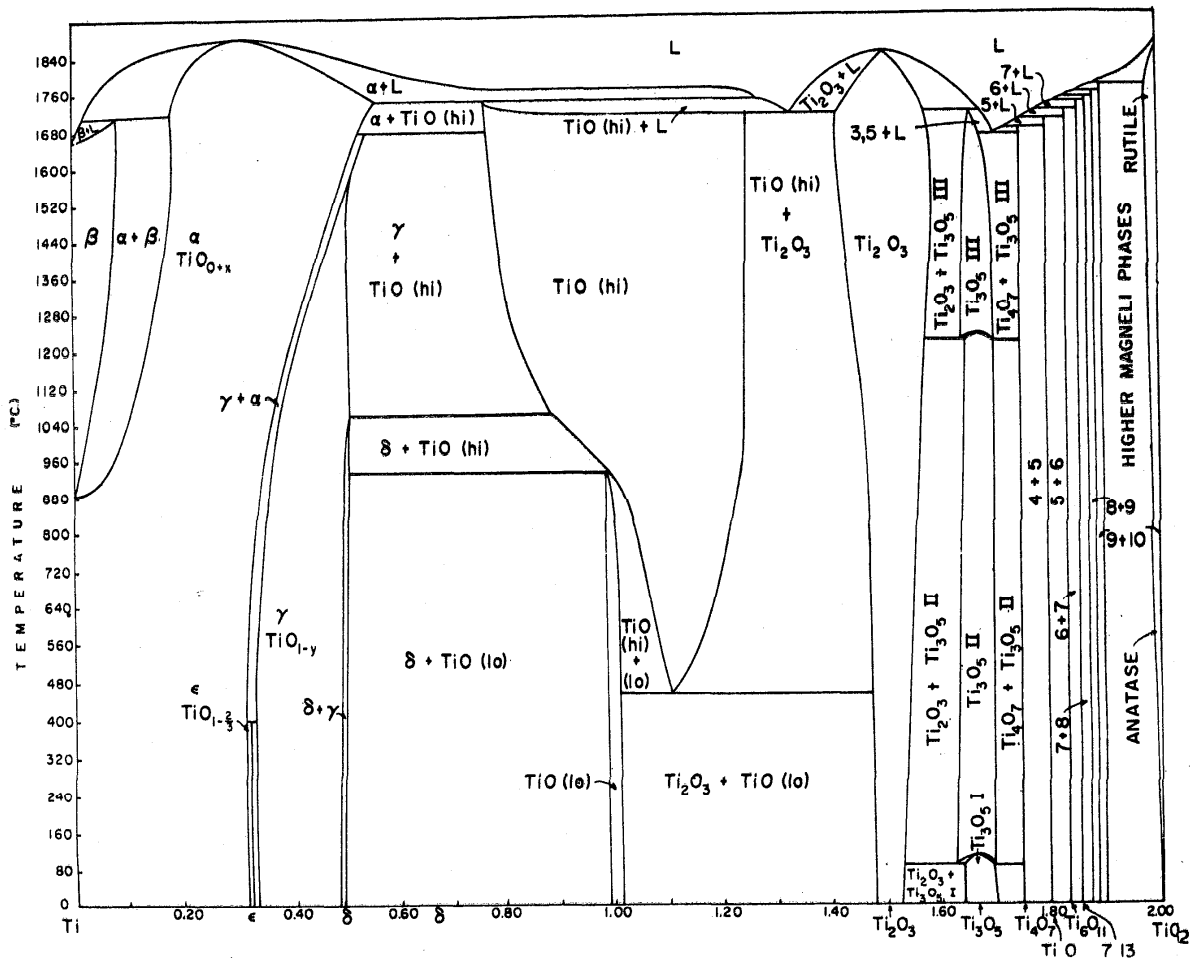

FIGURE I.1. Ti-TiO_2 *phase phase diagram showing various oxide phases (after Porter and Roy* [5]).

TiO_x ($x < 0.70$): Metallic titanium exists in two allotropic modifications, α (low temperature, hexagonal) and β (high temperature, bcc). The $\alpha \rightarrow \beta$ transition occurs at 1155 K [2, 6]. Oxygen addition to Ti stabilizes the α phase and oxygen can be dissolved interstitially up to ~30 atom percent [6]. From measurements of resistivity [7, 24], Seebeck coefficient [7] and rate of oxidation [25], it was suggested that a stable phase, Ti_6O, may exist. Recently, Yamaguchi et al. [9] have fully characterized this phase. Ti_6O is hexagonal with ordered superlattice structure. Electron/neutron diffraction and DTA studies show an order-disorder transition at ~710 K; the phase is stable up to ~1100 K.

Ti_3O and Ti_2O have a hexagonal ordered structure and they differ from the solid solutions of Ti and oxygen by the ordered arrangement of the oxygens in the suboxide lattice and by the greater stability of the chemical bond [3, 4, 7, 8, 10]. Andersson [26] found that the so-called δ-phase of TiO_x ($x = 0.65$) has a hexagonal structure and the isotropy in TEC values are probably connected with the occurrence of the close metal-metal contacts, which are present both parallel and perpendicular to the c axis.

TiO_x ($0.70 \leqslant x \leqslant 1.30$): The rock salt type TiO phase exists over a wide composition range depending on the temperature, e.g., from $TiO_{0.70}$ to $TiO_{1.25}$ at 1673 K and $TiO_{0.9}$ to $TiO_{1.25}$ at temperatures below 1260 K [3–6]. An important feature of this phase, as shown from density and lattice parameter measurements, is that its crystal structure has varying proportions of both titanium and oxygen vacancies [3, 4, 12–14, 16, 27–30]. At the composition $TiO_{0.70}$, the titanium lattice is almost perfect (~4 percent vacancies, extrapolating to zero at ~$TiO_{0.5}$) and about 30 percent of the oxygen sites are vacant. In $TiO_{1.30}$, the oxygen lattice is perfect and about 25 percent of the Ti sites are vacant. Even in the stoichiometric oxide, $TiO_{1.00}$, about 15 percent of both Ti and O sites are vacant. These vacancies are arranged randomly at temperatures above the equilibrium temperature, 1260 K; at lower temperatures, however, ordering of the vacancies occurs and the cubic rock salt structure of $TiO_{1.00}$ transforms to monoclinic phase [3, 4, 12, 17, 20, 31]. This monoclinic phase was first noticed by Naylor [32] from enthalpy studies. The oxygen-rich $TiO_{1.25}$ becomes ordered after long annealing treatments at 1070 K and the crystal symmetry changes from cubic to tetragonal [18]. There is another ordered structure, the so-called 'transition structure' [17] observed over a wide composition range $TiO_{0.7}$-$TiO_{1.25}$; this has an orthorhombic structure and is observed in specimens which were rapidly cooled from the melt (of TiO_x; cubic high temperature modification) and not well annealed at low temperatures as well as in thin foils (of TiO_x) annealed at temperatures greater than 870 K or heated by an intense electron beam [17, 31]. Thus, the high temperature cubic $TiO_{0.7}$-$TiO_{1.25}$ phase transforms, on cooling, to various ordered phases having different crystal symmetries by means of vacancy (both cation and anion) disorder-order mechanism. It is important to note, however, that it is possible to retain the cubic phase at room temperature by quenching from above 1270 K and a great deal of work has been done on these quenched cubic phases.

Detailed investigations on well-characterized samples by Banus and Reed [28] and Taylor and Doyle [29] have shown that the cubic lattice parameter and the density increase with increasing x in TiO_x (in the range 0.86–1.24); ρ and $d\rho/DT$ (negative) are small and increase slightly, α (n-type) increases and χ_M is extremely small and unchanging, indicating that TiO is a typical metallic oxide [14, 28–30, 33]. TiO becomes superconducting at liquid helium temperatures [15–34]; Hulm et al. [15] found that T_{sc} varies from 0.1–1.0 K as x increases from 0.92 to 1.10; for other values of x, at atmospheric pressure, the materials are normal conductors down to $T < 0.08$ K.

Annealing TiO_x at 50–60 kbar pressure and at 1573 K decreases the total number of vacancies considerably (by ~17 percent) [28, 35]; according to Taylor and Doyle [29], complete removal of vacancies in TiO_x is possible by proper selection of temperature and pressure (e.g., 77 kbar and ~1850 K). The removal of vacancies is accompanied by a rise (for a given x) in lattice parameter, density and T_{sc} (from 0.7 to 2.3 K for $TiO_{1.00}$), slight increase in ρ and α and decrease in compressibility and TEC. These changes in properties are completely reversible and are unambiguously due to the pressure effect because reheating the samples in the absence of applied pressure (say at ~1570 K) causes them to revert to the original vacancy concentration and lattice parameter [28, 29]. Recently, Iwasaki et al. [36] have studied the effect of pressure on the lattice parameters of $TiO_{0.82}$ and $TiO_{1.25}$ and essentially obtained the same results as those of Banus and Reed [28] and Taylor and Doyle [29]. The change in a parameter is small for both the samples; for $TiO_{0.82}$ the decrease is considerable for smaller pressures while $TiO_{1.25}$ shows a decrease at relatively higher pressures (10–60 kbar).

TiO_x forms solid solutions with VO_x and NbO_x but the solubility is low (~10 percent) [30, 37]. On the other hand, Gel'd et al. [37] noticed that the oxygen-rich phases $TiO_{1.20}$ and $VO_{1.25}$ have an appreciable mutual solubility (~20–25%). BeO, MgO, and CaO also appear to form solid solutions (up to ~50%) [37]. Loehman, Rao, and Honig [30] found that the vacancy concentration is decreased in TiO_x after solid solution formation; both TiO and $(Ti_{0.95}V_{0.05})O$ show metallic behavior.

Since the low temperature ordered TiO_x phases have been characterized only recently, reliable data on the physical properties are lacking at present on these materials.

Ti_2O_3: Ti_2O_3 has a narrow range of homogeneity ($x=1.49$–1.51 in TiO_x) [3, 4] and has the rhombohedral crystal structure at room temperature [12, 38, 39] and shows an unusual behavior in the thermal expansion of the lattice parameters in the range 450 to 650 K [12]. A more recent study [40] on pure material shows that the abrupt change in lattice parameters sets in at a lower temperature (~400 K); the c/a ratio increases and there is a 7 percent decrease in the volume of the unit cell in the range 390 to 470 K. There is no change in the crystal symmetry in this temperature range. Magnetic susceptibility does not show any significant anomaly in the range 400 to 550 K even though a two fold increase in the magnitude has been noted [12, 41–43]. The existence of long range magnetic order in Ti_2O_3 has been much debated on the basis of various experimental investigations [38, 44–46], but recent neutron diffraction study by Moon et al. [47] have clearly confirmed the absence of antiferromagnetism in Ti_2O_3 below 400 K. A specific heat anomaly has been reported in Ti_2O_3 in the range 450 to 600 K [32, 48]. Rao et al. [49] have found a broad endothermic peak (centered around 410 K) in the DTA curve (see figure 2 in introduction section).

Electrical properties have been examined by many workers in the literature [12, 33, 38, 50, 51]. Morin [33] found that below 450 K Ti_2O_3 is a semiconductor with a small energy gap (E_g~0.05 eV); above this temperature it behaves like a metal with a ten-fold drop in resistivity at T_t. Yahia and Frederikse [51] observed the semiconductor-to-metal transition at 450 K, the drop in resistivity being of a factor of 40. Abrahams [38] noticed the transition, but found that T_t was ~660 K. Honig and Reed [52] have carried out a detailed investigation on highly pure and nearly stoichiometric single crystals of Ti_2O_3; they have noted that in the range 100 to 300 K, the material behaves as an intrinsic semiconductor with a band gap of 0.03–0.05 eV (depending on the sample) and the drop in ρ beginning at ~400 K and extending up to 470 K. The drop in ρ in the 400 to 470 K range was about hundred-fold. The resistivity of Ti_2O_3 goes through a shallow minimum at ~800 K and rises again with further increase in temperature. Hall data [52] below 273 K indicated the charge carriers to be positively charged and with high mobilities. Seebeck coefficient of pure Ti_2O_3 is positive at ordinary temperatures [51, 53] (Loehman [53] reports smaller values compared to Yahia and Frederikse [51] for pure Ti_2O_3) and drops to smaller values in going through the transition region (400 to 470 K).

The nature of the semiconductor-to-metal transition in Ti_2O_3 has been discussed by various workers in the literature [54–64]. The gradual decrease in ρ and α in the region of the transition, the broad nature of the anomalies in χ, heat capacity and DTA measurements indicate that Ti_2O_3 is a relatively wide band material and that the semiconductor-to-metal transition is of higher order [52, 54, 58–64]. Since the absence of antiferromagnetism is definitely established in this material [47], a plausible mechanism appears to be that of band broadening or shifting [58, 61, 62, 64–66]. The presence of c axis pairs in the corundum structure to produce a cation sublattice band [54] together with a strong trigonal crystal field will produce a filled band with one $3d$ electron per Ti^{3+} ion (figure I.2). The rapidly in-

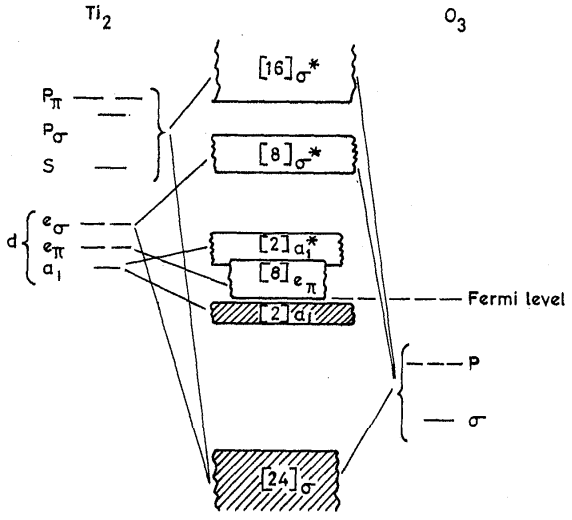

FIGURE I.2. *Schematic band strurture of* Ti_2O_3 (*after* [65]).

creasing c/a ratio in the vicinity of 400 to 470 K [40] brings the anions and cations much closer and thus provides for a progressively greater overlap among the corresponding wave functions (Note that c/a ratio at room temperature is anomalously small; see figure I.5). This, in turn, leads to narrowing and then to a disappearance of the valence band-conduction band separation (figure I.2). The p-type nature of the charge carriers can be explained by assuming that either the carriers in the valence band dominate the conduction or with a model involving joint participation of electrons and of holes with comparable effectiveness.

Honig and co-workers [52, 67] have shown that a slight amount of impurity remarkably affects the electrical properties of this material. A variety of values of T_t as well as the magnitude of the change in ρ (at T_t) reported in the literature [33, 38, 51] may as well be due to the small amounts of impurities in the samples of Ti_2O_3 employed in the investigations.

Ti_2O_3 forms solid solutions with V_2O_3 throughout the composition, but the solid solutions so formed are not ideal and do not obey Vegard's law [30, 68]. The interesting observation is that at $x \approx 0.1$ in $(Ti_{1-x}V_x)_2O_3$ the values of a, c, and α are the same as the corresponding values for pure Ti_2O_3 after it undergoes the electrical transition [30, 40]; the c parameter of Ti_2O_3 is increased by $\sim$3 percent by the incorporation of $\sim$20 percent V_2O_3 while the corresponding a parameter contracts by $\sim$1.5 percent. This strongly lends support to the idea [39] that strong metal-metal bonding across the octahedral edges takes place in Ti_2O_3. Recent resistivity data [69] on $(Ti_{1-x}V_x)_2O_3$ show that for $0 \leqslant x \leqslant 0.04$, ρ undergoes a change in almost the same temperature range as undoped Ti_2O_3; samples with high x are metallic at room temperature and exhibit no transition. This observation is consistent with the crystal data of Loehman, Rao, and Honig [30].

Ti_3O_5: Ti_3O_5, the precursor of the Ti_nO_{2n-1} Magnéli shear structures, is monoclinic at room temperature. Åsbrink and Magnéli [70] reported that Ti_3O_5 transforms to a distorted-orthohombic (more exactly, monoclinic) structure reversibly at $\sim$390 K, where as Naylor [32] from his enthalpy data, indicated a transition at $\sim$450 K. Keys and Mulay [43], Mulay and Danley [71], and Vasilév and Ariya [72] showed that χ_M of Ti_3O_5 shows a sharp discontinuity at $\sim$460 K, with a 30 K hysteresis on cooling; both above and below the T_t, χ_M is temperature independent. Keys, Mulay, and Danley [43, 71] and Keys [73] have suggested that the transition in Ti_3O_5 may correspond to a semiconductor-to-metal transition. X-ray studies of Åsbrink and Magnéli [70] showed the presence of metal-metal bonding in the low temperature form of Ti_3O_5 and above T_t, these bonds get broken. Based on considerations of the localized versus collective electron behavior of the d electrons in Ti_nO_{2n-1} Magnéli phases, Goodenough [74] has suggested that a semiconductor-to-metal transition may exist in Ti_3O_5.

Bartholomew and Frankl [75] made resistivity measurements on flux grown Ti_3O_5 single crystals and confirmed the semiconductor-to-metal transition in this material. Recently, Rao and co-workers [49] have examined the transition in Ti_3O_5 in detail employing high temperature x-ray diffraction, DTA, electrical resistivity, ESR and Mössbauer techniques. These workers established the first order nature of the transition in Ti_3O_5 with appreciable latent heat and hysteresis; no magnetic ordering was noted in the low temperature phase. At T_t (448 K), ρ drops by two orders of magnitude and below T_t, Ti_3O_5 is semiconducting with E_a of $\sim$0.3 eV. Slight amounts of Fe and W reduce the transition temperature and the magnitude of resistivity discontinuity and at about 5 percent Fe dopant concentration completely suppress the transition.

Since metal-metal bonding in Ti_3O_5 has been definitely established [70], it appears that Goodenough's model [54, 55, 61, 74] would be applicable in explaining the transition in this material. According to Goodenough, in the titanium and vanadium oxides, in the high temperature high symmetry phases, the cation-cation distance is greater than the critical cation-cation separation (see [61] for details) and the charge carriers move in partially filled cation sublattice d bands and metallic behavior is exhibited only in the materials with well-defined Fermi surface. As the temperature is lowered through T_t, however, the band breaks up into pairs of atoms that are bonded by homopolar bonds in which the conduction electrons are trapped and a change to lower crystal symmetry (and semiconducting phase) occurs to produce a filled band separated from an empty band by a finite energy gap. The atomic rearrangements at T_t are subtle in Ti_3O_5 [49, 70] and it appears that these are sufficient to bring about an electrical transition in this material. According to Goodenough's model, we expect electrons to be the charge carriers in Ti_3O_5 and the available Seebeck coefficient data [76] seem to confirm this prediction.

Iwasaki et al. [77] have reported the existence of a metastable form of Ti_3O_5 (designated as D) which is identical with the high temperature form of Ti_3O_5 [49, 70] (D′ form), but the two differ in their properties with respect to oxidation. D and D′ forms can be prepared by the hydrogen reduction of anatase and rutile respectively at ~1520 K and give almost identical x-ray diffraction patterns, but on oxidation at ~920 K, D gives rutile while D′ gives a mixture of anatase and rutile modifications of TiO_2. The low temperature form (M form of Iwasaki et al. [77]) can be prepared by the vacuum sintering of TiO_2 (anatase form) and Ti metal at ~1520 to 1570 K and yields rutile and anatase on oxidation. For the phase transition D′→M, Iwasaki and his co-workers report a T_t slightly greater than 373 K. The D form could easily be changed to the M form by cooling from 1620 K under vacuum. These observations suggest that differences in the oxygen coordination around Ti may give rise to stable and metastable modifications of Ti_3O_5 and the T_t as well as electrical and related properties may also differ accordingly. From this point of view, careful reinvestigation of the transition in Ti_3O_5 is worthwhile on well characterized samples of this material.

Ti_nO_{2n-1}: The existence of Magnéli phases in the Ti-O system was first reported by Andersson et al. [3, 4] in 1957. These are a homologous series of triclinic phases of composition Ti_nO_{2n-1} with $4 \leqslant n \leqslant 9$. They are bounded by monoclinic Ti_3O_5 on one side and by reduced rutile (TiO_{2-x}) on the other. The structures with $4 \leqslant n \leqslant 9$ can be described [3, 4, 22, 23, 78–84] as being built-up of slabs of rutile-type structure which have infinite extension parallel to the (121) plane and have a characteristic finite width corresponding to n TiO_6 octahedra (where n is the integer in the chemical formula, Ti_nO_{2n-1}) in the third direction. The adjacent slabs are mutually related by crystallographic shear (CS), the shear plane and shear vector being (121) and $\frac{1}{2}$ [01$\bar{1}$] respectively in the idealized Ti_nO_{2n-1} structure. This CS causes the titanium atom positions in one slab to correspond to unoccupied or interstitial positions in the next slab and decreases the crystal symmetry from tetragonal to triclinic while decreasing the size of the unit cell. However, the structure of $Ti_{10}O_{19}$ ($n=10$) cannot be explained in this way and the structure is not yet known.

Anderson and Hyde [81] suggested that rutile-based shear structures other than the (121) family probably exist, in particular, a (132) family in reduced rutile. Detailed studies using electron microscopy and diffraction by Hyde and co-workers [22, 23] showed the existence of a new family of ordered phases, Ti_nO_{2n-1} ($15 \leqslant n \leqslant 36$) derived by CS planes parallel to (132). Possibility of the existence of another Ti_nO_{2n-1} ($n>35$) family (011) shear planes was suggested by these workers since continuous streaking along ⟨011⟩ directions was observed occasionally in the electron diffraction patterns of reduced rutile and detailed studies are yet to be made. Studies are also necessary in the composition range $9<n<15$, (i.e., $TiO_{1.889}$–$TiO_{1.933}$).

The rutile based Ti_nO_{2n-1} series with $4 \leqslant n \leqslant 9$ have periodic stacking faults introducing extra planes of metal ions for every n planes in one crystallographic direction (121) and Magnéli [79, 82] has pointed out that the condensation of the defects into common planes can minimize the elastic energy of the crystal. Goodenough [74, 85] has recognized that such systems exhibiting shear structures may contain collective d orbitals and that the regularity of the spacings between these shear planes is due to the existence of a Fermi surface and to the energy stabilization achieved by either creating or increasing the energy discontinuity across a Brillouin zone surface at the Fermi surface. This stabilization is greater, the narrower the bands are, and hence spontaneous crystallographic distortions could result at lower temperatures. Also, since the existence of a Fermi surface is a collective electron property [61], it can be argued that crystallographic distortions in the Magnéli phases may also be associated with the metal-to-semiconductor transitions (on cooling). As a matter of fact, the available data indicate that electronic transitions do occur in these materials associated with crystal distortions; however, the crystal distortions appear to be minor (at least in Ti_4O_7, for which detailed high temperature x-ray data are available [75, 86]) and do not involve structural changes but only minor discontinuities in the lattice parameters at the transition temperature.

Detailed x-ray [75, 86], χ_M-T [43, 71, 72], DTA [75] and P-T [75, 87] studies show that there are two phase transitions in Ti_4O_7, at ~125 and at 150 K. There is 8 to 10 K hysteresis associated with the first transition and some structural changes; the 150 K transition is associated with a change from semiconductor to metal behaviour as well as magnetic susceptibility and DTA anomalies, but no apparent structural change. Ti_5O_9 exhibits transitions at 130 and 136 K and resistivity measurements indicate discontinuities at these temperatures, but the sample remains semiconducting above T_t [43, 71, 75]. DTA and χ_M-T measurements indicate a

transition in Ti_6O_{11} at 122 K [43, 71, 75], but the resistivity data indicate a T_t of ~130 K and semiconductor behavior above and below this temperature [75]. According to Bartholomew and Frankl [75], Ti_8O_{15} exhibits semiconductor behavior in the range 78 to 295 K and no transitions exist in this material. χ_M-T data are not available at present. The detailed physical properties of Ti_7O_{13} and Ti_9O_{17} are not known at present.

TiO_2: Titanium dioxide, TiO_2, has a narrow homgeneity range (x~1.983–2.000 in TiO_x) [3–6, 88], and exists in three polymorphic forms, namely, anatase (tetragonal), brookite (orthohombic), and rutile (tetragonal) at atmospheric pressure. In each of these, Ti^{4+} ion is surrounded by an irregular octahedra of oxide ions, but the number of edges shared by the octahedra of oxide ions, but the number of edges shared by the octahedra increases from two (out of twelve) in rutile to three in brookite and to four in anatase. The rutile form of TiO_2 is the most stable form and both anatase and brookite transform to rutile on heating. High pressure modifications of TiO_2 have been reported by Dachille and Roy [89], Bendeliani et al. [90], and McQueen et al. [91]. Phase transformations involving various modifications of TiO_2 have been extensively studied in the literature.

Anatase transforms irreversibly and exothermally to rutile in the range 880 to 1200 K depending on the method of preparation of the sample and at atmospheric pressure, the transformation is time and temperature dependent and is also a function of the impurity concentration. Rao and co-workers [92–96], Sullivan and Cole [97], Iida and Ozaki [98], Suzuki and Kotera [99], and Shannon and Pask [100] have carried out systematic investigations of the anatase-rutile transformation. The rate of transformation of spectroscopically pure TiO_2 in the anatase modification was found to be immeasurably slow below 885 K and extremely rapid above 1000 K [92, 101]. The transition is a nucleation-growth process, and follows the first order rate law with an activation energy of ~90 kcal/mol (fig. I.3a). Impurities like CuO, CoO, Li_2O, and Na_2O and reducing atmospheres accelerate the transformation while sulphate, phosphate, and fluoride anions, P^{5+} and S^{6+} ions and vacuum stabilize the anatase modification and inhibit the transition process [94–96, 98, 100, 102–104]. Values of T_t and activation energy are generally higher in impure samples than in the pure sample.

The defect structure of TiO_2 is not yet fully understood. There is considerable evidence for the formation of both titanium interstitials and oxygen vacancies [61, 104–108]; the atmosphere in which the defects are formed seems to be an important factor. Since the anatase-rutile transformation involves an overall contraction or shrinkage of the oxygen structure as indicated by a volume shrinkage of ~8 percent and a cooperative movement of ions (displacive and reconstructive transformation [94, 109, 110]), the removal of the oxygen ions would be expected to accelerate the transformation; formation of titanium interstitials would inhibit the transformation. This implies that a reducing atmosphere or doping with an ion of lesser valence state (Cu^{2+} or Co^{2+}) would accelerate the transition as indeed found experimentally. Vacuum or doping with anions will similarly give rise to Ti^{3+} interstitials and hence the inhibition of the transformation process and would increase the temperature of the anatase-rutile transition.

Yoganarasimhan and Rao [94] noticed that the particle size and crystallite size of anatase increase markedly in the region of the crystal structure transformation; smaller particle size and larger surface area of anatase samples favor the transition. Detailed x-ray studies indicated that the unit cell expands prior to the transformation to rutile.

Recently, Vahldiek [111] examined the effect of pressure on the anatase-rutile transformation. Electrical resistance and quenching experiments indicated that T_t and ΔH for the transition decrease with the applied pressure; at a pressure of 1 bar, $\Delta H \sim -2.8$ kcal/mol and his observations corroborated the data of earlier workers. Discontinuous change in ρ was observed at T_t at various applied pressures and the irreversibility of the anatase-rutile transition at high pressures (up to 24 kbar) was confirmed.

Kubo et al. [112] and Tekiz and Legrand [113] observed the transition of anatase to rutile by grinding; anatase-type TiO_2 obtained from $TiCl_4$ method is changed to rutile after grinding for 96 h, while TiO_2 (anatase form) obtained from the H_2SO_4 method changed to an amorphous state.

Brookite, the orthorhombic modification of TiO_2 occurs in nature; it has not been possible to prepare this polymorph in pure form in the laboratory. Brookite-rutile transformation was first reported by Schossberger [114] and examined in detail by Rao and co-workers [115]. Below 990 K, the rate of transition is extremely slow and sluggish and above this temperature, it follows a first order rate law with little or no induction time (fig. I.3b). The

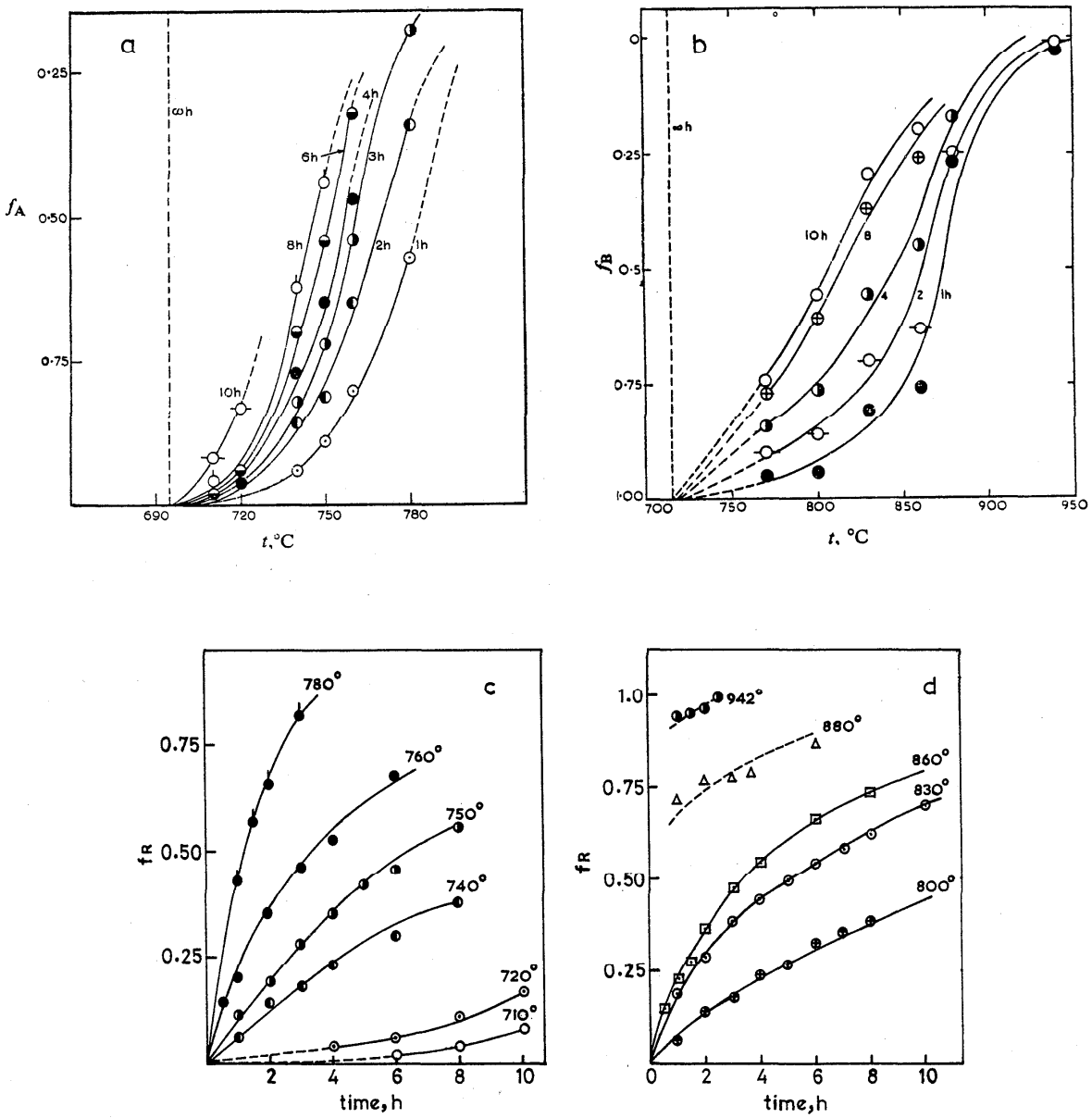

FIGURE I.3. *Transformation of anatase (a) and brookite (b) as a function of temperature at different times (after Rao and co-workers* **[94, 115]**.

f_A and f_B are the fractions of anatase and brookite forms in the mixture. Kinetics of transformation of anatase and brookite to rutile are shown in (c) and (d) respectively (f_r = fraction of rutile).

transition is irreversible with an energy of activation ~60 kcal/mol and $\Delta H \sim -(100 \pm 75)$ cal/mol. DTA studies give $T_t \approx 1020$ K.

As regards the comparison of the anatase-rutile and brookite-rutile transformations, it may be mentioned that the kinetics and mechanism are exactly similar (fig. I.3c and I.3d), but the energy of activation is larger in the anatase-rutile transition; the entropy of activation is large and negative for the brookite-rutile transition while it is small and has a positive value for the anatase-rutile transition. This discrepancy may be understood in terms of the change of symmetry (lower to higher) in the former case and the absence of such a change in the latter case.

A new high pressure modification of TiO_2 was synthesized by Dachille and Roy [89] at pressure 15–100 kbar and temperatures 298 to 773 K. It forms easily from anatase, but appears to be metastable with respect to rutile. The structure of this modification is not known. The new form converts slowly to rutile on heating between 770 to 973 K via a short-range order phase.

According to McQueen et al. [91], rutile at ordinary temperatures transforms to an orthorhombic modification at 330 kbar pressure with considerable decrease in volume (~21%). Bendeliani et al. [90] have synthesized the orthorhombic modification at ~70 kbar pressure and 970 K (pressures 40–120 kbar and 670 to 1770 K, under hydrothermal conditions). This phase reverts to rutile on heating to 720 to 870 K. The detailed physical properties of this phase are not known at present.

Even though the anatase and brookite modifications have not been investigated in detail, extensive literature is available on various physical properties of the rutile modification of TiO_2 [43, 116–120] and have been treated in detail in many review articles [57, 61, 63, 116, 121, 122]. Stoichiometric TiO_2 shows a temperature independent susceptibility consisting of a diamagnetic and a Van Vleck contribution [43, 121, 122a]. TiO_2 has a high room temperature resistivity and exhibits semiconducting behavior; intrinsic conduction seems to set in only at very high temperatures (>1500 K) with a large energy gap (~3 eV). Doped or reduced TiO_2 has a lower resistivity and exhibits impurity conduction. Detailed resistivity, Seebeck coefficient and Hall mobility studies over a range of temperatures have not been able to provide a clear understanding of the mechanism of conduction in pure and doped TiO_2 [116–120; 122b–122d]; multiple band conduction seems to be conclusively proved, but the existence of band or hopping (large or small polaron) type of conduction is still in dispute.

As mentioned earlier, the defect structure of TiO_2 is not yet completely understood and evidence is in favor of both anion vacancies and Ti interstitials [61, 104–108, 123, 123a]. Hauffe [123a] and Rudolph [123b] noted that in the range 882 to 1273 K, $\rho \propto p_{O_2}^{-1/n}$ where n varies from 5.7 to 4.4 whereas Greener et al. [123] obtained $n=4$ above 1470 K and no dependence of ρ on p_{O_2} below 1170 K (ideally, n should be 6, 5, and 4 for anion vacancy, Ti^{4+} and Ti^{3+} interstitial mechanisms respectively). High temperature E_a values (1.8 eV) of both workers agree very well. Internal friction measurements [123c] on vacuum-reduced rutile (for 1–3 h at 1530 K), on the other hand, indicate that the predominant point-defects are neither anion vacancies nor cation interstitials and the observed data in the range 50 to 300 K are best explained by assuming that Ti interstitials are associated in pairs in TiO_2. Resistivity studies on rutile under various pressures [124] indicate a large decrease in ρ up to ~6 kbar; at higher pressures (up to ~100 kbar), the resistance change was small suggesting that TiO_2 retains semiconductor behavior over a large pressure range with the possibility of exhibiting metallic conduction at very high pressures [124, 125]. Preliminary results of Kawai and Mochizuki [125a] actually indicate a highly conductive state in TiO_2 at pressures greater than 2 Mbar.

TiO_2 in the rutile modification forms solid solutions with other transition metal oxides with rutile related structures; thus, solid solutions with VO_2 [126–131], ZrO_2 [132, 133], NbO_2 [134–136], MoO_2 [134], TaO_2 [135], WO_2 [137, 138], IrO_2 [139] are known and the physical properties are well investigated. In most of the cases, undistorted rutile structures are formed and the properties of ZO_2 (Z = transition metal) are modified by the presence of TiO_2.

Oxide and description of the study	Data	Remarks and inferences	References
TiO_x ($x<0.70$)			
Ti_6O			
Crystal structure and phase transformation.	Hexagonal; space group, P31C; $a=5.14$ Å, $c=9.48$ Å. DTA shows a transition at ~710 K; $\Delta H=360$ cal/mol; $\Delta S=0.51$ e.u.	The transition appears to be an order-disorder type with respect to the interstitial positions of the oxygens; no superlattice reflections are noted in electron diffraction patterns of a sample quenched from 970 K.	[9]
Ti_3O			
Crystal structure.	Hexagonal; space group, P312; $a=5.1418$ Å, $c=14.308$ Å.	The structure consists essentially of a close-packed hexagonal arrangement of Ti atoms with every second layer of octahedral interstices normal to the c axis vacant; one third of the oxygen sites in the occupied layers are empty and these vacancies have an ordered arrangement in the direction of the c axis. Physical properties of Ti_3O are not known in detail at present; it appears to be stable up to ~1670 K.	[10].
Ti_2O			
Crystal structure.	Rhombohedral; space group, $P\bar{3}m1$; $a=2.959\pm0.003$ Å; $c=4.845\pm0.004$ Å. TEC (293–773 K): $\|\|^a$: 10.3×10^{-6}/°C; $\|\|^c$: 9.2×10^{-6}/°C.	The ordered structure, described as Ti_2O_{1-y} exhibits a homogeneity range which increases as the temperature is lowered.	[4, 11, 26]
$TiO_{0.65}$ (δ-oxide)	Hexagonal; space group, P6/mmm; $Z=3$; $a=4.9915$ Å; $c=2.8794$ Å. TEC: (293–773 K): $\|\|^a=10.0\times10^{-6}$/°C; $\|\|^c=9.0\times10^{-6}$/°C.	This is a deficient interstitial solution of oxygen in a metal atom lattice.	[26].
TiO_x ($0.70\leqslant x\leqslant1.25$)			
Crystal structure and physical properties.			[28]

Oxide and description of the study	Data	Remarks and inferences	References

High temperature quenched (cubic, Fm3m) phases:

Composition x	Density (g/cm³)	Lattice parameter, a (Å)	% Vacancies (Total)	Decrease in vacancies (after pressure treatment), %	T_{SC}* (K)	ρ (300 K) (10^4 Ω cm)	$-\alpha$ (μV/°C)
0.86	5.057	4.189	31.5	14	<1.3	2.8	4
0.91	5.025	4.186	29.9	12	<1.25	~3.0	5
1.00	5.000	4.184	28.0	17	1.35	2.8	8
1.18	4.907	4.173	24.7	11	1.7	3.4	11
1.24	4.870	4.170	23.3	22	2.0	3.6	12

* Pressure treated samples (at 50–60 kbar and 1370 to 2070 K).
No magnetic susceptibility was observed for any TiO_x samples down to the limit of the senstiivity of the magnetometer ($\chi_M \sim 150 \times 10^{-6}$ emu); Hall voltage observed was very small and no meaningful results could be obtained.

Vacancy filling in $TiO_{1.00}$ and physical properties. [29].

Conditions of study	Density (g/cm³)	Lattice parameter, a (Å)	% Vacancies (total)	Compressibility ($\times 10^{13}$ cm²/dyne)	TEC ($\times 10^6$ deg^{-1}) at 298 K	γ_G	T_{SC} (K)
1773 K, 1 bar; 2 days, quenched.	4.97±0.003	4.1796	28.8	5.5±0.08	6.73	1.18	0.7
1923 K, 77.4 kbar; sudden quench.	5.69±0.009	4.2062	0.0	4.2±0.008	6.30	—	2.3

The gradual increase in density and lattice parameter with decrease in vacancy concentration under various pressure and temperature treatments are studied in detail. An empirical equation correlating the lattice parameter, pressure and temperature is deduced from experimental data.

Oxide and description of the study	Data	Remarks and inferences	References
Compressibilities of TiO_x.	Experimental values are 1.6(4) and 2.8(7)$\times 10^{-13}$ cm^2/dyne for $x=0.82$ and 1.25 respectively.	These values compare well with those of other transition metal monoxides.	[34].
Seebeck coefficients of TiO_x ($0.3 \leqslant x \leqslant 1.2$).	Small and negative (-5 to -10 μV/°C) for all x in TiO_x·α increases with x and temperature.	These results are in agreement with those of Banus and Reed [28]. Qualitative description of the band structure is given; E_F changed appreciably with the composition x.	[140, 141].
Plasma resonance in TiO_x.	Reflectance data show the plasma edges in TiO_x in the range 3.6–4.0 eV and the actual value depends on x to some extent. The color of TiO_x is correlated with these plasma edges.	The studies indicate the metallic nature of TiO_x. A band of 2.5 eV in the reflectance spectrum is assigned to an interband transition.	[14, 142].
Band structure of TiO.	Tight binding and APW methods of theoretical calculation of the band structure of TiO indicate that the 3*d* bands are wide (~6 eV) and the electrical conduction can be assumed to take place in the wide band. Most of the transport properties are predicted in good agreement with experiment.	Calculations on TiO_x taking into account the vacancy concentration and composition do not seem to be satisfactory in explaining the observed data. As pointed out by Honig et al. (ref. [4], p. 130) cation-anion-cation overlaps also should be taken into account in computing the band structure in addition to the direct cation-cation overlap in order to get a reasonable picture of the band model in oxide materials. Results of Kawano [141] indicate that the Fermi level and density of states shift with the stoichiometry in TiO_x.	[143–145].
Low temperature ordered structures			
Phase, stability range and conditions of observation:			
$TiO_{0.7}$–$TiO_{0.9}$; thin foils (of TiO_x) heated above 870 K in the electron microscope or heating by an intense electron beam.	Orthorhombic; space group, I222; Z=6; $a'=a/\sqrt{2}$; $b'=3a/\sqrt{2}$; $c'=a$ (a is the lattice parameter of the original, high temperature, cubic cell of TiO_x).	This structure results from the ordering of the oxygen vacancies only since there are more oxygen vacancies than titanium vacancies in the oxygen deficient alloys; all oxygen vacancies are distributed on every third (110) plane in the original rock salt type lattice while the Ti vacancies are distributed randomly.	[17, 19, 31].

Oxide and description of the study	Data	Remarks and inferences	References
$TiO_{1.00}$ (composition range $TiO_{0.90}$–$TiO_{1.10}$); quenched from 1773 K and annealed for two days (1170–1220 K).	Monoclinic: space group. A2/m; Z = 12; a = 5.855 Å; b = 9.340 Å; c = 4.142 Å; β = 107.53°. Vacancy concentration, 16.7%. ρ (300 K) = 2×10^{-4} Ω cm; ρ (77 K) = 7×10^{-5} Ω cm. Positive temperature coefficient; Absolute value of ρ is much lower than that of the cubic phase.	The transition temperature is around 1190–1220 K; but the process is slow (and requires long periods of annealing) since this is a disorder-order transformation. This structure can be described in terms of vacancy ordering: i.e., in every third (110) plane of the original cubic cell, half of the titanium and half of the oxygen atoms are missing alternately. The spacing of this (110) plane is slightly larger than that of the other {110} planes, and as a result, the symmetry of the original cubic structure is lowered to monoclinic. Essentially the same structure has been observed in the composition range $TiO_{0.90}$–$TiO_{1.10}$ which implies that a small excess or deficiency of titanium and oxygen vacancies can be tolerated in $TiO_{1.00}$ structure.	[14, 17, 19, 20, 28, 31].
$TiO_{1.19}$			
Samples annealed for long periods below 973 K.	Both types of ordered structures, TiO and $TiO_{1.25}$, are noticed.	Electron diffraction patterns indicate that the ordered phases coexist as alternate thin layers of $TiO_{1.00}$ and $TiO_{1.25}$ parallel to $\{210\}_c$ planes.	[18, 31].
$TiO_{1.25}$			
Alloy annealed for 7 days at 973 K and then at 673 K.	Tetragonal; space group I4/m; Z = 10; $a = a_0\sqrt{10}/2$ = 6.594 Å; $c = a_0 \equiv$ 4.171 Å. (a_0 is the original cube cell edge). [Vacancy concentration, ~22%].	The type of ordered structure in $TiO_{1.25}$ is different from that in $TiO_{1.00}$; the oxygen sublattice is fcc and fully occupied while the titanium sites get ordered similar to Ni_4Mo and Au_4Mn type super structures.	[18, 31, 146, 147].
Transition structure (range $TiO_{0.7}$–$TiO_{1.25}$). Samples rapidly cooled from the melt and not well annealed at lower temperatures.	Both ordered TiO and $TiO_{1.25}$ structures coexist, the amount of the latter increasing with the oxygen content of the specimen. The transition structure observed occasionally in the $TiO_{1.25}$ specimen seem to be due to insufficient ordering treatment and it is considered that the transition structure would ultimately transform to the ordered $TiO_{1.25}$ structure.	The appearance of the transition structure is of importance for understanding the process of transformation from the disordered to the ordered form. When the disordered specimen of any composition is cooled to the equilibrium temperature, the vacancies concentrate firstly on every third atomic plane parallel to the (110) plane of the original	[31].

Oxide and description of the study	Data	Remarks and inferences	References
		rock salt structure, but are randomly distributed on these planes giving a diffraction pattern of the transition structure. On further annealing, the vacancies are distributed into the proper positions to make the ordered structure of $TiO_{1.25}$ type. Watanabe et al. [31] point out that the high temperature cubic and orthorhombic TiO_2 observed by Hilti [19] are the same as the 'transition structures.'	
Ti_2O_3			
Crystal structure and high temperature x-ray studies.	$T=300$ K: Hexagonal (corundum); space group, $R\bar{3}C$; $Z=6$; $a=5.1572\pm0.0002$ Å; $c=13.600\pm0.001$ Å. $T=540$ K: Hexagonal; space group, $R\bar{3}C$; $Z=6$; $a=5.122$ Å; $c=13.90$ Å. ΔV (on heating from 300 to 500 K) $= -7\%$.	There is no change in the crystal symmetry in the range 300–500 K but the thermal expansion parameters behave in an anomalous way; the a parameter decreases while c parameter increases. The unit cell volume decreases.	[30, 39, 40].
Magnetic properties.	χ_M (300 K)$\sim1.0\times10^{-4}$ cgs units and shows a two fold increase in the range 400—550 K. χ_M below 400 K is almost temperature independent. Magnetic moment <0.03 μ_B.	χ_M-T data and polarized neutron diffraction data do not indicate magnetic order in Ti_2O_3 below 400 K.	[12, 41–43, 47].
Thermal properties.	C_p (400 K)$\sim$0.2 cal/mol, deg. and shows a broad λ-type anomaly in the range 450–600 K. ΔH (calc.)$\sim$36 cal/mol [48]; 215 cal/mol [32]. DTA shows a broad endothermic peak (centered at $\sim$410 K).	These data show the second (or higher) order nature of the transition	[32, 48, 49].

Oxide and description of the study	Data	Remarks and inferences	References
Electrical properties of $TiO_{1.501}$.	<table><tr><th>Temperature (K)</th><th>ρ (Ω cm)</th><th>R_c (cm^3/C)</th><th>$\Delta\rho/\rho^a$</th><th>α (μV/K)</th></tr><tr><td>4.2 K</td><td>(1.3–1.8) $\times 10^4$</td><td>—[b]</td><td>3–4 ($\geq$200 kG)</td><td>—</td></tr><tr><td>77 K</td><td>0.2–0.8</td><td>0.4–1.5</td><td>$<10^{-3}$</td><td>—</td></tr><tr><td>273 K</td><td>$\sim 10^{-2}$</td><td>0.08–0.11</td><td>$<10^{-3}$</td><td>56</td></tr><tr><td>600 K</td><td>$\sim 3\times 10^{-4}$</td><td>—</td><td>—</td><td>45[c]</td></tr></table> (a) Magnetoresistance; $\Delta\rho/\rho_0 \propto H^2$. (b) Not measurable. (c) At 400 K. E_a (<20 K)$\sim$0.001–0.003 eV; E_a (100–300 K)$\sim$0.027–0.050 eV. T=4.2 K: μ_H (calc.)$\sim$720–840 cm^2/Vs; $n_c\sim 10^{10}$, cm^{-3}.	This is a careful study on well characterized pure single crystals. Various ranges of ρ and R_c values are encountered because of variable sample purity; common impurities like C, N affect the properties. The study by Honig and Reed [52] emphasizes the need for painstaking efforts in the preparation and characterization of oxide materials. Slight anisotropy in ρ has been noted. Impurity conduction seems to be predominant below 20 K; in the range 100–300 K, intrinsic behavior is noted. Hall mobilities are the highest encountered hitherto in pure oxide materials; at higher temperatures, μ_H seems to decrease. Magnetoresistance data indicate that a multiband conduction exists in Ti_2O_3. The band model proposed (fig. I.2) can explain the observed data without invoking a magnetic ordering in Ti_2O_3 at low temperatures.	[52, 53].
UHF Dielectric constant studies.	UHF ($\sim$10 GHz): ϵ (T=77 K)=30; ρ (UHF)>ρ (DC).	The imaginary part of the dielectric constant shows a maximum at 225 K, but this is not connected with any transition in Ti_2O_3.	[148].
Raman spectroscopy	Raman spectrum of Ti_2O_3 exhibits seven modes as predicted for the corundum structure. All the modes persist above the semiconductor-metal transition temperature indicating absence of space group change. The A_{1g} mode at 269 cm^{-1} (300 K) shows a 16% change in frequency and increase in intensity at the transition.	The Raman results can be interpreted in terms of the electronic and structural changes during the transition.	[149].
Ti_3O_5			
Crystal structure and x-ray studies.	T=300 K: Monoclinic; space group, C2/m; Z=4; a=9.80 Å; b=3.79 Å; c=9.45 Å; β=91.75°. T>460 K: Monoclinic; a=9.90 Å; b=3.78 Å; c=10.02 Å; β=90.75°. The c parameter and the unit cell volume show jump at T_t (448 K) on heating.	There is not much change in crystal symmetry at T_t but the unit cell volume increases. The transition is of first order.	[49].
Magnetic properties.	χ_M (300 K)$\sim 10^{-6}$ cgs units; χ_M (600 K)$\sim 2\times 10^{-4}$ cgs units. χ_M is temperature inde-	Mulay and Danley [71] proposed a new model to explain the mag-	[43, 49, 71].

Titanium oxides—Continued

Oxide and description of the study	Data	Remarks and inferences	References
	pendent both above and below T_t; large jump at T_t is noted with hysteresis; T_t (heating) $\approx$462 K; T_t (cooling) $\approx$432 K. χ_M-T data and Mössbauer studies do not indicate long range magnetic ordering in the low temperature phase. Rao et al. [49] have pointed out that the Mössbauer data on Fe-doped Ti_3O_5 should be interpreted with caution since Fe is known to stabilize the high temperature phase of Ti_3O_5. Neutron diffraction studies are urgently needed on Ti_3O_5 to establish the presence or absence of magnetic order in this material.	netic behavior of Ti_3O_5 and the Magnéli phases. According to this, below T_t, groups of cations are distributed periodically throughout the lattice; within these groups, the d electrons are localized. However, 'constrained type' antiferromagnetism sets in between specific neighboring d electrons through homopolar bonding of cations. Neighboring groups interact via thermal excitation of electrons. Above the transition, this type of ordering is modified by crystal structure changes and 3d orbital overlap is large enough to bring about a nearly complete delocalization of electrons over the entire lattice and the behavior is described by the 'free electron gas' model. This approach is a slightly modified form of the one proposed by Goodenough [74].	
Thermal properties.	Heat content data on Ti_3O_5 exhibit an anomaly at $\sim$450 K. DTA shows a sharp endothermic peak at 450 K; the peak is shown in the cooling curve at $\sim$415 K; $\Delta H = 1.6 \pm 0.4$ kcal/mol.	The first order nature of the transition is established. Fe doping reduces T_t and at higher concentrations (5%) suppresses the transition; the transition at lower concentrations does not seem to be strictly first order.	[32, 49, 75].
Electrical properties.	ρ (340 K) $\approx$20 Ω cm; ρ (500 K) $\approx$0.6 Ω cm. Semiconductor behavior below 450 K; $E_a = 0.29$ eV. Large drop in ρ at T_t (Bartholomew and Frankl [75] report a continuous change in ρ through T_t). Metallic behavior above T_t; m^* (calc., high temperature form) $\approx$20 m; α (340 K) ~ -60 μV/°C [76].	The first order semiconductor-to-metal transition is confirmed in Ti_3O_5; Rao et al. [49] stress the the importance of the purity of the material in determining the resistivity discontinuity at T_t.	[49, 71, 75, 76].
ESR Studies.	Multiplet structure is noted in the ESR spectra at 77 K. Well defined spectra are not obtained at higher temperatures and in doped samples (at 77 K).	The multiplet structure appears to be due to inequivalent cation sites in the structure of Ti_3O_5.	[49, 73].

Magnéli phases, Ti_nO_{n-1}

n: phase	Crystal structure, χ-T and DTA studies	Electrical properties	References
	(T=298 K: All phases are triclinic; space group, $P\bar{1}$; Z=2)		
4; Ti_4O_7	a=5.600Å; b=7.134 Å; c=12. 468 Å; α=95.05°; β=95.20°; γ=108.70°; (calc. density, 4.32 g/cm³). T_t=125 and 149±2 K. Discontinuities in the lattice parameters are noted at the 149 K transition; the volume change is <0.001 and the extra reflections observed below 149 K suggest a doubling of the unit cell. The 125 K transition is associated with ~8–10 K hysteresis and some structural changes seem to take place at this temperature. DTA (heating curve) indicates both the transitions but the cooling curve indicates only the 149 K transition. ΔH values not known. χ-T data do not indicate the low temperature transition. Probably long range magnetic order is absent.	Ti_4O_7 is metallic at 300 K and ρ increases by a factor of 10^3 at 149 K on cooling and semiconductor behavior in the range 130–149 K (E_a~0.04 eV). At ~125 K, ρ shows an increase by about three orders of magnitude. No Seebeck coefficient data available. At 300 K, $m^*\approx 13m$ and Hall data give a mobility of ~1 cm²/V s, increasing to 4 at ~160 K; below 149 K, no Hall voltage could be measured and hence μ_H<0.01 cm²/V s. Least square refinement of the structure has shown that the sharing of octahedral faces, edges and corners between rutile layers is similar to that in corundum structures. Average Ti-O and O-O distances are 2.012 and 2.826 Å respectively. Average Ti-Ti distances in a rutile layer are 2.972 and 3.576 Å across a shared octahedral edge and corner respectively.	[43, 71, 72, 75, 79, 84, 86, 87].
5; Ti_5O_9	a=5.569 Å; b=7.120 Å; c=8.865 Å; α=97.55°; β=112.34°; γ=108.50°. T_t=130 and 136 K. DTA and χ-T studies show anomalies at these phase transitions; no ΔH values are known. Probably long range magnetic order is absent.	Discontinuities in ρ are noted at T_t; however, the sample appears to be semiconducting above 136 K. E_a (<130 K)~0.04 eV; m^* (>136 K)$\approx 11m$.	[43, 71, 72, 75, 78, 79, 84].
6; Ti_6O_{11}	a=5.56 Å; b=7.14 Å; c=24.04 Å; α=98.5°; β=120.8°; γ=108.5°. T_t=122 K. DTA and χ-T studies show this transition; no ΔH is known. Probably long range magnetic order is absent.	ρ drops by a factor of 10 at 130 K and the sample is semiconducting both below and above T_t. E_a (<130 K)~0.08 eV; m^* (>130 K)≈ 16 m. The T_t noted here is less than that obtained (122 K) from DTA and χ-T data.	[43, 71, 72, 75, 79, 84].
7; Ti_7O_{13}	a=5.54 Å; b=7.13 Å; c=15.36 Å; α=98.9°; β=125.5°; γ=108.5°. No χ-T, DTA data are available.	No data are available	[79, 84].
8; Ti_8O_{15}	a=5.57 Å; b=7.10 Å; c=37.46 Å; α=97.2°; β=128.8°; γ=109.6°. DTA studies do not indicate a transition in the temperature range 78–295 K. χ-T data not available.	Semiconductor behavior in the temperature range 78–295 K; no indication of transformation. E_a~0.09 eV.	[75, 79, 84].
9; Ti_9O_{17}	a=5.57 Å; b=7.10 Å; c=22.15 Å; α=97.1°; β=131.0°; γ=109.8°. No χ-T, DTA data are available.	No data are available	[79, 84].

Oxide and description of the study	Data	Remarks and inferences	References
TiO_2 (*anatase*)			
Crystal structure and x-ray studies.	$T=298$ K: Tetragonal; space group, I4/amd; $Z=4$; $a=3.7845\pm0.0001$ Å; $c=9.5143\pm0.0004$ Å. TEC (300–985 K) (/°C): $\|^c$: $7.380\times10^{-6}+6.620\times10^{-9}\,t+1.771\times10^{-11}\,t^2$; $\perp^c$: $3.533\times10^{-6}+5.610\times10^{-9}\,t+4.315\times10^{-12}\,t^2$, where t is the temperature in °C.	Careful work up to the transition point; the variation in the relative magnitudes of the values of TEC are explained in terms of the inter-ionic distances. Earlier literature survey presented.	[150].
Kinetics of transformation of anatase → rutile and thermal properties.	The rate of transformation of pure anatase is exponential (fig. I.3); energy of activation is ~90 kcal/mol. The transition is immeasurably slow below 880 K and extremely rapid above 1000 K and is accompanied by ~8% decrease in the unit cell volume. ΔH is ~ −2.8 kcal/mol (exothermic). Impurities usually stabilize the the anatase modification; T_t as well as the energy of activation are greater in these doped materials compared to pure rutile. Smaller particle size and larger surface area seem to favor the transition.	The irreversible transformation of anatase to rutile is reconstructive and involves changes in the secondary coordination. The particle size, the crystallite size and the volume of the unit cell seem to increase prior to the transformation. The impurities seem to act by way of creating anion vacancies or cation interstitials in stabilizing the anatase phase.	[92–98, 100, 102–104].
Effect of pressure on the transition and resistivity studies.	Discontinuous changes in the resistance of the anatase samples noted at T_t. In the range 3.8–24 kbar pressure, T_t decreases with the application of pressure; $(dT_t/dP) = -0.02°$ bar^{-1}. ρ (300 K, prepressed specimens, anatase) $\sim10^{12}$ Ω cm; ρ (300 K, pressed at 3.8–24) kbar $\sim10^{7}$ Ω cm.	Detailed work on the effect of pressure on the transition. ΔH for the transition also decreases with pressure; the oxygen deficiency seems to be responsible for the acceleration of the rate of transition at higher temperatures. The results are in accord with the volume change associated with the anatase-rutile transition.	[111].
Magnetic properties of anatase.	$\chi=0.02\times10^{-6}$ emu/g (essentially independent of temperature)	Not a very accurate value [122a] because of the presence of impurities; the observed variation of χ with T is expalined on the basis of the presence of Ti^{+3} ions in the anatase samples.	
TiO_2 (*brookite*)			
Crystal structure	$T=298$ K Orthorhombic; space group, P_{cab}; $Z=8$; $a=9.25\pm0.03$ Å; $b=5.46\pm0.02$ Å; $c=5.16\pm0.01$ Å.	Data on the naturally occurring pure brookite sample; contains references to the earlier data.	[151].
Kinetics of brookite rutile transition and thermal properties.	The transition is irreversible and time and temperature dependent (fig. I.3); below 990 K, the transition is extremely slow. Above 990 K, first order rate law is obeyed. Energy and entropy of activation	The enthalpy of transition is small compared to the anatase-rutile transition. This indicates that the polymorphic transformation may not be of the reconstructive	[115].

Oxide and description of the study	Data	Remarks and inferences	References
	are ~60 kcal/mol and ~ −18 cal/mol (at 1070 K) respectively. DTA shows an exothermic peak at 1020 K; $\Delta H \sim -(100 \pm 75)$ cal/mol.	type but only a modified order-disorder type as applied to diffusionless transitions in solids.	
TiO_2 (*high pressure*)			
Crystal structure and transformation to rutile.	Orthorhombic; space group, Pban; $Z=4$; $a=4.529$ Å; $b=5.464$ Å; $c=4.905$ Å. This phase is formed from rutile at ~330 kbar pressure at ordinary temperatures; it reverts to rutile on heating at 720–870 K. A lower bound of 60 kbar is necessary to stabilize the higher pressure form with respect to rutile at room temperature.	The high pressure phase reported by two groups of workers prepared under different experimental conditions appears to be identical. As expected, the high pressure phase is denser than rutile and can be retained without changes under normal conditions of temperature and pressure after quenching for indefinite periods of time. Anatase is metastable with respect to the rutile and the high pressure forms. Reaction boundaries for these phases have been reported.	[90, 91].
TiO_2 (*rutile*)			
Crystal structure and x-ray studies.	$T=298$ K; Tetragonal, space group, $P4_2/mnm$; $Z=2$; $a=4.5941\pm0.0001$ Å; $c=2.9589\pm0.0001$ Å. TEC (303°–923 K) (/°C): $\|\|^c$: $8.816\times10^{-6}+3.653\times10^{-9}\,t+6.329\times10^{-12}\,t^2$; $\perp^c$: $7.249\times10^{-6}+2.198\times10^{-9}\,t+1.298\times10^{-12}\,t^2$, where t is the temperature in °C. High pressure x-ray studies indicate volume change, (V/V_0) of 0.91 at 102 kbar [152] and 0.94 at 158 kbar pressure [91].	Careful work up to the high temperatures. Slight anisotropy in the TEC parameters is obvious and is explained in terms of the interatomic distances in the unit cell of rutile.	[150, 152].
Magnetic, optical and dielectric properties.	$\chi=(0.067\pm0.0015)\times10^{-6}$ emu/g for high purity single crystal rutile and temperature independent in the range 55–372 K; negligible anisotropy. Stoichiometric rutile shows continuous absorption in the IR region [122b] but reduced samples exhibit free career absorption and characteristic bands (at 0.75 or 1.18 eV) depending on the sample resistivity or degree of reduction. Optical energy gap = 3.05 eV. ϵ_0 has a high value and exhibits anisotropy; at 300 K, ϵ_0 $(\|^c)=170$; $\epsilon_0(\|^a)=86$; $n(\|^c)$ 2.903; $n(\|^a)=2.616$. At low temperatures, ϵ_0 approaches limiting values; at $T\to0$ K, $\epsilon_0(\|^c)=257$; $\epsilon_0(\|^a)=111$. Parker's data [153] in the range 1.6–1060 K indicate that rutile is not a ferroelectric or antiferroelectric; however, the ionic polarizability of Ti is close	The temperature independent χ is due to diamagnetic and Van Vleck contributions. The free carrier absorption is due to the electrons released by the oxygen upon reduction; the bands in the reduced samples are believed to be due to polaron absorption. The environment of Ti sites in rutile, the anisotropy and high numerical values of ϵ_0 make an interesting comparison with $BaTiO_3$.	[43, 119–121, 122b, 123a, 153].

Oxide and description of the study	Data	Remarks and inferences	References
	to the critical value for a ferroelectric polarization catastrophe at all temperatures.		
Electrical properties and high pressure studies.	ρ (300 K) $\sim 10^9$ Ωcm for stoichiometric rutile; $E_g \sim 3.1$–3.4 eV; impurity conduction is always predominant at low temperatures; donor levels of 0.03–0.15 eV are encountered. Reduced specimens have low resistivity ($\sim 10^{-2}$ to 10^4 Ωcm), are n-type and exhibit anisotropy in R_H, μ_H and ρ. Anisotropy ratios, (ρ_a/ρ_c) and $(R_a/R_c)_H$ vary from 2.0 to 3.5 and 0.2 to 2.5 respectively and exhibit interesting temperature dependence. $\mu_H \approx 0.1$ cm^2/V s. at 500 K; α (100 K) = -1.0 mV/K. $m^* = 20\ m_0$. α shows large phonon drag effect at T below 20 K. In the range 882–1273 K, $\rho \propto p_{O_2}^{-1/n}$, n 4.4 to 5.7; $n = 4$ above 1470 K according to Greener et al. [123]; both anion vacancies and cation interstitials appear to play significant role. E_a ($T > 1000$ K) = 1.8 eV. High pressure studies indicate a large decrease in ρ up to 6 kbar ($d\rho/dP = -0.2 \times 10^4$ Ωbar^{-1}); in the range 6–100 kbar, change in ρ is small ($d\rho/dP = 0.08$ Ωbar^{-1}). Data of Kawai and Mochizuki [125a] indicate that at pressures >2Mbar ρ of TiO_2 drops by a factor of 10^6 and exhibits metallic behavior at room temperature.	Multiple band conduction is indicated by the ρ, R_H and α data but many workers feel that polaron type conduction is predominant at low temperatures. The defect structure of TiO_2 is not yet completely understood. Kawai and Mochizuki [125a] experiments at high pressures on the ρ behavior of TiO_2 are significant; x-ray data at these high pressures are highly desirable and will indicate whether the resistivity behavior actually corresponds to the insulator-metal (Mott) transition or not.	[116–125a, 154].
Thermal and mechanical properties.	$C_p = 1$ millijoule/K, mol at 4.2 K; $C_p \propto T^3$ below 4 K with $\theta_D = 758$ K. Reduced TiO_2 has large additional contribution and independent of T below 13 K and is attributed to electrons which do not become degenerate above 1 K. κ (200 K) = 0.1 W/cm, K and exhibits anisotropy above 25 K; goes through a maximum at $\sim$15 K indicating phonon-phonon scattering in TiO_2. Internal friction (Q^{-1}) goes through a maximum at 323° in pure rutile with $Q^{-1}(\|^a) = 1 \times 10^{-4}$ at 1842 Hz and activation energy of 14 ± 0.4 kcal/mol. Reduced rutile exhibits a pronounced maximum ($Q^{-1}(\|^a) = 12 \times 10^{-4}$ at 394 K and 1838 Hz with activation energy = 23.5 ± 1.0 kcal/mol) only along [100] direction and not along [110] and [001] direction. The results are discussed in terms of simple and associated defects in pure and reduced rutile.	It is evident that the degree and type of reduction brings about marked changes in these properties in rutile.	[118, 123c, 155].

Oxide and description of the study	Data	Remarks and inferences	References
Band structure of rutile	Calculations using tight binding method indicate relatively wide valence and conduction bands (~4 eV). The available transport data can be interpreted assuming multiband conduction in TiO_2 even at low temperatures (~100 K).	Since there are no magnetic order complications in TiO_2 it is worth while to compute the detailed band structure of TiO_2 using various methods including spin-orbit coupling effects.	[156].

References

[1] DeVries, R. C., and Roy, R., Bull. Am. Ceram. Soc. 33, 370 (1954).
[2] Schofield, T. H., and Bacon, A. E., J. Inst. Metals 84, 47 (1955–56).
[3] Andersson, S., Collen, B., Kuylenstierna, U., and Magnéli, A., Acta Chem. Scand. 11, 1641 (1957).
[4] Andersson, S., Collen, B., Kruuse, G., Kuylenstierna, U., Magnéli, A., Pestmalis, H., and Asbrink, S., Acta Chem. Scand. 11, 1653 (1957).
[5] Porter, V., and Roy, R., Bull. Am. Ceram. Soc. 43, 263 (1964); Porter, V., Ph.D. Dissertation, The Pennsylvania State Univ. (1965); McCarthy, G. J., White, W. B., and Roy, R., J. Inorg. Nucl. Chem. 31, 329 (1969).
[6] Wahlbeck, P. G., and Gilles, P. W., J. Am. Ceram. Soc. 49, 180 (1966).
[7] Kornilov, I. I., and Glazova, V. V., Dokl. Akad. Nauk SSSR 150, 313 (1963); 154, 638 (1964).
[8] Kornilov, I. I., Dokl. Akad. Nauk SSSR 183, 1087 (1968).
[9] Yamaguchi, S., Koiwa, M., and Hirabayashi, M., J. Phys. Soc. Japan 21, 2096 (1966).
[10] Jostsons, A., and Malin, A. S., Acta Cryst. 24B, 211 (1968).
[11] Holmberg, B., Acta Chem. Scand. 16, 1245 (1962).
[12] Pearson, A. D., J. Phys. Chem. Solids 5, 316 (1958).
[13] Bright, N. F. H., Adv. in X-ray Analysis 4, 175 (1961) (Univ. of Denver Press).
[14] Denker, S. P., J. Phys. Chem. Solids 25, 1397 (1964); J. Appl. Phys. 37, 142 (1966).
[15] Hulm, J. K., Jones, C. K., Mozelsky, R., Miller, R. C., Hein, R. A., and Gibson, J. W., Proc. 9th Intern. Conf. on Low Temp. Phys., (eds., J. G. Dount et al.), Plenum Press, New York, 1965, p. 600.
[16] Takeuchi, S., and Suzuki, K., Nippon Kinzoku Gakkaishi 31, 611 (1967); Chem. Abstr. 67, 120746c (1967).
[17] Watanabe, D., Castles, J. R., Jostsons, A., and Malin, A. S., Nature (Lond.) 210, 934 (1966); Acta Cryst. 23, 307 (1967).
[18] Watanabe, D., Terasaki, O., Jostsons, A., and Castles, J. R., J. Phys. Soc. Japan 25, 292 (1968).
[19] Hilti, E., Naturwiss. 55, 130 (1968).
[20] Hilti, E., and Laves, F., Naturwiss. 55, 131 (1968).
[21] Hirabayashi, M., Koiwa, M., and Yamaguchi, S., quoted by B. G. Hyde in 'The Chemistry of Extended Defects in non-Metallic Solids', Eds. L. Eyring and M. O'Keeffe (North-Holland Publ. Co., Amsterdam, 1970), p 90.
[22] Bursill, L. A., Hyde, B. G., Terasaki, O., and Watanabe, D., Phil. Mag. 20, 347 (1969).
[23] Hyde, B. G., and Bursill, L. A., in The Chemistry of Extended Defects in non-Metallic Solids, Eds. L. Eyring and M. O'Keeffe (North-Holland Publ. Co., Amsterdam, 1970), pp 347–378.
[24] Wasilewski, R. J., Trans. AIME 224, 8 (1962).
[25] Hurlen, T., J. Inst. Metals 89, 128 (1960–61).
[26] Andersson, S., Acta Chem. Scand. 13, 415 (1959); Arkiv för Kemi 15, 247 (1960).
[27] Ehrlich, P., Z. Elektrochem., 45, 362 (1939); Z. anorg. allgem. Chem. 247, 53 (1941).
[28] Banus, M. D., and Reed, T. B., in The Chemistry of Extended Defects in non-Metallic Solids, Eds. L. Eyring and M. O'Keeffe (North-Holland Publ. Co., Amsterdam, 1970), pp 488–522; Phys. Rev. B5, 2775 (1972).
[29] Taylor, A., and Doyle, N. J., in The Chemistry of Extended Defects in non-Metallic Solids, Eds. L. Eyring and M. O'Keeffe (North-Holland Publ. Co., Amsterdam, 1970), pp 523–540.
[30] Loehman, R. E., Rao, C. N. R., and Honig, J. M., J. Phys. Chem. 73, 1781 (1969).
[31] Watanabe, D., Terasaki, O., Jostsons, A., and Castles, J. R., in The Chemistry of Extended Defects in non-Metallic Solids, Eds. L. Eyring and M. O'Keeffe (North-Holland Publ. Co., Amsterdam, 1970), pp 238–258.
[32] Naylor, B. F., J. Am. Chem. Soc. 68, 1077 (1946).
[33] Morin, F. J., Phys. Rev. Letters 3, 34 (1959).
[34] Doyle, N. J., Hulm, J. K., Jones, C. K., Miller, R. C., and Taylor, A., Phys. Letters 26A, 604 (1968).
[35] Banus, M. D., Mat. Res. Bull. 3, 723 (1968).
[36] Iwasaki, H., Asaumi, K., Kamigaki, K., Ogawa, S., Terasaki, O., and Watanabe, D., J. Phys. Soc. Japan 30, 180 (1971).
[37] Gel'd, P. V., Shveikin, G. P., Alyamovskii, S. I., and Tskhai, V. A., Russ. J. Inorg. Chem. 12, 1053 (1967).
[38] Abrahams, S. C., Phys. Rev. 130, 2230 (1963).
[39] Prewitt, C. T., Shannon, R. D., Rogers, D. B., and Sleight, A. W., Inorg. Chem. 8, 1985 (1969).
[40] Rao, C. N. R., Loehman, R. E., and Honig, J. M., Phys. Letters 27A, 271 (1968).
[41] Foëx, M., and Wucher, J., Compt. Rend. (Paris) 241, 184 (1955).
[42] Carr, P. H., and Foner, S., J. Appl. Phys. 31, 344S (1960).
[43] Keys, L. K., and Mulay, L. N., Appl. Phys. Letters 9, 248 (1966); Phys. Rev. 154, 453 (1967).
[44] Shirane, G., Pickart, S. J., and Newnham, R., J. Phys. Chem. Solids 13, 167 (1960).
[45] Keys, L. K., Phys. Stat. Solidi 25, K5 (1968).
[46] Kendrick, H., Arrott, A., and Werner, S. A., J. Appl. Phys. 39, 585 (1968).
[47] Moon, R. M., Riste, T., Kochler, W. C., and Abrahams, S. C., J. Appl. Phys. 40, 1445 (1969).
[48] Nomura, S., J. Phys. Soc. Japan 16, 706 (1961).
[49] Rao, C. N. R., Ramdas, S., Loehman, R. E., and Honig, J. M., J. Solid State Chem. 3, 83 (1971).
[50] Foëx, M., and Loriers, J., Compt. Rend. (Paris) 226, 901 (1948).
[51] Yahia, J., and Frederikse, H. P. R., Phys. Rev. 123, 1257 (1961).
[52] Honig, J. M., and Reed, T. B., Phys. Rev. 174, 1020 (1968).

[53] Loehman, R. E., Ph.D. Thesis, Purdue Univ. (U.S.A.) 1969.
[54] Goodenough, J. B., Magnetism and the Chemical Bond (Interscience Publ. Inc., New York, 1963).
[55] Goodenough, J. B., Bull. Soc. Chim. France 4, 1200 (1965).
[56] Adler, D., Feinleib, J., Brooks, H., and Paul, W., Phys. Rev. 155, 851 (1967).
[57] Adler, D., Solid State Phys. 21, 1 (1968); Rev. Mod. Phys. 40, 714 (1968).
[58] Honig, J. M., Rev. Mod. Phys. 40, 748 (1968); IBM J. Res. & Develop. 14, 232 (1970).
[59] Mott, N. F., Phil. Mag. 20, 1 (1969).
[60] Doniac, S., Adv. Phys. 18, 819 (1969).
[61] Rao, C. N. R., and Subba Rao, G. V., Phys. Stat. Solidi (a) 1, 597 (1970).
[62] Rao, C. N. R., editor, Modern Aspects of Solid State Chemistry (Plenum Press, New York, 1970).
[63] Bosman, A. J., and van Daal, H. J., Adv. Phys. 19, 1 (1970).
[64] Hyland, G. J., J. Solid State Chem. 2, 318 (1970).
[65] Van Zandt, L. L., Honig, J. M., and Goodenough, J. B., J. Appl. Phys. 39, 594 (1968).
[66] Goodenough, J. B., in Proc. of 10th Intern. Conf. on Phys. of Semiconductors, Cambridge, Mass., 1970; Solid State Commun. 8 (23) pp i–xxvii (1970).
[67] Reed, T. B., Fahey, R. E., and Honig, J. M., Mat. Res. Bull. 2, 561 (1967).
[68] Kawakubo, T., Yamayi, T., and Namouri, S., J. Phys. Soc. Japan 15, 2102 (1960).
[69] Chandrashekhar, G. V., Won Choi, Q., Moyo, J., and Honig, J. M., Mat. Res. Bull. 5, 999 (1970).
[70] Asbrink, S., and Magnéli, A., Acta Cryst. 12, 575 (1959).
[71] Mulay, L. N., and Danley, W. J., J. Appl. Phys. 41, 877 (1970).
[72] Vasil'ev, Ya. V., and Ariya, S. M., Izv. Akad. Nauk. SSSR, Neorg. Mater. 1, 347 (1965).
[73] Keys, L. K., Phys. Letters 24A, 628 (1967).
[74] Goodenough, J. B., Mat. Res. Bull. 2, 37 (1967); 2, 165 (1967).
[75] Bartholomew, R. F., and Frankl, D. R., Phys. Rev. 187, 828 (1969).
[76] Rao, C. N. R., and co-workers (unpublished results, 1970).
[77] Iwasaki, H., Bright, N. F. H., and Rowland, J. F., J. Less-Comm. Metals 17, 99 (1969).
[78] Andersson, S., Acta Chem. Scand. 14, 1161 (1960).
[79] Magnéli, A., in Transition Metal Compounds, Ed. E. R. Schatz, (Gordon and Breach, Science Publishers, New York, 1964), pp 109–122.
[80] Andersson, S., and Jahnberg, L., Arkiv för Kemi 21, 413 (1963).
[81] Anderson, J. S., and Hyde, B. G., Bull. Soc. Chim. France 4, 1215 (1965); J. Phys. Chem. Solids 28, 1393 (1967).
[82] Magnéli, A., in The Chemistry of Extended Defects in non-Metallic Solids, Eds. L. Eyring and M. O'Keeffe (North-Holland Publ. Co., Amsterdam, 1970), pp 148–163 and references therein.
[83] Anderson, J. S., and Khan, A. S., J. Less-Comm. Metals 22, 219 (1970).
[84] Terasaki, O., and Watanabe, D., Japan J. Appl. Phys. 10, 292 (1971).
[85] Goodenough, J. B., Czech. J. Phys. 17B, 304 (1967).
[86] Marezio, M., Dernier, P. D., McWhan, D. B., and Remeika, J. P., Mat. Res. Bull. 5, 1015 (1970); See also, Marezio, M., and Dernier, P. D., J. Solid State Chem. 3, 340 (1971).
[87] Nagasawa, K., Kato, Y., Bando, Y., and Takada, T., J. Phys. Soc. Japan 29, 241 (1970).
[88] Straumanis, M. E., Eijma, T., and James, W. J., Acta Cryst. 14, 493 (1961).
[89] Dachille, F., and Roy, R., Bull. Amer. Ceram. Soc. 41, 225 (1962).
[90] Bendeliani, N. A., Popova, S. P., and Vereschagin, L. F., Geokhimiya 5, 499 (1966); Chem. Abstr. 65, 3296f (1966).
[91] McQueen, R. G., Jamieson, J. C., and Marsh, S. P., Science 155, 1401 (1967); see also, Jamieson, J. C., and Glinger, B., Am. Mineral. 54, 1478 (1969) and Science 161, 893 (1968).
[92] Czanderna, A. W., Rao, C. N. R., and Honig, J. M., Trans. Faraday Soc. 54, 1069 (1958).
[93] Rao, C. N. R., Canad. J. Chem. 39, 498 (1961).
[94] Yoganarasimhan, S. R., and Rao, C. N. R., Trans. Faraday Soc. 58, 1579 (1962).
[95] Rao, C. N. R., and Lewis, M. P., Curr. Sci. (India) 29, 52 (1960).
[96] Rao, C. N. R., Turner, A., and Honig, J. M., J. Phys. Chem. Solids 11, 173 (1959).
[97] Sullivan, W. F., and Cole, S. S., J. Am. Ceram. Soc. 42, 127 (1959).
[98] Iida, Y., and Ozaki, S., J. Am. Ceram. Soc. 44, 120 (1961).
[99] Suzuki, A. S., and Kotera, Y., Bull. Chem. Soc. Japan 35, 1353 (1962).
[100] Shannon, R. D., and Pask, J. A., J. Am. Ceram. Soc. 48, 391 (1965).
[101] Czanderna, A. W., Clifford, A. F., and Honig, J. M., J. Am. Chem. Soc. 79, 5407 (1957).
[102] Knoll, H., and Kühnhold, U., Naturwiss. 44, 394 (1957).
[103] Sullivan, W. F., and Coleman, J. R., J. Inorg. Nucl. Chem. 24, 645 (1962).
[104] Shannon, R. D., J. Appl. Phys. 35, 3414 (1964).
[105] Chester, P. F., J. Appl. Phys. 32, 2233 (1961).
[106] Carnahan, R. D., and Brittain, J. O., J. Appl. Phys. 34, 3095 (1963).
[107] Tannhauser, D. S., Solid State Commun. 1, 223 (1963).
[108] Blumenthal, R. N., Baukus, J., and Hirthe, W. M., J. Electrochem. Soc. 114, 172 (1967).
[109] Buerger, M. J., in Phase Transformations in Solids, Ed. Smoluchowski (John Wiley, New York, 1957).
[110] Rao, C. N. R., and Rao, K. J., Progr. Solid State Chem. 4, 131 (1967).
[111] Vahldieck, F. W., J. Less-Comm. Metals 11, 99 (1966).
[112] Kubo, T., Kato, M., Mitarai, Y., Takahashi, J., and Ohkura, K., Kogyo Kagaku Zasshi 66, 318 (1963); Chem. Abstr. 59, 10824f (1963).
[113] Tekiz, Y., and Legrand, C., Compt. Rend. (Paris) 261, 3619 (1965).
[114] Schossberger, F., Z. Krist. 104, 358 (1942).
[115] Rao, C. N. R., Yoganarasimhan, S. R., and Faeth, P. A., Trans. Faraday Soc. 57, 504 (1961).
[116] Frederikse, H. P. R., J. Appl. Phys. 32 2211 (1961).
[117] Becker, J. H., and Hosler, W. R., Phys. Rev. 137A, 1872 (1965).
[118] Thurber, W. R., and Mante, A. J. H., Phys. Rev. 139A, 1655 (1965).
[119] Bogomolov, V. N., and Zhuze, V. P., Sov. Phys.—Solid State (English Transl.) 8, 1904 (1967).
[120] Bogomolov, V. N., Kudinov, E. K., and Firsov, Yu. A., Sov. Phys.—Solid State (English Transl.) 9, 2502 (1968).
[121] Grant, F. A., Rev. Mod. Phys. 31, 646 (1959).
[122] Austin, I. G., and Mott, N. F., Adv. Phys. 18, 41 (1969).
[122a] Senftle, F. E., Pankey, T., and Grant, F. A., Phys. Rev. 120, 820 (1960).
[122b] Breckenridge, R. G., and Hosler, W. R., Phys. Rev. 91, 793 (1953).
[122c] Acket, G. A., and Volger, J., Physica 29, 225 (1963); Phys. Letters 8, 244 (1964).
[122d] Bogomolov, V. N., and Shavkunov, P. M., Sov. Phys.—Solid State (English Transl.) 5, 1481 (1963).
[123] Greener, E. H., Barone, F. J., and Hirthe, W. M., J. Am. Ceram. Soc. 48, 623 (1965).
[123a] Hauffe, K., Reaktionen in und an festen stoffen. (Springer Verlag, Berlin, 1955), pp 135–140.
[123b] Rudolph, J., Z. Naturforsch. 14a, 727 (1959).
[123c] Wachtman, J. B., Jr. and Doyle, L. R., Phys. Rev. 135, A276 (1964).
[124] Vahldiek, F. H., J. Less-Comm. Metals 14, 133 (1968).
[125] Minomura, S., and Drickamer, H. G., J. Appl. Phys. 34, 3043 (1963).
[126] Marinder, B.-O., and Magnéli, A., Acta Chem. Scand. 11, 1635 (1957).
[127] Rüdorff, W., Walter, G., and Stadler, J., Z. anorg. allgem. Chem. 297, 1 (1958).

[128] Ariya, S. M., and Grossman, G., Sov. Phys.—Solid State (English Transl.) 2, 1166 (1960).
[129] Sakata, K., and Sakata, T., Japan J. Appl. Phys. 6, 112 (1967).
[130] Kristensen, I. K., J. Appl. Phys. 39, 5341 (1968).
[131] Rao, C. N. R., Natarajan, M., Subba Rao, G. V., and Loehman, R. E., J. Phys. Chem. Solids 32, 1147 (1971).
[132] Ksendzov, Ya. M., and Prokhvatilov, V. G., Zhur. Fiz. Khim. 31, 321 (1957).
[133] Keler, E. K., and Andreeva, A. B., Ogneupory 25, 320 (1960); Chem. Abstr. 54, 25663i (1960).
[134] Marinder, B.-O., Dorm, E., and Seleborg, A., Acta Chem. Scand. 16, 293 (1962).
[135] Rüdorff, W., and Luginsland, H. H., Z. anorg. allgem. Chem. 334, 125 (1964).
[136] Sakata, K., Nishida, I., Matsushima, M., and Sakata, T., J. Phys. Soc. Japan 27, 506 (1969).
[137] Chang, L. L. Y., Scroger, M. G., and Phillips, B., J. Less-Comm. Metals 12, 51 (1967).
[138] Chang, L. L. Y., J. Am. Ceram. Soc. 51, 295 (1968).
[139] McDaniel, C. L., and Schneider, S. J., J. Res. Nat. Bur. Stand. (U.S.), 71A (Phys. and Chem.), No. 2, 119–123 (Mar. Apr. 1967).
[140] Samakhvalov, A. A., and Rustamov, A. C., Sov. Phys.—Solid State (English Transl.) 5, 877 (1963).
[141] Kawano, S., Japan J. Appl. Phys. 8, 1264 (1969).
[142] Rao, C. N. R., Wahnsiedler, W. E., and Honig, J. M., J. Solid State Chem. 2, 315 (1970).
[143] Yamashita, J., J. Phys. Soc. Japan 10, 1010 (1963).
[144] Ern, V., and Switendick, A. C., Phys. Rev. 137A, 1927 (1965).
[145] Schoen, J. M., and Denker, S. P., Phys. Rev. 184, 864 (1969).
[146] Harker, D., J. Chem. Phys. 12, 315 (1944).
[147] Watanabe, D., Acta Cryst. 10, 483 (1957); J. Phys. Soc. Japan 15, 1251 (1960).
[148] Samokhvalov, A. A., Sov. Phys.—Solid State (English Transl.) 3, 2613 (1962).
[149] Mooradian, A., and Raccah, P. M., Phys. Rev. B3, 4253 (1971).
[150] Krishna Rao, K. V., Nagender Naidu, S. V., and Iyengar, L., J. Am. Ceram. Soc. 53, 124 (1970).
[151] Yoganarasimhan, S. R., and Rao, C. N. R., Anal. Chem. 33, 155 (1961).
[152] Clendenen, R. L., and Drickamer, H. G., J. Chem. Phys. 44, 4223 (1966).
[153] Parker, R. A., Phys. Rev. 124, 1719 (1961).
[154] Hernandez, W. C., and Kahn, A. H., J. Res. Nat. Bur. Stand. (U.S.), 67A (Phys. and Chem.), No. 4, 293–299 (July–Aug. 1963).
[155] Keesom, P. H., and Pearlman, N., Phys. Rev. 112, 800 (1958).
[156] Kahn, A. H., Frederikse, H. P. R., and Becker, J. H., in Transition Metal Compounds, Ed. E. R. Schatz (Gordon and Breach, Science Publishers, New York, 1964).

I.3. Vanadium Oxides

The vanadium-oxygen system has been extensively studied by several workers in the different homogeneity ranges by employing a variety techniques. In the range V-VO, by Seybolt and Sumsion [1], Schönberg [2], Rostoker and Yamamoto [3], Ozerov [4], and Cambini et al. [5]; in the range V-V_2O_3, by Klemm and Grimm [6], and Westmann and Nordmark [7]; in the range V_2O_3-V_2O_4, by Morozova et al. [8], Katsura and Hasegawa [9], and recently by Kimizuka et al. [10], Okinaka et al. [11], and Anderson and Khan [12]; in the range V_2O_3-V_2O_5, by Hoschek and Klemm [13], Burdese [14], Grossman et al. [15], Abei [16], and Kosuge [17]; in the range VO-V_2O_5, by Andersson [18] and Andersson [19] and in the range VO_2-V_2O_5, by MacChesney et al. [20], Theobald et al. [21], Sata et al. [22, 23], and Tilley and Hyde [24]. The available data have been summarized by a few workers [25, 26]. Stringer [26] constructed a schematic phase diagram and suggested a systematic nomenclature of the phases. A modified phase diagram of Stringer [26] and MacChesney et al. [20] (in the region VO_2-V_2O_5) are shown in figure I.4.

The V-O system is quite a complex one. In addition to the stable compounds like V_2O_3, VO_2, and V_2O_5 having narrow homogeneity ranges, compounds with wide homogeneity range like VO, Magnéli phases of the general formula V_nO_{2n-1} ($4 \leqslant n \leqslant 8$) and V_nO_{2n+1} ($n = 3$, 4, and 6) exist. Several new unidentified phases also exist in the region VO_2-V_2O_5 [21–24].

Oxygen forms a solid solution with metallic vanadium up to about 11 mol percent ($VO_{0.4}$) distorting the cubic lattice of V [1, 2, 5]. Range $VO_{0.5}$-$VO_{0.8}$ has not been accurately studied.

Vanadium monoxide has a wide homogeneity range ($VO_{0.85}$-$VO_{1.27}$) and all the compositions have been investigated experimentally. $VO_{1.5}$ (V_2O_3)appears to have a very narrow range of homogeneity [27]; different phases have been detected in alloys having compositions $VO_{1.44}$ and $VO_{1.65}$. The existence and stability of the Magnéli phases, V_nO_{2n-1}, with respect to the oxygen partial pressure and temperature have been examined by various workers [9, 11, 12, 17, 18]. VO_2 (V_nO_{2n-1}, $n = \infty$) has a narrow homogeneity range [10, 28]. Besides V_2O_5, in the series V_nO_{2n+1}, V_3O_7 [29], V_4O_9 [30] and V_6O_{13} [18] have been prepared and characterized.

VO: VO is unique in having an extremely wide composition range essentially symmetric about the stoichiometric composition together with an extraordinarily high vacancy content (~20%). It has a cubic rock salt structure and the lattice parameter a increases with increasing oxygen content but the density decreases; however, the increase in a is not linear with x in VO_x whereas the density versus x plot is linear. According to the recent study on well-characterized and annealed VO_x samples, the lower limit for the single phase cubic region appears to be between 0.75 and 0.79 and the upper limit, 1.30 [31]. Mathewson et al. [32] first noticed that the x-ray density of $VO_{1.00}$ (6.50 g/cm^3) is approximately 15 percent higher than the pycknometric value (5.6 g/cm^3) suggesting that the lattice is highly defective at the stoichiometric composition. The

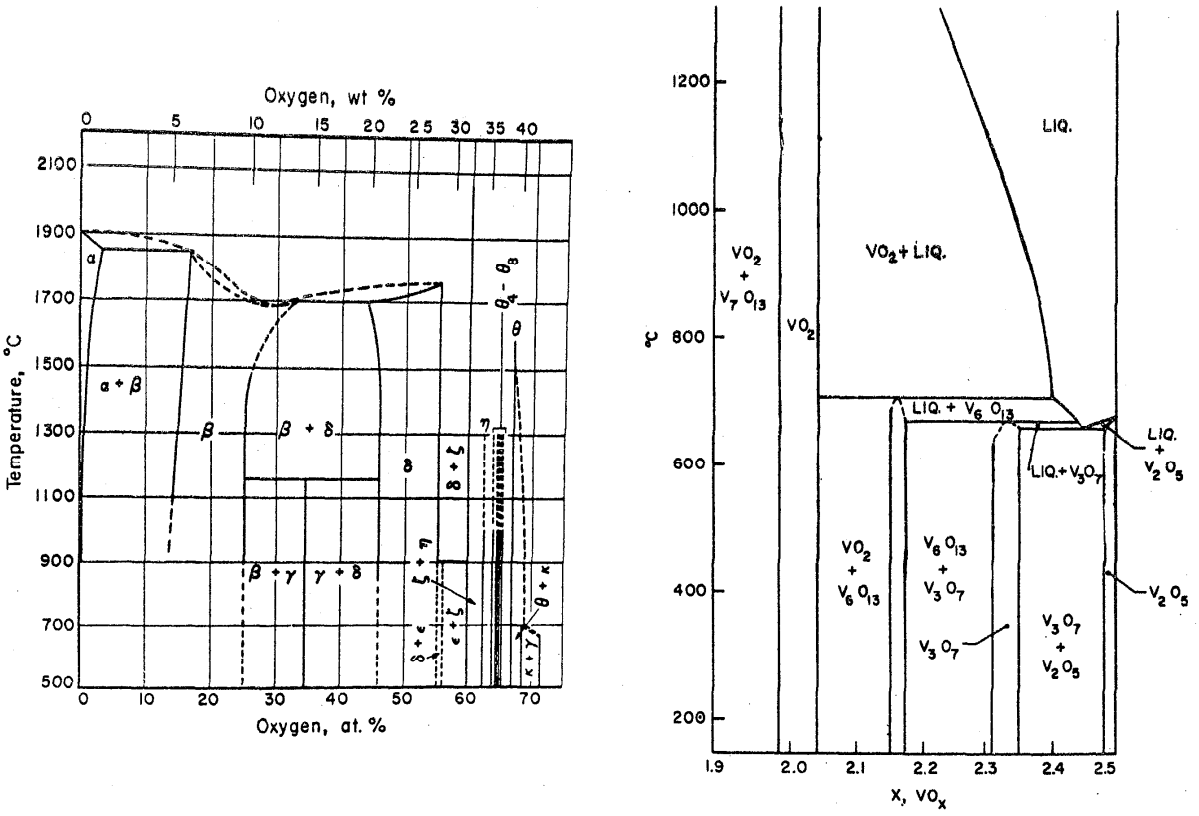

FIGURE I.4. (a) V–O *phase diagram (after* [26]). *The various phases and stability ranges have been discussed in detail by Stringer.* (b) VO_2–V_2O_5 *phase diagram showing the* V_nO_{2n+1} *phases (after* [20]).

variation of the defect concentration of the cationic and anionic lattices across the phase field has been examined by many workers [7, 27, 31, 33–36]. At the oxygen rich phase limit the anion lattice is nearly perfect with almost zero anion vacancies while at the vanadium rich phase limit, however, the cation lattice still contains ~13 percent vacancies. Banus and Reed [31] and Taylor and Doyle [36] have found that annealing the VO_x at high temperatures (~1570 K) and high pressures (~50–60 kbar) decreases the total number of vacancies (by about 6–13%) resulting in an increase in the density by ~1 percent and a 0.1 percent increase in the lattice parameter. These changes are unambiguously the result of the high pressure treatment, since reannealing the samples at 1 atm pressure at 1570 K gave samples with the same lattice parameter as the material before pressure treatment. Loehman, Rao, and Honig [35] have found that the vacancies in VO can be reduced by solid solution with TiO.

Because of the wide homogeneity range and large number of vacancies, VO_x shows interesting physical and chemical properties. With increase in x in VO_x, ρ, $d\rho/dT$, and χ_M increase linearly with abrupt increases in slopes at $x = 1.00$, while α changes smoothly from n-type to p-type at $x = 1.02$. The metal rich VO is a semimetal with weak temperature-independent paramagnetism and higher x changes to a semiconductor with a small energy gap and a stronger temperature-dependent paramagnetism. Contrary to the earlier reports [37–40], recent studies on well characterized samples of VO_x indicated no metal-to-semiconductor transition for any composition on decreasing the temperature to 77 K [31, 35, 41–43]. Oxygen rich VO shows [31] only a weak temperature dependent paramagnetism in the range 4.3 to 273 K with no evidence of magnetic ordering, in contrast to the findings of Kawano et al. [41] who observed definite evidence of antiferromagnetic ordering for $x = 1.15$ and 1.26.

The decrease in vacancy concentration on annealing at high pressure results in slight changes in the electrical and magnetic properties. The pressure annealing of VO does not significantly change the magnitude of ρ, the slope of ρ versus T or χ_M. At all compositions, there is a 10–20 percent decrease in χ_M in the range 4.2–100 K; a decrease in anion vacancies (caused by pressure anneal) affects the χ_M in an opposite direction to that caused by increase in x. This indicates that χ_M is more sensitive to the cation vacancies than the anion vacancies. The magnitude of α increases after pressure annealing and $VO_{1.02}$ changes from n-type to p-type behavior.

V_2O_3: Vanadium sesquioxide, V_2O_3, exhibits two transitions. Because of the dramatic changes in physical properties accompanying these phase transitions and the unique behavior with respect to pressure, temperature and impurity content, this oxide has been studied extensively in recent years both from theoretical and experimental points of view. The metal-to-insulator transition exhibited by V_2O_3 is a field of intense research activity at the present time (See fig. 2 in the introduction) and several review articles have recently appeared [44–56] on this aspect of the problem.

At room temperature, V_2O_3 has the corundum structure with rhombohedral symmetry [57, 58]. There is a unique c axis perpendicular to the basal plane which contains three identical crystal axes. Near 150 K, a phase transition occurs to the monoclinic structure [59–64] involving a slight tilting of the hexagonal c axis of the rhombohedral phase. The transition is accompanied by discontinuous changes in the c/a ratio (fig. I.5) and the unit cell volume (increase by about 1.4 percent) [63]. There is also a high temperature anomaly in V_2O_3 around 500 K where there is no change in the crystal parameters [63]; Kosuge [17], however, finds a DTA transition at 430 K. Recent neutron diffraction study on V_2O_3 [65] has confirmed the presence of antiferromagnetic ordering in the low temperature monoclinic phase (earlier measurements using various techniques gave contradictory conclusions; see, for example, reference [53]). According to Moon [65], the antiferromagnetic axis lies in a plane parallel to the c axis (in the hexagonal cell) and perpendicular to one of the a axes and makes an angle of about 71° to the c axis in this plane; the V moments are ferromagnetically coupled in monoclinic (010) or hexagonal (110) layers, with a reversal between adjacent layers. The ordered moment is 1.2 μ_B per

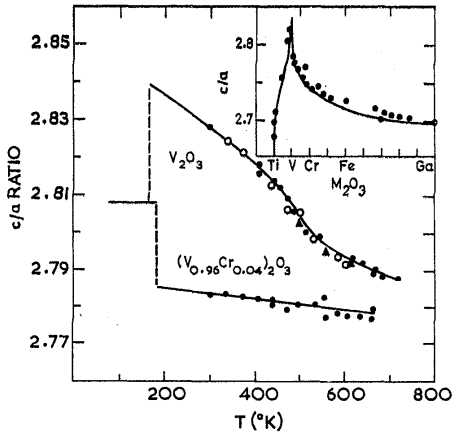

FIGURE I.5. *Variation of the c/a ratio of V_2O_3 with temperature* [63].

At the transition temperature we see a drastic change in the ratio. Chromium substitution markedly affects the c/a ratio. In the Insert we have shown the variation of c/a ratio in various sesquioxides; the ratio is anomalously high in V_2O_3 and low in Ti_2O_3.

V atom. Neutron diffraction [65] and magnetic susceptibility studies [66–68] indicate that the antiferromagnetic ordering in V_2O_3 disappears at the transition point (154 K) where the crystallographic transition also occurs. The high temperature anomaly is associated with a discontinuity in the χ_M, but the substance remains paramagnetic throughout the temperature range, 150 to 1000 K [68].

Associated with the phase transitions in V_2O_3, there occur dramatic changes in the electrical properties. At room temperature, V_2O_3 is a fairly good metal (with the purest samples showing resistivities of the order of 10^{-3} Ω cm and a positive temperature coefficient of ρ). When the temperature is decreased to 150 K (crystallographic transition point), it undergoes a transition from the metallic state to an insulating state with an accompanying increase in resistivity by about seven orders of magnitude. This transition has been first discovered by Foëx [69] and since then confirmed by many workers [37, 38, 63, 66, 70–78]. The characteristic metallic resistivity in V_2O_3 shows an anomaly in the high temperature region as well. Both the c axis and basal plane resistivities show a rapid increase with temperature in the region near 525 K, but keep monotically increasing up to 800 K [76]. Foëx et al. [66] on the other hand, have noted a maximum at 525 K and a semiconductor behavior in V_2O_3 above 525 K. Discontinuity in α was noted at the low temperature crystallographic transition in V_2O_3 [78, 79]. Above 150 K, α was positive and small and below this temperature, it changed sign and became very small.

R_H was negative in the entire range of temperature studied (7–800 K) and did not indicate any anomaly; α did not indicate anomaly at the high temperature transition of V_2O_3 [78].

λ-type anomalies are noted in the heat capacities at the low and high temperature transitions in V_2O_3 [66, 80]; DTA studies indicate endothermic peaks corresponding to the transitions [17]. Anomalous behavior of V_2O_3 in the region of the transition point has been noted in the measurements made by a variety of techniques like NMR spectroscopy [81–84], Mössbauer spectroscopy [74], positron annihilation [85], UHF (~10 GHz) dielectric constant [86] and optical spectroscopy [76, 87].

The effect of pressure on the transition has been studied by a few workers [38, 39, 61, 76, 77]. The transition temperature ($T_t \equiv T_N$) decreases with pressure (~4 K/kbar). Application of pressures greater than 25 kbar suppresses the transition completely [77] and V_2O_3 remains metallic and Pauli paramagnetic down to 2.2 K without indication of any long range magnetic order.

All the available data seem to establish that the low temperature transition in pure V_2O_3 is of first order and the high temperature one is of second order. The low temperature transition is sharp and marked by a hysteresis. T_t is sensitive to stoichiometry [88] and the magnitude of the discontinuity in ρ seems to depend on sample purity and stress. The properties of the metallic state of V_2O_3 are highly anomalous and they change rapidly with pressure in the direction of making it more metallic. It, therefore, appears that pure V_2O_3 is near a critical region and that the application of negative pressure would induce a transition; doping with chromium has an empirical correspondance with the negative pressure, and indeed, it is found that a metal-to-insulator transition occurs with Cr doping in this material.

As early as 1949, Mott [89] predicted that an abrupt metal-insulator (collective electron-localized electron) transition will occur in an ionic solid when the interionic separation is forced to pass through a critical value. Since each of the two resistance anomalies in V_2O_3 is accompanied by an anomaly in the thermal expansion, it would appear that they may both be metal-insulator transitions of the type envisioned by Mott. The basis for the ideas that the V_2O_3 transitions are Mott-type transitions is contained in the recent work of McWhan and co-workers [62, 63, 84, 90]. These workers have examined the resistivity and the lattice distortion of V_2O_3 as a function of pressure, temperature, and chromium and

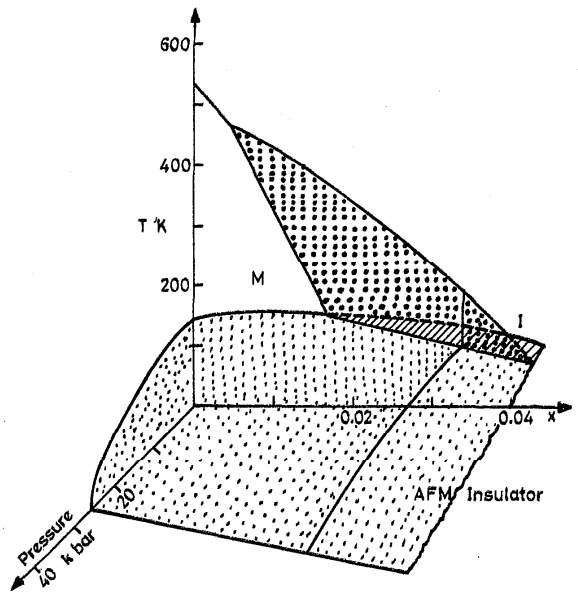

FIGURE I.6. *Pressure-temperature-composition (Cr) phase diagram* $(V_{1-x}Cr_x)_2O_3$.
M, I, and AFM insulator phases have been indicated; the metal-insulator phase boundary terminates at a critical point (~530 K) (after [63]).

titanium doping. Three types of phases have been suggested to be present in V_2O_3: the metallic (M), the insulating (I) and antiferromagnetic insulating (AF) phases. Depending on the temperature, pressure and dopant concentration, all the three phases and the transitions between any two ($M \rightleftharpoons I$; $M \rightleftharpoons AF$; $AF \rightleftharpoons I$) can be realized experimentally. The temperature-pressure-composition phase diagram for $(V_{1-x}Cr_x)_2O_3$ is reproduced in figure I.6.

At room temperature and atmospheric pressure, pure V_2O_3 is situated in the metallic phase. As the temperature is lowered, the undoped material passes through the M-AF phase surface at ~160 K. Conversely, as the temperature is raised, pure V_2O_3 appears to pass through the extension of the M-I phase boundary at ~550 K. However, the M-I phase boundary terminates at a critical point (fig. I.6), so that the high temperature transition in pure V_2O_3 reflects a critical behavior. The phase transition is no longer a well-defined, abrupt, first order transition, but is a gradual change from metallic to insulating behavior. When a small percentage of Cr ions is substituted for vanadium in V_2O_3, a definite first order phase transition between the metallic and insulating phases exists, with the transition temperature rapidly decreasing as a function of chromium doping. At a critical concentration (~3

percent), the M→I and M→AF transition temperatures are equal (~160 K). For Cr dopings greater than 3 percent, an intermediate metallic state does not exist and the only observed transition is a direct I→AF transition (at atmospheric pressure). Similarly, at a given temperature (say, 298 K) and Cr-concentration (say, 4 percent), I→M transition can take place with the application of pressure without the intervening AF phase. Doping with increasing amounts of Ti has the empirical correspondance to the application of pressure (3.6 kbar/atom %) and the system tends to become more and more metallic [79]; at about 7 atom percent Ti, both the transitions in V_2O_3 are suppressed and the system is metallic in the entire range of temperatures as is the case in pure V_2O_3 above 25 kbar pressure [62].

Various theories have been put forward to explain the metal-insulator transitions in oxide materials ([91–93]; for a review of various earlier theories see [53]), but each of them is able to explain the experimental findings on a specific oxide material and fail to explain the behavior of other oxides. Any discussion of the theories would be outside the scope of this review and it would suffice to point out that there is still a need for unifying theoretical approaches to the understanding of metal-insulator transitions. In figure I.7 we have shown the schematic band structure of V_2O_3 (following Goodenough) in the rhombohedral, nonmagnetic monoclinic and magnetic monoclinic structures to illustrate the nature of changes accompanying the low-temperature transition.

V_nO_{2n-1}: The Magnéli phases, V_nO_{2n-1}, $(4 \leqslant n \leqslant 8)$, have a triclinic structure based upon the rutile structure with periodic sheared planes resembling stacking

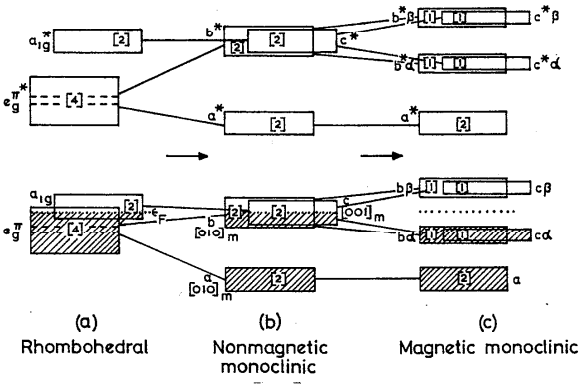

FIGURE I.7. *Changes in the* d*-electron band strurture of* V_2O_3 *accompanying the transition at* ~150 *K (After Goodenough).*

faults into which extra planes of metal atoms are introduced. Because of the shear planes, metal-metal bonding can occur leading to interesting electrical and magnetic properties. Whenever these metal-metal bonds are broken up, anomalies in the physical properties occur, but there appears to be no case where structural transformation occurs; only a discontinuity in the lattice parameters is noticed. Nagasawa and co-workers have grown single crystals of these Magnéli phases by the vapor transport method [94–97] and have carried out various measurements.

V_3O_5, even though it corresponds to V_nO_{2n-1} with $n=3$, is not a Magnéli phase since the structure is different (monoclinic). It shows a discontinuity in the χ-T plot around 133 K [95], but in contrast to the earlier studies [73] (which showed a semiconductor-to-metal transition in the range 150 to 180 K), only a semiconductor behavior was noted in the range 130 to 300 K [72, 98]. Kosuge [17] does not observe a DTA peak, or a χ-T anomaly. X-ray studies of Åsbrink et al. [99] up to 1270 K, also do not indicate a phase transition.

Magnetic susceptibility and electrical transport (on single crystal materials), x-ray, DTA and Mössbauer studies indicate semiconductor-to-metal transitions (on heating; first order) in V_4O_7 at 250±5 K [17, 94, 100, 101]; in V_5O_9 at 135±5 K [17, 96, 102]; in V_6O_{11} at 177±2 K [17, 95, 103]; in V_8O_{15} at 70 K [97, 104, 105]. Detailed studies [17, 94, 103] indicate that V_7O_{13} is paramagnetic (Pauli ?) and metallic in the range 4.2 to 300 K. In their recent study published in 1973, Kachi, Kosuge, and Okinaka [105] have presented the data on all the V_nO_{2n-1} (n = 3–9) systems and find that all but V_3O_5 and V_7O_{13} show metal-sinulstor transitions. These workers have established the phase relationships and structures of these oxides.

It is difficult to rationalize this wealth of experimental data without a proper understanding of the theory underlying the semiconductor-to-metal transitions; unfortunately, present day theory has not yet developed to such sophistication, to satisfactorily explain the transitions even in simple substances like V_2O_3 and VO_2. However, in the V_nO_{2n-1} series, two important generalizations may be noted: (i) all the phases are triclinic and detailed x-ray study on V_4O_7 indicate no crystal structure change at T_t, but only discontinuity in lattice parameters. Probably the same case may be true for other Magnéli phases as well. (ii) Recent studies [105] show that there is antiferromagnetic ordering in all the V_nO_{2n-1} phases at low temperatures in addition to first order transi-

tions in many of them at higher temperatures; in these respects, these phases are similar to V_2O_3. It appears that the first order transitions in these Magnéli phases are explainable in terms of Goodenough's qualitative picture ([44, 106, 107]; for a detailed discussion, see [53]) of metal-metal bonding and trapping of the conduction electrons in the semiconducting phase and the breaking of these bonds and creation of Fermi surface at T_t in the high temperature metallic phase. Like VO_2, V_nO_{2n-1} oxides also show only a single transition (V_2O_3 and Ti_4O_7 on the other hand, show two transitions).

VO_2: Vanadium dioxide, VO_2, exhibits a crystallographic transition at 340 K. The transition is accompanied by interesting changes in physical properties (see fig. 2 in introduction). In view of the possible practical applications of this material in electrical switching circuits and in other devices, the crystal growth and physical properties of this material have been extensively studied and reviewed by various workers in recent years [44–56, 108].

VO_2 is monoclinic at room temperature [101, 109–113] and transforms to a tetragonal rutile structure at 340 K [101, 114–116]. The transition is of first order and is accompanied by hysteresis effects and changes in latent heat and volume [101, 114–119]. Magnetic susceptibility [15, 114, 117, 119–122], Mössbauer [75, 123] and NMR [84, 124, 125] studies have failed to show any evidence of long range magnetic ordering in VO_2 in the temperature range 1.7 to 400 K; however, a jump in χ is noted at T_t and χ is almost temperature independent both above and below T_t. The electrical characteristics of VO_2 change from those of a semiconductor to those of a metal at T_t with a large drop in resistivity (by a factor of $\sim 10^5$ for pure and single crystalline material) [37, 73, 75, 113, 114, 117, 126–134]. Seebeck coefficient [117, 128, 135, 136] and Hall effect [130, 137] also show anomalies at T_t. Studies of DTA [17, 113, 116], heat capacity [114, 117, 138] as well as infrared spectra and other optical properties [130, 139] clearly show the first order nature of the transition in this material, but thermal conductivity does not show an anomaly at T_t [117].

Recently, some workers have found evidence for the existence of an intermediate triclinic phase of VO_2 in the range 325 to 340 K by means of NMR [125], DTA [116] and x-ray diffraction [115] studies. The temperature range of stability of this intermediate phase may become vanishingly small for pure VO_2 [101], but impurities like Al, Fe, Cr, Mo, and hydrogen reduction appear to be effective in the stabilization of this phase by way of Magnéli defects [115, 116][2].

The effect of pressure on the VO_2 transition has been examined by a few workers [39, 61, 140]. T_t increases linearly with pressure at a rate of 0.082 ± 0.005°C/kbar. The conductivity activation energy in the semiconducting phase decreases linearly with pressure typically at a rate of 1–2 mV/kbar. Assuming intrinsic behavior below T_t for VO_2, this indicates that the carrier concentration increases with pressure but no metallic conduction is encountered up to pressures of $\sim$300 kbar at 300 K.

The effect of various impurities on the temperature and nature of the transition in VO_2 has been investigated extensively in the literature. Many elements like Ti, Nb, Mo, Tc, Ta, W, and Re, form complete solid solutions with VO_2 [113, 116, 120, 121, 133, 141–148] and at appreciable concentrations stabilize the high temperature rutile from of VO_2 at room temperature; the T_t of VO_2 is lowered appreciably and the nature of the transition (at not too high impurity concentrations) is changed from that of a semiconductor-to-metal to that of a semiconductor-to-semiconductor. The same effect is produced by the addition of ions like Fe, Co, and Ni, but Al, Cr, and Ge raise the T_t appreciably [133, 146, 148]. Unfortunately, each system is complicated in itself and no generalizations are possible on the effect of impurities on the transition in VO_2 until the detailed mechanism of the semiconductor-metal transition in pure VO_2 is clearly understood.

Since long range magnetic order is absent in VO_2, it might be considered that the Adler-Brooks crystal distortion model ([149, 53]) would be applicable to the transition in VO_2, but quantitative agreement between theory and experiment is lacking [56, 108, 134]. Since the metal-metal bonding in VO_2 and other rutile type oxides at low temperatures has been established beyond doubt, Goodenough's approach seems to be applicable (for detailed discussion, see [53]), but the treatment is only qualitative. Paul [108], Hyland [56], and others [150, 151] strongly argue for an electron-phonon interaction mechanism and phonon instability [152] as the basic driving force for the transition in VO_2. In figure I.8 we have shown the elementary band structure scheme for tetragonal and monoclinic VO_2 to illustrate the nature of changes accompanying the transition.

---

[2] Goodenough, [116a] J. Solid State Chem. 3: 490 (1971), has recently identified two distinguishable mechanisms of the monoclinic-tetragonal transition of VO_2: an antiferroelectric-paraelectric transition at a temperature T_t and a change from homopolar to metallic V–V bonding at T_t'. Both T_t and T_t' are at 340 K in pure VO_2. In the presence of impurities the two components seem to get separated with $T_t' < T_t$ (see ref. [136], and [148] for example).

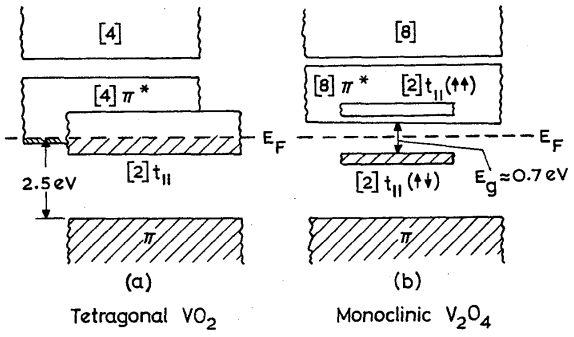

FIGURE I.8. *Schematic band structure of* VO_2 *in the monoclinic and tetragonal phases (after Goodenough).*

V_nO_{2n+1}: V_6O_{13} is monoclinic at room temperature [16, 18]. Kosuge [17] reported an endothermic peak in DTA at 177 K where a χ-T anomaly has also been noted. Recently, Kanazawa [153] has noticed a semiconductor-to-metal transition (on heating) in this material at 149 K with a drop in resistivity by a factor of 10^4. The transition may be first order but the structure of the low temperature phase is not yet established.

In the series V_nO_{2n+1}, in which V_2O_5 and V_6O_{13} are known members, V_4O_9 and V_3O_7 have been recently prepared and characterized. V_4O_9 is orthorhombic [30] whereas V_3O_7 has a monoclinic crystal symmetry [29, 154, 155] at room temperature and decomposes at 930 K. No DTA peak was noticed by Kosuge [17] in the range 130 to 950 K. The other physical properties are not yet known.

Vanadium pentoxide has a narrow range of homogeneity [26]. It is orthorhombic at room temperature and has a corrugated sheet type structure and is built up from distorted trigonal bipyramidal coordination polyhedra of oxygens around vanadium, sharing edges to form zig-zag double chains along [001] and are cross-linked along [100] through shared corners, thus forming sheets in the xz plane [156–159]. This special type of structure predicts anisotropy in thermal expansion of the lattice parameters and is observed experimentally [160–162]. V_2O_5 does not show any phase transformations up to the melting point (~940 K) at one atmosphere [17, 163]. Minomura and Drickamer [39] have noticed a phase transition in V_2O_5 at pressures ~100–105 kbar, associated with a large increase in the resistivity. V_2O_5 remains semiconducting both below and above the transition. Electrical properties and the mechanism of conduction in V_2O_5 have been discussed by a few workers [164–169]. Small amounts of alkali and other metals form 'vanadium bronzes' with V_2O_5. These important materials have been discussed in detail in the literature [53, 170].

Vanadium oxides

Oxide and description of the study	Data			Remarks and inferences				References
	Oxide	a, Å (cubic, rock salt)	Density (g/cm³)	% Vacancies (Total)	ρ (300 K) (Ωcm)	α (μV/°C)	χ_M (273 K)	
VO								
Crystal structure and physical properties of VO_x ($0.8 < x < 1.25$).	$VO_{0.86}$	4.034	5.736	37.0	6.0×10^{-4}	−10.9	0.5×10^{-3}	[31, 35].
	$VO_{0.99}$	4.068	5.602	30.8	2.2×10^{-3}	−4.2	0.6×10^{-3}	
	$VO_{1.02}$	4.077	5.583	28.9	3.5×10^{-3}	−2.0	0.6×10^{-3}	
	$VO_{1.23}$	4.133	5.329	21.2	—	+22.1	0.8×10^{-3}	

Oxide and description of the study	Data	Remarks and inferences	References
	Melting point (VO_x)~2170 K	Most comprehensive study on 30 well-characterized samples; contains literature survey up to 1970; High pressure annealing studies conducted; VO_x ($0.86 \leqslant x \leqslant 1.02$) is metallic and show temperature-independent χ_M while samples of VO_x ($1.02 \leqslant x \leqslant 1.23$) are semiconducting and show weak temperature-dependent χ_M. No metal-to-semiconductor transition nor magnetic ordering noticed in any sample in the range 4.2–300 K for all x.	
Vacancy annealing in VO.	High temperature (~1920 K) and high pressure (~56 kbar) produced substantial decrease in the vacancies (vacancy filling); In common with other workers, difficulties were encountered in the preparation of pure single phase $VO_{1.00}$.	A critical value of $P\Delta T$ (>90,000 kbar. °C) where P is the applied pressure and ΔT is the temperature above ambient at which the pressure is applied, seems to eliminate the vacancies completely in TiO. A similar (but higher) value is predicted for complete vacancy filling in VO.	[36].
NMR studies of VO.	V^{51} NMR studies on single crystals and pressure annealed VO_x ($x=0.86$, 1.02 and 1.23) using cw and spin echo techniques in fields of 9–50 kOe in the range 1.4–300 K. Resonance was observable in all compounds at all temperatures indicating the absence of metal-insulator transition in the observed materials.	Results indicate that the bulk of the temperature-dependent magnetization comes from local moments on a minority of sites whose nuclear resonances are unobservable.	[42].
Resistivity and Hall coefficient studies.	VO_x ($0.82 \leqslant x \leqslant 1.0$) samples studied at 4.2, 77, and 300 K. ρ (300 K) is in the range 10^{-3}–10^{-4} Ωcm with small negative values of $d\rho/dT$; R_H is $\sim 5\times10^{-4}$ cm³/C and positive $\Delta\rho/\rho$ at 4.2 K. The samples did not exhibit metal-insulator transition.	An overlapping band model is suggested to explain the observed properties.	[43].

Vanadium oxides—Continued

Oxide and description of the study	Data	Remarks and inferences	References
Seebeck coefficient studies on VO_x.	For VO_x samples with $x<1.0$, α is negative; for $x>1.0$, α is positive and for $x\approx1.0$, $\alpha\approx0$. The numerical values are small (-5 to $+20$ μV/°C).	The data indicate that electrons and holes are competing together for the contribution to α and the consequent complications in the band structure related to a large concentration of metal and anion vacancies.	[171].
Crystallography and defect chemistry of VO and solid solutions with TiO.	The solubility of TiO in VO is small (~10%). The concentration of defects are lower than in pure VO_x at any given composition. Semiconductor behavior was noticed for VO ($x\geqslant1.0$) and its solid solutions in the range 100–300 K. No metal-semiconductor transition was noticed for VO or in the solid solutions in the temperature range investigated.	It appears that $VO_{0.8}$ does not belong to the same family of cubic VO_x with ($0.9\leqslant x\leqslant1.2$) and higher disorder in cation sublattice exists compared to anion sublattice. The low solubility of TiO in VO is explained in terms of the different degree of disorder in the two crystal lattices.	[35].
Electronic structure and solubility of other oxides in VO.	Mutual solubility of VO and TiO at 1870 K is ~18–20%; in the oxygen rich phases ($x>1.0$), solubility is greater (20–25%). Solubility of BeO, CaO, and MgO are small in VO.	The observed behavior is explained in terms of the electronic structure and valence states of the metal in these compounds.	[172].
Plasma resonance in VO.	Reflectance minima are found in the range 3.8–4.0 eV in VO_x depending on the composition.	The reflectance minima correspond to the plasma edges in these materials.	[173].
Infrared studies of VO_x.	$VO_{1.05}$ and $VO_{1.11}$ give rise to bands at 1075 ± 15 and 1080 ± 10 cm^{-1} respectively.	The band corresponds to the metal-oxygen vibrations and results indicate that the band position is not much sensitive to the nature of the cation or the phase composition.	[174].
Band structure of VO.	Band structure calculations by the tight binding method indicate that the *d* bands are about 7 eV wide, lying below the vanadium 4*s* band so that conductivity in VO is primarily due to the *d* electrons. The Fermi level falls in the *d* band.	The energy bands in VO seem to be sensitive to the degree ionicity assumed in the calculation; the density of states at the Fermi level is large, suggesting that VO might exhibit some sort of magnetism. See also (ref. [9], p. 130) for band structure calculations.	[175].
V_2O_3			
Crystal structures of the phases and x-ray studies.	Range 77–160 K: Monoclinic; space group, $I2/a$; $Z=4$; $a=7.255\pm0.003$ Å; $b=5.002\pm0.002$ Å; $c=5.548\pm0.002$; $\beta=96.75\pm0.02°$; $V=99.97\pm0.08$ Å^3. TEC of this phase is $<2\times10^{-6}$ K^{-1}.	Earlier workers [59, 176] interpreted the low temperature monoclinic distortion in terms of a orthohexagonal cell or *c*-centered monoclinic cell but the present choice in terms of a hexagonal cell appears to be the most easily conceived. Single crystal	[63, 64].

Oxide and description of the study	Data	Remarks and inferences	References
	Range 160–700 K: Rhombohedral (pseudo hexagonal); space group, $R\bar{3}C$; $Z=2$, $a_H=4.9515\pm0.0003$ Å; $c_H=14.003\pm0.001$ Å; $c/a=2.8281$; $V=98.61\pm0.05$ Å^3. TEC (/K) at 298 K: $\|^a=(20.2\pm0.3)\times10^{-6}$; $\|^c=-(8.6\pm0.3)\times10^{-6}$. The c/a ratio (pseudo c/a for monoclinic cell) shows a sharp jump at ~160 K and slight nonlinear decrease in the region 450–600 K; the 4% Cr doped samples show the exact opposite behavior. ΔV (mono.→rhombo.) = $-(1.4\pm0.1)$%; the value is much less for doped samples (4%). With pressure, volume decreases gradually with increasing pressure but doped samples give discontinuity depending on the concentration. Lattice parameters vary smoothly with the application of pressure; $d\ln(c/a)/d(\ln V) = -0.7$. Melting point of pure V_2O_3~2240 K.	growth conditions established. V_2O_3 has an unusually high c/a ratio (at 298 K); detailed studies indicate that in going to the monoclinic structure, nearest neighbor V–V distances show a discontinuous expansion while the average V–O distance remains unchanged. Contrary to the earlier interpretations [45, 76, 177], pair-wise contraction of the basal plane cations does not, in fact, occur but the oxygen octahedra become skewed up about the central metal atom and the triply twinned monoclinic structure is a logical consequence of the distortion.	[58, 62, 63].
Magnetic susceptibility, magnetic ordering and neutron diffraction studies.	Range 4.2–1000 K: $\chi_M=1.0\times10^{-4}$ (cgs units) ($T<150$ K) $\chi_M=2.1\times10^{-4}+1.40/(T+600)$ ($180°<T<350$ K); $\chi_M=2.1\times10^{-4}+1.78/(T+600)$ ($580<T<1000$ K). χ_M shows little anisotropy (<20%) and is essentially temperature independent. χ_M shows a jump in going through T_t while heating and shows Curie-Weiss behavior; a hysteresis of ~12° was noted. $T_t\approx155$ K. A shallow maximum is indicated in χ_M-T curve in the range 400–500 K. This seems to correspond to the high temperature anomaly in pure V_2O_3. The magnetic moment changes from 2.37 μ_B to 2.69 μ_B in going through this transition (spin only value for V^{3+} is 2.83 μ_B). χ_M-T studies were also made on doped samples. Internal field value ~175±15 kOe was obtained in V_2O_3 at 105 K using inelastic spin-flip	The ordering of magnetic dipoles in V_2O_3 is of special type compared to the other transition metal sesquioxides. The estimated latent heat at low temperature transition is ~700 cal/mol.	[65, 67, 68, 76, 77, 79, 178–181].

Vanadium oxides—Continued

Oxide and description of the study	Data	Remarks and inferences	References
	scattering of neutrons. The ordered moment (calculated) is 1.25 μ_B. The existence of antiferromagnetic ordering in the low temperature phase is confirmed. The observations are in accord with a model in which the vanadium moments are ferromagnetically coupled in monoclinic (010) layers with a reversal between adjacent layers. The ordered moment is (1.2 ± 0.1) μ_B per V atom. Neutron diffraction study shows that the magnetic ordering disappears at 154 K which is the Néel temperature (T_N). Application of pressure decreases the transition temperature ($dT_N/dP = -3.78$ K/kbar). Above 26 kbar pressure, the magnetic order disappears and the material remains paramagnetic down to 4.2 K.		
Electrical properties.	*Semiconductor behavior below* T_t $(151\pm3$ K); ρ (125 K) $\sim 10^5$ Ωcm; $E_a\sim0.12$–0.18 eV; below 40 K, evidence of impurity conduction with $E_a\sim0.001$ eV. Below T_t, α is ~ -3 $\mu V/°C$ and $R_H<0.3$ cm^3/C (at $\rho\sim10^3$ Ωcm). *Metallic behavior above* T_t; ρ drops by a factor 10^7 at T_t while heating; hysteresis of $\sim$12 K noted. α becomes positive and jumps to $\sim$12 μV/°C and shows slight decrease with temperature thereafter. ρ shows an anomaly (broad maximum) in the range 500–600 K. No anomalous behavior in α and R_H in this temperature region. Resistance decreases with the application of pressure: 1 atm: $\rho=227\pm1.4$ T $(150<T<350$ K). 26 kbar: $\rho=182\pm0.7$ T $(200<T<300$ K); $\rho=3.1\pm0.042$ T^2 $(T<50$ K). $(d\ln\rho/d\ln V)=30$ (basal plane); $=16$ (parallel to c-axis). $R_H=2.3\times10^{-4}$ cm^3/C (p-type); no change in R_H at the high temperature transition. $\mu_H=$ 0.2–0.6 cm^2/V s in the range 300–600 K; $m^*\approx50$ m; Mean free path $\sim$2 Å.	The low temperature behavior is usually interpreted in terms of intrinsic behavior. According to McWhan et al. [63], the properties of both the high temperature phases (metallic, M and insulating, I, phase) are anomalous and are modified by the impending transition in the range 500–600 K. The order of the transition may be second or higher order but can be made first order under proper conditions (by doping with Cr). A generalized picture of the transitions in V_2O_3 has emerged from the work of these investigators.	[38, 63, 71, 76–78, 182].

Vanadium oxides—Continued

Oxide and description of the study	Data	Remarks and inferences	References
Thermal properties.	Endothermic peaks in DTA were noted at 168 and 430 K; no ΔH value reported. λ-type anomaly was noted in the heat capacity of V_2O_3 at 169 K; $\Delta H = 692$ cal/mol; ΔS for the transition = 4.1 e.u. McWhan et al. [62] estimate a value of $\Delta S = 2.6$ e.u. A nuclear specific heat measurement in the temperature range below 0.5 K indicated a Schottky anomaly varying with T^{-2} for pure V_2O_3.	The thermal properties are showing up the two transitions in V_2O_3 but there is need for quantitative studies on the ΔH and ΔS of transition.	[17, 62, 76, 80, 183].
Optical properties.	Energy gap of ~0.1 eV is obtained from the optical measurements at 77 K in pure V_2O_3. The reflectivity of pure V_2O_3 at 300 K is small but has the general shape characteristics of a metal; plasma edge is at ~1 eV.	The fundamental absorption edge in the antiferromagnetic phase appears to be very soft and shifts to lower energies on entering the high temperature insulating phase.	[76, 87].
NMR Studies.	Knight shift (%): $k = 1.52 - 18.1/(T+684)$ ($T > 150$ K). An abrupt change in k is noted at the high temperature transition, while the resonance signal vanishes at the low-temperature transition (150 K). No anisotropy in k is noted nor any observed nuclear quadrupole splitting. Antiferromagnetic state is suppressed in pure V_2O_3 at high pressure and low temperatures. V^{51} NMR signal is observable down to 4.2 K. $k = (-1.0 \pm 0.2) + (0.01 \pm 0.005)\ P$ ($20 < P < 65$ kbar and $T = 4.2$ K). The effect of doping V_2O_3 with Cr and Al has also been studied in detail.	This study is a strong evidence for magnetic ordering at low temperatures in pure V_2O_3. From the 'NMR-phase diagram', Rubenstein [83] concludes that the metal-insulator (high temperature region) phase boundary is not sharp and uniform below the critical point, but corresponds to an inhomogeneous transition. It is postulated that the high temperature phase transition is produced by an instability in a normal mode vibration of the crystal lattice and that the low-temperature transition (150 K) is driven by large magnetostriction by the antiferromagnetic ordering aided by the presence of this 'soft' acoustic phonon mode. The lattice instability is believed to be caused by the close proximity of a van Hove singularity to the Fermi energy in the metallic state of the crystal. The pressure dependence of the Knight shift implies that the d spin component of the susceptibility (χ_d) is unusually strongly dependent on volume with $(\partial \ln \chi_d / \partial \ln V) = 8 \pm 5$.	[81–84].
Mössbauer studies.	Studies of Fe-doped V_2O_3 in the range 4.2–300 K: Magnetic hyperfine splitting was noted be-	The calculated T_N was ~200 K. It is inferred that the larger discrepancy between T_t and T_N	[74].

Vanadium oxides—Continued

Oxide and description of the study	Data	Remarks and inferences	References
	low T_t ($\sim$140 K) which disappeared above T_t and the substance was paramagnetic. The internal field decreased with temperature (400 and 315 kO_e at 4.2 and 131 K respectively) and abruptly disappeared at T_t; isomer shift showed a jump at T_t.	(calc) might indicate that magnetic ordering is not a major cause of the transition.	
UHF dielectric properties.	Wave guide method using a frequency of 9.5 GHz: $\epsilon \approx 18$ ($T <$ 160 K); $\epsilon \approx 36$ ($T > 160$ K). ϵ slowly varies with temperature; in the region of the transition a jump by a factor of 2 is noted. Complex conductivity also exhibits an anomaly at T_t.	The high value of ϵ indicates the relative importance of nonpolar type of bonding in V_2O_3 and the transition is accompanied by a change in the type of chemical bonding, electron-energy spectrum and consequently the dielectric properties.	[86]
Electric field effect on the transition.	When the applied field reaches a critical value ($\sim 10^4$ V/cm at 77 K) the current increases rapidly; this threshold field depends weakly on the sample thickness. Switching behavior also is noted in the samples of pure V_2O_3.	—	[184]
Effect of stoichiometry on the low temperature transition.	For low stoichiometric deviations in $VO_{1.5+x}$, both a and c parameters of hexagonal form at room temperature, decrease linearly and c/a is a constant. With large x ($x > 0.015$), a decreases more rapidly than c suggesting a probable change in the distribution of defects involved in the crystals. The magnitude of the discontinuous change in χ_M at T_N and T_N become smaller with increasing x; no transition is observed observed for $x = 0.034$ either in terms of a change in the crystal structure or in χ_M.	—	[88]
Band structure of V_2O_3.	The band structure of the hexagonal V_2O_3 lattice is examined by the tight-binding method. The stability of the structure in relation to the distortions and the splitting of the d bands is investigated.	The model appears to account for a transition from a distorted, insulating state to an undistorted semimetallic one, for certain values of the d–d interactions.	[185]
V_3O_5			
Crystal structure	Monoclinic; space group, C2/c or Cc; $Z = 4$; $a = 9.98$ Å; $b = 5.03$ Å;		[99]

Oxide and description of the study	Data	Remarks and inferences	References
	$c=9.84$ Å; $\beta=138.8°$. X-ray studies do not indicate any phase transition up to ~1270 K.		
Physical properties.	χ-T plot shows an anomaly at ~133 K, but DTA does not indicate a peak at this temperature. Probably the substance is paramagnetic in the range 77—300 K. Semiconductor behavior in the range 130–300 K; $E_a=0.4$ eV. α data (~280 μV/°C at 273 K) indicates n-type behavior; α decreases with T.	Earlier studies [73] might have contained some V_5O_9 impurity; the cause of χ-T anomaly is not known.	[17, 72, 95, 98, 105].
Magnéli phases, V_nO_{2n-1}	Crystal structure and transition temperature	Magnetic, electrical, DTA and Mössbauer studies	References
n; phase	All phases are triclinic; space group, $P\bar{1}$; $Z=2$.		
4; V_4O_7	$a=5.502$ Å; $b=6.997$ Å; $c=12.248$ Å; $\alpha=95.09°$; $\beta=95.17°$; $\gamma=109.28°$. $T_t=250\pm5$ K. Discontinuity in the lattice parameters at T_t; no change in the crystal structure; the volume change for the semiconductor-to-metal transition = $+0.0011\pm0.0006$; the pressure dependence of T_t is -0.2 ± 0.1 K/kbar.	χ-T anomaly at T_t. Semiconductor-to-metal transition; $\Delta\rho=10^2$ at T_t; α shows discontinuity at T_t; α is negative in the range 120–300 K; α above T_t is ~10–12 μV/°C. Endothermic DTA peak. No magnetic order below T_t; Isomer shift and quadrupole splitting show discontinuities at T_t; T_t decreases by Fe^{3+} doping but jump in χ remains almost the same.	[17, 94, 100, 101, 105, 186].
5; V_5O_9	$a=5.475$ Å; $b=6.994$ Å; $c=8.718$ Å; $\alpha=97.53°$, $\beta=112.44°$; $\gamma=108.99°$. $T_t=135\pm5$ K.	χ-T anomaly at T_t. Semiconductor-to-metal transition at T_t; $\Delta\rho\sim10^4$–10^6; E_a below $T_t=0.1$–0.2 eV. α decreases with increase in T; anomaly at T_t; above T_t, $\alpha\sim10$–20 μV/°C (n-type). Endothermic DTA peak at T_t. No magnetic order below T_t; Isomer shift and quadrupole splitting show discontinuities at T_t; Fe^{3+} doping decreases T_t slightly.	[17, 96, 102, 105, 186, 187].
6; V_6O_{11}	$a=5.44$ Å; $b=6.99$ Å; $c=23.66$ Å; $\alpha=98.5°$; $\beta=120.9°$; $\gamma=108.9°$. $T_t=170$–177 K.	χ-T anomaly at T_t. Semiconductor-to-metal transition at T_t; $\Delta\rho\sim10^4$; E_a below $T_t=0.12$ eV. α is negative in the range 120–300 K and goes through a sharp maximum at T_t. Above T_t, $\alpha=10$–13 μV/°C. DTA endothermical peak.	[17, 95, 103, 105, 186].

Oxide and description of the study	Crystal structure and transition temperature	Magnetic, electrical, DTA and Mössbauer studies	References
7; V_7O_{13}	$a=5.43$ Å; $b=7.00$ Å; $c=15.16$ Å; $\alpha=98.9°$; $\beta=125.5°$; $\gamma=108.9°$. No transition.	χ continuously decreases with increase in T. Metallic in the range 4.2–300 K; ρ (300 K)$\sim 10^{-3}$ Ωcm. α is negative and small in the range 4.2–300 K, decreases slightly with T and below 120 K, nearly constant ($\sim$1 μV/°C). No endothermic peak in DTA.	[17, 94, 103, 105, 186].
8; V_8O_{15}	$a=5.43$ Å; $b=6.99$ Å; $c=37.08$ Å; $\alpha=99.0°$; $\beta=128.5°$; $\gamma=109.0°$. $T_t=70$ K.	χ-T anomaly at T_t. Semiconductor-to-metal transition at T_t: $\Delta\rho\approx 10$; ρ (200 K) $\sim 10^{-3}$ Ωcm. α is negative and drops from -70 to -5 μV/°C at T_t; Above T_t, α is constant.	[97, 104, 105, 186].

The general characteristics of all the Magnéli phases, V_nO_{2n-1} are: (i) All have triclinic crystal structure at room temperature. (ii) Antiferromagnetic ordering is present at low temperatures and semiconductor-metal transitions are present at higher temperatures, T_t [105]. T_N is 70, 40, 30, 23, 43, and 7 K respectively, when n is 3, 4, 5, 6, 7, and 8. V_2O_3 ($n=2$), V_nO_{2n-1} ($3\leq n\leq 8$) and VO_2 ($n=\infty$) make an interesting comparison: $n=2$, $T_N=T_t$; $n=3$–8, $T_N<T_t$; $n=\infty$, $0=T_N<T_t$. (iii) α of all the phases is negative below and above T_t which shows that the predominant carriers are electrons. Above T_t, α is $\sim$10–12 μV/°C in all the phases which is characteristic of metallic conduction. Below T_t, α-T curve is complicated. (iv) DTA [105] gives ΔH (cal mol^{-1}) and ΔS (e.u.) values at T_t as follows: $n=4$, 142, 0.57; $n=5$, 215, 1.59; $n=6$, 222, 1.31; No data for $n=8$; V_3O_5 and V_7O_{13} show no transitions and are semiconducting and metallic respectively in the ranges 77 to 127 K and 4.2 to 300 K.

VO_2			
Crystal growth.	Single crystals of VO_2 are grown from V_2O_5 at high temperatures under various oxygen partial pressures.	Depending on the conditions large single crystals of varying stoichiometry can be grown.	[10, 28, 133].
Crystal structures of the phases and x-ray studies.	$T<340$ K: Monoclinic; space group, $P2_1/c$; $Z=4$; density, 4.65 g/cm^3 (obs.); 4.67 g/cm^3 (cacl.). $a=5.7517\pm 30$ Å; $b=4.5378\pm 25$ Å; $c=5.3825\pm 25$ Å; $\beta=122.646\pm 96°$. $T=346$ K: Tetragonal; space group, $P4/mnm$; $Z=2$; $a=4.551\pm 0.001$ Å; $c=2.851\pm 0.001$ Å. ΔV at the transition $=0.02\pm 0.05$ cm^3/mol. TEC (350–690 K)/°C: $\|^c$: $29.638\times 10^{-6}-2.930\times 10^{-8}\,t+2.576\times 10^{-11}\,t^2$; $\|^a$: $5.828\times 10^{-6}-7.091\times 10^{-9}\,t+6.946\times 10^{-12}\,t^2$. $325<T<340$ K: Triclinic, $a=5.80$ Å; $b=4.52$ Å; $c=5.38$ Å. $\alpha=91.5(5)°$; $\beta=122.7(8)°$; $\gamma=90.0°$.	Crystal symmetry changes at the transition; volume change is very small. Above T_t both a and c parameters increase but the relative increase in the c parameter is greater. NMR evidence shows the triclinic phase formation at 325 K. Cr, Al, and Fe are supposed to stabilize this phase. Also see [116a] for structural aspects of VO_2.	[61, 101, 109, 111, 112, 115, 116, 118, 125, 189].

Vanadium oxides—Continued

Oxide and description of the study	Data	Remarks and inferences	References
Magnetic properties.	Paramagnetic in the range 1.7–400 K; χ below and above T_t are almost temperature independent; slight anisotropy in χ is shown. $\chi = 1.0 \times 10^{-6}$ (emu/g) ($T < 340$ K); $\chi = 8.5 \times 10^{-6}$ (emu/g) ($T > 340$ K).	Jump in χ at T_t is noted; the exact cause of this is not understood clearly.	[17, 117, 120–122].
Electrical properties.	$T < 340$ K: Semiconductor behavior. $\rho \sim 10^{-3} - 10$ Ωcm; $E_a \sim$ 0.1–0.65 eV; $\alpha \sim 30$–1000 μV/°C (negative); $\mu_H \sim 0.1$–1.0 cm^{-2}/V s; $n_c \sim 10^{18}$–10^{19} cm^{-3} ($T \lesssim 340$ K); $m^* \sim 1.6$–7 m; $\alpha_F^* \sim 2$. $T > 340$ K: Metallic behavior $\rho \sim 2$ 5 ($\times 10^{-4}$) Ωcm; ρ lincarly increases with T; $\alpha \sim 23$ μV/°C (negative); $\mu_H \sim 1$–10 cm^{-2}/V s; $n_c \sim 10^{21}$–10^{23} cm^{-3}; $m^* \approx 0.5$ m. $dT/dP = +(0.082 \pm 0.005)$°C/kbar; $-dE_a/dP \sim (0.001$–$0.002)$ mV/kbar. ρ decreases with pressure at 300 K but no metallic behavior noted up to 300 kbar.	The wide variation in the properties of VO_2 in the low and high temperature region are believed to be due to the purity, method of preparation etc. Slight anisotropy exists in all the properties. Discontinuities at T_t in ρ, α, and R_H are noticed by various workers. A hysteresis of ~2° is noticed in ρ-T data. The pressure effects on T_t indicate qualitatively different behavior than that encountered in V_2O_3. Slight increase in carrier concentration is noticed with pressure but the effect is small and superpressures seem to be required to produce metallic conduction in VO_2 at room temperature.	[39, 61, 120, 128, 130, 134–137, 140].
Optical properties.	VO_2 exhibits infrared active phonon modes for $T < T_t$ (=341 K) in the energy range 0.02–0.09 eV. Above T_t, the infrared spectra show sudden increase in reflectivity. Reflectivity and transmission measurements in the range 0.25–5.0 eV below T_t indicate prominent absorption peaks at 0.85, 1.3, 2.8, and 3.6 eV. Above T_t, metallic free carrier absorption is observed below 2.0 eV, but the same two absorption peaks near 3 and 4 eV are present in the high temperature phase. $\epsilon_\infty = 5.54$ (300 K); 4.17 (355 K). According to Kawakubo [150], ϵ of VO_2 measured at 24 GHz increases monotonically from 22 to 26 in the range 100–300 K and attains a high value of 60 within a few degrees below T_t (340 K). This seems to indicate the onset of an intermediate ferro- or anti-ferroelectric phase [151] possessing a distinct triclinic structure [115, 125].	The data are consistent with the assumption of the appearance of ~10^{21} quasi free electrons per cm^3 in the metallic state and a filled oxygen 2p band ~2.5 eV below from the partially filled bands arising primarily from vanadium 3d orbitals. Transitions from the filled 2p bands are responsible for the high-energy peaks in optical absorption in both the high- and low-temperature phases. In the metallic phase there is evidence of overlap among the 3d bands such that at least two bands are partially occupied by the extra d electron per vanadium ion. In the semiconducting phase, a band gap of ~0.6 eV opens up within the 3d bands separating two filled bands from higher-lying empty bands.	[130, 139].

Vanadium oxides—Continued

Oxide and description of the study	Data	Remarks and inferences	References
Thermal properties.	DTA of pure VO_2 shows an endothermic reversible peak at 340 K. Some workers [116] have noticed two peaks at 342 and 346 K with slow heating rates (0.5°/min). $\Delta H = 750$ cal/mol; $C_p = 13$ cal/mol, °C (300 K) and shows a λ-type anomaly at T_t; $\theta_D = 750$ K; $\kappa \sim 40$–70 mW/cm°C at 300 K and is independent of temperature in the range 300–360 K.	First order nature of the transition is confirmed. DTA evidence is presented for the existence of a triclinic phase of VO_2 just below the transition.	[17, 80, 113, 116, 117, 119, 138].
Mössbauer studies.	No magnetic hyperfine splitting is noticed at any temperature in Fe^{57} doped VO_2. Isomer shift shows an anomaly at T_t while the quadrupole splitting goes to zero.	No long range magnetic order exists in VO_2 and the absence of quadrupole splitting in the high temperature phase indicates shielding of the nucleus by conduction electrons.	[75, 123, 190].
Electron and optical microscopic study of the phase transition.	The boundaries between the monoclinic and tetragonal phases during the transition in VO_2 have been observed in an electron microscope by the diffraction contrast at the interfaces which are revealed as fringe patterns. The growth of transformed regions from sites of nucleation is observed in micrographs.	This is a direct observation of the transition and various domains formed according to the different modes of transformation can easily be distinguished. It appears that the T_t and the rate of growth of domains are dependent on the mechanical strain.	[115, 191].
Infrared study of VO_2.	Bands at 720 and 1115 cm^{-1} are noted.	These seem to correspond to metal-oxygen vibrations.	[174].
V_nO_{2n+1} phases			
V_6O_{13}			
Crystal structure and properties.	$T = 300$ K: Monoclinic; space group, C2/m; $a = 11.90$ Å; $b = 3.67$ Å; $c = 10.12$ Å; $\beta = 100.87°$. Low temperature structure not known. DTA endothermic peak and χ-T anomaly at 177 ± 2 K; semiconductor-to-metal transition at 149 K.	The transition may be first order but the detailed properties are not known at present.	[16–18, 153].
V_4O_9			
Crystal structure.	$T = 300$ K: Orthorhombic; space group, Pnma; $Z = 4$; $a = 17.926 \pm 0.004$ Å; $b = 3.631 \pm 0.001$ Å; $c = 9.396 \pm 0.002$ Å.	The structure appears to be closely related to that of V_2O_5. The physical properties are not known at present.	[30].
V_3O_7			
Crystal structure and properties.	$T = 300$ K Monoclinic; space group, C2/C; $Z = 12$; $a = 21.92$ Å;	Detailed physical properties are not known at present.	[17, 29, 154, 155].

Magnéli phases, V_nO_{2n-1}	Crystal structure and transition temperature	Magnetic, electrical, DTA and Mössbauer studies	References
	$b=3.68$ Å; $c=18.34$ Å; $\beta=95.62°$. DTA does not indicate any transition in the range 130–950 K.		
V_2O_5			
Crystal structure and magnetic properties.	$T=300$ K: Orthorhombic; space group, Pmnm; $Z=2$; density, 3.357 g/cm³ (obs.); 3.37 g/cm³ (calc.); $a=11.519\pm0.006$ Å; $b=4.373\pm0.002$ Å; $c=3.564\pm0.002$ Å. $\chi=3.7\times10^{-6}$ cgs/g. TEC (300–870 K) ($\times10^6$/°C): $\|\|^a$, 2.0; $\|\|^b$, 55.4; $\|\|^c$, 8.0; average, 21.8; polycrystalline, 13.0.	V_2O_5 has a corrugated sheet type structure and predicts anisotropy in the TEC values; this is observed experimentally.	[157, 162].
Electrical properties.	Range, 77–450 K: Semiconductor; $\rho\sim10^3$ Ωcm; $\alpha\sim10$ μV/°C (negative). ρ-T plot shows breaks at 250 and 390 K. α goes through a maximum at 250 K. Anisotropy in ρ, E_a and α are noted. μ_D increases with T in the range 350–390 K.	Anisotropy in electrical transport properties is understandable because of the peculiar sheet type structure of V_2O_5. The breaks in ρ-T plots may correspond to the change in the mechanism of conduction (extrinsic to intrinsic).	[168, 192].

References

[1] Seybolt, A. U., and Sumsion, H. T., Trans. AIME 197, 292 (1953); J. Metals 5, 292 (1953).
[2] Schönberg, N., Acta Chem. Scand. 8, 221 (1954).
[3] Rostoker, W., and Yamamoto, A., Trans. Am. Soc. Metals 46, 1136 (1954); 47, 1002 (1955).
[4] Ozerov, R. P., Usp. Khim. 24, 951 (1955).
[5] Cambini, M., Heerschap, M., and Gevers, R., Mat. Res. Bull. 4, 633 (1969).
[6] Klemm, W., and Grimm, L., Z. anorg. allgem. Chem. 250, 142 (1942).
[7] Westman, S., and Nordmark, C., Acta Chem. Scand. 14, 465 (1960).
[8] Morozova, M. P., Konopel'ko, M. V., and Pinchuk, I. V., Vetn. Leningrad Univ., Ser. Fiz. i Khim. 19, 109 (1964).
[9] Katsura, T., and Hasegawa, M., Bull. Chem. Soc. Japan 40, 561 (1967).
[10] Kimizuka, N., Saeki, M., and Nakahira, M., Mat. Res. Bull. 5, 403 (1970).
[11] Okinaka, H., Kosuge, K., and Kachi, S., Japan J. Appl. Phys. 9, 224 (1970).
[12] Anderson, J. S., and Khan, A. S., J. Less-Comm. Metals 22, 209 (1970).
[13] Hoschek, E., and Klemm, W., Z. anorg. allgem. Chem. 242, 63 (1939).
[14] Burdese, A., Ann. Chim. (Rome) 47, 785 (1957); Chem. Abstr. 51, 17555d (1957).
[15] Grossmann, G., Proskurenko, O. W., and Ariya, S. M., Z. anorg. allgem. Chem. 305, 121 (1960).
[16] Aebi, F., Helv. Chim. Acta 31, 8 (1948).
[17] Kosuge, K., J. Phys. Chem. Solids 28, 1613 (1967).
[18] Andersson, G., Acta Chem. Scand. 8, 1599 (1954).
[19] Andersson, S., Acta Chem. Scand. 14, 1161 (1960).
[20] MacChesney, J. B., Potter, J. F., and Guggenheim, H. J., J. Electrochem. Soc. 115, 52 (1968).
[21] Theobald, F., Cabala, R., and Bernard, J., Compt. Rend. (Paris) 266C, 1534 (1968).
[22] Sata, T., Komada, E., and Ito, Y., Kogyo Kagaku Zasshi 71, 643 (1968).
[23] Sata, T., and Ito, Y., Kogyo Kagaku Zasshi 71, 647 (1968); Chem. Abstr. 69, 90305e (1968).
[24] Tilley, R. J. D., and Hyde, B. G., J. Phys. Chem. Solids 31, 1613 (1970).
[25] Pearson, W. B., J. Iron and Steel Inst. 164, 149 (1950).
[26] Stringer, J., J. Less-Comm. Metals 8, 1 (1965).
[27] Gel'd, P. V., Alyamovskii, S. I., and Matveenko, I. I., Zh. Strukt. Khim. 2, 301 (1961).
[28] Aramaki, S., and Roy, R., J. Mat. Sci. 3, 643 (1968).
[29] Tudo, J., and Tridot, G., Compt. Rend. (Paris) 261, 2911 (1965).
[30] Wilhelmi, K.-A., and Waltersson, K., Acta Chem. Scand. 24, 3409 (1970).
[31] Banus, M. D., and Reed, T. B., in The Chemistry of Extended Defects in non-Metallic Solids, Eds. L. Eyring and M. O'Keeffe (North Holand Publ. Co., Amsterdam, 1970), pp 488–522.
[32] Mathewson, C. H., Spire, E., and Samans, C. H., Trans. Am. Soc. Steel Treating 20, 357 (1932).
[33] Ariya, S. M., and Popov, Yu. G., Zh. Obshch. Khim. 32, 2077 (1962).
[34] Takeuchi, S., and Suzuki, K., Nippon Kinzoku Gak kaishi 31, 611 (1967).
[35] Loehman, R. E., Rao, C. N. R., and Honig, J. M., J. Phys. Chem. 73, 1781 (1969).

[36] Taylor, A., and Doyle, N. J., in The Chemistry of Extended Defects in non-Metallic Solids, Eds. L. Eyring and M. O'Keeffe (North Holland Publ. Co., Amsterdam, 1970), pp 523–540.
[37] Morin, F. J., Phys. Rev. Letters 3, 34 (1959).
[38] Austin, I. G., Phil. Mag. 7, 961 (1962).
[39] Minomura, S., and Drickamer, H. G., J. Appl. Phys. 34, 3043 (1963).
[40] Warren, W. W., Jr., Miranda, G. A., and Clark, W. G., Bull. Am. Phys. Soc. 12, 1117 (1967).
[41] Kawano, S., Kosuge, K., and Kachi, S., J. Phys. Soc. Japan 21, 2744 (1966).
[42] Warren, W. W., Jr., Gossard, A. C., and Banus, M. D., J. Appl. Phys. 41, 881 (1970).
[43] Honig, J. M., Wahnsiedler, W. E., Banus, M. D., and Reed, T. B., J. Solid State Chem. 2, 74 (1970).
[44] Goodenough, J. B., Bull. Soc. Chim. France 4, 1200 (1965).
[45] Adler, D., Feinleib, J., Brooks, H., and Paul, W., Phys. Rev. 155, 851 (1967).
[46] Adler, D., Solid State Phys. 21, 1 (1968).
[47] Adler, D., Rev. Mod. Phys. 40, 714 (1968).
[48] Hyland, G. J., J. Phys. C (Proc. Phys. Soc. Ser. 2) 1, 189 (1968).
[49] Mott, N. F., Phil. Mag. 20, 1 (1969).
[50] Doniach, S., Adv. Phys. 18, 819 (1969).
[51] Honig, J. M., IBM J. Res. & Develop. 14, 232 (1970).
[52] Rice, T. M., and McWhan, D. B., IBM J. Res. & Develop. 14, 251 (1970).
[53] Rao, C. N. R., and Subba Rao, G. V., Phys. Stat. Solidi (a) 1, 597 (1970).
[54] Rao, C. N. R., Ed., Modern Aspects of Solid State Chemistry, (Plenum Press, New York), 1970.
[55] Bosman, A. J., and van Daal, H. J., Adv. Phys. 19, 1 (1970).
[56] Hyland, G. J., J. Solid State Chem. 2, 318 (1970).
[57] Newnham, R. E., and de Haan, Y. M., Z. Krist. 117, 235 (1962).
[58] Dernier, P. D., J. Phys. Chem. Solids 31, 2569 (1970).
[59] Warekois, E. P., J. Appl. Phys. 31, 346 (1960).
[60] Jaffray, J., and Dumas, A., J. Rech. Centre Natl. Rech. Sci. Lab. Bellevue (Paris) 5, 360 (1954); Chem. Abstr. 49, 6759d (1955).
[61] Minomura, S., and Nagasaki, H., J. Phys. Soc. Japan 19, 131 (1964).
[62] McWhan, D. B., Rice, T. M., and Remeika, J. P., Phys. Rev. Letters 23, 1384 (1969).
[63] McWhan, D. B., and Remeika, J. P., Phys. Rev. B2, 3734 (1970).
[64] Dernier, P. D., and Marezio, M., Phys. Rev. B2, 3771 (1970).
[65] Moon, R. M., Phys. Rev. Letters 25, 527 (1970); J. Appl. Phys. 41, 883 (1970).
[66] Foëx, M., Goldsztaub, J., Jaffrey, R., Lyand, R., Wey, R., and Wucher, J., J. Rech. Centre Natl. Rech. Sci. Lab., Bellevue (Paris) 21, 237 (1952).
[67] Carr, P. H., and Foner, S., J. Appl. Phys. 31, 344S (1960).
[68] Menth, A., and Remeika, J. P., Phys. Rev. B 2, 3756 (1970).
[69] Foëx, M., Compt. Rend. (Paris) 223, 1126 (1946); 229, 880 (1949).
[70] Goodman, G., Phys. Rev. Letters 9, 305 (1962).
[71] Acket, G. A., and Volger, J., Physica 28, 277 (1962).
[72] Kachi, S., Takada, T., and Kosuge, K., J. Phys. Soc. Japan 18, 1839 (1963).
[73] Takei, H., and Koide, S., J. Phys. Soc. Japan 21, 1010 (1966).
[74] Shinjo, T., and Kosuge, K., J. Phys. Soc. Japan 21, 2622 (1966).
[75] Kosuge, K., J. Phys. Soc. Japan 22, 551 (1967).
[76] Feinleib, J., and Paul, W., Phys. Rev. 155, 841 (1967).
[77] McWhan, D. B., and Rice, T. M., Phys. Rev. Letters 22, 887 (1969).
[78] Austin, I. G., and Turner, C. E., Phil. Mag. 19, 939 (1969).
[79] MacMillan, A. J., Laboratory for Insulation Res., M.I.T. Tech. Rept. No. 172, 1962 (unpublished); quoted in [76].
[80] Anderson, C. T., J. Amer. Chem. Soc. 58, 564 (1936).
[81] Jones, E. D., Phys. Rev. 137, A978 (1965); J. Phys. Soc. Japan 20, 1292 (1965).
[82] Nagasawa, H., Takeshita, S. K., Tomono, Y., Minomura, S., and Okai, B., J. Phys. Soc. Japan 19, 2232 (1964).
[83] Rubenstein, M., Solid State Commun. 8, 1469 (1970); Phys. Rev. B 2, 4731 (1970).
[84] Gossard, A. C., McWhan, D. B., and Remeika, J. P., Phys. Rev. B 2, 3762 (1970); J. Appl. Phys. 41, 864 (1970).
[85] Gainotti, A., Ghezzi, C., and Manfredi, M., Nuovo Cimento 62B, 121 (1969).
[86] Samokhvalov, A. A., Sov. Phys.—Solid State (English Transl.) 3, 2613 (1962).
[87] Barker, A. S., Jr., and Remeika, J. P., Solid State Commun. 8, 1521 (1970).
[88] Nakahira, M., Horiuchi, S., and Ooshima, H., J. Appl. Phys. 41, 836 (1970).
[89] Mott, N. F., Canad. J. Phys. 34, 1356 (1956) and references there in.
[90] Jayaraman, A., McWhan, D. B., Remeika, J. P., and Dernier, P. D., Phys. Rev. B 2, 3751 (1970).
[91] Aronov, A. G., and Kudinov, E. K., Sov. Phys.—JETP (English Transl.) 28, 704 (1969).
[92] Brinkman, W. F., and Rice, T. M., Phys. Rev. B 2, 1324 (1970).
[93] Ramirez, R., Falicov, L. M., and Kimball, J. C., Phys. Rev. B 2, 3283 (1970).
[94] Nagasawa, K., Bando, Y., and Takada, T., Japan J. Appl. Phys. 8, 1262 (1969).
[95] Nagasawa, K., Bando, Y., and Takada, T., Japan J. Appl. Phys. 8, 1267 (1969).
[96] Nagasawa, K., Bando, Y., and Takada, T., Japan J. Appl. Phys. 9, 407 (1970).
[97] Nagasawa, K., Bando, Y., Takada, T., Horiuchi, H., Tokonami, M., and Morimoto, N., Japan J. Appl. Phys. 9, 841 (1970).
[98] Okinaka, H., Nagasawa, K., Kosuge, K., Bando, Y., Takada, T., and Kachi, S., J. Phys. Soc. Japan 27, 1366 (1969).
[99] Asbrink, S., Friberg, S., Magnéli, A., and Andersson, G., Acta Chem. Scand. 13, 603 (1959).
[100] Okinaka, H., Nagasawa, K., Kosuge, K., Bando, Y., Kachi, S., and Takada, T., J. Phys. Soc. Japan 28, 798 (1970).
[101] Marezio, M., Dernier, P. D., McWhan, D. B., and Remeika, J. P., Mat. Res. Bull. 5, 1015 (1970).
[102] Okinaka, H., Nagasawa, K., Kosuge, K., Bando, Y, Kachi, S., and Takada, T., J. Phys. Soc. Japan 28, 803 (1970).
[103] Okinaka, H., Nagasawa, K., Kosuge, K., Bando, Y., Kachi, S., and Takada, T., J. Phys. Soc. Japan 29, 245 (1970).
[104] Okinaka, H., Kosuge, K., Kachi, S., Nagasawa, K., Bando, Y., and Takada, T., Phys. Letters 33A, 370 (1970).
[105] Kachi, S., Kosuge, K., and Okinaka, H., J. Solid State Chem. 6, 258 (1973).
[106] Goodenough, J. B., Czech. J. Phys. 17B, 304 (1967).
[107] Goodenough, J. B., Mat. Res. Bull. 2, 37 (1967); 2, 165 (1967).
[108] Paul, W., Mat. Res. Bull. 5, 691 (1970).
[109] Andersson, G., Acta Chem. Scand. 10, 623 (1956).
[110] Westman, S., Acta Chem. Scand. 15, 217 (1961).
[111] Rogers, D. B., Shannon, R. D., Sleight, A. W., and Gillson, J. L., Inorg. Chem. 8, 841 (1969).
[112] Longo, J. M., and Kierkegaard, P., Acta Chem. Scand. 24, 420 (1970).
[113] Rao, C. N. R., Natarajan, M., Subba Rao, G. V., and Loehman, R. E., J. Phys. Chem. Solids 32, 1147 (1971).
[114] Kawakubo, T., and Nakagawa, T., J. Phys. Soc. Japan 19, 517 (1964).
[115] Mitsuishi, T., Japan J. Appl. Phys. 6, 1060 (1967).
[116] Nygren, M., and Israelson, M., Mat. Res. Bull 4, 881 (1969).
[117] Berglund, C. N., and Guggenheim, H. J., Phys. Rev. 185, 1022 (1969).

[118] Hyland, G. J., and Taylor, A. W. B., J. Phys. Soc. Japan **21**, 819 (1966).
[119] Klemm, W., and Grimm, L., Naturwiss. **27**, 787 (1939).
[120] Rüdorff, W., Walter, G., and Stadler, J., Z. anorg. allgem. Chem. **297**, 1 (1958).
[121] Ariya, S. M., and Grossmann, G., Sov. Phys.—Solid State (English Transl.) **2**, 1166 (1960).
[122] Kosuge, K., Takada, T., and Kachi, S., J. Phys. Soc. Japan **18**, 318 (1963).
[123] Wertheim, G. K., Buchanen, O. N. E., and Guggenheim, H. J., Bull. Amer. Phys. Soc. **12**, 23 (1967).
[124] Umeda, J., Kusumoto, H., Narita, K., and Yamada, E., J. Chem. Phys. **42**, 1458 (1965).
[125] Umeda, J., Ashida, S., Kusumoto, H., and Narita, K., J. Phys. Soc. Japan **21**, 1461 (1966).
[126] Neuman, C. H., Lawson, A. W., and Brown, R. F., J. Chem. Phys. **41**, 1591 (1964).
[127] Sasaki, H., and Watanabe, A., Phys. J. Phys. Soc. Japan **19**, 1748 (1964).
[128] Bongers, P. F., Solid State Commun. **3**, 275 (1965).
[129] Ohashi, T., and Watanabe, A., J. Am. Ceram. Soc. **49**, 519 (1966).
[130] Barker, A. S., Jr., Verleur, H. W., and Guggenheim, H. J., Phys. Rev. Letters **17**, 1286 (1966).
[131] Hill, G. J., and Martin, R. H., Phys. Letters **27A**, 34 (1968).
[132] Everhart, C. R., and MacChesney, J. B., J. Appl. Phys. **39**, 2872 (1968).
[133] MacChesney, J. B., and Guggenheim, H. J., J. Phys. Chem. Solids **30**, 225 (1969).
[134] Ladd, L., and Paul, W., Solid State Commun. **7**, 425 (1969).
[135] Kitahiro, I., and Watanabe, A., J. Phys. Soc. Japan **21**, 2423 (1966).
[136] Rao, C. N. R., and co-workers, unpublished results.
[137] Kitahiro, I., Ohashi, T., and Watanabe, A., J. Phys. Soc. Japan **21**, 2422 (1966).
[138] Cook, O. A., J. Am. Chem. Soc. **69**, 331 (1947).
[139] Verleur, H. W., Barker, A. S., Jr., and Berglund, C. N., Phys. Rev. **172**, 788 (1968).
[140] Berglund, C. N., and Jayaraman, A., Phys. Rev. **185**, 1034 (1969).
[141] Marinder, B.-O., and Magnéli, A., Acta Chem. Scand. **11**, 1635 (1957).
[142] Rüdorff, W., and Marklin, J., Z. anorg. allgem. Chem. **334**, 142 (1964).
[143] Sakata, K., and Sakata, T., Japan J. Appl. Phys. **6**, 112 (1967).
[144] Kristensen, I. K., J. Appl. Phys. **39**, 5341 (1968).
[145] Kristensen, I. K., J. Appl. Phys. **40**, 4992 (1969).
[146] Futaki, H., and Aoki, M., Japan J. Appl. Phys. **8**, 1008 (1969).
[147] Israelson, M., and Kihlborg, L., Mat. Res. Bull. **5**, 19 (1970).
[148] Villeneuve, G., Bordet, A., Casalot, A., and Hagen-Muller, P., Mat. Res. Bull. **6**, 119 (1971).
[149] Adler, D., and Brooks, H., Phys. Rev. **155**, 826 (1967).
[150] Kawakubo, T., (quoted in [56]).
[151] Fröhlich, H., in Ferroelectricity, Ed. E. F. Weller (Elsevier Publ. Co., Amsterdam, 1967).
[152] Brews, J. R., Phys. Rev. B **1**, 2556 (1970).
[153] Kanazawa, K. K., Bull. Amer. Phys. Soc. **12**, 1120 (1967).
[154] Thomas, D., Tudo, J., and Tridot, G., Compt. Rend. (Paris) **265**, 183 (1967).
[155] Andersson, S., Galy, J., and Wilhelmi, K. A., Acta Chem. Scand. **24**, 1473 (1970).
[156] Bystrom, A., Wilhelmi, K. A., and Brotzen, O., Acta Chem. Scand. **4**, 1119 (1950).
[157] Bachmann, H. G., Ahmed, F. R., and Barnes, W. H., Z. Krist. **115**, 110 (1961).
[158] Bachmann, H. G., and Barnes, W. H., Z. Krist. **115**, 215 (1961).
[159] Abdullaev, A. A., Belyaev, L. M., Binarov, I. V., Dobrzhanskii, G. F., and Yankelevich, R. G., Sov. Phys.—Crystallogr. (English Transl.) **14**, 957 (1970).
[160] King, B. W., and Suber, L. L., J. Am. Ceram. Soc. **38**, 306 (1955).
[161] Corvin, I., and Cartz, L., J. Am. Ceram. Soc. **48**, 328 (1965).
[162] Kennedy, T. N., Hakim, R., and Mackenzie, J. D., Mat. Res. Bull. **2**, 193 (1967).
[163] Holtzberg, F., Reisman, A., Berry, M., and Berkenblit, M., J. Am. Chem. Soc. **78**, 1536 (1956).
[164] Simard, G. L., Stegar, J. F., and Arnott, R. J., Ind. Eng. Chem. **47**, 1424 (1955).
[165] Clark, H., and Berets, D. J., Advances in Catalysis (Academic Press, N.Y.) **9**, 204 (1957).
[166] Patrina, I. B., and Ioffe, V. A., Sov. Phys.—Solid State (English Transl.) **6**, 2581 (1965).
[167] Allersma, T., Hakim, R., Kennedy, T. N., and MacKenzie, J. D., J. Chem. Phys. **46**, 154 (1967).
[168] Volzhenskii, D. S., and Pashkavskii, M. V., Sov. Phys.—Solid State (English Transl.) **11**, 950 (1969).
[169] Haemers, J., Compt. Bend. (Paris) **259**, 3740 (1964).
[170] Hagenmuller, P., in The Chemistry of Extended Defects in non-Metallic Solids, Eds. L. Eyring and M. O'Keeffe (North Holland Publishing Comp., Amsterdam, 1970), pp 91–108.
[171] Kawano, S., Kosuge, K., and Kachi, S., J. Phys. Soc. Japan **27**, 1076 (1969).
[172] Gel'd, P. V., Shveikin, G. P., Alyamovskii, S. I., and Tskhai, V. A., Russ. J. Inorg. Chem. **12**, 1053 (1967).
[173] Rao, C. N. R., Wahnsiedler, W. E., and Honig, J. M., J. Solid State Chem. **2**, 315 (1970).
[174] Alyamovskii, S. I., Shveikin, G. P., and Gel'd, P. V., Russian J. Inorg. Chem. **12**, 915 (1967).
[175] Norwood, T. E., and Fry, J. L., Phys. Rev. B **2**, 472 (1970).
[176] Abrahams, S. C., Phys. Rev. **130**, 2230 (1963).
[177] Goodenough, J. B., Magnetism and the Chemical Bond (Interscience, John Wiley and Sons, New York-London) 1963.
[178] Jesser, R., and Silhouette, D., Compt. Rend. (Paris) **264B**, 1123 (1967).
[179] Kosuge, K., and Kachi, S., J. Phys. Soc. Japan **20**, 627 (1965).
[180] Arnold, D. J., and Mires, R. W., J. Chem. Phys. **48**, 2231 (1968).
[181] Heidemann, A., Z. Physik. **238**, 208 (1970).
[182] Zhuze, V. P., Andreev, A. A., and Shelykh, A. I., Sov. Phys.—Solid State (English Transl.) **10**, 2914 (1969).
[183] Andres, K., Phys. Rev. B **2**, 3769 (1970).
[184] Andreev, V. N., Aronov, A. G., and Chudnovskii, F. A., Sov. Phys.—Solid State (English Transl.) **12**, 1230 (1970).
[185] Nebenzahl, I., and Weger, M., Phys. Rev. **184**, 936 (1969).
[186] Magnéli, A., in Transition Metal Compounds, Informal Proc. of the Bukl Intern. Conf. on Materials, ed. E. R., Schatz (Gordon and Breach, New York, 1964).
[187] Magnéli, A., Andersson, S., Åsbrink, S., Westman, S., and Holmberg, B., PB Rep., 145923, U.S. Dept. Comm. Office of Tech. Ser. 1961.
[188] Krishna Rao, K. V., Naidu, S. V. N., and Iyengar, L., J. Phys. Soc. Japan **23**, 1380 (1967).
[189] Hazony, Y., and Perkins, H. K., J. Appl. Phys. **41**, 5130 (1970).
[190] Rao, C. N. R., Ramdas, S., Loehman, R. E., and Honig, J. M., J. Solid State Chem. **3**, 83 (1971).
[191] Hayashi, Y., van Landuyt, J., and Amelinckx, S., Phys. Stat. Solidi **39**, 189 (1970).
[192] Elyutin, V. P., Povlov, Yu. A., and Manukhin, A. V., Sb. Mosk. Inst. Stali Splavov, No. 49, 46 (1968); Chem. Abstr. **70**, 32635x (1969).

I.4. Chromium Oxides

Many binary oxides are known in the Cr-O system. Schonberg [1] described the existence of Cr_3O, but detailed investigations have not yet been carried out. CrO does not exist in the stable state and attempts have been made to stabilize it in the form of solid solutions [2]. The known oxides of chromium are Cr_2O_3 [3], CrO_2 [4], Cr_5O_{12} [5], an oxide of the composition $CrO_{2.44}$ [6], Cr_6O_{15}, or Cr_2O_5 [6–8], a nonstoichiometric oxide $CrO_{2.65}$ [6], Cr_3O_8 [8] and CrO_3 [6–9]. Cr_3O_4 has been reported by a few workers [10, 11], but recent work [12] has failed to indicate the existence of this material as a stable phase. Cr_2O_3 and CrO_2 have been extensively investigated in the literature.

Cr_2O_3: Cr_2O_3 is rhombohedral (pseudo hexagonal) and is antiferromagnetic below 308 K. Even though it has the same corundum structure as α-Fe_2O_3, the spin structure differs and precludes the possibility of superimposed ferromagnetism below T_N [13–19]. The crystal structure does not change at T_N, but discontinuities in the lattice parameters are noted [20]; in particular, the body diagonal c parameter is contracted slightly on heating through T_N. Below T_N, χ (perpendicular to the [111] direction) is almost temperature independent whilst χ parallel to the [111] direction approaches (but does not become) zero at 0 K [14, 21]. Cr_2O_3 exhibits magnetoelectric effect below T_N and various workers have studied this phenomenon [22–27]. Anomalies in ρ [28, 29], ultrasonic sound velocity [30–32], Young's modulus [33] and dielectric constant [25, 26, 34] have been noted in Cr_2O_3 at $\sim T_N$.

High pressure x-ray studies [35] indicate no crystallographic transition in Cr_2O_3; however, T_N decreases linearly with pressure up to ~13 kbar [36]. T_N also seems to depend on particle size of Cr_2O_3 [37] to a small extent. Recently, Kawai and Mochizuki [38] noticed a transition from insulator to highly conductive state in Cr_2O_3 under static high pressure conditions (>2 Mbar).

Cr_2O_3 forms solid solutions with other oxides of corundum structure like Al_2O_3 [3, 39–41], Fe_2O_3 [18, 42] and Mn_2O_3 [42] and the nature of magnetic interactions and other physical properties have been investigated in detail.

CrO_2: The dioxide of chromium, CrO_2, has a number of interesting properties which include ferromagnetism and metallic electrical conductivity. Many methods have been reported in the literature for the preparation of CrO_2 [2, 6, 8, 43–52] but the material is actually a metastable form and will, on heating to ~720 K, transform irreversibly to Cr_2O_3 [53]. Recent work has shown [51, 54] that CrO_2 can be held for considerable period of time without decomposition at temperatures 1170 to 1770 K at pressures of 60–65 kbar.

CrO_2 has a tetragonal rutile structure and its lattice constants do not vary with slight changes in the O/Cr ratio [48, 51, 52] and the rutile structure exists in the range 300 to 673 K [55, 56]. Magnetic measurements [4, 57–59] and Mössbauer data [60] indicate that the oxide is ferromagnetic with $T_c \sim$ 395 K. ρ-T data in the range 80–575 K indicate that it exhibits a positive temperature coefficient of ρ and is a typical metal [4, 48, 49, 51, 61–64]; discontinuities in ρ and α are noted at T_c. Optical and heat capacity data [65, 66] are also consistent with the metallic nature of CrO_2.

CrO_2 forms solid solutions with VO_2 [67, 68] and MnO_2 [69] with the associated changes in the physical properties.

Cr_5O_{12}: Cr_5O_{12} is formed under high pressure conditions at ~500 K and has orthorhombic symmetry [6, 7]; the substance appears to be nonferromagnetic but detailed physical properties are not known at present.

$CrO_{2.44}$: This oxide is obtained by the decomposition of CrO_3 at a pressure of 600 bar and ~510 K [6]; the structure and other properties have not yet been investigated.

Cr_6O_{15} (Cr_2O_5): Kubota [8] reported the formation of Cr_2O_5 by the decomposition of CrO_3 at high oxygen pressures but the structure is not known. On the other hand, Wilhelmi [6, 7] reported the formation of orthorhombic Cr_6O_{15} at pressures >1 kbar and 490 K; pertinent physical properties, however, are not known at present.

$CrO_{2.65}$: This nonstoichiometric oxide reported by Wilhelmi [6] is obtained by the decomposition of CrO_3 in air at 540 to 570 K. Detailed data are lacking.

Cr_3O_8: This oxide is formed by the decomposition of anhydrous CrO_3 [8]. It is not very stable and decomposes at 650 K. The crystal structure and other properties are not known.

CrO_3: Chromium trioxide, CrO_3, is a stable material but absorbs moisture. It is orthorhombic and the structure consists of linear chains of corner-sharing CrO_4 tetrahedra [6, 9, 70]. Electrical transport studies [71] indicate it to be a semiconductor over a wide temperature range. No crystal structure transitions at ordinary pressures are known but ρ studies at high pressures [72] indicate a first order transition at ~140–145 kbar pressure and the sample retains the semiconductor behavior. Other properties of CrO_3 have not been investigated in detail.

Oxide and description of the study	Data	Remarks and inferences	References
Cr_2O_3			
Crystal structure and x-ray studies.	Hexagonal; space group, $R\bar{3}C$; $Z=6$. $T=291$ K: $a=4.9575$ Å; $c=13.5976$ Å. $T=313$ K: $a=4.9605$ Å; $c=13.5945$ Å. Discontinuities are encountered in a and c parameters at $\sim T_N$ (308 K); c axis contracts on heating through T_N. Pressure also decreases c parameter.	No change in the crystal structure takes place through the transition region.	[6, 20, 35, 73].
χ-T data.	$T=4.2$ K; $\chi=22.4\times10^{-6}$ emu/g (parallel to [111] direction). The sublattice magnetization drops from ~1.5 to zero at T_N. Magnetic moment $= 2.76\pm0.03$ μ_B. Anisotropy in χ is shown. $T_N=308\pm1$ K; T_N decreases linearly with pressure; $\partial T_N/\partial P=-1.6\pm0.3$ K/kbar.	χ-T plot is typical of an antiferromagnetic material. Increase of pressure seems to bring about the collapse of the antiferromagnetic spin structure at a given temperature.	[14, 21, 36, 74, 75].
Electrical properties.	Semiconductor behavior in the range 300–1600 K. $\rho\sim10^5$ Ωcm at 300 K; $E_a\sim0.4$ eV ($T<1500$ K); $E_a\sim2.5$ eV ($T>1520$ K). $\alpha=0.2$–0.4 mV/°C at ~500 K; p type; $\mu_D\sim10^5$ cm²/V s at ~500 K.	The available data indicate that the conduction is extrinsic below 1200 K dominated by impurities or native defects with hopping of holes between Cr^{4+} and Cr^{3+} sites. Intrinsic conduction sets in at $T\gtrsim1500$ X.	[28, 29, 71, 76–82].
Dielectric properties.	$\epsilon_\infty\approx8$ (300 K) and the ϵ value at zero and high magnetic fields and at high frequencies show anomalies at T_N.	The magnetoelectric effect associated with Cr_2O_3 below T_N is because of the magnetic ordering of the Cr^{3+} spins.	[25, 26, 34].
Mechanical properties.	Young's modulus $\approx$ 96 dyn/cm² at 273 K and shows anomalous variation in going through T_N. Compressibility $\sim4.5\times10^{-4}$ (kbar)$^{-1}$ at 300 K.	The anomaly in the Young's modulus in Cr_2O_3 is quite different from the one encountered in CoO and NiO and is attributed to the domain phenomena and differences in the magnetic order.	[33, 40].
Optical properties.	Bands are noted at 14 390, 16 610, 21 690, 27 030 and 39 220 cm^{-1} and are attributed to the crystal field transitions. Well defined infrared bands are encountered in region 300–750 cm^{-1} and are due to vibrations of the Cr-O bond. $10\,Dq=16\,610$ cm^{-1}; $B=478$ cm^{-1}.	The data indicate the localized nature of the electrons in Cr_2O_3.	[83].
CrO_2			
Crystal structure and x-ray studies.	Tetragonal; space group, $P4/mnm$; $Z=2$; $a=4.421$ Å; $c=2.916$ Å.	Typical rutile structure; TEC shows high anisotropy and in	[4, 8, 51, 52, 55, 56].

Chromium oxides—Continued

Oxide and description of the study	Data	Remarks and inferences	References
	TEC (/°C): $T=303$ K: $\|\|^c = -14.84\times10^{-6}$; $\|\|^a = +18.61\times10^{-6}$. $T=640$ K: $\|\|^c = -0.1\times10^{-6}$; $\|\|^a = +13.52\times10^{-6}$.	fact $\|\|^c$ axis is negative. No crystal structure change in going through T_c.	
Magnetic properties.	Ferromagnetic; T_c~392–398 K depending on the sample. Magnetic moment = 2.07±0.03 μ_B. Specific magnetization = 138.3 at 0 K. $\chi\sim2\times10^{-4}$ emu/g. at 500 K.	Typical ferromagnetic behavior exhibited by single and polycrystalline samples. The properties of CrO_2 are adequately explained on the basis of Goodenough's model [48, 84, 85].	[4, 48, 57–59, 84, 85].
Electrical properties.	Metallic in the range 80–575 K; $\rho\sim10^{-4}$ Ωcm (300 K); $\alpha\approx-10$ μV/K (300 K); exhibits discontinuities in ρ, α at T_c. Semiconductor behavior is not encountered above T_c contrary to the expectations. Magnetoresistance effects noted; at 298 K in a field of 29 kOe (applied parallel to [001] axis), $(\Delta\rho/\rho)=(-1.8\pm0.2)\%$.	Typical metallic behavior; the electrical properties are explained in a rational manner by the Goodenough's model [48, 84, 85].	[4, 48, 49, 51, 61–64, 84, 85].
Mössbauer studies of ^{57}Fe doped CrO_2.	Fe atoms exist as Fe^{3+}; hyperfine splitting of the spectra disappears at T_c (397 K). Magnetic moment = $2\mu_B$ per Cr^{4+} ion at 0 K; internal magnetic field = 530 kOe.	A novel study of the transition in CrO_2; T_c agrees well with other measured values; internal field drops to zero at T_c as expected.	[60].
Cr_5O_{12}			
Crystal structure at 300 K.	Orthorhombic; space group, Pbcn; $Z=4$; $a=12.044$ Å; $b=8.212$ Å; $c=8.177$ Å. The structure contains pairs of CrO_6 octahedra joined by sharing edges; by sharing corners, the pairs of octahedra are linked with CrO_4 tetrahedra to form a three dimensional frame work. Trivalent and hexavalent Cr atoms seem to be present.	—	[6, 7].
Cr_6O_{15} (Cr_2O_5)			
Crystal structure at 300 K.	Orthorhombic; space group, Cmcm or C2cm or Cmc2; $Z=4$; $a=8.47$ Å; $b=12.90$ Å; $c=10.08$ Å. Kubota [8] reports that Cr_2O_5 has a high value of ρ ($\sim10^{10}$ Ωcm) at 300 K.	Detailed structural and other data are lacking.	[6–8]
CrO_3			
Crystal structure at 300 K.	Orthorhombic, space group, C2cm; $Z=4$; $a=4.789\pm0.005$ Å; $b=8.557\pm0.005$ Å; $c=5.743\pm0.004$ Å.	CrO_3 has a chain structure.	[6, 9, 70].

Oxide and description of the study	Data	Remarks and inferences	References
	The structure consists of linear chains of corner-sharing CrO_4 tetrahedra.		
Electrical properties.	Semiconductor behavior; $\rho \sim 10^5$–10^6 Ωcm. ρ studies at high pressures indicate a transition at ~140–145 kbars with considerable decrease in the value of ρ but CrO_3 remains semiconducting up to very high pressures.	Detailed data are, however, lacking on CrO_3 at present.	[71, 72].

References

[1] Schönberg, N., Acta Chem. Scand. 8, 221 (1954).
[2] Brauer, G., Reuther, H., Walz, H., and Zapp, K. H., Z. anorg. allgem. Chem. 369, 144 (1969).
[3] Bunting, E. N., J. Res. Nat. Bur. Stand. (U.S.), 6, 947 (1931).
[4] Guillaud, C., Michael, A., Binard, J., and Fallot, M., Compt. Rend. (Paris) 219, 58 (1944).
[5] Wilhelmi, K.-A., Acta Chem. Scand. 19, 165 (1965).
[6] Wilhelmi, K.-A., Acta Chem. Scand. 22, 2565 (1968).
[7] Wilhelmi, K.-A., Nature (Lond.) 203, 967 (1964).
[8] Kubota, B., J. Am. Ceram. Soc. 44, 239 (1961).
[9] Bystrom, A., and Wilhelmi, K.-A., Acta Chem. Scand. 4, 1131 (1950).
[10] Hilty, D. C., Forgeng, W. D., and Folkman, R. L., J. Metals 7, 253 (1955); Trans. AIME 203, 253 (1955).
[11] Layden, G. K., J. Am. Ceram. Soc. 48, 219 (1965).
[12] Johnson, R. E., and Muan, A., J. Am. Ceram. Soc. 51, 430 (1968).
[13] Brockhouse, B. N. J., J. Chem. Phys. 21, 961 (1953).
[14] McGuire, T. R., Scott, E. J., and Grannis, F. H., Phys. Rev. 102, 1000 (1956).
[15] Li, Y. Y., Phys. Rev. 102, 1015 (1956).
[16] Goodenough, J. B., Phys. Rev. 117, 1442 (1960).
[17] Osmond, W. P., Proc. Phys. Soc. (Lond.) 79, 394 (1962).
[18] Cox, D. E., Takei, W. J., and Shirane, G., J. Phys. Chem. Solids 24, 405 (1963).
[19] Pratt, G. W., Jr., and Bailey, P. T., Phys. Rev. 131, 1923 (1963).
[20] Greenwald, S., Nature (Lond.) 177, 286 (1956).
[21] Foner, S., Phys. Rev. 130, 183 (1963).
[22] Asrov, D. N., Sov. Phys.—JETP (English Transl.) 13, 729 (1961).
[23] Shtrikman, S., and Treves, D., Phys. Rev. 130, 986 (1963).
[24] Hornreich, R., and Shtrikman, S., Phys. Rev. 161, 506 (1967).
[25] Lal, H. B., Srivastava, R., and Srivastava, K. G., Phys. Rev. 154, 505 (1967).
[26] Srivastava, K. G., Kant, P., and Srivastava, R., Ind. J. Pure and Appl. Phys. 8, 755 (1970).
[27] O'Dell, T. H., and White, E. A. D., Phil. Mag. 22, 649 (1970).
[28] Roche, J., and Jaffrey, J., Compt. Rend. (Paris) 240 2212 (1955).
[29] Hagel, W. C., J. Appl. Phys. 36, 2586 (1965).
[30] Shapira, Y., Phys. Letters 24A, 361 (1967); J. Appl. Phys. 42, 1588 (1971).
[31] Street, R., Munday, B. C., Window, B., and Williams, I. R., J. Appl. Phys. 39, 1050 (1968).
[32] Tani, H., J. Phys. C (Solid State Phys.) 3, 1597 (1970).
[33] Street, R., and Lewis, B., Phil. Mag. 1, 663 (1956).
[34] Samokhvalov, A. A., Sov. Phys.—Solid State (English Transl.) 3, 2613 (1962).
[35] Lewis, G. K., Jr., and Drickamer, H. G., J. Chem. Phys. 45, 224 (1966).
[36] Worlton, T. G., Brugger, R. M., and Bennion, R. B., J. Phys. Chem. Solids 29, 435 (1968).
[37] Gunsser, W., Hille, W., and Knappwost, A., Z. Naturforsch. 23a, 781 (1968).
[38] Kawai, N., and Mochizuki, S., Phys. Letters 36A, 54 (1971).
[39] Saalfeld, H., Z. Krist. 120, 342 (1964).
[40] Rossi, L. R., and Lawrence, W. G., J. Am. Ceram. Soc. 53, 604 (1970).
[41] Schultz, A. H., and Stubican, V. S., J. Am. Ceram. Soc. 53, 613 (1970).
[42] Wretblad, P. E., Z. anorg. allgem. Chem. 189, 329 (1930).
[43] Michel, A., and Benard, J., Compt. Rend. (Paris) 200, 1316 (1935); Bull. Soc. Chim. 10, 315 (1943).
[44] Schwartz, R. S., Funkuchen, I., and Ward, R., J. Am. Chem. Soc. 74, 1676 (1952).
[45] Ariya, S. M., Shchukarev, S. A., and Glushkova, V. B., Zhur. Obschchei. Khim. 23, 1241 (1953).
[46] Thamer, B. J., Douglass, R. M., and Staritzky, E., J. Am. Chem. Soc. 79, 547 (1957).
[47] Kubota, B., Nishikawa, T., Yanase, A., Hirota, E., Mihara, T., and Iida, Y., J. Am. Ceram. Soc. 46, 550 (1963).
[48] Chapin, D. S., Kafalas, J. A., and Honig, J. M., J. Phys. Chem. 69, 1402 (1965).
[49] Nakayama, N., Hirota, E., and Nishikawa, T., J. Am. Ceram. Soc. 49, 52 (1966).
[50] DeVries, K. J., Naturwiss, 54, 563 (1967).
[51] Chamberland, B. L., Mat. Res. Bull. 2, 827 (1967).
[52] Shibasaki, Y., Kanamura, F., Koizumi, M., Ado, K., and Kume, S., Mat. Res. Bull. 5, 1051 (1970).
[53] Rodbell, D., and DeVries, R., Mat. Res. Bull. 2, 491 (1967).
[54] DeVries, R. C., Mat. Res. Bull. 2, 999 (1967).
[55] Siratori, K., and Iida, S., J. Phys. Soc. Japan 17B (Suppl.), 208 (1962).
[56] Krishna Rao, K. V., and Iyengar, L., Acta Cryst. 25A, 302 (1969).
[57] Flippen, R. B., J. Appl. Phys. 34, 2026 (1963).
[58] Rodbell, D. S., J. Phys. Soc. Japan 21, 1224 (1966).
[59] Stoffel, A. M., J. Appl. Phys. 40, 1238 (1969).
[60] Shinjo, T., Takada, T., and Tamagawa, N., J. Phys. Soc. Japan 26 1404 (1969).

[61] Kubota, D., and Hirota, E., J. Phys. Soc. Japan 16, 345 (1961).
[62] Rodbell, D. S., Lommel, J. M., and DeVries, R. C., J. Phys. Soc. Japan 21, 2430 (1966).
[63] Nishikawa, T., Nakayama, N., and Hirota, E., Yogyo Kyokaishi 74, 256 (1966); Chem. Abstr. 69, 81508w (1968).
[64] Nygren, M., and Magnéli, A., Arkiv för Kemi 28, 217 (1967).
[65] Chrenko, R. M., and Rodbell, D. S., Phys. Letters 24A, 211 (1967).
[66] Druilhe, R., and Bonnerot, J., Compt. Rend. (Paris) 263B, 55 (1966).
[67] Kubota, B., Nishikawa, T., and Yanase, A., J. Phys. Soc. Japan 16, 2340 (1961).
[68] Villeneuve, G., Bordet, A., Casalot, A., and Hagenmuller, P., Mat. Res. Bull. 6, 119 (1971).
[69] Stradley, J. G., Shevlin, T. S., and Everhart, J. O., Ohio State Univ. Res. Found. Prog. Rept. 806-1, Contract AF 35(616)-5515 (1958).
[70] Stephens, J. S., and Cruickshank, D. W. J., Acta Cryst. 26B, 222 (1970).
[71] Cojocaru, L. N., Costea, T., and Negoescu, I., Z. Phys. Chem. (N.F.) 60, 152 (1968).
[72] Minomura, S., and Drickamer, H. G., J. Appl. Phys. 34, 3043 (1963).
[73] Newnham, R. E., and de Haan, Y. M., Z. Krist. 117, 235 (1962).
[74] Corliss, L., Hastings, J. M., Nathans, R., and Shirane, G., J. Appl. Phys. 36, 1099 (1965).
[75] Samuelson, E. J., Hutchings, M. T., and Shirane, G., Physica 48, 13 (1970).
[76] Chapman, P. R., Griffith, R. H., and Marsh, T. D. F., Proc. Roy. Soc. (Lond.) 224A, 419 (1954).
[77] Fischer, W. A., and Lorenz, G., Z. Phys. Chem. (N.F.) 18, 308 (1958).
[78] Hagel, W. C., and Seybolt, A. U., J. Electrochem. Soc. 108, 1146 (1961).
[79] Crawford, J. A., and Vest, R. W., J. Appl. Phys. 35, 2413 (1964).
[80] Vaisnys, J. R., J. Appl. Phys. 38, 2153 (1967).
[81] Cojocaru, L. N., Z. Phys. Chem. (N.F.) 64, 255 (1969).
[82] Subba Rao, G. V., Wanklyn, B. M., and Rao, C. N. R., J. Phys. Chem. Solids 32, 345 (1971).
[83] Subba Rao, G. V., Rao, C. N. R., and Ferraro, J. R., Appl. Spec. 24, 436 (1970) and references therein.
[84] Rao, C. N. R., and Subba Rao, G. V., Phys. Stat. Solidi (a) 1, 597 (1900).
[85] Honig, J. M., in Modern Aspects of Solid State Chemistry, Ed. C. N. R. Rao, (Plenum Press, New York, 1970).

I.5. Manganese Oxides

Detailed phase relation studies of the Mn-O system [1–5] have shown that MnO, Mn_3O_4, Mn_2O_3, and MnO_2 are the stable solid oxides. All the oxides show interesting crystallographic and magnetic transitions and have been widely investigated in the literature.

MnO: MnO shows slight deviations from stoichiometry ($\lesssim 2\%$) at high temperatures ($\sim$1400 K) [5–10]. It is cubic with the rock salt structure at room temperature and undergoes a trigonal distortion as well as a volume contraction on cooling to $\sim$118 K and changes from a paramagnetic to an antiferromagnetic state [6, 11–15]. The structure in the antiferromagnetic phase has been examined by a few workers [11, 15, 16–24] and detailed χ-T measurements made. The magnetic moments in MnO are arranged in ferromagnetic sheets parallel to {111} planes, with neighboring planes coupled in an antiferromagnetic arrangement. The long range order parameter increases progressively with decreasing T below T_N. Neutron diffraction measurements show considerable short range magnetic order in MnO above T_N [16, 22]. Even though many workers have argued for a continuous (higher order) transition in MnO because no hysteresis effects are noted at T_N, the available x-ray diffraction [14], χ-T [21], exchange striction [14, 15], TEC [25], Mössbauer [26], internal friction and Young's modulus [27], acoustic attenuation [28], elastic moduli [29] and NMR [21, 30–32] data indicate that the antiferromagnetic-paramagnetic transition is indeed first order. High pressure studies on MnO have been carried out and the x-ray data [33] indicate a transition in MnO at $\sim$100 kbar to a phase which is tetragonal or of lower symmetry. Bartholin et al. [34] found that the T_N increases with P up to $\sim$3 kbar.

Electrical properties of pure [9, 35–41] and doped (with Li or Cr) [9, 42–44] MnO have been examined in detail. MnO is unique among the transition metal monoxides in that there is a maximum in the ρ versus p_{O_2} plot indicating a transition from p to n type semiconducting behavior at $\sim$1370 K; changes in sign of μ_H and α have also been noted [5, 35, 38–40] to corroborate the resistivity data. The electron mobility in MnO is higher than the hole mobility at high temperatures ($\mu_D^n/\mu_D^p \approx 10$ at $\sim$1450 K) [45, 46] and the defect structure seems to involve doubly ionized cation vacancies at high temperatures and at low oxygen partial pressures [5, 9, 35–37, 41, 42, 45, 46]. The charge carriers are localized in pure and doped MnO and at low enough temperatures ($<$700 K) hopping type of conduction occurs by holes in the 3d-band with a small E_a whereas the dominant mechanism of conduction is by holes in the oxygen 2p-band [9, 47, 48]. The EMF data on MnO at high temperatures [10] indicate second or higher order transitions within the homogeneity region.

Optical properties of MnO have been studied in the literature [49–51]; the absorption edge appears to be $\sim$3.8 eV. Far infrared antiferromagnetic resonance studies [52–54] show that the resonance frequency at 27.5 cm^{-1} is dependent on temperature and impurity content.

MnO forms solid solutions with other transition metal monoxides having the rock salt structure [55, 56] and the physical properties show variations with the composition.

Mn_3O_4: Mn_3O_4 has a tetragonal structure at room temperature and can be considered as a distorted spinel because of the Jahn-Teller distortion at the Mn^{3+} sites [57]; the ionic formula is probably very close to $Mn^{2+}[Mn_2^{3+}]O_4$ corresponding to a 'normal' spinel. Preparation of Mn_3O_4 in both polycrystalline and single crystal forms has been reported in the literature [6, 58–65]. The degree of tetragonal distortion in Mn_3O_4 decreases with increase in T and a rapid structural transition to cubic phase takes place at ~1435 K [66, 67]. The high temperature cubic form can not be preserved by quenching and the thermodynamic parameters indicate the first order nature of the transition [10, 66, 67].

Mn_3O_4 is ferrimagnetic below 43 K which is the curie temperature [65, 68, 69]. At 33 K a rearrangement of the moments occurs such that the chemical and magnetic unit cells become identical. Measurements of C_p [70] in the range 20–49 K show that there are no anomalies except for a peak at T_c. The material is a semiconductor [71–73] and has a higher resistivity than the analogous material Fe_3O_4.

Mn_3O_4 forms complete series of solid solutions with Fe_3O_4 and Co_3O_4 [67, 74].

Mn_2O_3: The common form of manganese sesquioxide is the α-modification which is closely related to the bixbyite, $(Mn, Fe)_2O_3$, structure [6]. γ-Mn_2O_3 having a structure nearly identical to that of Mn_3O_4 has been reported [6, 75], but detailed data are lacking. Moore et al. [6] have noted that γ-Mn_2O_3 transforms to the α-modification either by heating in vacuum for 48 h at ~770 K or by keeping at room temperature for one year.

Among the transition metal sesquioxides, α-Mn_2O_3 is the only oxide which does not possess a corundum structure and instead, it assumes a deformed cubic C-type rare-earth oxide structure [76–78] possibly as a result of the large Jahn-Teller distortion associated with the Mn^{3+} ion [79, 80]. Geller and coworkers [79–84], employing x-ray diffraction, χ-T and Mössbauer studies have shown that α-Mn_2O_3 undergoes a crystallographic transition (cubic to orthorhombic) at 302 K, a paramagnetic-antiferromagnetic transition at 80 K and another magnetic transition (of the Néel type) at 25 K. Crystal structure of α-Mn_2O_3 does not change below 300 K and x-ray data at 6.5 K show no additional lines or symmetry change implying that the transition at 25 K involves a shift in the symmetry center of the structure (characteristic of a diffusionless, but probably, first-order transition).

Mn_2O_3 behaves as a semiconductor in the range 400 to 1000 K [85, 86]. It decomposes at high temperatures.

Trivalent cations can be doped successfully into Mn_2O_3 and the structural and magnetic ordering aspects have been examined by Geller and co-workers [80–84] and by Hase et al. [87].

MnO_2: MnO_2 apparently exists only in the rutile modification and found in nature as pyrolusite [6]. An orthorhombic modification has been reported in the naturally occurring samples, but detailed data are lacking; laboratory preparation of the orthorhombic form has, however, not been successful [6]. MnO_2 is always associated with slight nonstoichiometry [6, 88, 90] and decomposes above 800 K to Mn_2O_3.

The usual wet chemical methods of preparation of MnO_2 result in nonstiochiometry and water of hydration and are less characterized [6, 88, 89]. Atomic or molecular oxygen is evolved on heating these 'disperse' forms of MnO_2 and serve as good oxidizing agents in organic chemical reactions; most probably the 'active' oxygen is present in the lattice as defects or adsorbed on the surface. The activity seems to depend on the particle size and the method of preparation etc.

No crystal structure transitions are known in MnO_2. It is antiferromagnetic below 92 K [90–94] and has a screw-type spin structure such that the spins, aligned parallel in the c plane, screw along the c axis; the magnetic unit cell is as large as 7 times the chemical unit cell.

MnO_2 has a low resistivity (~0.1Ω cm at 300 K) and shows anomalous temperature dependence in the range 4 to 300 K [90]. Anomalies in ρ and C_p have been noted at T_N [90, 94, 95]. Bhide and Damle [96] reported MnO_2 to be ferroelectric with a T_c of 325 K and Samokhvalov [97] finds a (UHF) dielectric anomaly at around this temperature; however, the anomaly does not correspond to that of a typical ferroelectric material. Ferroelectricity in MnO_2 is doubtful since no other relevant data are available in the literature.

Solid solutions, $(Mn_{1-x}Cr_x)O_2$, have been reported by Siratori and Iida [98].

Oxide and description of the study	Data	Remarks and inferences	References
MnO			
Crystal structure and x-ray studies.	$T=296$ K: Cubic; space group, Fm3m; $Z=4$; $a=4.4457\pm0.0002$ Å. $T\approx4$ K: Rhombohedral; $a=4.4316\pm0.0003$ Å; $\alpha=90.624\pm0.008°$. T_t ($\equiv T_N$) $=118\pm2$ K. TEC (/°C): 64×10^{-6} at $\sim T_N$. High pressure x-ray studies at 300 K indicate a phase transition at ~100 kbar to a tetragonal or lower symmetry phase.	The cubic lattice distorts to rhombohedral structure at T_t on cooling; slight volume changes also occur. TEC also touches maximum at T_t. The structure of the high pressure form is not known.	[6, 11–15, 25, 33].
Magnetic properties.	χ (122 K) $=83\times10^{-6}$ emu/g; χ (4.2 K) $=79\times10^{-6}$ emu/g. Typical antiferromagnetic behavior with $T_N=118\pm3$ K. T_N increases with pressure; $(\partial T_N/\partial P)=0.3\times10^{-3}$ deg/bar. In the presence of a magnetic field, below T_N, the direction of antiferromagnetism is modified which leads to an increase in χ.	In the antiferromagnetic state the magnetic moments are arranged in ferromagnetic sheets parallel to (111) planes and the direction of magnetization in neighboring planes is antiparallel. Neutron diffraction shows the persistence of short range magnetic order above T_N. The magnetic transition appears to be first order.	[11, 15, 16–24, 34].
Electrical properties.	**Pure MnO:** ρ (300 K)~10^{15} Ωcm in stoichiometric MnO. Semiconductor behavior up to ~1500 K; E_a~1.0 eV; α (500 K)~400 μV/K; Changes from p- to n-type behavior as a function of p_{O_2} (at ~10^{-12} atm), at ~1370 K; α changes sign at this temperature; $(\mu_D^n/\mu_D^p)\approx10$. **Li doped MnO:** ρ~10^{-3}–10^{-1} Ωcm; E_a~0.7 eV; $\mu_H=0.007$ cm²/V s (400–700 K); $\mu_D=$ (calc.)~0.03 cm²/V s; $m^*=7\,m_0$ at 700 K. ρ decreases with pressure and no transitions are indicated up to 200 kbar.	The data on pure MnO can be interpreted as due to hopping of charge carriers with a band gap of ~2.2 eV or with a band conduction for electrons with a smaller band gap. The change from p- to n-type behavior is due to the greater mobility of electrons compared to holes at high temperatures and low oxygen partial pressures and due to the cation vacancy defects. In doped materials, conduction is always extrinsic at ordinary temperatures and mainly occurs by hopping; intrinsic conduction seems to set in at very high temperatures.	[5, 9, 35–37, 42, 45, 46–48, 99].
Optical properties.	$Dq=1010$ cm^{-1}; $B=601$ cm^{-1}; Absorption edge is at ~3.8 eV. Far infrared antiferromagnetic resonance is at ~27.5 cm^{-1} at 2 K; the frequency decreases with rise in T and varies with the impurity content.	Optical data indicate the localized nature of the charge carriers in MnO.	[49–54].
Mössbauer studies of ^{57}Fe doped MnO.	$T_N=116.9$ K. Magnetic hyperfine splitting noted below T_N. Internal magnetic field is maximum (170 kG) at 90 K and decreases to 97 kG at 4.2 K.	The magnetic transition appears to be first order but no temperatures hysteresis is noted in the transition.	[26].

Manganese oxides—Continued

Oxide and description of the study	Data	Remarks and inferences	References
NMR studies of MnO.	The ^{55}Mn NMR frequency shifts are found to be temperature dependent and proportional to χ; magnetic field dependence also is noted. Hyperfine coupling constant = $-(81.5\pm2.5)\times10^{-4}$ cm^{-1}.	Guenther et al. [32] speculate that weak ferromagnetism may exist in MnO at very low temperatures.	[21, 30–32].
Mechanical properties.	Compressibility = 6.48×10^{-7} bar^{-1}. Elastic moduli (measured at 30 MHz): $C_{11}=(1.768\pm0.006)\times10^{12}$ dyn/cm^2; $C_{14}=(6.8\pm0.1)\times10^{11}$ $dyne/cm^2$ (at $T>T_N$). At T_N, C_{11} drops by ~19% and greater decrease is shown by C_{14}. Young's modulus (at T_N) $=2\times10^{11}$ dyn/cm and internal friction $\approx20\times10^{-3}$; both the properties show anomalous behavior near T_N.	The discontinuous changes in the elastic moduli, Young's modulus and internal friction are taken as strong evidence for a first order magnetic transition in MnO.	[14, 15, 27, 29].
Mn_3O_4			
Crystal structure and x-ray studies.	$T=300$ K: Tetragonal; space group, $I4_1/amd$; $Z=4$; $a=5.762$ Å; $c=9.463$ Å. $T_t=1435$ K. $T>T_t$: Cubic; $a=8.42$ Å.	Mn_3O_4 can be considered as a distorted spinel because of the Jahn-Teller distortion at the Mn^{3+} sites; the ionic formula can be written as $Mn^{2+}/[Mn_2^{3+}]O_4$. The transition is first order and the high temperature phase cannot be quenched to room temperature.	[6, 58–67].
Magnetic properties.	*Ferrimagnetic below 43 K (T_C); a* rearrangement of the spin moments occurs at 33 K such that the magnetic and chemical unit cells become identical. χ_M (290 K) ~12×10^{-3} emu; Magnetic moment = 5.27 μ_B below T_C.	*The observed ferrimagnetism is* consistent with the spinel structure. $1/\chi$-T behavior is of the Neel type above T_C and consistent with the Yafet-Kittel model.	*[60, 65, 68,* 69].
Electrical and thermal properties.	Semiconductor behavior; ρ (300 K) ~10^7 Ωcm; $\alpha\approx0.2$ mV/°C in the range 500–900 K (p-type); $\Delta H=-(5.9\pm0.7)$ kcal/mol; $\Delta S=(4.2\pm0.5)$ et at T_t; C_p shows an anomaly at T_t.	Detailed electrical data are lacking; Mn_3O_4 has a higher value of ρ than Fe_3O_4. The enthalpy and C_p data indicate that the transition is first order.	[10, 66, 67, 70, 71–73].
Infrared spectra.	Bands at 474 and 550 cm^{-1} are noted.	The data are correlated with the spectra of other oxide spinels.	[100].
Mn_2O_3			
Crystal structure and x-ray studies.	$T=298$ K: Orthorhombic; space group, Pbca; $Z=4$; $a=9.414$ Å; $b=9.424$ Å; $c=9.405$ Å. $T_t=302$ K. $T=314$ K: Cubic; space group, Ia3; $Z=16$; $a=9.414$ Å.	Earlier workers concluded that only cubic structure exists in Mn_2O_3; this oxide does not have a corundum structure and instead has a distorted C-type rare-earth oxide structure. The transi-	[76–84].

Manganese oxides—Continued

Oxide and description of the study	Data	Remarks and inferences	References
		tion appears to be first order but detailed data on other properties are lacking.	
Magnetic properties.	χ_M (100 K)$\sim 7\times10^{-3}$ emu. Paramagnetic—antiferromagnetic transition, T_{N_1}, at 80 K and another magnetic transition at 25 K (T_{N_2}). No crystal structure transition below 300 K up to 4 K; Both the low temperature phases are antiferromagnetic. T_{N_1} and T_{N_2} are greatly affected by impurities.	Geller et al. [82] proposed a magnetic structure in the antiferromagnetic phase. Chevalier et al. [102] find that the low temperature (25 K) transition is at 50 K and is of second order.	[79–84, 101, 102].
Optical and electrical properties.	Band at $\sim$20,000 cm^{-1} is ascribed to the spin allowed transition. Infrared bands are in the range 320–670 cm^{-1} and are ascribed to the stretching and bending vibrations of the Mn-O bond. Semiconductor behavior in the range 400–1100 K: ρ (200 K)$\sim 7\times10^{3}$ Ωcm; ρ (500 K)$\sim$50 Ωcm; E_a = 0.6 eV.	Detailed electrical data on single crystal material are lacking.	[85, 86, 103].
MnO_2			
Crystal structure and x-ray studies.	T=298 K: Tetragonal; space group $P4_2/mnm$; Z=4; a=4.3980 ±0.0002 Å; c=2.8738±0.0002 Å. TEC (300–670 K) ($\times10^7$/°C): $\|\|^c$=69; $\|\|^a$=67. With pressure, c axis expands at low pressures, then passes through a maximum (at $\sim$40 kbar) and ultimately contracts; a axis, on the other hand, decreases smoothly with pressure. The compressibility is low at low pressures and then increases at pressures beyond the maximum in c axis.	No crystal structure transitions are known and it is very difficult to prepare exactly stoichiometric MnO_2.	[6, 33, 88–90, 104, 105].
Magnetic properties.	Antiferromagnetic with T_N=92±2 K. χ (100 K)$\approx 36\times10^{-6}$ emu/g; χ (300 K)$\approx 32\times10^{-6}$ emu/g. Curie-Weiss Law is satisfied above 150 K. A screw type spin structure exists below T_N and the magnetic unit cell is 7 times the chemical unit cell.	The characteristic screw structure is exclusive to MnO_2.	[90–94].
Electrical and other properties.	Resistivity is low; ρ (4.2 K)$\approx 2.6\times10^{-2}$ Ωcm; ρ (300 K)$\approx 1.1\times10^{-1}$ Ωcm. Anomalous T dependence in the range 4–300 K. Anomalies	The anomalous ρ-T behavior is not clearly understood; MnO_2 may be classified as a degenerate semiconductor [57]. The magnetic	[90, 94, 96].

Manganese oxides—Continued

Oxide and description of the study	Data	Remarks and inferences	References
	in ρ and C_p noted at T_N. Ferroelectricity with a $T_C \sim 325$ K reported.	transition may be classified as second order. The details of the ferroelectric behavior are not understood and ferroelectricity is doubtful.	

References

[1] Hahn, W. C., Jr., and Muan, A., Am. J. Sci. **258**, 66 (1960).
[2] Otto, E. M., J. Electrochem. Soc. **111**, 88 (1964).
[3] Schmahl, N. G., and Stemmler, B., J. Electrochem. Soc. **112**, 365 (1965).
[4] Muan, A., Nucl. Sci. Abstr. **20**, 50 (1966).
[5] Hed, A. Z., and Tannhauser, D. S., J. Electrochem. Soc. **114**, 314 (1967).
[6] Moore, T. E., Ellis, M., and Selwood, P. W., J. Am. Chem. Soc. **72**, 856 (1950).
[7] Davies, M. W., and Richardson, F. D., Trans. Faraday Soc. **55**, 604 (1959).
[8] Turnock, A. C., J. Am. Ceram. Soc. **49**, 382 (1966).
[9] O'Keeffe, M., and Valigi, M., J. Phys. Chem. Solids **31**, 947 (1970).
[10] Fender, B. E. F., and Riley, F. D., in The Chemistry of Extended Defects in non-Metallic Solids, Eds. L. Eyring and M. O'Keeffe (North Holland Publ. Co., Amsterdam, 1970), p 54.
[11] Roth, W. L., Phys. Rev. **110**, 1333 (1958); **111**, 772 (1958); J. Appl. Phys. **31**, 2000 (1961).
[12] Rodbell, D. S., Osika, L. M., and Lawrence, P. E., J. Appl. Phys. **36**, 666 (1965).
[13] Bloch, D., Charbit, P., and Georges, R., Compt. Rend. (Paris) **266B**, 430 (1968).
[14] Morosin, B., Phys. Rev. B **1**, 236 (1970).
[15] Bartel, L. C., Phys. Rev. B **1**, 1254 (1970); Bull. Am. Phys. Soc. **15**, 271 (1970); J. Appl. Phys. **41**, 5132 (1970).
[16] Shull, C. G., Strauser, W. A., and Wollan, E. O., Phys. Rev. **83**, 333 (1951).
[17] Kaplan, J. I., J. Chem. Phys. **22**, 1709 (1954).
[18] Keffer, F., and O'Sullivan, W., Phys. Rev. **108**, 637 (1957).
[19] Uchida, E., Kondoh, H., Nakamuzi, Y., and Nagamiya, T., J. Phys. Soc. Japan **15**, 466 (1960).
[20] Slack, G. A., J. Appl. Phys. **31**, 1571 (1960).
[21] Lines, M. E., and Jones, E. D., Phys. Rev. **139A**, 1313 (1965).
[22] Blech, I. A., and Averbach, B. L., Phys. Rev. **142**, 287 (1966).
[23] Bloch, D., Feron, J. L., Georges, R., and Jacobs, I. S., J. Appl. Phys. **38**, 1474 (1967).
[24] Bloch, D., Georges, R., and Jacobs, I. S., J. de Physique **31**, 589 (1970).
[25] Foëx, M., Compt. Rend. (Paris) **227**, 193 (1948).
[26] Siegwarth, J. D., Phys. Rev. **155**, 285 (1967).
[27] Belov, K. P., Katayev, G. I., and Levitin, R. Z., J. Appl. Phys. Suppl. **31**, 153 (1960).
[28] Evans, R. G., and Daniel, M. R., Phys. Letters **26A**, 276 (1968).
[29] Cracknell, M. F., and Evans, R. G., Solid State Commun. **8**, 359 (1970).
[30] Jones, E. D., Phys. Rev. **151**, 315 (1966).
[31] Tompa, K., Toth, F., and Gruner, G., Phys. Stat. Solidi **22**, K11 (1967).
[32] Guenther, B. D., Christensen, C. R., and Daniel, A. C., Phys. Letters **30A**, 391 (1969).
[33] Clendenen, R. L., and Drickamer, H. G., J. Chem. Phys. **44**, 4223 (1966).
[34] Bartholin, H., Bloch, D., and Georges, R., Compt. Rend. (Paris) **264B**, 360 (1967).
[35] Hed, A. Z., and Tannhauser, D. S., J. Chem. Phys. **47**, 2090 (1967).
[36] Duquesnoy, A., and Marion, F. C., Compt. Rend. (Paris) **256**, 2862 (1963).
[37] Eror, N. G., Ph.D. Thesis, Northwestern Univ., Illinois, U.S.A. (1965).
[38] Gvishi, M., Tallan, N. M., and Tannhauser, D. S., Solid State Commun. **6**, 135 (1968).
[39] DeWit, H. J., and Crevecoeur, C., Phys. Letters **25A**, 393 (1967).
[40] Bocquet, J. P., Kawahara, M., and Lacombe, P., Compt. Rend. (Paris) **265C**, 1318 (1967).
[41] Le Brusq, H., Oehlig, J.-J., and Marion, F., Compt. Rend. (Paris) **266C**, 965 (1968).
[42] Nagels, P., Denayer, M., DeWit, H. J., and Crevecoeur, C., Solid State Commun. **6**, 695 (1968).
[43] Ali, M., Fridman, M., Denayer, M., and Nagels, P., Phys. Stat. Solidi **28**, 193 (1968).
[44] Crevecoeur, C., and DeWit, H. J., J. Phys. Chem. Solids **31**, 783 (1970).
[45] Wagner, J. B., Jr., in Mass Transport in Oxides, Nat. Bur. Stand. (U.S.), Spec. Publ. 296, (1968), p. 65.
[46] Tannhauser, D. S., Tallan, N. M., and Gvishi, M., in Mass Transport in Oxides, N.B.S. Special Public. 296, 1968.
[47] Adler, D., Solid State Phys. **21**, 1 (1968).
[48] Adler, D., and Feinleib, J., Phys. Rev. **B2**, 3112 (1970).
[49] Iskenderov, R. N., Drabkin, I. A., Emel'yanova, L. T., and Ksendzov, Ya. M., Sov. Phys.—Solid State (English Transl.) **10**, 2031 (1969).
[50] Huffman, D. R., J. Appl. Phys. **40**, 1334 (1969).
[51] Huffman, D. R., Wild, R. L., and Shinmei, M., J. Chem. Phys. **50**, 4092 (1969).
[52] Sievers, A. J., and Tinkham, M., Phys. Rev. **129**, 1566 (1963).
[53] Richards, P. L., J. Appl. Phys. **34**, 1237 (1963).
[54] Hughes, A. E., Phys. Rev. **B3**, 877 (1971).
[55] Bizette, H., and Mainard, R., Bull. Soc. Sci. Bretagne **42**, 209 (1967).
[56] Brezny, B., Ryall, W. R., and Muan, A., Mat. Res. Bull. **5**, 481 (1970).
[57] Rao, C. N. R., and Subba Rao, G. V., Phys. Stat. Solidi (a) **1**, 597 (1970).
[58] Scott, E. J., J. Chem. Phys. **23**, 2459 (1955).
[59] Kleinert, P., Z. Chem. **3**, 353 (1963).
[60] Perthel, R., and Jahn, H., Phys. Stat. Solidi **5**, 563 (1964).
[61] Rozdestvenskaya, M. V., Mokievskii, V. A., and Stogova, V. A., Sov. Phys.—Crystallogr. (English Transl.) **11**, 765 (1967).
[62] Smith, B. A., and Austin, I. G., J. Cryst. Growth **1**, 79 (1967).

[63] Buhl, R., J. Phys. Chem. Solids 30, 805 (1969).
[64] Caslavska, V., and Roy, R., J. Appl. Phys. 41, 825 (1970).
[65] Boucher, B., Buhl, R., and Perrin, M., J. Appl. Phys. 42, 1615 (1971).
[66] Southard, J. C., and Moore, G. E., J. Am. Chem. Soc. 64, 1769 (1942).
[67] van Hook, H. J., and Keith, M. L., Am. Mineral. 43, 69 (1958).
[68] Jacobs, I. S., J. Phys. Chem. Solids 11, 1 (1959).
[69] Dwight, K., and Menyuk, N., Phys. Rev. 119, 1470 (1960).
[70] Lecomte, M., quoted in [65].
[71] Verwey, E. J. W., and deBoer, J. H., Rec. Trav. Chim. 55, 531 (1936).
[72] Bhide, V. G., and Dani, R. H., Physica 27, 821 (1961).
[73] Oehlig, J. J., Le Brusq, H., Duquesnoy, A., and Marion, F., Compt. Rend. (Paris) 265C, 421 (1967).
[74] Wickham, D. J., and Croft, W. J., J. Phys. Chem. Solids 7, 351 (1958).
[75] Gattöw, V. G., and Glemser, O., Z. anorg. allgem. Chem. 309, 121 (1961).
[76] Banks, E., and Kostiner, E., J. Appl. Phys. 37, 1423 (1966).
[77] Hase, W., Kleinstuck, K., and Schulze, G. E. R., Z. Krist. 124, 428 (1967).
[78] Norrestam, R., Acta Chem. Scand. 21, 2871 (1967).
[79] Geller, S., Cape, J. A., Grant, R. W., and Espinosa, G. P., Phys. Letters 24A, 369 (1967).
[80] Grant, R. W., Cape, J. A., Geller, S., and Espinosa, G. P., Bull. Am. Phys. Soc. 13, 462 (1968).
[81] Geller, S., Grant, R. W., Cape, J. A., and Espinosa, G. P., J. Appl. Phys. 38, 1457 (1967).
[82] Grant, R. W., Geller, S., Cape, J. A., and Espinosa, G. P., Phys. Rev. 175, 686 (1968).
[83] Geller, S., and Espinosa, G. P., Phys. Rev. B1, 3763 (1970).
[84] Geller, S., Acta Cryst. 27, 821 (1971).
[85] Drotschman, C., Batterien 18, 686 (1964); Chem. Abstr. 62, 8472g (1965).
[86] Subba Rao, G. V., Wanklyn, B. M., and Rao, C. N. R., J. Phys. Chem. Solids 32, 345 (1971).
[87] Hase, W., Bruckner, W., Tobsisch, J., Ullrich, H.-J., and Wegerer, G., Z. Krist. 129, 360 (1969).
[88] Wadsley, A. D., and Walkley, A., Rev. Pure & Appl. Chem. 1, 203 (1951), and references therein.
[89] Malinin, G. V., and Tolmachev, Yu. M., Russ. J. Phys. Chem. (English Transl.) 43, 1129 (1969).
[90] Rogers, D. B., Shannon, R. D., Sleight, A. W., and Gillson, J. L., Inorg. Chem. 8, 841 (1969).
[91] Bizette, H., J. Phys. Rad. 12, 161 (1951).
[92] Bacon, D., Usp. Fiz. Nauk. 8, 335 (1963).
[93] Yoshimori, A., J. Phys. Soc. Japan 14, 807 (1959).
[94] Ohama, N., and Hamaguchi, Y., J. Phys. Soc. Japan 30, 1311 (1971).
[95] Kelley, K. K., and Moore, G. E., J. Am. Chem. Soc. 65, 782 (1943).
[96] Bhide, V. G., and Damle, R. V., Physica 26, 33 (1960).
[97] Samokhvalov, A. A., Sov. Phys.—Solid State (English Transl.) 3, 2613 (1962).
[98] Siratori, K., and Iida, S., J. Phys. Soc. Japan 15, 210 (1960).
[99] Minomura, S., and Drickamer, H. G., J. Appl. Phys. 34, 3043 (1963).
[100] Hafner, S., Z. Krist. 115, 331 (1961).
[101] Banks, E., Kostiner, E., and Wertheim, G. K., J. Chem. Phys. 45, 1189 (1966).
[102] Chevalier, R. R., Roult, G., and Bertaut, E. F., Solid State Commun. 5, 7 (1967).
[103] Subba Rao, G. V., Rao, C. N. R., and Ferraro, J. R., Appl. Spec. 24, 436 (1970).
[104] Bradt, R. C., and Wiley, J. S., J. Electrochem. Soc. 109, 651 (1962).
[105] Kirchner, H. P., J. Am. Ceram. Soc. 52, 379 (1969).

I.6. Iron Oxides

The Fe-O system has been a subject of extensive investigation over the past several decades [1–4]. The available data up to 1957 has been summarized in the literature [2]. The most important iron oxides are the oxygen deficient ferrous oxide (wüstite), $Fe_{1-x}O$, magnetite, Fe_3O_4 and hematite, Fe_2O_3. The dioxide, FeO_2 has been recently reported [5], but the existance of stable FeO_2 still appears doubtful [6].

$Fe_{1-x}O$: Wüstite at ordinary pressures is always nonstoichio-metric and the homogeneity range extends from $Fe_{0.84}O$ to $Fe_{0.95}O$ at ~1620 K and the material is unstable below 840 K with respect to decomposition into Fe_3O_4 and Fe metal; the metastable phase can, however, be retained by quenching [1, 2, 7–10]. The thermodynamics and the defect structure at high temperatures has been examined [4, 11–20]. The deviation from stoichiometry in wüstite is due to cation vacancies, with each cation vacancy requiring the presence of two Fe^{3+} ions to maintain charge balance; thus, $Fe_{1-x}O$ may be regarded as a solid solution of Fe^{2+} and cation vacancies in FeO. The average structure at room temperature is cubic [7–10] and the material is paramagnetic. Magnetic ordering into antiferromagnetic state occurs at 198 K accompanied by a change from cubic to rhombohedral structure. Below T_N, the magnetic moments are arrayed in ferromagnetic sheets parallel to (111) planes and the direction of magnetization in neighboring planes is antiparallel; the magnetic axis in $Fe_{1-x}O$ is perpendicular to the ferromagnetic sheets [9, 10, 21].

Detailed studies employing x-ray and neutron diffraction techniques of the quenched phases of $Fe_{1-x}O$ indicate defect cluster formation [10, 18, 22–24]; it appears that the oxygen sublattice is continuous and the defect cluster is a region in which there are vacancies in cation sites and interstitial ions in some tetrahedral sites. The results are in agreement with a model which assumes that the average defect cluster contains about 4 vacancies and 2 interstitials in powder samples and 13 vacancies and 4 interstitials in single crystalline samples. Order-disorder transitions have been noted in $Fe_{1-x}O$ at high temperatures [19].

The cubic lattice parameter of $Fe_{1-x}O$ shows variation with the stoichiometry and generally, a increases with increasing Fe content [8]. Magnetic cluster

formation [22] also affects the spin structure and directions in $Fe_{1-x}O$ below T_N, but T_N is almost unaffected by variation in x [21]. This behavior is indicative of the existence of defect clusters of cation vacancies by virtue of which the remaining part of the cation sublattice is left intact thereby not weakening the antiferromagnetic interaction; random vacancies, on the other hand, would be expected to weaken the antiferromagnetic interaction and lower the T_N.

Stoichiometric $FeO_{1.00}$ lies outside the phase field under ordinary pressure conditions [24], but under high pressure conditions and in the presence of excess metallic iron, the cation deficient structure of wüstite might not be formed; Katsura et al. [25] have indeed successfully synthesized $FeO_{1.00}$ from $FeO_{0.95}$ and Fe at a pressure of 36 kbar and at 1040 K. Hentschel [26] has recently concluded on the basis of x-ray and Mössbauer data that $FeO_{1.00}$ is formed as a metastable intermediate in the decomposition of wüstite at relatively low temperatures (~500 K).

Resistivity measurements [4, 13, 14, 27–29] on $Fe_{1-x}O$ indicate that ρ decreases with temperature as well as the oxygen content. Low oxygen content samples are p type as evidenced by the α data; a p- to n-type transition is noted at higher oxygen content or with higher p_{O_2} in the system. The defect structure is interpreted as due to doubly ionized cation vacancies.

Anomalous behavior of TEC [30], C_p [31] and UHF dielectric constant [32] have been noted at T_N in $Fe_{1-x}O$. High pressure x-ray studies [33] do not indicate a transition up to several hundred kilobars.

Solid solution formation of $Fe_{1-x}O$ with MnO and MgO has been reported in the literature [8, 34].

Fe_3O_4: This oxide is encountered in nature as the magnetic oxide of iron or magnetite; it can also be prepared in the laboratory and has a narrow range of homogeneity [1–3]. Fe_3O_4 has the cubic inverse spinel structure [35] at room temperature where Fe^{3+} ions occupy all the A sites and one-half the B sites, while the Fe^{2+} ions occupy the other half of the B sites. The material is ferrimagnetic with $T_N \approx$ 858 K [36–38].

On cooling to 119 K, Fe_3O_4 undergoes a crystallographic transition to an orthorhombic modification [39–44]. This has been explained by Verwey et al. [39, 40] as due to the ordering of the octahedral Fe^{2+} and Fe^{3+} ions into perpendicular rows with the associated reduction in crystal symmetry. This transition is commonly referred to as the Verwey transition and detailed investigations have been carried out to understand the nature of the transition.

Magnetic properties of Fe_3O_4 are not affected below the Verwey transition, but χ shows anisotropy [41, 43–46]. Fe_3O_4 has a low resistivity at room temperature and the ordering of the ions below T_t (119 K) appears as a sudden increase of ρ by a factor of >90 and also causes an anisotropy in ρ [41, 43]. Verwey et al. [39, 40] have explained this observation as due to the fast electron exchange in Fe_3O_4 which is inhibited below T_t because of the ordering process. Many workers [47, 48] have proposed that this phenomenon is similar to a metal-semiconductor transition, but the actual electrical behavior above T_t is more complex and does not correspond to the typical metallic behavior. Semiconductor behavior is noted in the range 80 to 119 K and 119 to 250 K; ρ is essentially constant in the range 250 to 1700 K showing slight maxima and minima at 350 and ~850 K respectively [43, 49]; the low value of ρ and constancy over a wide temperature range (250 to 1700 K) seem to indicate that Fe_3O_4 can be classified as a degenerate semiconductor above room temperature [35, 50–53]. Discontinuities in α, R_H and μ_H have also been noted at T_t [53–56].

Mössbauer studies of the ordering transition in Fe_3O_4 have been reported by many workers in the literature [57–67]. Careful studies on untwinned crystals of Fe_3O_4 have revealed that the Mössbauer spectrum is composed of five components below T_t corresponding to a tetrahedral Fe^{3+} site, two octahedral Fe^{3+} and two octahedral Fe^{2+} sites. One would expect, on the basis of the Verwey mechanism, a three component spectrum of equal intensity (due to octahedral Fe^{2+} and Fe^{3+} and tetrahedral Fe^{3+} sites). In order to explain the observed spectrum, it is proposed [64, 65] that the Verwey-ordering is not entirely correct and the unit cell must at least be doubled to enable the different sites to contribute to the hyperfine component. This is corroborated by the recent studies employing neutron diffraction [68] and electron microscopy [69].

Several properties of Fe_3O_4 exhibit discontinuities at T_t; among them are TEC [70], saturation magnetization [41], magnetostriction [70], Young's modulus and internal friction [71], elastic constants and sound wave velocity [72], magnetocaloric effect [73] and NMR relaxation [74, 75]. However, T_t determined by different techniques differ slightly, possibly due to slight nonstoichiometry or sample purity [66]. Discontinuities in the ultrasonic sound velocities have been noted near T_N in Fe_3O_4 [76]. High pres-

sure studies [47, 77] indicate that T_t decreases whereas T_N increases in a linear fashion.

Fe_3O_4 forms solid solutions with Mn_3O_4 and Co_3O_4 giving spinel type structures [34, 78].

Fe_2O_3: Iron sesquioxide, Fe_2O_3 (hematite), exists in several modifications: α-Fe_2O_3, the most stable form having a corundum structure [1, 2, 4], β-form (supposedly metastable) possessing a cubic bixbyite structure [79, 80] and the γ-modification having a tetragonal structure which is metastable at all conditions of temperature and pressure [2, 79, 81–84]. The structure of δ-Fe_2O_3 is not well established and even its composition is open to doubt (a better description might be δ-FeOOH) [85–88]; the ϵ-form having a monoclinic structure has been recently characterized [89] and a high pressure form of Fe_2O_3 having a hypothetical perovskite structure has been deduced from shock wave experiments [90].

γ-Fe_2O_3: γ-Fe_2O_3 has a tetragonal structure and consists of three spinel blocks stacked on top of each other; the unit cell has the formula $Fe_{64}O_{96}$ instead of $Fe_{72}O_{96}$ to be expected with a spinel compound. The eight *vacancies* are distributed among the octahedral spinel sites in an ordered manner [79, 83, 91]. The material is ferrimagnetic [91, 92] and transforms to α-Fe_2O_3 above $\sim$670 K [2, 79, 81, 92–94]; the transition occurs gradually and it is easy to control the conversion. Goto [95] investigated the phase transformation of γ-Fe_2O_3 up to 33 kbar pressure and up to 570 K. The rate constant primarily depends on the thermo-dynamic parameter $P\Delta V$ where ΔV ($\sim$7%) is the volume difference between α- and γ-modifications.

ϵ-Fe_2O_3: The monoclinic ϵ-Fe_2O_3 has a dark brown color and is ferromagnetic with T_c $\sim$485 to 500 K [89, 96]. It decomposes to α-Fe_2O_3 above 770 K.

α-Fe_2O_3: This is the most stable sesquioxide of iron and has a very narrow range of homogeneity [1–4, 97]. It has a rhombohedral structure [98] and is antiferromagnetic with a high Néel point ($T_N \approx 960$ K) [99–104]; discontinuities in the lattice parameters are noted at T_N [105]. Of special interest in Fe_2O_3 is the magnetic transition which takes place at $\sim$263 K (T_M) and is usually referred to as the Morin transition [106] and has been extensively studied in recent years. Below T_M and in the absence of magnetic field, the Fe^{3+} spins are aligned along the (111) or z axis of the crystal and the magnetic structure is that of a pure antiferromagnet; above T_M, the crystal exhibits weak ferromagnetism with canted spins lying in the (111) plane. On application of a sufficiently large magnetic field in the z-direction below T_M, a field induced first order spin-flip transition is observed. The Morin transition in Fe_2O_3 has been examined by a variety of experimental techniques like neutron diffraction [100, 107, 108], static magnetization [106, 109–113], AFMR [110, 114, 115], Mössbauer spectroscopy [102, 116–120], NMR [121], ultrasonic attenuation [122], Cotton-Mouton effect [123] and inelastic neutron scattering [124–127]. The effect of pulsed magnetic field has also been studied [128].

Several theoretical approaches have been attempted to gain an insight into the mechanism of the Morin transition [113, 128, 129–132]. The effect of pressure on the transition indicates that T_M increases in a linear fashion; $(\partial T_M/\partial P) = +3.6°$/kbar [133–135]. T_M also depends on the particle size, the method of preparation and the purity of the sample [136, 137]. The effect of doping Fe_2O_3 (with impurities) on T_M has been studied by a few workers; Al^{3+}, Ga^{3+}, Cr^{3+}, Sc^{3+}, Ti^{4+}, and Sn^{4+} ions seem to lower T_M (broadening the range of existence of weak ferromagnetism) [112, 138, 139] while Rh^{3+} raises the T_M considerably [140–142].

Electrical properties of pure [143–146] and doped [147–150] Fe_2O_3 have been examined by various workers in the literature. The material is a semiconductor in the entire temperature range investigated (200 to 1600 K). Highly pure Fe_2O_3 shows some what complex behavior with different activation energies in the region 300 to 700K, 700 to 950K, and 950 to 1600 K whereas impure Fe_2O_3 shows linear variation of $\ln\rho$ with $1/T$ in the range 400 to 1500 K with $E_a \sim 1.0$ eV. Anomalies in ρ and α at T_t and T_N have not been noted, but n-type Fe_2O_3 samples show a sign reversal in R_H at $\sim T_N$ while μ_H goes through a minimum around this temperature. Because of the ease with which the valence state of Fe can be changed by slight impurities, it is highly improbable that the conduction is intrinsic in Fe_2O_3.

High pressure x-ray studies do not indicate any phase transition [151], but recent resistivity studies at ultrahigh pressures seem to indicate a transition from the insulating phase to a highly conducting state (at $\geqslant$2 Mbar pressure) [152].

Solid solutions of Fe_2O_3 with Mn_2O_3 [153–157], Cr_2O_3 [158], Ga_2O_3 [159, 160], and In_2O_3 [160–162] have been examined in detail in the literature.

Oxide and description of the study	Data	Remarks and inferences	References
$Fe_{1-x}O$			
Crystal structure and x-ray diffraction studies.	$T=300$ K: Cubic; space group, Fm3m; $Z=4$. a varies from 4.2886 to 4. 3012 Å with increasing Fe content in $Fe_{1-x}O$ ($Fe_{0.84}O$ to $Fe_{0.95}O$). For $FeO_{1.00}$ synthesized at high pressure, $a=4.323\pm0.001$ Å. $T_t=198$ K. Below T_t, the structure is rhombohedral. The rhombohedral distortion is sensitive to the Fe content; at 90 K, $\alpha\approx60°$ for high Fe content $Fe_{1-x}O$ and $\approx59.04°$ for low Fe content sample. High pressure x-ray studies do not indicate any phase transition up to several hundred kilobars pressures.	At ordinary pressures, FeO is always nonstoichiometric due to the cation vacancies. Studies on quenched high temperature phases ($Fe_{1-x}O$ is unstable below 850 K) indicate defect cluster formation. Below T_t, the rhombohedral distortion varies with the stoichiometry but T_t itself remains unaffected. Hentschel [26] found evidence for the formation of intermediate stoichiometric $FeO_{1.00}$ in the decomposition of wüstite at relatively low temperatures.	[1, 2, 7, 8, 10, 18, 19, 22–25, 33].
Magnetic properties.	Antiferromagnetic below 198 K ($\equiv T_N$) and the magnetic moments are arrayed in ferromagnetic sheets parallel to (111) planes and the direction of magnetization in neighboring planes is antiparallel; the magnetic axis is perpendicular to the ferromagnetic sheet. χ_M obeys a Curie-Weiss law; $\chi_M=3.56/(T+136)$. Magnetic cluster formation is noted anologous to the cationic defect clusters which affect the spin structure and spin directions below T_N. T_N is not much affected by variation of x in $Fe_{1-x}O$.	The spins in FeO are perpendicular to the (111) plane unlike in NiO and MnO which also show antiferromagnetism and have rock salt structure above T_N.	[9, 10, 21, 22].
Electrical properties.	Semiconductor behavior (100–1100 K); ρ (300 K) ≈0.05 Ωcm; ρ decreases with increase in the oxygen content in $Fe_{1-x}O$. Three distinct regions in $\ln\rho$-T behavior: $E_a=0.008$ eV (<100 K); $E_a=0.3$ eV (125–175 K); $E_a=0.07$ eV (200–1100 K). The samples are p-type but high oxygen content samples are n-type. The defect structure is of the doubly ionized cation vacancy type.	Unusually low resistivity exhibited by $Fe_{1-x}O$ compared to other 3d transition metal monoxides and controlled by stoichiometry; ρ-T behavior is extrinsic.	[4, 13, 14, 27–29].
TEC and UHF dielectric constant studies.	TEC and UHF (~10 GHz) dielectric constant data indicate anomalies at T_N. TEC (186 K) $=41\times10^{-6}$/°C; $\epsilon_\infty=12.7$.	—	[30, 32].

Oxide and description of the study	Data	Remarks and inferences	References
Fe_3O_4			
Crystal structure and x-ray data.	$T=295$ K: cubic; space group, Fd3m; $Z=8$; $a=8.394\pm0.0005$ Å. $T_t=119$ K. $T=78$ K: Orthorhombic; space group, Imma; $a=5.912$ Å; $b=5.945$ Å; $c=8.388$ Å. TEC (128–295 K): 7.7×10^{-6}/°C. TEC is negative near T_t (-20×10^{-6}/°C) with a peak at T_t. T_t decreases with pressure; $(\partial T_t/\partial P)=-(0.46\pm0.02)$ K/kbar.	The substance is an inverse spinel. The Verwey transition in Fe_3O_4 changes the lattice symmetry from cubic to orthorhombic and causes an ordering of the Fe^{2+} and Fe^{3+} ions on the B sites which are randomly distributed above the transition temperature. The octahedral ferric ions lie along the orthorhombic a axis and the ferrous ions along the b axis in alternate rows that are mutually perpendicular.	[40–43, 47, 70].
Magnetic properties.	Ferrimagnetic; $T_N\approx860$ K. χ does not show anomaly at T_t (119 K) but anisotropy behavior noted with or without a magnetic field. $(M_s/M_o)=0.026$ at T_N. Magnetic moment = 4 μ_B. T_N increases with pressure; $(\partial T_N/\partial P)=(2.05\pm0.10)$ K/kbar.	The magnetic behavior is unaffected at the ordering transition. The magnetic moment corresponds to the spin-only value (since Fe_3O_4 is an inverse spinel), the contribution from the Fe^{3+} ions must vanish and the entire net moment must be due to the Fe^{2+} ions.	[36–38, 41, 43–46, 77].
Electrical properties.	Below T_t (119 K) semiconductor behavior; E_a increases from 0.03 to 0.15 eV just below T_t. At T_t (on heating), ρ drops by a factor of 10^2 to the order of 10^{-2} Ωcm. Above T_t, ρ continues to decrease (with $E_a\sim0.06$ eV) and in the range 250–1700 K, ρ is essentially constant ($\sim4\times10^{-3}$ Ωcm) with a slight maximum at ~350 K and a minimum at $\sim T_N$. α (500 K) ≈-60 μV/°C. R_H, however, is +ve. At 300 K, $R_H\approx5\times10^{-4}$ cm³/C; $\mu_H\sim0.1$ cm²/V s. α shows discontinuities at T_t and T_N. R_H and μ_H decrease with T below T_t and remain constant or show an increasing trend above T_t.	The electrical properties of Fe_3O_4 are a little bit complex; some workers [47, 48] assume that it exhibits a semiconductor-metal transition at T_t (119 K). However, the ρ-T behavior above T_t indicates that of a typical degenerate semiconductor. The maxima and minima at 350 and 860 K in the ρ-T plot may be spurious and requires confirmation by a detailed investigation on well-characterized, stoichiometric Fe_3O_4. The abrupt drop in ρ at T_t is explained as due to the rapid electron exchange between the octahedral Fe^{2+} and Fe^{3+} ions; this is inhibited below T_t because of the ordering process.	[39–41, 43, 49, 53–56].
Mössbauer studies.	Careful results on untwinned crystals of Fe_3O_4 indicate that the spectrum can be resolved into five individual components corresponding to a tetrahedral Fe^{2+}, two octahedral Fe^{3+} and two octahedral Fe^{2+} sites. The lines below T_t are broadened. The results are interpreted in terms of a modi-	Mössbauer studies have provided the most direct evidence of the electron exchange and ordering process in Fe_3O_4 at T_t.	[57–67].

Iron oxides—Continued

Oxide and description of the study	Data	Remarks and inferences	References
	fied Verwey model consisting of twice as large as the unit cell originally proposed. The relaxation time of the electron hopping is estimated to be 1.1 ± 0.2 ns.		
Mechanical properties.	Young's modulus drops by ~30% at 108 K; internal friction exhibits a peak at ~95 K. At 300 K, $v_L = 6.75 \times 10^5$ cm/s; $v_S = 3.69 \times 10^5$ cm/s. Both v_L and v_S along [100] axis show sharp increases of 7.5 and 0.2% respectively at 119 K. v_L also exhibits an anomaly at 130 K where there is an easy axis change in Fe_3O_4 from the [100] to the [111] axis. v_L and v_S also go through a minimum at $\sim T_N$.	These observations indicate that the 119 K transition is of first order.	[71, 72, 76].
Magnetocaloric effect.	The temperature change of a sample upon applying magnetic field has been examined through T_t in Fe_3O_4. ΔT is negative below T_t and reaches a maximum at T_t; ΔT passes through zero and becomes +ve. The sign reversal shifts to lower temperatures as the applied field gets stronger.	—	[73].
Infrared spectra.	A band at 595 cm^{-1} is noted and correlated with the bands noted in other oxide spinels.	—	[163].
γ-Fe_2O_3			
Crystal structure and properties.	Tetragonal; space group $P4_1$; $Z = 32$; $a = 8.33$ Å; $c = 24.99$ Å. γ-Fe_2O_3 is ferrimagnetic and transforms to α-modification above 670 K. $\Delta V \sim 7\%$ and high pressure studies indicate no abrupt transition at any given P and T. Detailed physical properties not known.	The structure consists of three spinel blocks stacked on top of each other; the unit cell has cation vacancies arranged in an ordered manner.	[79, 83, 91, 92—95].
ϵ-Fe_2O_3			
Crystal structure and properties.	Monoclinic; $Z = 20$; $a = 12.97$ Å; $b = 10.21$ Å; $c = 8.44$ Å; $\beta = 95.33°$. Ferromagnetic; $T_C \sim 485$–500 K. Transforms to α-form above 770 K.	Detailed properties not known.	[89, 96].
α-Fe_2O_3			
Crystal structure and x-ray studies.	$T = 300$ K: Rhombohedral (pseudo-hexagonal); space group, $R\bar{3}c$; $Z = 6$; $a = 5.0351 \pm$	Typical corundum structure assumed by many transition metal sesquioxides and α-Al_2O_3.	[98, 105, 151, 160].

Oxide and description of the study	Data	Remarks and inferences	References
	0.0003 Å; $c=13.750\pm0.001$ Å. Discontinuities in lattice parameters noted at T_N ($\approx$960 K). High pressure studies do not indicate any phase transitions up to several hundred kilobars.		
Magnetic properties.	Antiferromagnetic; $T_N\approx960$ K. $\chi\sim1.7$–2.3×10^{-5} emu/g. Magnetic moment = 2.45 μ_B. Above 263 ± 2 K (T_M), Fe_2O_3 exhibits weak superimposed ferromagnetism due to slight canting of the spins in (111) plane. The spin-flip transition has been observed in the presence of a magnetic field. Careful neutron diffraction studies show that the transition is spread over a 25–30° range, centered at 261 K. T_M depends on the particle size and stoichiometry of the sample. T_M increases with pressure; $(\partial T_M/\partial P)=3.6\pm0.3$ K/kbar.	The superimposed weak ferromagnetism in the range 260–960 K is characteristic of only α-Fe_2O_3 and the mechanism which causes the Morin transition is the change in the spin-direction from parallel to perpendicular to the c-axis. The observed pressure dependence of T_M can be explained if we assume a change in sign of the total magnetic anisotropy energy.	[99–104, 106–113, 133–137].
Electrical properties (200–1600 K).	Semiconductor behavior; ρ (300 K) $\sim10^3$–10^5 Ωcm. Pure Fe_2O_3 shows a three-region behavior with various E_a values in the range 300–1600 K; usually p type behavior but some samples show change of sign of α on heating. Impure or doped samples exhibit linear $\ln\rho$-T plots with $E_a\sim1.0$ eV. Both p- and n-type samples can be obtained by doping. For n-type Fe_2O_3, at 1000 K, $\rho\sim1$–10 Ωcm; $\alpha\sim-(400$–$700)$ μV/K; $\mu_H\sim10^{-2}$ cm²/V s. R_H changes sign at T_N.	The conductivity behavior appears to be extrinsic or controlled by native defects in the entire temperature range investigated. The reason for the sign reversal of R_H is not exactly known.	[143–150].
Mössbauer studies (100–1050 K).	Characteristic six-line spectra noted below T_N. Anomalies in isomer shift and quadrupole splitting noted at $\sim T_M$. The electric field gradient shows an abrupt increase at $\sim T_N$. The temperature dependence of the internal field is in agreement with the predictions of the molecular field theory.	Results indicate that Fe_2O_3 in the form of fine particles exhibit superparamagnetic behavior.	[102, 116–120].
Optical properties.	Absorption bands noted at 1.4, 1.9, 2.4 and 3.2 eV. Morin [164] observed a band at 0.7 eV which	The 0.7 eV peak observed by Morin seems to be associated with donor levels. The higher	[164–166].

Oxide and description of the study	Data	Remarks and inferences	References
	increases strikingly as Ti is added. Infrared bands noted in the range 285–560 cm^{-1} and are associated with the metal oxygen vibrations.	energy bands are ascribed to the crystal field transitions [166].	

References

[1] Darken, L. S., and Gurry, R. W., J. Am. Chem. Soc. 67, 1398 (1945).
[2] A.·E. Vol, Ed., Hand Book of Binary Metallic Systems: Structure and Properties, Vol. *II* (English Transl.), Israel Progr. for Scientific Translation, Jerusalem, 1967.
[3] Muan, A., Am. J. Science **256**, 171 (1958).
[4] Tannhauser, D. S., J. Phys. Chem. Solids **23**, 25 (1962).
[5] Addison, C. C., Johnson, B. F. G., and Logan, N., J. Chem. Soc. (Lond.) 4490 (1965).
[6] Roy, R., Bull. Soc. Chim. France 4, 1065 (1965).
[7] Willis, B. T. M., and Rooksby, H. P., Acta Cryst. **6**, 827 (1953).
[8] Foster, P. K., and Welch, A. J. E., Trans. Faraday Soc. **52**, 1626 (1956).
[9] Roth, W. L., Phys. Rev. **110**, 1333 (1958).
[10] Roth, W. L., Acta Cryst. **13**, 140 (1960).
[11] Berbi, G. B., J. Phys. Chem. **68**, 2912 (1964).
[12] Vallet, P., and Raccah, P., Compt. Rend. (Paris) **258**, 3679 (1964).
[13] Geiger, G. H., Levin, R. L., and Wagner, J. B., Jr., J. Phys. Chem. Solids **27**, 947 (1966).
[14] Bransky, I., and Tannhauser, D. S., Trans. AMIE **239**, 75 (1967).
[15] Wagner, J. B., Jr., in Mass Transport in Oxides, Nat. Bur. Stand. (U.S.), Spec. Publ. 296 (1968), p. 65.
[16] Libowitz, G. G., in Mass Transport in Oxides, Nat. Bur. Stand. (U.S.), Spec. Publ. 296 (1968), p. 109.
[17] Rizzo, H. F., Gordon, R. S., and Cutler, I. B., in Mass Transport in Oxides, Nat. Bur. Stand. (U.S.), Spec. Publ. 296 (1968), p. 129.
[18] Koch, F., and Cohen, J. B., Acta Cryst. **25B**, 275 (1969).
[19] Fender, B. E. F., and Riley, F. D., J. Phys. Chem. Solids **30**, 793 (1969).
[20] Fender, B. E. F., and Riley, F. D., in The Chemistry of Extended Defects in non-Metallic Solids, Eds. L. Eyring and M. O'Keeffe (North Holland Publ. Co., Amsterdam, 1970).
[21] Koch, F. B., and Fine, M. E., J. Appl. Phys. **38**, 1470 (1967); **39**, 2478 (1968).
[22] Roth, W. L., J. Appl. Phys. Suppl. **30**, 303 (1959).
[23] Childs, P. E., D. Phil, Thesis, Univ. of Oxford, England, 1967.
[24] Anderson, J. S., in Modern Aspects of Solid State Chemistry, Ed. C. N. R. Rao (Plenum Press, New York, 1970).
[25] Katsura, T., Iwasaki, B., Kimura, S., and Akimoto, S., J. Chem. Phys. **47**, 4559 (1967).
[26] Hentschel, B., Z. Naturforsch. **25a**, 1996 (1970).
[27] Aubry, J., and Marion, F., Compt. Rend. (Paris) **241**, 1778 (1955).
[28] Ofstad, P. K., and Hed, A. Z., J. Electrochem. Soc. **115**, 102 (1968).
[29] Seltzer, M. S., and Hed, A. Z., J. Electrochem. Soc. **117**, 815 (1970).
[30] Foëx, M., Compt. Rend. (Paris) **227**, 193 (1948).
[31] Mainard, R., Boubel, M., and Fousse, H., Compt. Rend. (Paris) **266B**, 1299 (1968).
[32] Samokhvalov, A. A., Sov. Phys.—Solid State (English Transl.) **3**, 2613 (1962).
[33] Clendenen, R. L., and Drickamer, H. G., J. Chem. Phys. **44**, 4223 (1966).
[34] Muan, A., Nucl. Sci. Abstr. **20**, 50 (1966).
[35] Rao, C. N. R., and Subba Rao, G. V., Phys. Stat. Solidi (a) **1**, 597 (1970).
[36] Pauthenet, R., Compt. Rend. (Paris) **230**, 1842 (1950).
[37] Sato, T., Sugihara, M., and Saito, M., Rev. Elec. Commun. Lab. **11**, 26 (1963).
[38] Gerber, R., Simsa, Z., and Vichr, M., Czech. J. Phys. **16B**, 913 (1966).
[39] Verwey, E. J. W., and Heilman, E. L., J. Chem. Phys. **15**, 174 (1947).
[40] Verwey, E. J. W., Haayman, P. W., and Romeijn, F. C., J. Chem. Phys. **15**, 181 (1947).
[41] Domenicali, C. A., Phys. Rev. **78**, 458 (1950).
[42] Abrahams, S. C., and Calhoun, B. A., Acta Cryst. **6**, 105 (1953).
[43] Calhoun, B. A., Phys. Rev. **94**, 1577 (1954).
[44] Smith, D. O., Phys. Rev. **102**, 959 (1956).
[45] Bickford, L. R., Jr., Rev. Mod. Phys. **25**, 75 (1953).
[46] Hamilton, W. C., Phys. Rev. **110**, 1050 (1958).
[47] Samara, G. A., Phys. Rev. Letters **21**, 795 (1968).
[48] Cullen, J. R., and Callen, E., J. Appl. Phys. **41**, 879 (1970); Phys. Rev. Letters **26**, 236 (1971).
[49] Miles, P. A., Westphal, W. B., and von Hippel, A., Rev. Mod. Phys. **29**, 279 (1957).
[50] Adler, D., Solid State Phys. **21**, 1 (1968).
[51] Adler, D., Rev. Mod. Phys. **40**, 714 (1968).
[52] Rosencwaig, A., Phys. Rev. **181**, 946 (1969).
[53] Siemons, W. J., IBM J. Res. & Develop. **14**, 245 (1970).
[54] Verwey, E. J. W., and Haayman, P. W., Physica **8**, 979 (1941).
[55] Kostopoulos, D., and Thedossiou, A., Phys. Stat. Solidi (a) **2**, 73 (1970).
[56] Griffiths, B. A., Elwell, D., and Parker, R., Phil. Mag. **22**, 163 (1970).
[57] Solomon, I., Compt. Rend. (Paris) **251**, 2675 (1960).
[58] Bauminger, R., Cohen, S. G., Marinov, A., Ofer, S., and Segal, E., Phys. Rev. **122**, 1447 (1961).
[59] Ito, A., Ono, V., and Ishikawa, J., J. Phys. Soc. Japan **18**, 1465 (1963).
[60] Evans, B. J., and Hafner, S. S., J. Appl. Phys. **40**, 1411 (1969).
[61] Sawatzky, G. A., Coey, J. M. D., and Morrish, A. H., J. Appl. Phys. **40**, 1402 (1969).
[62] Kündig, W., and Hargrove, R. S., Solid State Commun. **7**, 223 (1969).
[63] Romanov, V. P., Checherskii, V. D., and Eremenko, V. V., Phys. Stat. Solidi **31**, K153 (1969).
[64] Hargrove, R. S., and Kündig, W., Solid State Commun. **8**, 303 (1970).

[65] Daniels, J. M., and Rosencwaig, A., J. Phys. Chem. Solids **30**, 1561 (1969).
[66] Romanov, V. P., and Checherskii, V. D., Sov. Phys.—Solid State (English Transl.) **12**, 1474 (1970).
[67] Kuzmin, R. N., and Gendler, T. S., Sov. Phys.—Crystallogr. (English Transl.) **15**, 634 (1971).
[68] Samuelsen, E. J., Bleeker, E. J., Dobrzynski, L., and Riste, T., J. Appl. Phys. **39**, 1114 (1968).
[69] Yamada, T., Suzuki, K., and Chikazumi, S., Appl. Phys. Letters **13**, 172 (1968).
[70] Vittoratos, E., Baranov, I., and Meincke, P. P. M., J. Appl. Phys. **42**, 1633 (1971).
[71] Fine, M. E., and Kenney, N. T., Phys. Rev. **94**, 1573 (1954).
[72] Moran, T. J., and Lüthi, B., Phys. Rev. **187**, 710 (1969).
[73] Krasovskii, V. P., and Fakidov, I. G., Sov. Phys.—JETP (English Transl.) **12**, 170 (1961).
[74] Boyd, E. L., Phys. Rev. **129**, 1961 (1963).
[75] Mizoguchi, T., and Inoue, M., J. Phys. Soc. Japan **21**, 1310 (1966).
[76] Kamilov, I. M., and Aliev, Kh. K., Sov. Phys.—Solid State (English Transl.) **12**, 1476 (1970).
[77] Samara, G. A., and Giardini, A. A., Phys. Rev. **186**, 577 (1969).
[78] van Hook, H. J., and Keith, M. L., Am. Mineral. **43**, 69 (1958).
[79] Rooymans, C. J. M., Philips Res. Rep. Suppl. **1**, 95 (1968).
[80] Blackman, M., and Kaye, G., Proc. Phys. Soc. (Lond.) **75**, 364 (1960).
[81] Cirilli, V., Gazz. Chim. ital. **80**, 347 (1950).
[82] Michel, A., and Lensen, M., Compt. Rend. (Paris) **243**, 1422 (1956).
[83] van Oosterhout, G. W., and Rooymans, C. J. M., Nature (Lond.) **181**, 44 (1958).
[84] Tejima, N., Chem. Abstr. **69**, 44935n (1968).
[85] Glemser, O., and Gwinner, E., Naturwiss. **26**, 739 (1938); Z. anorg. allgem. Chem. **240**, 161 (1939).
[86] Conley, R. F., J. Am. Ceram. Soc. **50**, 124 (1967).
[87] Okamoto, S., J. Am. Ceram. Soc. **51**, 54 (1968).
[88] Cook, W. R., Jr., J. Am. Ceram. Soc. **51**, 408 (1968).
[89] Schrader, R., and Büttner, G., Z. anorg. allgem. Chem. **320**, 220 (1963).
[90] Clark, S. P., Ed., Hand Book of Phys. Constants, Geol. Soc. Am. Mem. **97**, 153 (1966).
[91] Takei, H., and Chiba, S., J. Phys. Soc. Japan **21**, 1068 (1966).
[92] Senno, H., and Tawara, T., Japan J. Appl. Phys. **6**, 509 (1967).
[93] Senno, H., Tawara, T., and Iida, Y., Japan J. Appl. Phys. **6**, 1347 (1967).
[94] Oles, A., Szytula, A., and Wanic, A., Phys. Stat. Solidi **41**, 173 (1970).
[95] Coto, Y., Japan J. Appl. Phys. **3**, 739 (1964).
[96] Trautman, J.-M., and Forestier, H., Compt. Rend. (Paris) **261**, 4423 (1965).
[97] Drakeford, R. W., and Quinn, C. M., J. Mat. Sci. **6**, 175 (1971).
[98] Newnham, R. E., and de Haan, Y. M., Z. Krist. **117**, 235 (1962).
[99] Gullaud, C., J. Phys. Rad. **12**, 489 (1951).
[100] Shull, C., Strauser, W. A., and Wollan, E. O., Phys. Rev. **83**, 333 (1951).
[101] Corliss, L. M., Hastings, J. M., and Goldman, J. E., Phys. Rev. **93**, 893 (1954).
[102] Freier, S., Greenshpan, M., Hillman, P., and Shechter, H., Phys. Letters **2**, 191 (1962).
[103] Gilad, P., Greenshpan, M., Hillman, P., and Shechter, H., Phys. Letters **7**, 239 (1963).
[104] Lielmezs, J., and Chaklader, A. C. D., Science **160**, 1137 (1968).
[105] Willis, B. T. M., and Rooksby, H. P., Proc. Phys. Soc. (Lond.) **65B**, 950 (1952).
[106] Morin, F. J., Phys. Rev. **78**, 819 (1950).
[107] Nathans, R., Pickart, S. J., Alperin, H. A., and Brown, P. J., Phys. Rev. **136A**, 1641 (1964).
[108] Curry, N. A., Johnston, G. B., Besser, P. J., and Morrish, A. H., Phil. Mag. **12**, 221 (1965).
[109] Bizette, H., Chevallier, R., and Tsai, B., Compt. Rend. (Paris) **236**, 2043 (1953).
[110] Tasaki, A., and Iida, S., J. Phys. Soc. Japan **18**, 1148 (1963).
[111] Besser, P. J., and Morrish, A. H., Phys. Letters **13**, 289 (1964).
[112] Flanders, P. J., and Remeika, J. P., Phil. Mag. **11**, 1271 (1965).
[113] Cinader, G., Flanders, P. J., and Shtrikman, S., Phys. Rev. **162**, 419 (1967).
[114] Fouer, S., and Williamson, S. J., J. Appl. Phys. **36**, 1154 (1965).
[115] Ozhogin, V. I., and Shapiro, V. G., Sov. Phys.—JETP (English Transl.) **28**, 915 (1969).
[116] Ono, K., and Ito, A., J. Phys. Soc. Japan **17**, 1012 (1962).
[117] Kundig, W., Bommel, H., Constabaris, G., and Lindquist, R. H., Phys. Rev. **142**, 327 (1966).
[118] van Der Woude, F., Phys. Stat. Solidi **17**, 417 (1966).
[119] Vlasov, A. Ya., Loseva, G. V., Makarov, F., Murashko, N. V., Petukhov, E. P., and Povitskii, V. A., Sov. Phys.—Solid State (English Transl.) **12**, 1177 (1970).
[120] Fabrichnyi, P. B., Babeshkin, A. M., Nesmeyanov, A. N., and Onuchak, V. N., Sov. Phys.—Solid State (English Transl.) **12**, 1614 (1971).
[121] Anderson, D. H., Phys. Rev. **151**, 247 (1966).
[122] Shapira, Y., Phys. Rev. **184**, 589 (1969); J. Appl. Phys. **42**, 1588 (1971).
[123] Pisarev, R. V., Sinii, I. G., and Smolenskii, G. A., Sov. Phys.—JETP Letters (English Transl.) **9**, 172 (1969).
[124] Riste, T., and Wanic, A., J. Phys. Chem. Solids **17**, 318 (1961).
[125] Dimitrijevic, Z., Kraśnicki, S., Rjany, H., Todorovic, J., Wanic, A., Curieu, H., and Milojevic, A., Phys. Stat. Solidi **21**, K163 (1967).
[126] Samuelsen, E. J., Physica **34**, 241 (1967).
[127] Samuelsen, E. J., and Shirane, G., Phys. Stat. Solidi **42**, 241 (1970).
[128] Novotny, P., and Kaczer, J., Czech. J. Phys. **20B**, 979 (1970).
[129] Dzyaloshinski, I. E., Sov. Phys.—JETP (English (Transl.) **6**, 1120 (1960); J. Phys. Chem. Solids **4**, 241 (1958).
[130] Moriya, T., Phys. Rev. **120**, 91 (1960).
[131] Artman, J. O., Murphy, J. C., and Fouer, S., Phys. Rev. **138A**, 912 (1965).
[132] Herbert, D. C., Phys. Rev. Letters **22**, 1184 (1969); J. Phys. C (Solid State) **2**, 1606 (1969); **2**, 1614 (1969); **3**, 891 (1970).
[133] Kawai, N., and Ono, F., Phys. Letters **21**, 279 (1966).
[134] Umebayashi, H., Frazer, B. C., Shirane, G., and Daniels, W. B., Phys. Letters **22**, 407 (1966).
[135] Wayne, R. C., and Anderson, D. H., Phys. Rev. **155**, 496 (1967).
[136] Schroeer, S., and Nininger, R. C., Jr., Phys. Rev. Letters **19**, 632 (1967).
[137] Gallagher, P. K., and Gyorgy, E. M., Phys. Rev. **180**, 622 (1969).
[138] Besser, P. J., Morrish, A. H., and Searle, C. W., Phys. Rev. **153**, 632 (1967).
[139] Voskanyan, R. A., Sov. Phys.—JETP (English Transl.) **30**, 457 (1970).
[140] Kren, E., Szabo, P., and Konczos, G., Phys. Letters **19**, 103 (1965).
[141] Dezsi, I., Erlaki, Gy., and Keszthelyi, L., Phys. Stat. Solidi **21**, K121 (1967).
[142] Morrish, A. H., and Eaton, J. A., J. Appl. Phys. **42**, 1495 (1971).
[143] Morin, F. J., Phys. Rev. **83**, 1005 (1951).
[144] Gardner, R. F. G., Swett, F., and Tanner, D. W., J. Phys. Chem. Solids **24**, 1175 (1963); **24**, 1183 (1963).
[145] Tanner, D. W., Swett, F., and Gardner, R. F. G., Brit. J. Appl. Phys. **15**, 1041 (1964).
[146] Subba Rao, G. V., Wanklyn, B. M., and Rao, C. N. R., J. Phys. Chem. Solids **32**, 345 (1971).
[147] Bevan, D. J. M., Shelton, J. P., and Anderson, J. S., J. Chem. Soc. (Lond.) 1729 (1948).

[148] Lessoff, H., Kersey, Y., and Horne, R. A., J. Chem. Phys. 31, 1141 (1959).
[149] Nakau, T., J. Phys. Soc. Japan 15, 727 (1960).
[150] van Daal, H. J., and Bosman, A. J., Phys. Rev. 158, 736 (1967).
[151] Lewis, G. K., Jr., and Drickamer, H. G., J. Chem. Phys. 45, 224 (1966).
[152] Kawai, N., and Mochizuki, S., Phys. Letters 36A, 54 (1971).
[153] Geller, S., Grant, R. W., Cape, J. A., and Espinosa, G. P., J. Appl. Phys. 38, 1457 (1967).
[154] Chevalier, R. R., Roult, G., and Bertaut, E. F., Solid State Commun. 5, 7 (1967).
[155] Grant, R. W., Geller, S., Cape, J. A., and Espinosa, G. P., Phys. Rev. 175, 686 (1968).
[156] Hase, W., Brückner, W., Tobsisch, J., Ullrich, H.-J., and Wegerer, G., Z. Krist. 129, 360 (1969).
[157] Geller, S., J. Appl. Phys. 42, 1499 (1971).
[158] Cox, D. E., Takei, W. J., and Shirane, G., J. Phys. Chem. Solids 24, 405 (1963).
[159] Marezio, M., and Remeika, J. P., J. Chem. Phys. 46, 1862 (1967).
[160] Prewitt, C. T., Shannon, R. D., Rogers, D. B., and Sleight, A. W., Inorg. Chem. 8, 1985 (1969).
[161] Schneider, S J., Roth, R. S., and Waring, J. L., J. Res. Nat. Bur. Stand. (U.S.), 65A (Phys. and Chem.), No. 4, 345–374 (July–Aug. 1961).
[162] Geller, S., Williams, H. J., and Sherwood, R. C., J. Chem. Phys. 35, 1908 (1961).
[162] Hafner, S., Z. Krist. 115, 331 (1961).
[164] Morin, F. J., Phys. Rev. 93, 1195 (1954).
[165] Bailey, P. C., J. Appl. Phys. 31, 39S (1960).
[166] Subba Rao, G. V., Rao, C. N. R., and Ferraro, J. R., Appl. Spec. 24, 436 (1970).

I.7. Cobalt Oxides

In the Co-O system, CoO and Co_3O_4 are the stable oxides which have been investigated in detail. Although many workers have reported the preparation and properties of a sesquioxide, Co_2O_3, characterization with respect to stoichiometry and method of preparation seems to be still in doubt and many a time, hydrated forms of the oxides are obtained.

Cobalt monoxide, CoO, has a narrow range of homogeneity [1–4]. It has a cubic rock salt structure at room temperature and is paramagnetic [5–8]. Below 289 K, it becomes antiferromagnetic followed by a crystal distortion to tetragonal symmetry [5–7, 9] and the tetragonality increases with decrease in temperature. Detailed x-ray diffraction studies [10] at low temperatures indicated that a rhombohedral deformation is superimposed on the tetragonal distortion and at 123 K, the true symmetry is monoclinic. The magnetic structure in the low temperature phase of CoO has been examined by various workers [11–13]. Although a number of non-collinear spin-axis structures are possible in CoO [12, 14], available experimental evidence points to a collinear structure [10, 13, 15] with the moments tipped out of the {111} planes 7.85° toward the c axis.

The transition in CoO has been studied by a variety of techniques in recent years. χ-T data on powder and single crystalline CoO indicate typical antiferromagnetic behavior below T_N [16–19]. CoO is semiconducting at all temperatures and discontinuities in ρ, α, and R_H are exhibited at the Néel temperature by pure and Li-doped CoO [20–22]. Similarly, anomalies in C_p [23–26], κ [25, 27], elastic wave velocity [27, 28–30], elastic constants, internal friction and Young's modulus [27–29, 31] and α_{td} [25] have been noted at $\sim T_N$ in CoO. The continuous nature of the transition as indicated by κ, C_p and neutron scattering experiments [9, 23–27] seem to infer that the antiferromagnetic→paramagnetic transition in CoO is of the order greater than unity. CoO was one of the first compounds to be studied by Mössbauer spectroscopy and many workers have examined the spectrum as a function of temperature [32–39]. Below T_N, a six-line pattern indicating magnetic hyperfine splitting is seen; this disappears in the paramagnetic state. The Néel temperatures obtained from Mössbauer studies agree excellently with those obtained by other techniques.

Effect of pressure on the magnetization and magnetic ordering temperature of CoO has been investigated by a few workers [40, 41]; the results indicate that T_N increases with increasing pressure and decreasing volume. X-ray diffraction [8] and resistivity [42] studies do not indicate any high pressure transitions in CoO up to pressures of ~250 kbar.

According to Ok and Mullen [37, 43], there exist two forms of cobalt monoxide, CoO (I) and CoO (II). Both have cubic rock salt structure at room temperature but CoO (II) has a lesser density and the lattice has ~25 percent vacancies. CoO (II) can only be prepared at room temperatures and is very reactive with atmospheric oxygen at ordinary temperatures. The two forms show different Mössbauer patterns and their Néel temperatures differ. CoO (II) transforms to CoO (I) above ~573 K with a transformation rate that increases with temperature; on the other hand, the transition is not complete on heating CoO (II) in an argon atmosphere up to ~1270 K for several hours and generally CoO (I, II) is obtained which can be treated as a mixture of forms I and II in varying amounts. Ok and Mullen point out that pressures of ~10 kbar are not sufficient to transform II→I at 300 K in an inert atmosphere. These authors indicate that the usual chemical methods of preparation of CoO yield always CoO (I, II).

It should be mentioned that the Mössbauer spectra of the oxides reported by Ok and Mullen [37] differ nontrivially with the work of others; complete characterization of CoO (I) and CoO (II) is less

unequivocally established [43]. Further detailed work is urgently needed.

Optical properties of CoO have been examined by many workers over a wide energy range (0.02–26.0 eV) [44–53]. Studies in the UV region have provided an understanding of the density of states in CoO [44, 45, 49, 50, 52]; some of the bands observed in the far infrared region have been ascribed to the antiferromagnetic resonance [19, 46, 47, 53] but the resonance frequencies are insensitive to temperature [53].

Small amounts of Li and Ti can be incorporated in CoO and a great deal of work has been carried out on these doped materials [3, 20–22, 50, 54, 55]. Generally, doping with Li decreases the resistivity compared to the pure stoichiometric material. CoO forms solid solutions with other metallic oxides like MnO, FeO, NiO and MgO [24, 51, 56, 57]. The magnetic, electrical, optical and thermal properties show variations depending on the composition of the solid solution.

Co_3O_4 is a normal spinel and has the ionic structure $Co^{2+}[Co^{3+}]_2O_4$; it is cubic [58, 59] and paramagnetic but not ferrimagnetic, although it crystallizes in the magnetite structure. The Co^{3+} ions have zero permanent moment as a consequence of the splitting of the $3d$ levels by the octahedral cubic field. At ~40 K, Co_3O_4 undergoes a transition to form an ordered antiferromagnetic state [58]; the magnetic structure is due to antiferromagnetic ordering of spins in the A sites of the spinel structure [60] and each Co^{2+} ion in an A site is surrounded by four nearest neighbors with oppositely directed spins. χ_M-T curve follows a Curie-Weiss law with a deviation at high temperatures in the range 90–500 K and the abnormally low value of χ_M in Co_3O_4 is ascribed to the fact that the material is a 2–3 spinel in which Co^{3+} give no contribution to the magnetic moment [61, 62].

Co_3O_4 is a semiconductor [42, 63, 64] at ordinary and at high pressures [42]; however, detailed studies on single crystal materials have not been made. Mössbauer studies on Co_3O_4 have been reported by a few workers [38, 39, 65]. Above T_N ($=33\pm1$ K), two quadrupole split lines corresponding to A and B site Fe^{3+} are noted while below T_N the A site Fe^{3+} spectrum is magnetically split due to the antiferromagnetic Co^{2+} sublattice. NMR studies [66, 67] of Co_3O_4 fully confirm the spinel structure and different oxidation states of cobalt ion at the A and B sites.

Cobalt oxides

Oxide and description of the study	Data	Remarks and inferences	References
CoO			
Crystal structure and x-ray study.	$T=290$ K: Cubic, space group, Fm3m; $Z=4$; $a=4.260$ Å. $T=250$ K: Tetragonal; $a=4.263$ Å; $c=4.247$ Å. $T=123$ K: Monoclinic; space group, C2/m; $Z=2$; $a=5.18\pm0.03$ Å; $b=3.01\pm0.05$ Å; $c=3.01\pm0.07$ Å; $\beta=125.55\pm0.01°$. X-ray studies conducted in the range 210–330 K indicate the change in crystal symmetry at 284 ± 1 K which is recognized as the T_N.	The low temperature structure (at and below 123 K) is shown to be strictly monoclinic and not tetragonal.	[5–7, 10].
Magnetic susceptibility in the range 90–500 K and the effect of pressure.	$\chi_M \sim 10^{-3}$ cgs units; slight anisotropy noted. $T_N=287.25$ K and T_N increases with pressure; $(dT_N/dP)=0.6\pm0.03$ K/kbar.	The calculated values of χ_M on the basis of Kanamori's theory [19] are in agreement with the experimental values.	[16–19, 41].

Cobalt oxides—Continued

Oxide and description of the study	Data	Remarks and inferences	References
Electrical properties.	Pure oxide: $\rho \sim 10^{7}$–10^{11} Ωcm in the range 200–300 K; ρ(1300 K)$\sim$ 0.5 Ωcm; μ_D (1300 K)$\sim$0.4 cm^2/V s; E_a changes at T_N and slightly depends on the stoichiometry. Li doped CoO (0.05–0.15%): $\rho \sim 0.5$ Ωcm; $\alpha \sim +500$ μV/K; $\mu_D = 0.25$ cm^2/V s (1200 K); $\mu_D \sim 6$ cm^2/V s (300 K); R_H is +ve; ρ and R_H show discontinuities at T_N. μ_H is constant in the range 200–1500 K ($\sim$0.1 cm^2/V s); p type behavior. ρ decreases with pressure but no transition occurs up to 250 kbars.	Typical semiconductor behavior in the temperature range investigated. Band and polaron theories have been applied to explain the mechanism of conduction in pure and doped CoO and the weight of experimental evidence seems to point out the validity of band model in this oxide.	[1, 3, 20–22, 42, 68].
Optical reflectance spectra (range 1–26 eV).	Optical reflectance spectra give bands at 5.5, 7.5, 12.6 and 17.5 eV. The observed bands at 0.97 and 2.28 eV are attributed to $^4T_{1g} \rightarrow {}^4T_{2g}$ and $^4T_{1g} \rightarrow {}^4T_{1g}(P)$ respectively [49].	The low energy bands are interpreted as the exciton transitions whereas the higher energy bands may be due to the transitions in the conduction band. The data show the localization of the d electrons in CoO and the $2p$ band of oxygen seems to lie $\sim$8.5 eV below the vacuum level.	[44, 49, 50, [52].
Infrared spectra (100–300 cm^{-1})	Prominent bands are at 146, 215, 222, 233, 243, 250, 260, and 297 cm^{-1}. Most of the bands are presumed to be the antiferromagnetic resonance modes but temperature variation in the range 2–300 K shows the band to be insensitive.	The data are in agreement with the theoretically predicted values using time-dependent molecular field theory.	[19, 45–49, 53].
Mössbauer studies of ^{57}Fe doped CoO at ordinary and high pressures.	1 atmospheric pressure: The hyperfine splitting disappears at T_N (291 K); Isomer shift, screening parameter and magnetic hyperfine field show discontinuities at T_N. High pressures: T_N increases with pressure; $(d \ln T_N / d \ln V) = -3$. Isomer shift and screening parameter show small changes on the application of pressure. Ok and Mullen [43] report different values of Mössbauer parameters for CoO(I) and CoO(II).	Quantitative features of the spectra seem to differ for various investigations but the general agreement with the values of T_N is excellent.	[32–40, 43].
Thermal properties.	Dilatometric study shows that the coefficient of expansion passes through a sharp maximum at 292 K for CoO; TEC at 292 K = 3.0×10^{-5}/K. C_p and κ show anomalies at T_N; C_p (290 K) = 32 cal/mol, K.	The discontinuous nature of the transition indicates that it is probably of a higher order transformation.	[24–27, 69].

Oxide and description of the study	Data	Remarks and inferences	References
Mechanical properties.	Sound velocities in various crystallographic directions change discontinuously above T_N by 10–20%. Elastic moduli ($\times 10^{11}$ dyn/cm^2) (300 K): $c_{11}=26.17\pm 0.03$; $c_{12}=14.5\pm 0.2$; $c_{44}=8.32\pm 0.02$. During phase transition, c_{11} and c_{12} exhibit jumps. In the region of the transition, Young's modulus increases rapidly from 6.3 to 17×10^{11} dyn/cm, with increase in temperature and the moduli are approximately step functions of temperature; on the other hand, the internal friction in CoO falls from 91 to 2 ($\times 10^{-4}$) at T_N for a constant strain amplitude of 10^{-7}. Increasing the strain amplitude has little effect on the Young's modulus and internal friction.		[28, 29, 31].
Co_3O_4			
Crystal structure and magnetic properties.	$T=300$ K: Cubic; $a=8.0835$ Å; space group: Fd3m ($T>T_N$); F$\bar{4}$3m ($T<T_N$). $T_N=40$ K. χ_M (100 K) $=1.4\times 10^{-2}$; χ_M (300 K) $=0.71\times 10^{-2}$. The Co^{2+} moment below T_N is 3.02 μ_B.	The crystal structure does not change in going through T_N but the space group changes. The low value of χ_M is believed to be due to the absence of permanent moment of Co^{3+} and the magnetic structure is due to the antiferromagnetic ordering of the spins of Co^{2+} ions on the A sites of the spinel structure.	[58, 59, 61, 62].
Electrical properties.	Semiconductor; $\rho\sim 10^3$–10^4 Ωcm; ρ decreases with P and a minimum is noted at 215 kbars in the ρ-P plot. Detailed data not available.		[42].
Mössbauer studies.	T_N is found to be 33 ± 1 K; above T_N, two quadrupole split lines are observed corresponding to A and B spinel sites whereas below T_N, the A site Fe^{3+} spectrum is magnetically split due to the antiferromagnetic Co^{2+} sublattice.	T_N obtained from Mössbauer work is less than that reported by χ_M-T measurements. The behavior of ultrafine particles of Co_3O_4 towards Mössbauer spectra is interesting and needs further detailed study.	[38, 39, 65].

Oxide and description of the study	Data	Remarks and inferences	References
	Above T_N, the spectra of the ultrafine particles (diameter = 100 Å) of Co_3O_4 is found to be identical to that of the bulk material. Below T_N, the fine particles display superparamagnetic behavior and the B site spectral broadening is enhanced. The anisotropy constant estimated from the superparamagnetic-antiferromagnetic transition is 4×10^4 erg/cm^3. Effective θ_D = 185 K.		
NMR studies of ^{59}Co in the paramagnetic state.	The Co signal is identified with the Co^{3+} ions at the B sites and the line shift is separated into T-dependent and T-independent terms; the line shapes are studied and the thermal relaxation time is estimated to be $\sim1.5\times10^{-5}$ s.	The T-independent shift (1.5%) is interpreted as the second order chemical shift due to the mixing of the low-lying excited state; the T-dependent shift is attributed to the hyperfine coupling between the Co nuclear spin and the electron spins on the Co^{2+} ions at the A sites in Co_3O_4. The super-exchange mechanisms are examined and it is concluded that 2% fractional spin density in the Co^{3+} e_g orbital mainly contributes to the super-exchange.	[66, 67].
Diffuse reflectance spectral studies.	Absorption bands at 0.81 and 1.85 eV are noted. These are attributed to Co^{2+} at A sites ($^4A_2\rightarrow{}^4T_2$) and Co^{3+} at B sites ($^1T_{1g}\rightarrow{}^1A_{1g}$) transitions respectively; corresponding Dq values are 0.08 and 0.19 eV.	It is concluded that the forbidden band widths in CoO and Co_3O_4 are almost identical.	[49].
Infrared spectral studies.	The prominent bands are at 570 and 665 cm^{-1}; other bands are at 350, 460 and 635 cm^{-1}.	The spectra have been discussed in relation to other oxide spinels and and covalency effects.	[48, 70, 71].
Co_2O_3			
Crystal structure and phase transition	Low-spin phase (with $t_{2g}^6e_g^0$ configuration) is obtained at high pressures. This phase has corundum structure (a = 4.782 Å and c = 12.96 Å). The low-spin phase transforms to the high-spin corundum phase ($t_{2g}^4e_g^2$) around 670 K (a = 4.8882 Å, c = 13.34 Å).	The high-spin phase appears to be the stable phase at atmospheric pressure.	[72].

References

[1] Fisher, B., and Tannhauser, D. S., J. Electrochem. Soc. **111**, 1194 (1964); J. Chem. Phys. **44**, 1663 (1966).
[2] Wagner, J. B., Jr., in Mass Transport in Oxides, NBS Special Publ. 296 (1968).
[3] Eror, N. G., and Wagner, J. B., Jr., J. Phys. Chem. Solids **29**, 1597 (1968).
[4] Reed, T. B., in The Chemistry of Extended Defects in non-Metallic Solids, Eds. L. Eyring and M. O'Keeffe (North Holland Publ. Co., Amsterdam, 1970), pp 21–35.
[5] Tombs, N. C., and Rooksby, H. P., Nature (Lond.) **165**, 442 (1950).
[6] Greenwald, S., and Smart, J. S., Nature (Lond.) **166**, 523 (1950).
[7] Greenwald, S., Acta Cryst. **6**, 396 (1953).
[8] Clendenen, R. L., and Drickamer, H. G., J. Chem. Phys. **44**, 4223 (1966).
[9] Rechtin, M. D., Moss, S. C., and Averbach, B. L., Phys. Rev. Letters **24**, 1485 (1970).
[10] Saito, S., Nakagihashi, K., and Shimomura, Y., J. Phys. Soc. Japan **21**, 850 (1966).
[11] Roth, W. L., Phys. Rev. **110**, 1333 (1958); **111**, 772 (1958).
[12] Van Laar, B., Phys. Rev. **138A**, 584 (1965); J. Phys. Soc. Japan **20**, 1282 (1965).
[13] Khan, D. C., and Drickson, R. A., J. Phys. Chem. Solids **29**, 2087 (1968).
[14] Bertaut, E. F., J. Phys. Chem. Solids **30**, 763 (1969).
[15] Nagamiya, T., Saito, S., Shimomura, Y., and Uchida, E., J. Phys. Soc. Japan **20**, 1285 (1965).
[16] La Blanchetais, C. H., J. Phys. Radium **12**, 765 (1951).
[17] Singer, J. R., Phys. Rev. **104**, 929 (1956).
[18] Uchida, E., Fukuoka, N., Kondo, H., Takeda, T., Nakazumi, Y., and Nagamiya, T., J. Phys. Soc. Japan **19**, 2088 (1964).
[19] Tachiki, M., J. Phys. Soc. Japan **19**, 454 (1964).
[20] Van Daal, H. J., and Bosman, A. J., Phys. Rev. **158**, 736 (1967).
[21] Austin, I. G., Springthorpe, A. J., Smith, B. A., and Turner, C. E., Proc. Phys. Soc. (Lond.) **90**, 157 (1967).
[22] Bosman, A. J., and Crevecoeur, C., J. Phys. Chem. Solids **30**, 1151 (1969).
[23] Assayag, C., and Bizette, H., Compt. Rend. (Paris) **239**, 238 (1954).
[24] Bizette, H., and Mainard, R., Bull. Soc. Sci. Bretagne **42**, 209 (1967).
[25] Zhuze, V. P., Novruzov, O. N., and Shelykh, A. I., Sov. Phys.—Solid State (English Transl.) **11**, 1044 (1969).
[26] Salamon, M. B., Phys. Rev. B **2**, 214 (1970).
[27] Slack, G. A., Phys. Rev. **126**, 427 (1962).
[28] Fine, M. E., Phys. Rev. **87**, 1143 (1952); Rev. Mod. Phys. **25**, 158 (1953).
[29] Aleksandrov, K. S., Shabanova, L. A., and Reshchikova, L. M., Sov. Phys.—Solid State (English Transl.) **10**, 1316 (1968).
[30] Ikushima, A., Phys. Letters **29A**, 417 (1969).
[31] Street, R., and Lewis, B., Nature (Lond.) **168**, 1036 (1951); Phil. Mag. **1**, 663 (1956).
[32] Wertheim, G. K., Phys. Rev. **124**, 764 (1961).
[33] Bearden, A. I., Mattern, P. L., and Hart, T. R., Rev. Mod. Phys. **36**, 470 (1964).
[34] Coston, C. I., Ingalls, R., and Drickamer, H. G., Phys. Rev. **145**, 409 (1966).
[35] Bhide, V. G., and Shenoy, G. K., Phys. Rev. **147**, A306 (1966).
[36] Triftshauser, W., and Craig, P. P., Phys. Rev. Letters **16**, 1161 (1966).
[37] Ok, H. N., and Mullen, J. G., Phys. Rev. **168**, 550 (1968); **168**, 563 (1968).
[38] Murin, A. N., Lur'e, B. G., and Seregin, P. P., Sov. Phys.—Solid State (English Transl.) **10**, 1000 (1968); **10**, 2006 (1968).
[39] Bondarevskii, S. I., Shipatov, V. T., Seregin, P. P., and Perepech, K. V., Sov. Phys.—Solid State (English Transl.) **11**, 1929 (1969).
[40] Coston, C. J., Ingalls, R., and Drickamer, H. G., J. Appl. Phys. **37**, 1400 (1966).
[41] Bloch, D., Chaissé, F., and Pauthenet, R., J. Appl. Phys. **37**, 1401 (1966).
[42] Minomura, S., and Drickamer, H. G., J. Chem. Phys. **34**, 3043 (1963).
[43] Ok, H. N., and Mullen, J. G., Phys. Rev. **181**, 986 (1969).
[44] Doyle, W. P., and Lonergan, G. A., Disc. Faraday Soc. (Lond.) **26**, 27 (1958).
[45] Newman, R., and Chrenko, R. M., Phys. Rev. **115**, 1147 (1959).
[46] Sakurai, J., Buyers, W. J. L., Cowley, R. A., and Dolling, G., Phys. Rev. **167**, 510 (1968).
[47] Daniel, M. R., and Cracknell, A. P., Phys. Rev. **177**, 932 (1969).
[48] Cherkashin, A. E., Vilesov, F. I., Semin, G. L., and Matvienko, L. G., Sov. Phys.—Solid State (English Transl.) **11**, 142 (1969).
[49] Cherkashin, A. E., and Vilesov, F. I., Sov. Phys.—Solid State (English Transl.) **11**, 1068 (1969).
[50] Cherkashin, A. E., Vilesov, F. I., and Semin, G. L., Sov. Phys.—Solid State (English Transl.) **11**, 511 (1969).
[51] Jacono, M. L., Sgamelotti, A., and Cimino, A., Z. Phys. Chem. (N.F.) **70**, 179 (1970).
[52] Powell, R. J., and Spicer, W. E., Phys. Rev. **B2**, 2182 (1970).
[53] Austin, I. G., and Garbett, E. S., J. Phys. C (Solid State Phys.) **3**, 1605 (1970).
[54] Bosman, A. J., and Crevecoeur, C., J. Phys. Chem. Solids **29**, 109 (1968).
[55] Gvishi, M., and Tannhauser, D. S., Solid State Commun. **8**, 485 (1970).
[56] Muan, A., Nucl. Sci. Abstr. **20**, 50 (1966).
[57] Cimino, A., Jacono, M. L., Porta, P., and Valigi, M., Z. Phys. Chem. (N.F.) **70**, 166 (1970).
[58] Roth, W. L., J. Phys. Chem. Solids **25**, 1 (1964).
[59] Knop, O., Reid, K. I. G., Sutarno, and Nakagawa, Y., Canadian J. Chem. **46**, 3463 (1968).
[60] Rao, C. N. R., and Subba Rao, G. V., Phys. Stat. Solidi (a) **1**, 597 (1970).
[61] Cossee, P., J. Inorg. Nucl. Chem. **8**, 483 (1958).
[62] Perthel, R., and Jahn, H., Phys. Stat. Solidi **5**, 563 (1964).
[63] Goodenough, J. B., Magnetism and the Chemical Bond (Interscience Publ., Inc. and John Wiley Inc., New York, 1963).
[64] Oehlig, J. J., Le Brusq, H., Duquesnoy, A., and Marion, F., Compt. Rend. (Paris) **265**, 421 (1967).
[65] Kuendig, W., Kobelt, M., Appel, H., Constabaris, G., and Lindquist, R. H., J. Phys. Chem. Solids **30**, 819 (1969).
[66] Miyatani, K., Kohn, K., Kamimura, H., and Iida, S., J. Phys. Soc. Japan **21**, 464 (1966).
[67] Kamimura, H., J. Phys. Soc. Japan **21**, 484 (1966).
[68] Cox, J. T., and Quinn, C. M., J. Mat. Science **4**, 33 (1969).
[69] Foëx, M., Compt. Rend. (Paris) **227**, 193 (1948).
[70] Hafner, S., Z. Krist. **115**, 331 (1961).
[71] McDevit, N. T., and Baun, W. Z., Spectrochim. Acta **20**, 799 (1964).
[72] Chenavas, J., Joubert, J. C., and Marezio, M., Solid State Commun. **9**, 1057 (1971).

I.8. Nickel Oxides

Nickel monoxide, NiO, is the only stable oxide in the Ni-O system. Earlier literature [1, 2] contains reports of the existence of some 25 different oxides of nickel including Ni_3O_4, Ni_2O_3, and NiO_2 and Kuznetsov [3] has recently suggested that all the higher oxides and oxide solid solutions are merely partial hydroxide decomposition products. Detailed studies made recently [4–6] have shown that the monoxide is the only material known in the Ni-O system and slight deviations from stoichiometry are allowed [4–7]. The possibility of synthesizing Ni_3O_4 at high pressure has been pointed out [8].

NiO is one of the extensively studied transition metal oxides. In the paramagnetic state it has the fcc rock salt structure [9–17] and as the temperature is lowered through T_N ($\sim$523 K), there is a trigonal distortion in the unit cell [9–14, 16, 17] and the material becomes antiferromagnetic [11–13, 18]; in addition, there is an isotropic volume contraction associated with the magnetic behavior. In the antiferromagnetic state, the spins are ferromagnetically alligned in sheets parallel to (111) planes and antiparallel to those in adjacent sheets [11–13, 18]. This magnetic structure is characteristic of all the transition metal monoxides and is explained as due to the antiferromagnetic superexchange through the p orbitals of the intervening oxygen anions [19]. Below T_N, the unit cell contracts along the [111] axis perpendicular to the ferromagnetic sheets and the crystal becomes rhombohedral; the distortion from cubic is, however, small and the rhombohedral angle increases from 90° at T_N to 90.06° at 300 K [17]. χ-T data definitely indicate the antiferromagnetic behavior of NiO [20]. Magnetic anisotropy and antiferromagnetic domains in NiO have been studied by a few workers [13, 19, 21–24].

Pure, stoichiometric NiO is green in color and the reported black and grey colors are due to slight deviations from stoichiometry or the presence of impurities [25–27]. Stoichiometric NiO is a good electrical insulator ($\rho \sim 10^{13}\Omega$cm) but the ρ decreases drastically by slight changes in the stoichiometry or by lithium doping at small concentrations. Electrical properties of pure and doped NiO have been investigated by various workers for the past few years [4, 5, 28–48]. Discontinuities in ρ, E_a, α and R_H are encountered at T_N; R_H changes sign from positive to negative values at around T_N, but the exact cause of this behavior is not understood. Measurements in the range 10 to 1300 K and at various dopant concentrations (up to 40% [49]) and at high pressures [50] indicate that the samples of NiO remain semiconducting and that the d electrons are localized.

Even though it is definitely known that the d electrons in NiO are localized, the detailed mechanism of electrical conduction is not yet understood; the various properties of this material have been reviewed in several articles [51–56]. The available data on transport properties indicate that: (a) between 200 to 1000 K, the predominant conduction mechanism is the motion of holes in a band with an $m^* = 6$m; (b) the carrier concentration in lightly doped samples is thermally activated with an acceptor ionization energy of 0.3–0.4 eV; (c) Li acceptors are always self-compensated by donors; (d) μ_D (≈ 0.5 cm^2/V s at 300 K) decreases with rise in T and μ_H is proportional to μ_D in the range 300 to 600 K and (e) intrinsic conduction is observable at $T > 1000$ K in the more highly compensated samples. It appears that small polaron hopping by 3d-holes (with low E_a) contributes little to the total conductivity at ordinary temperatures (100–1000 K) whereas the major contribution is from the holes in the oxygen 2p-band of NiO. We may note here that until 1963 it was generally taken for granted that charge-transfer in doped NiO involved activated mobilities. Since then the weight of the evidence seems to have shifted in the other direction; for example, the studies of Bosman and Crevecoeur [42] are in favor of the band regime. Since most of the studies have been on doped or nonstoichiometric NiO, we have to view the various claims with some caution. Needless to mention, there is continuing need for careful experimental studies on pure NiO.

Optical absorption measurements have been carried out on pure and doped NiO from far infrared through x-ray frequencies [44, 57–68] and the results indicate that the d electrons are localized. There is a peak at 0.24 eV which begins to broaden and decrease in energy above 400 K and disappears above 600 K [58, 63]; it appears to be connected with antiferromagnetism since the band vanishes just above T_N and moves towards lower energies with decrease in sublattice magnetization by either increase of temperature [58] or dilution with MnO or CoO [59]. The main feature in the optical spectrum of NiO is the absorption edge at $\sim$3.8 eV [57, 58, 64, 67]. Infrared studies show restrahlen bands at $\sim$0.05 eV; the antiferromagnetic resonance peak is at 0.04 eV below T_N [46, 69–71]. The band structure that emerges from the optical absorption, electroreflectance [72] and photoemission [73] studies is consistent with the theoretically calculated band structure of NiO [74–76].

Mössbauer studies of ^{57}Fe doped NiO have been reported in the literature [77, 78] and accurate value of T_N obtained. Discontinuities in κ, C_p, α_{td}, Young's modulus and internal friction and TEC have been noted in pure and Li doped NiO [79–83].

NiO forms solid solutions with other oxides of rock salt structure [59, 66, 84, 85] and the properties are slightly modified depending on the nature of the oxide.

Nickel oxides

Oxide and description of the study	Data	Remarks and inferences	References
NiO			
Crystal strucrure, x-ray studies.	$T \to 0$ K: Rhombohedral; $a = 4.1705$ A; $\alpha = 90.075°$. $T = 298$ K: Rhombohedral; $a = 4.1759$ Å; $\alpha = 90.058°$. $T = 525$ K: Cubic; space group, Fm3m; $Z = 4$; $a = 4.177$ Å. Slight volume change at T_N (523 K). High pressure studies up to several hundred kilobars do not reveal any phase transition. TEC (/K): 7.93×10^{-6}; $\theta_D = 900$ K.	The rhombohedral distortion is small and the transition at T_N appears to be second order.	[9–17].
χ-T studies and observation of the magnetic domains by optical and neutron diffraction.	$\chi(T_N) = 11.7 \times 10^{-6}$ emu/g. The antiferromagnetic T (twin) and S (spin-rotation) walls studied. Crystals with only T or S walls can be produced; these can be displaced by the application of small mechanical stress or magnetic fields. Magnetic field dependence of χ also is noticed.	The antiferromagnetic-paramagnetic transition appears to be of order greater than unity and slight magnetic order has been noticed above T_N by neutron diffraction. The anomalous χ in (111) at higher magnetic fields is caused by spin rotation.	[11–13, 19–24].
Electrical properties.	Pure NiO: ρ (300 K)$\sim 10^{13}$ Ωcm; $\rho \propto p_{O_2}^{-1/4}$ (p_{O_2}, 10^{-4}–1 atm.; 1170–1473 K); $\rho \propto p_{O_2}^{-1/5}$ (p_{O_2}, 10^{-2}–10^{+3} atm; 1320 K); $\rho \propto p_{O_2}^{-1/6}$ ($p_{O_2} \sim 10^{-1}$ atm; 1070 1373°K). The data are interpreted in terms of the singly and doubly ionized cation vacancies; the conduction is of p type. Impurities in the range 100–500 ppm seem to affect the intrinsic electrical properties. $E_a \sim 0.9$ eV (200–500 K); above T_N, E_a drops to 0.6 eV and increases to 1.0 eV at 1000 K; Range 10–100 K, $E_a \sim 0.004$ eV. $\mu_H \sim 0.5$ cm²/V s, at 200 K and hole like behavior; no striking temperature variation in the range 200–400 K but μ_H gradually decreases with rise in T. Above 400 K, rapid decrease is shown and at ~600 K, μ_H reverses sign. $\alpha \sim 0.5$ mV/K at ~200 K and above 300 K, has	At very low temperatures, impurity conduction is noticed whereas in the range 100–1000 K 3d holes contribute to conduction (only a small part of the total σ) by hopping of the small polarons. Major part of the conductivity comes from the holes in the oxygen 2p band in pure and slightly doped NiO. The high temperature Hall data anomalies are suggested to be due to the formation or small phase separation of n type Ni_3O_4 or small regions of metallic Ni in the samples.	[4, 5, 28–50].

Oxide and description of the study	Data	Remarks and inferences	References
	the same slope as log ρ as a function of T. Doped NiO: $\rho \sim 1$ Ωcm at 300 K and E_a is much smaller than in pure samples; E_a varies with dopant concentration and slightly with T. μ_H and α behave in a qualitatively similar manner as the undoped samples. Application of pressure decreases ρ but the sample remains semiconducting up to the highest pressures measured (~500 kbar). Neutron irradiation seems to increase ρ and decrease α of pure NiO.		
Optical properties (0.03–26 eV).	The main features are (i) antiferromagnetic resonance peak at ~0.04 eV observed in NiO below T_N (and which disappears above T_N), (ii) restrahlen peaks in the vicinity of 0.05 eV, (iii) a peak at 0.24 eV which begins to broaden and decrease in energy above 400 K and disappears at ~600 K, (iv) absorption edge at ~0.38 eV and (iv) several high energy peaks in the range 5–18 eV connected with interband transitions. $\epsilon_0 \approx 12$; $\epsilon_\infty \approx 5$.	Most of the observations are consistent with other body of data and the band picture that emerged is in reasonable agreement with the theoretical predictions. The peak at 0.24 eV appears to be connected with antiferromagnetism in NiO.	[44, 57–72].
Mössbauer studies of ^{57}Fe doped NiO (4.2–550°K).	An electric field gradient which appears at the ^{57}Fe nucleus below T_N grows as T decreases. The internal magnetic field is maximum (216 kG) at ~300 K and decreases to ~55 kG at 4.2 K. T_N is found to be 524 K and the direction of spins of Ni^{2+} is found to be close to <112>.	The order of the transition in NiO appears to be greater than unity.	[77, 78].
Thermal and mechanical properties.	C_p shows a λ-type anomaly at T_N; maximum value of $C_p = 65$ cal/mol. α_{td} and κ also show anomalies at T_N. Large increase in Young's modulus noted at ~T_N (Maximum value = 8.5×10^{-11} dyn/cm²). Elastic wave velocity also increases at ~T_N in NiO.	Striking anomalies are noted inspite of the negligible volume change and only smooth variation of the lattice parameter at T_N in NiO.	[79–83].

References

[1] Bogatskii, D. P., Zhur. Obshchei Khim. **21**, 3 (1951); Chem. Abstr. 46, 7861d (1952).
[2] Bogatskii, D. P., and Mineeva, I. A., Fiz. Tverd. Tela Akad. Nauk SSSR, Sbornic Statie **2**, 361 (1959); Zhur. Obshchei Khim. **29**, 1382 (1959).
[3] Kuznetsov, A. N., Russian J. Inorg. Chem. (English Transl.) **13**, 1050 (1968).
[4] Mitoff, S. P., J. Chem. Phys. **35**, 882 (1961).
[5] Cox, J. T., and Quinn, C. M., J. Mat. Sci. **4**, 33 (1969).
[6] Drakeford, R. W., and Quinn, C. M., J. Mat. Sci. **6**, 175 (1971).
[7] Tretyakov, Y. D., and Rapp, R. A., Trans. Met. Soc. AIME **245**, 1235 (1969).
[8] Reed, T. B., in The Chemistry of Extended Defects in non-Metallic Solids, Eds. L. Eyring and M. O'Keeffe (North Holland Publ. Co., Amsterdam, 1970), pp 21–35.
[9] Rooksby, H. P., Acta Cryst. **1**, 226 (1948).
[10] Shimomura, Y., Tsubokawa, I., and Kojima, M., J. Phys. Soc. Japan **9**, 521 (1954).
[11] Roth, W. L., Phys. Rev. **110**, 1333 (1958); **111**, 772 (1958).
[12] Roth, W. L., and Slack, G. A., J. Appl. Phys. **31**, 352S (1960).
[13] Slack, G. A., J. Appl. Phys. **31**, 1571 (1960).
[14] Vernon, M. W., and Lovell, M. C., J. Phys. Chem. Solids **27**, 1125 (1966).
[15] Clendenen, R. L., and Drickamer, H. G., J. Chem. Phys. **44**, 4223 (1966).
[16] Vernon, M. W., Phys. Stat. Solidi **37**, K1 (1970).
[17] Bartel, L. C., and Morosin, B., Phys. Rev. **B3**, 1039 (1971).
[18] Shull, C. G., Strauser, W. A., and Wollan, E. O., Phys. Rev. **83**, 333 (1951).
[19] Roth, W. L., in The Chemistry of Extended Defects in non-Metallic Solids, Eds. L. Eyring and M. O'Keeffe (North Holland Publ. Co., Amsterdam, 1970), pp 455–487.
[20] Singer, J. R., Phys. Rev. **104**, 929 (1956).
[21] Kondoh, K., Uchida, E., Nakazumi, Y., and Nagamiya, T., J. Phys. Soc. Japan **13**, 579 (1958).
[22] Roth, W. L., J. Appl. Phys. **31**, 2000 (1960).
[23] Kondoh, H., and Takeda, T., J. Phys. Soc. Japan **19**, 2041 (1964).
[24] Yamada, T., J. Phys. Soc. Japan **21**, 650 (1966); **21**, 664 (1966).
[25] Francois, J., Compt. Rend. (Paris) **230**, 1282 (1950); **230**, 2183 (1950).
[26] Teichner, S. J., and Morrison, J. A., Trans. Faraday Soc. **51**, 961 (1955).
[27] Tourky, A. R., Hanafi, Z., and Salem, T. M., Z. Phys. Chem. (Leipzig) **243**, 145 (1970).
[28] Morin, F. J., Phys. Rev. **93**, 1199 (1954).
[29] Snowden, D. P., Saltsburg, H., and Perene, J. H., Jr., J. Phys. Chem. Solids **25**, 1099 (1964).
[30] Nachman, M., Cojocaru, L. N., and Ribco, L. V., Phys. Stat. Solidi **8**, 773 (1965).
[31] Pizzini, S., and Morlotti, R., J. Electrochem. Soc. **114**, 1179 (1967).
[32] Aiken, J. G., and Jordan, A. G., J. Phys. Chem. Solids **29**, 2153 (1968).
[33] Eror, N. G., and Wagner, J. B., Jr., Phys. Stat. Solidi **35**, 641 (1969).
[34] van Houten, S., J. Phys. Chem. Solids **17**, 7 (1960).
[35] Ksendzov, Ya. M., Ansel'm, L. N., Yasil'eva, L. L., and Latysheva, V. M., Sov. Phys.—Solid State (English Transl.) **5**, 1116 (1963).
[36] Zhuge, V. P., and Shelykh, A. I., Sov. Phys.—Solid State (English Transl.) **5**, 1278 (1963).
[37] Roilos, M., and Nagels, P., Solid State Commun. **2**, 285 (1964).
[38] Heikes, R. R., in Transition Metal Compounds, Ed. E. R. Schatz, (Gordon and Breach, Science Publ., New York, 1964).
[39] Koide, S., J. Phys. Soc. Japan **20**, 123 (1965).
[40] Ksendzov, Ya. M., and Drabkin, I. A., Sov. Phys.—Solid State (English Transl.) **7**, 1519 (1965).
[41] Snowden, D. P., and Saltsburg, H., Phys. Rev. Letters **14**, 497 (1965).
[42] Bosman, A. J., and Crevecouer, C., Phys. Rev. **144**, 763 (1966).
[43] Cojocaru, L. N., Phys. Stat. Solidi **22**, 361 (1967).
[44] Ksendzov, Ya. M., Avdeenko, B. K., and Makarov, V. V., Sov. Phys.—Solid State (English Transl.) **9**, 828 (1967).
[45] Van Daal, H. J., and Bosman, A. J., Phys. Rev. **158**, 736 (1967).
[46] Austin, I. G., Springthorpe, A. J., Smith, B. A., and Turner, C. E., Proc. Phys. Soc. (Lond.) **90**, 157 (1967).
[47] Uno, R., J. Phys. Soc. Japan **22**, 1502 (1967).
[48] Kabashima, S., and Kawakubo, T., J. Phys. Soc. Japan **24**, 493 (1968).
[49] Toussaint, C. J., and Vos, G., J. Appl. Cryst. **1**, 187 (1968).
[50] Minomura, S., and Drickamer, H. G., J. Appl. Phys. **34**, 3043 (1963).
[51] Adler, D., Solid State Phys. **21**, 1 (1968).
[52] Goodenough, J. B., J. Appl. Phys. **39**, 403 (1968).
[53] Austin, I. G., and Mott, N. F., Adv. Phys. **18**, 41 (1969).
[54] Rao, C. N. R., and Subba Rao, G. V., Phys. Stat. Solidi (a) **1**, 597 (1970).
[55] Bosman, A. J., and Van Daal, H. J., Adv. Phys. **19**, 1 (1970).
[56] Adler, D., and Feinleib, J., Phys. Rev. **B2**, 3112 (1970).
[57] Doyle, W. P., and Lonergan, G. A., Disc. Faraday Soc. **26**, 27 (1958).
[58] Newman, R., and Chrenko, R. M., Phys. Rev. **114**, 1507 (1959).
[59] Newman, R., and Chrenko, R. M., Phys. Rev. **115**, 882 (1959).
[60] Stephens, D. R., and Drickamer, H. G., J. Chem. Phys. **34**, 937 (1961).
[61] Haber, J., and Stone, F. S., Trans. Faraday Soc. **59**, 1 (1963); **59**, 192 (1963).
[62] Gielisse, P. J., Plendl, J. N., Mansur, L. C., Marshall, R., Mitra, S. S., Mykolajewycz, R., and Smakula, A., J. Appl. Phys. **36**, 2446 (1965).
[63] Austin, I. G., Clay, B. D., and Turner, C. E., J. Phys. C. (Ser. 2) **1**, 1418 (1968).
[64] Rossi, C. E., and Paul, W., J. Phys. Chem. Solids **30**, 2295 (1969).
[65] Cherkashin, A. E., and Vilesov, F. I., Sov. Phys.—Solid State (English Transl.) **11**, 1068 (1969).
[66] Jacono, M. L., Sgamellotti, A., and Cimino, A., Z. Phys. Chem. (N.F.) **70**, 179 (1970).
[67] Powell, R. J., and Spicer, W. E., Phys. Rev. **B2**, 2182 (1970).
[68] Brown, F. C., Gähwiller, C., and Kunz, A. B., Solid State Commun. **9**, 487 (1971).
[69] Kondoh, H., J. Phys. Soc. Japan **15**, 1970 (1960).
[70] Sievers, A. J., and Tinkham, M., Phys. Rev. **129**, 1566 (1963).
[71] Richards, P. L., J. Appl. Phys. **34**, 1237 (1963).
[72] McNatt, J. L., Phys. Rev. Letters **23**, 915 (1969).
[73] Cherkashin, A. E., Vilesov, F. I., Keier, N. P., and Bulgakov, N. N., Sov. Phys.—Solid State (English Transl.) **11**, 506 (1969).
[74] Yamashita, J., J. Phys. Soc. Japan **18**, 1010 (1963).
[75] Switendick, A. C., MIT Quart. Progr. Rept. No. 49, 1963 (unpublished, quoted in [51]).
[76] Wilson, T. M., J. Appl. Phys. **40**, 1588 (1969); Intern. J. Quant. Chem. IIIS, 757 (1970).
[77] Bhide, V. G., and Shenoy, G. K., Phys. Rev. **143**, 309 (1966).
[78] Siegwarth, J. D., Phys. Rev. **155**, 285 (1967).
[79] Zhuge, V. P., Novruzov, O. N., and Shelykh, A. I., Sov. Phys.—Solid State (English Transl.) **11**, 1044 (1969).
[80] Fine, M. E., Rev. Mod. Phys. **25**, 158 (1953).
[81] Street, R., and Lewis, B., Nature (Lond.) **168**, 1036 (1951).
[82] Slack, G. A., Phys. Rev. **126**, 427 (1962).
[83] Föex, M., Compt. Rend. (Paris) **227**, 193 (1948).
[84] Muan, A., Nucl. Sci. Abstr. **20**, 50 (1966).
[85] Bizette, H., and Mainard, R., Bull. Soc. Sci. Bretagne **42**, 209 (1967).

I.9. Copper Oxides

Phase equilibrium studies [1–3] on the Cu-O system indicate that Cu_2O and CuO are the only stable oxide phases in the solid state; both have narrow ranges of homogeneity. Frondel [4] has reported the existence of a tetragonal nonstoichiometric oxide of the formula $(Cu^{2+}_{1-2x}Cu^{+}_{2x})O_{1-x}$, $x=0.116$, but details are not known.

Cu_2O: Cuprous oxide, Cu_2O, has a cubic structure [5] and no phase transformations are known up to the melting point [3, 5]. Because of the extensive use of Cu_2O as a barrier layer photoelectric cell, many workers have successfully grown single crystals of the oxide [6, 7]. Cu_2O has considerable covalency associated with the Cu-O bond and exhibits plastic behavior above 870 K [5, 8]. The material is a semiconductor and the bulk and surface resistivities and photoconductivity have been examined by several workers [9–18]. Optical absorption studies [19–22] indicate several reflection bands with an absorption edge, corresponding to the optical energy gap, of ~2.02 eV. Cu_2O exhibits the interesting phenomena of exciton spectra at low temperatures which appear as hydrogen-like series of narrow lines at the absorption edge and towards the long-wavelength region (yellow series). Similar series of lines (called the green, blue-green and blue series) also appear near the other interband transitions [23–25] and are due to the optical excitation of the excitons in Cu_2O. Detailed investigation of these excitonic spectra contributed to the understanding of the photoconductivity and band structure of Cu_2O [23, 26].

CuO: Cupric oxide, CuO, has a monoclinic structure [27, 28] and has considerable covalency associated with the Cu-O bond [28]; no phase transformations are known at ordinary pressures. CuO is a semiconductor [29, 30] and resistivity studies at high pressure [29] seem to indicate a phase transition; however, detailed data are lacking.

CuO forms solid solutions with PdO [31, 32] and 'PtO' [33] having a tetragonal structure and with MgO, NiO and CoO having cubic rock salt structure [32]; the lattice constant-composition curve extrapolated to pure CuO suggest the existence of a tetragonal or cubic metastable (crypto-) modification of CuO [31–33].

Copper oxides

Oxide and description of the study	Data	Remarks and inferences	References
Cu_2O			
Crystal structure and x-ray studies.	Cubic; space group, $Pn3m$; $Z=2$; $a=4.268\pm0.001$ Å. TEC (120–470 K), /°C): 2×10^{-6}. Melting point ~1510 K.	Cu_2O has an unusual structure described as two interpenetrating and identical frame works of copper and oxygen atoms which are not cross connected by any primary Cu-O bonds. Considerable convalency is associated with the Cu-O bond.	]5, 8].
Electrical properties.	Semiconductor (300–670 K); ρ (400 K)~2×10^3 Ωcm; $E_a=0.26$ eV; α (400 K)$\approx+1$ mV/°C; μ_H (300 K)≈0.08 cm²/V s. Cu_2O may be nearly an ionic conductor and extrinsic hole conduction can occur by activated hopping.	The conductivity behavior in Cu_2O is complicated by surface and photoconductivity effects.	[9, 15].
Elastic properties by pulse echo technique (4.2–300 K).	Room temperature values of elastic constants ($\times10^{12}$ dyn/cm²): $C_{11}=1.165\pm0.005$; $c_{12}=1.003\pm0.04$; $c_{44}=0.121\pm0.003$. Limiting low temperature values (~4.2 K) ($\times10^{12}$ dyn/cm²): $c_{11}=1.211\pm0.005$; $c_{12}=1.054\pm0.04$; $c_{44}=$	—	[34].

Oxide and description of the study	Data	Remarks and inferences	References
	0.109±0.003. θ_D=181 K; compressibility (300 K)=0.946×10^{-6} cm²/kg.		
Optical properties and band structure.	Reflectivity bands at 2.67, 3.85, 4.64 and 5.00 eV are noted. Energy gap is estimated to be 2.02 eV. ϵ_0=7.60; ϵ_∞=6.46. Exciton spectra are noted at the band edge at low temperatures.	The data are discussed in terms of the band structure of Cu_2O.	[14, 19–26].
CuO			
Crystal structure and x-ray studies.	Monoclinic; space group, C2/c; Z=4; a=4.6837±0.005 Å; b=3.4226±0.0005 Å; c=5.1288±0.0006 Å; β=99.54±0.01°. TEC (293–973 K, /°C)≈6.5×10^{-6}. Each copper atom is coordinated to four coplanar oxygen atoms situated at the corners of an almost rectangular parallelogram; the oxygen atom is coordinated to four copper atoms situated at the corners of a distorted tetrahedron. Estimated ionic character 40%; hence the bonding in CuO appears to be predominantly covalent.	The structure can be described in the following manner: the building elements are the oxygen coordination parallelograms, which form chains by sharing edges. Such chains traverse the structure in the [110] and [$\bar{1}$10] directions, the two types of chains alternating in the [001] direction. Each type of chain is stacked in the [010] direction with a separation between the chains of ∼2.7 Å; each individual chain in a group of stacked chain of [110] type is linked to each chain in the two adjacent groups of [$\bar{1}$10] type by corner sharing.	[3, 27, 28].
Electrical properties.	ρ (296 K)∼2–4×10^3 Ωcm at 20 kbar pressure. High pressure studies indicate no transition up to 450 kbar at 300 K or up to 419 K at 17 kbars; however, at 391 K, ρ shows discontinuous drop at 187 kbar or 462 kbar at 360 K. α data indicate p type behavior. Detailed data are lacking.	The high pressure data seem to indicate a solid-solid phase transition in CuO but detailed studies are yet to be made.	[29, 30].

References

[1] Roberts, H. S., and Smyth, F. H., J. Am. Chem. Soc. 43, 1061 (1921).
[2] Gadalla, A. M. M., and White, J., Trans. Brit. Ceram. Soc. 63, 39 (1964).
[3] Pranatis, A. L., J. Am. Ceram., Soc. 51, 182 (1968).
[4] Frondel, C., Am. Mineral. 26, 657 (1941).
[5] Suzuki, T., J. Phys. Soc. Japan 15, 2018 (1960).
[6] Toth, R. S., Kilkson, R., and Trivich, D., J. Appl. Phys. 31, 1117 (1960).
[7] Brower, W. S., Jr. and Parker, H. S., J. Cryst. Growth 8, 227 (1971), and references therein.
[8] Vagnard, G., and Washburn, J., J. Am. Ceram. Soc. 51, 88 (1968).
[9] Toth, R. S., Kilkson, R., and Trivich, D., Phys. Rev. 122, 482 (1961).
[10] O'Keeffe, M., and Moore, W. J., J. Chem. Phys. 35, 1324 (1961); 36, 3009 (1962).
[11] Campbell, R. H., Kass, W. J., and O'Keeffe, M., in Mass Transport in Oxides, Nat. Bur. Stand. (U.S.), Spec. Publ. 296 (1968), p. 173.
[12] Young, A. P., and Schwartz, C. M., J. Phys. Chem. Solids 30, 249 (1969).

[13] Zielinger, J. P., Tapiero, M., Roubaud, Mme. C., and Zouaghi, M., Solid State Commun. 8, 1299 (1970).
[14] Kuzel, R., and Weichman, F. L., Canad. J. Phys. 48, 1585 (1970); 48, 2643 (1970).
[15] Kuzel, R., Cann, C. D., Sheinin, S. S., and Weichman, F. L., Canad. J. Phys. 48, 2657 (1970).
[16] Fortin, E., Zouaghi, M., and Zielinger, J. P., Phys. Letters 24A, 180 (1967).
[17] Zouaghi, M., Coret, A., and Eymann, J. O., Solid State Commun. 7, 311 (1969).
[18] Zouaghi, M., Tapiero, M., Zielinger, J. P., and Burgraf, R., Solid State Commun. 8, 1823 (1970).
[19] Balkanski, M., Petroff, Y., and Trivich, D., Solid State Commun. 5, 85 (1967).
[20] Tandon, S. P., and Gupta, J. P., Phys. stat. solidi 37, 43 (1970).
[21] Dahl, J. P., and Switendick, A. C., J. Phys. Chem. Solids 27, 931 (1966).
[22] Smirnov, V. P., Sov. Phys.—Solid State (English Transl.) 7, 2312 (1966); 8, 2020 (1967).
[23] Gross, E. F., Sov. Phys. Uspekhi (English Transl.) 5, 195 (1962).
[24] Deiss, J. L., Daunois, A., and Nikitine, S., Solid State Commun. 7, 1417 (1969); 8, 521 (1970).
[25] Forman, R. A., Brower, W. S., Jr., and Parker, H. S., Phys. Letters 36A, 395 (1971).
[26] Elliot, R. J., Phys. Rev. 108, 1384 (1957); 124, 340 (1961).
[27] Tunell, G., Posnjak, E., and Ksanda, C. J., Z. Krist. 90, 120 (1935).
[28] Åsbrink, S., and Norrby, L.-J., Acta Cryst. 26B, 8 (1970).
[29] Minomura, S., and Drickamer, H. G., J. Appl. Phys. 34, 3043 (1963).
[30] Zuev, K. P., and Dolgintsev, V. D., Izv. Akad. Nauk SSSR, Neorg. Mater. 4, 1498 (1968).
[31] Schmahl, N. G., and Minzl, E., Z. Physik. Chem. (N.F.) 47, 142 (1965).
[32] Schmahl, N. G., and Eikerling, G. F., Z. Physik. Chem. (N.F.) 62, 268 (1968).
[33] Muller, O., and Roy, R., J. Less-Comm. Metals 19, 209 (1969).
[34] Hallberg, J., and Hanson, R. C., Phys. stat. solidi 42, 305 (1970).

I.10. Zinc Oxides

ZnO is the stable oxide of zinc and it has the wurtzite (hexagonal) structure at room temperature. It is piezoelectric. No phase transformations are known in ZnO in the range 4.2 to 890 K. At high pressures, it transforms to the rock salt structure at room temperature.

Vannerberg [1] has reported a cubic form of zinc peroxide, ZnO_2 ($a=4.871\pm0.006$ Å), but apparently no other studies on this material are available in the literature.

Because of the technical importance, single crystals of ZnO have been grown by a variety of techniques including hydrothermal, flux growth, traveling solvent, vapor phase reaction and oxidation methods [2–7]. Lattice parameters and thermal expansion coefficients have been determined by various workers in the range 4.2 to 890 K [7–13]. ZnO is a semiconductor and the electrical transport properties and optical characteristics have been examined in detail in the literature [6, 14–18].

High pressure x-ray diffraction [19, 20] and optical studies [21] indicated that ZnO transforms from hexagonal to cubic structure at pressures ~100–125 kbar at 300 K (Bates et al. give a value 670 K). Studies of Bates and co-workers [20] indicate that NH_4Cl acts as a catalyst in the formation of the high pressure phase and the transformation is sluggish. The cubic phase does not revert back to the wurtzite structure even after prolonged standing (several weeks) at room temperature; however, at ~390 K, it reverts within three weeks time.

Zinc oxides

Oxide and description of the study	Data	Remarks and inferences	References
ZnO			
Crystal structure and x-ray studies.	Range, 4.2–890 K; Hexagonal; space group, $P6_3mc$; $Z=2$; $\theta_D=370$ K. $T=297$ K: $a=3.2497\pm0.0009$ Å; $c=5.206\pm0.0009$ Å. TEC (300–890 K; °/C): $\|\|^a=6.05\times10^{-6}+2.20\times10^{-9}\,t+2.29\times10^{-12}\,t^2$; $\|\|^c=3.53\times10^{-6}+2.38\times10^{-9}\,t+9.24\times10^{-12}\,t^2$ (t in °C). Ibach [12] and Reeber [9] find that in the range 4.2–300 K, a goes through a minimum at 93 K.	Reeber [9] has summarized all the earlier crystal data on ZnO. Slight anisotropy in TEC values is evident.	[9, 11, 12].

Oxide and description of the study	Data	Remarks and inferences	References
Pressure transition	High pressure x-ray study shows T_t to be 673 or 300 K at pressures ~105–110 kbars. Cubic phase; space group, Fm3m; $Z=4$; $a=4.28$ Å. $\Delta H=785$ cal/mol; $\Delta S=-2.5$ e.u.; $dP/dT = 42.5\times10^{-3}$ bar/°C; $\Delta V = -2.55$ cm³/mol. High pressure optical absorption indicates transition at 125 kbars at 300 K. Absorption edge is at 3.14 eV ($\equiv E_g$, at 1 bar); $d(\Delta E_g)/dP$ = 0.6–1.9$\times10^{-6}$ eV/bar (wurtzite); = 1.9×10^{-6} eV/bar (rock salt).	The 4:4 coordination of the wurtzite phase of ZnO changes to 6:6 coordination in the rock salt phase; the latter phase is denser.	[19–21].
Electrical properties.	Pure undoped crystals have ρ~1–100 Ωcm but doping increases the ρ by a factor ~10. The ρ of sintered and unsintered specimens behave differently with respect to temperature. Interstitial metal atoms appear to play a dominant part.	E_g is ~3 eV but donor levels of ~0.3 eV below the conduction band always create charge carriers thermally and contribute to to the conductivity.	[14–18].
	Hutson [16] obtained the following transport parameters at 300 K: $\alpha\approx1.7$ mV/K; $\mu_H=180$ cm²/V s; $n_c=2\times10^{16}$ cm^{-3}; $m^*\approx0.5$ m; $m_p^*=0.27$ m; $\alpha_F^*=0.85$; $\epsilon_0=8.5$; $\epsilon_\infty=3.73$; $\theta_D=920$ K.	In the range 150–900 K, T dependence of μ_H has been explained by the optical mode scattering; however, below 150 K, ionized impurity scattering and phonon-drag effects play a significant role.	

References

[1] Vannerberg, N. G., Arkiv Kemi 14, 119 (1959).
[2] Weaver, E. A., J. Cryst. Growth 1, 320 (1967).
[3] Kleber, W., and Mlodoch, R., Kriat. Tech. 1, 245 (1966); Chem. Abstr. 69, 46561m (1968).
[4] Hirose, M., and Kubo, I., Japan J. Appl. Phys 8, 402 (1969).
[5] Cleland, J. W., in Mass Transport in Oxides, Nat. Bur. Stand. (U.S.), Spec. Publ. 296, (1968), p. 195.
[6] Nielsen, K. F., J. Cryst. Growth 3–4, 141 (1968).
[7] Heller, R. B., McGannon, J., and Weber, A. H., J. Appl. Phys. 21, 1283 (1950).
[8] Abrahams, S. C., and Beinstein, J. L., Acta Cryst. 25B, 1233 (1969).
[9] Reeber, R. R., J. Appl. Phys. 41, 5063 (1970).
[10] Sirdeshmukh, D. B., and Deshpande, V. T., Curr. Sci. (India) 36, 630 (1967).
[11] Khan, A. A., Acta Cryst. 24A, 403 (1968).
[12] Ibach, H., Phys. Stat. solidi 33, 257 (1969).
[13] Kirchner, H. P., J. Am. Ceram. Soc. 52, 379 (1969).
[14] Hahn, E. E., J. Appl. Phys. 22, 855 (1951).
[15] Hutson, A. R., Phys. Rev. 108, 222 (1957).
[16] Hutson, A. R., in Semiconductors, Ed. N. B. Hannay (Reinhold Publ. Corp., New York, 1959), p. 541.
[17] Seitz, M. A., and Whitmore, D. H., J. Phys. Chem. Solids 29, 1033 (1968).
[18] Hideo, H., and Kasae, K., Nippon Kagaku Zasshi 90, 112 (1969); Chem. Abstr. 70, 71821z (1969).
[19] Class, W., Iannucci, A., and Nesor, H., Norelco Reporter 13, 87 (1966); 13, 94 (1966).
[20] Bates, C. H., White, W. B., and Roy, R., Science 137, 993 (1962).
[21] Edwards, A. L., Slykhouse, T. E., and Drickamer, H. G., J. Phys. Chem. Solids 11, 140 (1959).

II. Oxides of 4*d* Transition Elements

II.1. Yttrium Oxides

The fully oxidized form, Y_2O_3, is the only solid oxide of yttrium [1–3]; substoichiometric yttrium oxide, $YO_{1.5-x}$, has, however, been reported by a few workers [4–6]; with $x = 0.009$, the oxide possesses intense green color and is paramagnetic in nature, but the crystal structure is the same as that of stoichiometric Y_2O_3. Miller and Daane [5] report a higher lattice parameter and a lower density for $YO_{1.491}$ compared to $YO_{1.500}$. A monoxide, YO, was reported [7] as an impurity in Y metal on the basis of x-ray pattern, but it is likely to have been a surface film; the existence of YO as a bulk phase has not been reported.

Y_2O_3: *Y_2O_3 has a cubic C-type rare-earth oxide* structure at room temperature and 1 atmospheric pressure and can be described as a modified fluorite phase having one anion in four missing to balance the trivalent cationic charge with a slight readjustment of the positions of the remaining ions. The resulting unoccupied anion sites may be considered as forming nonintersecting strings along the four ⟨111⟩ directions of the cubic cell [1–3].

A hexagonal (H) form of Y_2O_3 at high temperatures (~2650 K) has been reported by Foëx and Traverse [8]. This H-form of Y_2O_3 is closely related to the A-type rare-earth oxide structure. The C→H transformation has been found to be reversible [8] and the two modifications are usually observed to coexist over a remarkably extended range of temperatures. Noguchi et al. [9] report a crystal structure transition (probably C→H) at ~2550 K. Mehrotra et al. [10] have reported a high temperature transformation in Y_2O_3 which is reversible and occurs over the range 670 to 1170 K. The high temperature phase has been indexed on a hexagonal basis but a monoclinic symmetry could not be ruled out.

The C-type structure of Y_2O_3 is relatively loose and is of lower density compared to the B-(monoclinic) and A-(hexagonal) type structures (usually adopted by rare earth sesquioxides). One would, therefore, expect that application of pressure should favor the denser structures. Accordingly, Hoekstra and Gingerich [11], Hoekstra [12] and Prewitt et al. [13] noticed that C→B conversion occurs in Y_2O_3 at ~25 kbar and at ~1270 K. The high pressure phase can be quenched and the reversibility of the phase transformation has been confirmed by heating the B-form in air at ~1270 K or annealing in air at ambient pressure and ~1170 K for several hours [11, 12]; *from the observed pressure-temperature* data, the enthalpy and entropy changes accompanying the C→B transformation in Y_2O_3 have been estimated [1, 14].

Electrical properties of Y_2O_3 have been examined by a few workers [15–22]. Y_2O_3 exhibits *p*-type semiconduction with considerable ionic contribution to the total conductivity. The ionic conductivity has been ascribed to the anionic migration [17, 18, 20–24] but the contribution is smaller the larger the temperature and is less than 1 percent above 1500 K; impurities in slight amounts seem to play a dominant role in ionic conduction [18, 24].

Y_2O_3 forms solid solutions with oxides of the type MO (M = Sr [25]), M_2O_3 (M = B [26], Al [27], Sc [28, 29], La [30] and Nd [30]) and MO_2 (M = Ti [31, 32], Zr [9, 31, 33–36], Hf [37–42], Ce [23], Th [43, 44] and Re [45, 46]) and their properties have been examined extensively. Some of the ThO_2-Y_2O_3 solid solutions exhibit 100 percent ionic conductivity and are used as solid electrolytes [47, 48].

Oxide and description of the study	Data	Remarks and inferences	References
Y_2O_3			
Crystal structure (including high temperature high pressure x-ray studies.	$T=300$ K, 1 atm pressure: Cubic (C-type); space group, Ia3; $Z=16$; $a=10.604$ Å. High temperature phases. $T=1170$ K: Hexagonal (A-type?); $a=9.80$ Å; $c=10.17$ Å. $T=2603$ K: Hexagonal (H-type); $a=3.805$ Å; $c=6.085$ Å. Cubic-monoclinic (B-type) transition at ~25 kbar and at ~1270 K. High pressure phase is monoclinic; space group, C2/m; $Z=6$; $a=13.91$ Å$\pm$0.01 Å; $b=3.483\pm0.003$ Å; $c=8.593\pm0.008$ Å; $\beta=100.15\pm0.05$ Å. ΔH (estimated) ~2 kcal/mol; ΔS (estimated) ~1.5 e.u. Melting point = 2959 ± 20 K [49].	The cubic structure of Y_2O_3 is the usual structure type adopted by the heavy rare earth oxides. It is remarkable that the structure change on heating is to that of a lower symmetry and is due to the changes in coordination and increase in density. The pressure transition does not go through the corundum phase and the detailed mechanism has been discussed by Prewitt et al. [13].	[1–3, 8, 10–12].
Electrical properties (300–1500 K).	Semiconductor; ρ (970 K)~10^7 Ωcm; E_a~1 eV; α (900 K)~2 mV/°C; p-type to n-type change at low oxygen partial pressures. Considerable ionic conductivity below 1000 K; above 1500 K, pure electronic conduction.	Y_2O_3 at low temperatures can be considered to be almost an insulator having a very high resistivity. Impurities exert a lot of influence in the ionic conductivity of the material; purest sample has a very low ionic contribution. The p- to n-type change in Y_2O_3 may be due to loss of oxygen and creation of anion vacancies at high temperatures.	[15–24].
Dielectric and infrared studies.	$\epsilon_0=9.77$; $\epsilon_\infty=3.58$. Several bands in the region 300–560 cm^{-1} are noted; weak bands in the region 800–1070 cm^{-1} also exist. The bands are attributed to metal-oxygen vibrations.	—	[50–53].
Heat capacity studies (300–1800 K).	C_p (1300 K) $=31.17\pm19$ cal/deg mol. An anomaly has been noted at 1330 K with a $\Delta H=310$ cal/mol; ΔH (estimated, by extrapolation) $=249\pm66$ cal/mol; $\Delta S=0.19\pm0.05$ e.u.	The cause of the C_p anomaly at 1330 K is not known.	[54, 55].

References

[1] Brauer, G., Progr. in the Science and Technology of Rare Earths Ed. L. Eyring (Pergamon, Oxford), 1, 152 (1964); 2, 312 (1966); 3, 434 (1968).

[2] Fert, A., Bull. Soc. Franc. Mineral Crist. 85, 267 (1962).

[3] Paton, M. G., and Maslen, E. N., Acta Cryst. 19, 307 (1965).

[4] Haefling, J. A., Schmidt, F. A., and Carlson, O. N., J. Less-Comm. Metals 7, 433 (1964).

[5] Miller, A. E., and Daane, A. H., J. Inorg. Nucl. Chem. 27, 1955 (1965).

6] Miller, A. E., Thesis, Iowa State Univ. of Sci. and Tech. 1964; Nucl. Sci. Abstr. **20**, 880 (1966).
[7] Huber, E. J., Jr., Head, E. L., and Holley, C. E., Jr., J. Phys. Chem. **61**, 497 (1957).
[8] Foëx, M., and Traverse, J.-P., Compt. Rend. (Paris) **261**, 2490 (1965).
[9] Noguchi, T., Mizuno, M., and Yamada, T., Bull. Chem. Soc. Japan **43**, 2614 (1970).
[10] Mehrotra, P. N., Chandrashekar, G. V., Rao, C. N. R., and Subbarao, E. C., Trans. Faraday Soc. **62**, 3586 (1966).
[11] Hoekstra, H. R., and Gingerich, K. A., Science **146**, 1163 (1964).
[12] Hoekstra, H. R., Inorg. Chem. **5**, 754 (1966).
[13] Prewitt, C. T., Shannon, R. D., Rogers, D. B., and Sleight, A. W., Inorg. Chem. **8**, 1985 (1969).
[14] Westrum, E. F., Jr., Progr. in the Science and Technology of Rare Earths, Ed. L. Eyring (Pergamon, Oxford) **3**, 459 (1968).
[15] Noddack, W., and Walch, H., Z. Elektrochem. **63**, 269 (1959); Z. Physik. Chem. (Leipzig) **211**, 194 (1959).
[16] Neuimin, A. D., and Pal'guev, S. F., Chem. Abstr. **59**, 9417g (1963).
[17] Tare, V. B., and Schmalzried, H., Z. Physik. Chem. (NF) **43**, 30 (1964).
[18] Tallan, N. M., and Vest, R. W., J. Am. Ceram. Soc. **49**, 401 (1966).
[19] Zyrin, A. V., Dubok, V. A., and Tresvyatskii, S. G., Chem. Abstr. **69**, 62562t (1968).
[20] Chandrashekar, G. V., Mehrotra, P. N., Subba Rao, G. V., Subbarao, E. C., and Rao, C. N. R., Trans. Faraday Soc. **63**, 1295 (1967).
[21] Subba Rao, G. V., Ph.D. Thesis, Indian Institute of Technology, Kanpur, India, 1969.
[22] Subba Rao, G. V., Ramdas, S., Mehrotra, P. N., and Rao, C. N. R., J. Solid State Chem. **2**, 377 (1970).
[23] Subba Rao, G. V., Ramdas, S., Tomar, M. S., and Rao, C. N. R., Ind. J. Chem. **9**, 242 (1971) and references therein.
[24] Etsell, T. H., and Flengas, S. N., Chem. Rev. **70**, 339 (1970).
[25] Lopato, L. M., Yaremenko, Z. A., and Tresvyatskii, S. G., Dopovidi Akad. Nauk Ukr RSR, 1493 (1965).
[26] Levin, E. M., Phys. Chem. Glasses **7**, 90 (1966).
[27] Bondar, I. A., and Toropov, N. A., Izv. Akad. Nauk SSSR, Ser. Khim. 212 (1966).
[28] Hajek, B., Petru, F., Kalalova, E., and Dolezalova, J., Z. Chem. **6**, 268 (1966).
[29] Trezebiatowski, W., and Horyn, R., Bull, Acad. Polon. Sci., Ser. Sci. Chim. **13**, 311 (1965).
[30] Andreeva, A. B., and Keler, E. K., Zh. Prikl. Khim. **39**, 489 (1966).
[31] Collongues, M. R., Queyroux, F., Perez, M., Jorba, Y., and Gilles, J.-C., Bull. Soc. Chim. France **4**, 1141 (1965).
[32] Ault, J. D., and Welch, A. J. E., Acta Cryst. **20**, 410 (1966).
[33] Rouanet, A., Compt. Rend. (Paris) **267C**, 1581 (1968).
[34] Takahashi, T., and Suzuki, Y., Deuxiemes Jour. Int. des piles a Combustible, Bruxelles 378 (1967).
[35] Strickler, D. W., and Carlson, W. G., J. Am. Ceram. Soc. **48**, 286 (1965).
[36] Duwez, P., Odell, F., and Brown, F. N., J. Electrochem. Soc. **98**, 356 (1951).
[37] Volchenkova, Z. S., and Pal'guev, S. F., Trans. Inst. Elektrokhim. Akad. Nauk SSSR, Ural. Flilial **5**, 133 (1964).
[38] Robert, G., Deportes, C., and Besson, J., Deuxiemes Jour. Int. des piles a Combustible, Bruxelles 368 (1967).
[39] Komissarova, L. N., Wang, C. S., and Spitsyn, V. I., Izv. Akad. Nauk SSSR Ser. Khim. **1**, 3 (1965).
[40] Caillet, M., Deportes, C., Robert, G., and Vitter, G., Rev. int. Hautes Temp. Refract. **4**, 269 (1967).
[41] Besson, J., Deportes, C., and Robert, G., Compt. Rend. (Paris) **262**, 527 (1966).
[42] Duclot, M., Vicat, J., and Deportes, C., J. Solid State Chem. **2**, 236 (1970).
[43] Wimmer, J. M., Bidwell, L. R., and Tallan, N. M., Nucl. Sci. Abstr. **19**, 42896 (1965).
[44] Subbarao, E. C., Sutter, P. H., and Hrizo, J., J. Am. Ceram. Soc. **48**, 443 (1965).
[45] Roy, R., McCarthy, G. J., Muller, O., and White, W. B., Nucl. Sci. Abstr. **20**, 36784 (1966).
[46] Roy, R., Kachi, S., McCarthy, G. J., Muller, O., and White, W. B., Nucl. Sci. Abstr. **20**, 13260 (1966).
[47] Wimmer, J. M., Bidwell, L. R., and Tallan, N. M., J. Am. Ceram. Soc. **50**, 198 (1967).
[48] Patterson, J. W., Bogren, E. C., and Rapp, R. A., J. Electrochem. Soc. **114**, 752 (1967).
[49] Noguchi, T., and Kozuka, T., Solar Energy **10**, 203 (1966).
[50] McDevitt, N. T., and Davidson, A. D., J. Opt. Soc. Amer. **56**, 636 (1966).
[51] Goldsmith, J. A., and Ross, S. D., Spectrochim. Acta **23A**, 1909 (1967).
[52] Subba Rao, G. V., Rao, C. N. R., and Ferraro, J. R., Appl. Spec. **24**, 436 (1970).
[53] Nigara, Y., Ishigame, M., and Sakurai, T., J. Phys. Soc. Japan **30**, 453 (1971).
[54] Pankratz, L. B., King, E. G., and Kelley, K. K., U.S. Bur. Mines, Rept. Invest. No. 6033, 1962.
[55] Holley, C. E., Jr., Huber, E. J., Jr. and Baker, F. B., Progr. in the Science and Technology of Rare Earths Ed. L. Evring (Pergamon, Oxford), **3**, 343 (1968).

II.2. Zirconium Oxides

The solubility of oxygen in α-zirconium (hexagonal, $a=3.231$ Å, $c=5.148$ Å) is appreciable and with increasing oxygen content, the c-axis of the metal elongates, the change being marked around $ZrO_{0.3}$ [1]; the a axis passes through a maximum around $ZrO_{0.25}$. The Zr_3O phase ($a=5.629$ Å, $c=5.197$ Å) is completely ordered, the compositions richer than Zr_3O being analogous to Zr_3O [1]. Electrical and mechanical properties of the solid solutions of oxygen in Zr have been measured and Zr_6O phase with a decomposition temperature of 1200 K has been identified in addition to the more stable Zr_3O [2]; both Zr_6O and Zr_3O are reported to be semiconductors. Both the Zr_6O and Zr_3O phases have been examined by electron microprobe and electron microscopic techniques and the ordered nature of the latter phase confirmed [3]. The structures of the solid solutions in the composition range 11–28.5 atomic percent oxygen have been examined by x-ray, neutron and electron diffraction techniques [1, 4, 5]. The compositions in the range 15–25 atomic percent oxygen can be described in terms of a one-dimensional long-period superstructure with a periodicity which increases with oxygen content [4]. The superstructure can be expressed in terms of the stacking sequence of octahedral interstitial sites in the lattice of α-Zr with ABCABC . . . in ZrO_x ($0.25<x<0.33$) and ABAB . . . in ZrO_y ($0.33<y<0.40$) respectively; Zr_3O exhibits an intermediate structure with ABC BC AC AB stacking with 9 layers period [5].

An examination of chemically thinned single crystals of zirconium by electron diffraction during an isobaric treatment with O_2 at 5×10^{-4} torr at 670 K

revealed superstructure patterns due to Zr_2O [6]. Zr_2O crystallizes in the hexagonal system with $a=16.16$ Å and $c=5.148$ Å. Six oxygens form a ring and a total of four such rings form the supercell.

The most stable oxide of zirconium is the important ceramic dioxide, ZrO_2 which normally crystallizes in the monoclinic structure ($P2_1/c$) possessing 4 ZrO_2 units in the unit cell [7–9]. The monoclinic structure reversibly transforms to a tetragonal structure around 1420 K and to a fluorite type cubic form at very high temperatures around 2500 K [10–14]. ZrO_2 melts at 2995 ± 20 K [15].

Oxygen equilibria over nonstoichiometric ZrO_2 (with oxygen deficiency) have been examined by Aronson and others [16] in the 1100 to 1400 K range at 10^{-12}-10^{-20} atm pressures. The compositions of the oxide in the 1670 to 2170 K range at $1\text{-}10^{-6}$ atm have been investigated exhaustively by Carniglia et al. [17] who find the ZrO_{2-x}-Zr boundary to be $x=0.014$ at 2070 K and 3.5×10^{-6} atm of oxygen. A black form of ZrO_2 has been prepared by heating hydrated ZrO_2 in argon or vacuum; this has a tetragonal structure [18, 19]. Amorphous hydrated ZrO_2 prepared by precipitation methods has been shown to possess short range order [19].

The phase transitions of ZrO_2 have been investigated extensively by several workers. Although there were some inconsistencies and uncertainties in the earlier literature [20] recent studies have clearly established the transition temperatures [21] and there appears to be no doubt regarding the monoclinic-tetragonal and tetragonal-cubic transitions mentioned earlier [10–14]. The monoclinic-tetragonal transition shows appreciable hysteresis similar to martensitic phase transitions [22] and is predominantly athermal [22, 23]; the formation of the cubic form is reversible [22]. Anomalous intensity changes in the x-ray pattern are noticed prior to the monoclinic-tetragonal transition (in the 1200 to 1370 K range) and hybrid crystal formation has been noticed [24]; orientation relationship between the monoclinic and tetragonal phases has been established. The tetragonal-cubic transition around 2550 K (observed by x-ray studies in vacuum), is undoubtedly accompanied by partial reduction of ZrO_2 and the phase boundary between the cubic and tetragonal forms is affected by the stoichiometry or oxygen deficiency [17, 25]. The lattice dimensions of monoclinic and tetragonal ZrO_2 decrease with increase in oxygen deficiency, but the phase does not appear to be significantly affected.

Pressure induced monoclinic-tetragonal transition of ZrO_2 has been reported [26–28]. Polymorphic behaviour of evaporated films of ZrO_2 has been investigated by electron microscopy and diffraction [29]. As mentioned earlier, the mechanism of the monoclinic-tetragonal transition of ZrO_2 has been examined by several workers [10–14, 21–24]. The kinetics of this transition with particular reference to its martensitic nature have been studied by Sukharevskii et al. [30]. The mechanism of the transition has also been studied with single crystals [31].

Preparation of finely-divided samples of the metastable phases of ZrO_2 has been described by several workers [10, 11, 21, 32–34]. ZrO_2 prepared by decomposition of alkoxides is cubic at room temperature and transforms to the metastable tetragonal phase around 570 K which then transforms to the monoclinic phase in the range 580 to 670 K [32]. Occurrence of the metastable tetragonal phase in high surface area (small crystallite size) samples of ZrO_2 has been examined by Garvie [33] and the kinetics of transformation of the metastable phase to the monoclinic phase have been investigated by Dow Whitney [34] and Surkarevskii et al. [30]. The low temperature metastable cubic and tetragonal phases possess lattice parameters identical to those of the corresponding high temperature phases [11, 21]. Thin evaporated films of ZrO_2 also exhibit the cubic structure at room temperature as shown by electron diffraction [29]; the cubic form transforms to the tetragonal and monoclinic forms on heating.

Electrical conductivity measurements of Vest and co-workers [35, 36] have clearly shown that ZrO_2 is a semiconductor, the sign of the majority carriers depending on the oxygen partial pressure and temperature; some evidence of ionic conduction in tetragonal ZrO_2 has been presented. Electrical conductivity of the tetragonal phase has been measured by other workers [37, 38] as well. Electrical conductivity measurements have been employed to study the monoclinic-tetragonal transformation under pressure [26].

Phase equilibria, phase transitions, defect chemistry, electrical properties and other aspects of solid solutions of ZrO_2 with a variety of oxides have been reported in the literature [39]. Solid solutions like ZrO_2-CaO [39, 40] are well-known solid electrolytes. Typical of the solid solutions investigated are ZrO_2-MgO [41, 42], ZrO_2-SrO [43], ZrO_2-MnO [44], ZrO_2-R_2O_3 where R = Sc, Y, or a rare earth [10, 39, 45–54], ZrO_2-CeO_2 [55], ZrO_2-GeO_2 [56], ZrO_2-TiO_2 [57–59] and ZrO_2-HfO_2 [60–62]. The monoclinic tetragonal transition of ZrO_2 is markedly affected in such solid solutions; as can be expected the cubic phase is stabilized in many of the solid solutions.

Oxide and description of the study	Data	Remarks and inferences	References
ZrO			
Crystal structures of the monoclinic, tetragonal and cubic phases of ZrO_2 by x-ray diffraction.	The stable room temperature monoclinic phase has the $P2_1/C$ space group with 4 ZrO_2 in unit cell: $a=5.1454\pm0.0005$ Å; $b=5.2075\pm0.0005$ Å; $c=5.3107\pm0.0005$ Å and $\beta=99°14'\pm0°05'$. The Zr-O distances vary from 2.05 to 2.28 Å (for the near neighbors) and there is a strong tendency to twin in the (100) direction and polymorphism can be understood in terms of the (fluorite type) layers parallel to (100).	The monoclinic structure can be considered to be a distorted fluorite structure. Detailed atomic positions in the monoclinic phase as well as structural rearrangements in polymorphic transitions to tetragonal and cubic phases have been discussed. The structures of ZrO_2 and HfO_2 have been compared.	[7–9].
	The tetragonal phase (D_{4h}^{15}–$P4_2/nmc$) has dimensions: $a=3.64$ Å and $c=5.27$ Å at 1520 K with 2 molecules in the cell. The fluorite type cubic phase has $a\approx5.26$ Å at the transition temperature.	The lattice dimension of the cubic phase will be a function of stoichiometry which in turn will depend on the temperature and oxygen partial pressure.	[11–13].
Phase transitions by x-ray diffraction.	The phase transition temperatures reported by different workers vary to some extent. The ranges are: monoclinic→tetragonal, 1320–1490 K; tetragonal→cubic, ~2550–2650 K.	The transitions of HfO_2 and ZrO_2 are similar.	[11–14, 21–25].
	There is considerable thermal hysteresis in the monoclinic-tetragonal transition just like in the transition of HfO_2. For example, the tetragonal→monoclinic transition (on cooling) has been reported in the range 1320–1170 K.	The transition is martensitic in character.	[14, 22–24].
	Coexistence of monoclinic and tetragonal phases as well as hybrid crystal formation have been observed in the range 1370–1490 K. The orientation relationship between the two phases is found in terms of the parallelism of the (100) and (010) planes of the tetragonal phase; the b axis of the monoclinic phase is similar to the c axis of the tetragonal phase.	The thermal hysteresis in the monoclinic-tetragonal transition arises from the differences between the forward and reverse transitions (i.e., heating *versus* cooling) The pretransformation region is between 1200 and 1370 K.	[24].
Stoichiometry and its relation to the tetragonal-cubic transition.	The tetragonal-cubic transition temperature found by x-ray diffraction (in vacuum) varies widely due to the changes in the stoichiometry of ZrO_2. For a	At ~2670 K and 10^{-6} torr of oxygen, the composition will be $ZrO_{1.960\pm0.002}$. At ~2670 K and 2×10^{-3} torr of oxygen, the composition will be $ZrO_{1.986}$.	[25].

Zirconium oxides—Continued

Oxide and description of the study	Data	Remarks and inferences	References
	composition of $ZrO_{1.97}$, the tetragonal-cubic transformation temperature corresponds to crossing of the (tetragonal ZrO_2+cubic ZrO_2)-(cubic ZrO_2) phase boundary.		
	The stoichiometry of ZrO_2 as a function of temperature and oxygen partial pressure has been investigated and the cubic-tetragonal transition temperature is significantly lowered in samples containing α-Zr and ZrO_2.	ZrO_2 is nearly stoichiometric at 1270 K and 1 atm p_{O_2}. The ZrO_{2-x}-Zr phase boundary is at $x=0.018$ at $p_{O_2}\approx 3.5\times10^{-6}$ atm and $T\approx 2070$ K.	[16, 17, 25].
	ZrO_2 is oxygen-deficient over the entire temperature range of 1370–2170 K at $p_{O_2}<1$ atm. In the 1670–2170 K range, oxygen deficiency is given by $\log x \approx -0.890[(0.400\times10^{-4})/T]-[(\log P)/6]$ where x is in ZrO_{2-x}, T is K and p is in atmospheres of oxygen.	Lattice thermal expansion is not affected by the oxygen deficiency although the dimensions of the monoclinic and tetragonal phases decrease; the monoclinic-tetragonal transition is not significantly affected. No change in Young's modulus and strength of ZrO_2 is noticed due to oxygen defciency in sintered samples.	
Metallographic observations.	The monoclinic-tetragonal phase transition has been examined on a vacuum hot-stage microscope (up to 1570 K). In the 1320–1420 K range, the platelet substructure within ZrO_2 grains forms rapidly. Photomicrographs and motion pictures were taken through the transformation.	Based on these observations the transformation has been shown to be diffusionless and athermal as in martensite transformations.	[23].
High pressure studies.	Monoclinic ZrO_2 reversibly transforms to the tetragonal form at 298 K on application of pressures greater than 37 kbar. The tetragonal phase cannot be retained at ambient conditions.	dT/dP of the transition has been reported to be -0.01°/bar in [27] and -0.003°/bar in [26].	[26–28].
Kinetics of monoclinic-tetragonal transformation.	Martensite (monoclinic⇌tetragonal) transformations in ZrO_2 show no principle difference between athermal and isothermal kinetics. At a certain supercooling, the transformation velocity increases sharply and the transformation becomes athermal. In the tetragonal-monoclinic transition, a change in the kinetics of diffusionless transition is observed. This phenomenon has also been studied with the metastable tetragonal phase prepared by decomposition of the oxychloride.	Transformation velocity decreases with decreasing temperature in isothermal runs; the energy of activation is 150 kcal/mol.	[30].

Zirconium oxides—Continued

Oxide and description of the study	Data	Remarks and inferences	References
Thermal expansion.	Thermal expansion of the lattice parameters up to 1370 K have been reported. The monoclinic-tetragonal transition occurs around 1370° and the reverse transition occurs at much lower temperatures (980–1250 K).	There is a critical Zr-O distance above which the monoclinic structure is no longer stable.	[14, 63].
	Thermal expansion data for the tetragonal phase are: $a=3.588_2+4.50\times10^{-5}\,t$ within 0.001_3 Å; $c=5.188_2+7.57\times10^{-5}\,t$ within 0.002_2 Å where t is in degrees centigrade between 1150 and 1700 °C.	The data are probably applicable up to 2270 K. At 1420 K, $a=3.639$ Å and $c=5.275$ Å and at 1970 K, $a=3.678$ Å and $c=5.339$ Å.	[64].
	Thermal expansion data for monoclinic ZrO_2 have been measured in detail along the three axes and found to be highly anisotropic.	The monoclinic-tetragonal transition is accompanied by a contraction of 3.42%.	[65].
Heat of transition.	The monoclinic-tetragonal transition is associated with an enthalpy change of 1420 cal/mol.		[66].
Superplasticity	Enhanced plasticity during the monoclinic-tetragonal transition has been studied.		[67].
Infrared spectra.	Cubic phase gives one band at 490 cm^{-1}. Monoclinic phase shows several bands as expected.		[52, 68].
Neutron induced transformation.	The monoclinic-cubic transformation by neutrons depends on the method of preparation.	Impurities stabilize the high symmetry phase.	[69].
Metastable cubic and tetragonal phases and their phase transitions.	Finely divided samples of ZrO_2 prepared by the decomposition of alkoxides, oxychloride and other salts give rise to the metastable cubic and tetragonal phases. The metastable cubic form prepared from alkoxides transforms to the metastable tetragonal form (~570 K), and then to the monoclinic form (580–670 K). The temperatures of transformation seem to vary with the method of sample preparation and some workers have reported cubic-monoclinic transitions. The lattice parameters of these low temperature cubic and tetragonal forms agree with those of the high temperature phases. The metastable tetragonal phase pre-	Cubic phase lattice parameter from electron diffraction is ~ 5.07 Å. Thin evaporated films of ZrO_2 (as shown by electron diffraction) also exist in cubic form and the transformation to tetragonal and monoclinic form is affected by annealing, oxygen pressure etc. The cubic lattice parameters are around 5 Å, the actual value varying with annealing.	[10, 11, 21, 29, 32, 33, 52, 70].

Oxide and description of the study	Data	Remarks and inferences	References
	pared by precipitation of alkaline aqueous solution or low-temperature calcination of zirconium nitrate has been found to be stable at room temperature due to the small crystallite size (or large surface area).		
	The kinetics and mechanism of transformation of the metastable tetragonal phase to the monoclinic phase have been studied and the kinetic data have been interpreted in terms of Avrami's equation and order-disorder theory.	No induction period was seen in the kinetics.	[34].
	The cubic-tetragonal transformation in thin films is monotropic while the tetragonal-monoclinic transformation exhibits the nucleation and growth mechanism.		[29].
Electrical properties.	Electrical properties have been reported by several workers. Monoclinic ZrO_2 is an amphoteric semiconductor at 1270 K and at high oxygen pressures ($1–10^{-6}$ atm), the predominant defects are ionized Zr vacancies which give rise to low mobility holes. The defect structure of tetragonal ZrO_2 has been examined by measuring the temperature and oxygen pressure dependence of conductivity and the electronic transference number. At high temperatures and low p_{O_2}, ZrO_2 is an n-type semiconductor (due to ionized oxygen vacancies). Tetragonal ZrO_2 is a mixed electronic and ionic conductor. The conductivity change accompanying the monoclinic-tetragonal transition is isothermal and the rate of change depends on thermal and sample history.	There is considerable disagreement regarding the ionic transport numbers in monoclinic and tetragonal ZrO_2 and the available data have been nicely reviewed by Etsell and Flengers [39]. There is no doubt that ZrO_2 is a mixed conductor. The conductivity minima have been reported at 10^{-9} and 10^{-16} atm at 1270 K for the monoclinic phase. For the tetragonal phase the minima are reported at 10^{-4}, 10^{-6} and 10^{-7} atm at 1570 K. The minima are at higher oxygen pressures at higher temperatures.	[35, 36, 39].

References

[1] Holmberg, B., and Dogerhamm, T., Acta Chem. Scand. **15,** 919 (1961).
[2] Kornilov, I. I., Glazova, V. V., and Kenina, E. M., Dokl. Akad Nauk SSSR **169,** 343 (1966).
[3] Ericson, T., Osteberg, G., and Lehtinen, B., J. Nucl. Materials **25,** 322 (1968).
[4] Fehlmann, M., Jostsons, A., and Napier, J. G., Z. Krist. **129,** 318 (1969).
[5] Yamaguchi, S., J. Phys. Soc. Japan **24,** 855 (1968).
[6] Steeb, S., and Rickert, A., J. Less Common Metals **17,** 429 (1969).
[7] McCullough, J. D., and Trueblood, K. N., Acta Cryst. **12,** 507 (1959).
[8] Adam, J., and Rogers, M. D., Acta Cryst. **12,** 951 (1959).
[9] Smith, D. K., and Newkirk, H. W., Acta Cryst. **18,** 983 (1965).
[10] Kuznetsov, A. K., Keler, E. K., and Fan, F. K., Zh. Prikl. Khim. **38,** 233 (1965).
[11] Boganov, A. G., Rudenko, V. S., and Makarov, L. P., Dokl. Akad Nauk SSSR, **160,** 1065 (1965).
[12] Smith, D. K., and Cline, C. F., J. Am. Ceram. Soc. **45,** 249 (1962).
[13] Teufer, G., Acta Cryst. **15,** 1187 (1962).
[14] Ruh, R., and Corfield, P. W., J. Am. Ceram. Soc. **53,** 126 (1970).
[15] Noguchi, T., and Kozuka, T., Solar. Energy **10,** 203 (1966).
[16] Aronson, S., J. Electrochem. Soc. **108,** 312 (1961); Kofstad, P., and Ruzicka, D. J., ibid. **110,** 181 (1963).
[17] Carniglia, S. C., Brown, S. D., and Schroeder, T. F., J. Am. Ceram. Soc. **54,** 13 (1971).
[18] Livage, J., and Mazieres, C., Compt. Rend. **261,** 4433 (1965).
[19] Livage, J., Doi, K., and Mazieres, C., J. Am. Ceram. Soc. **51,** 349 (1968).
[20] Weber, B. C., J. Am. Ceram. Soc. **45,** 614 (1962).
[21] Ruh, R., and Rockett, T. J., J. Am. Ceram. Soc. **53,** 360 (1970).
[22] Wolten, G. M., J. Am. Ceram. Soc. **46,** 418 (1963).
[23] Fehrenbacher, L. L., and Jacobson, L. J., J. Am. Ceram. Soc. **48,** 157 (1965).
[24] Patil, R. N., and Subbarao, E. C., Acta Cryst. **26A,** 535 (1970).
[25] Nicholson, P. S., J. Am. Ceram. Soc. **54,** 52 (1971); see also Ruh, R., and Garrett, H. J., ibid. **50,** 257 (1967).
[26] Dow-Whitney, E., J. Electrochem. Soc. **112,** 91 (1965).
[27] Vahldiek, F. W., and Lynch, C. T., Proc. Intern. Conf. on Sintering and Related Phenomena, Ed. G. C. Kuczinski, (Gordon and Breach, New York, 1966).
[28] Kulcinski, G. L., J. Am. Ceram. Soc. **51,** 582 (1968).
[29] El-Shanshoury, I. A., Rudenko, V. A., and Ibrahim, I. A., J. Am. Ceram. Soc. **53,** 264 (1970).
[30] Sukharevskii, B. Ya., Alapin, B. G., and Gavrish, A. M., Dokl. Akad. Nauk SSSR **156,** 677 (1967).
[31] Grain, C. F., and Garvia, R. C., U.S. Bur. Mines Rept. Invest No. 6619, 19 (1965), **CA, 63,** 5027A.
[32] Mazdiyasni, K. S., Lynch, C. T., and Smith, J. S., J. Am. Ceram. Soc. **48,** 372 (1965); ibid. **49,** 286 (1966).
[33] Garvie, R. C., J. Phys. Chem. **69,** 1238 (1965).
[34] Dow-Whitney, E., Trans. Faraday Soc. **61,** 1991 (1965).
[35] Vest, R. W., and Tallan, N. M., and Tripp, W. C., J. Am. Ceram. Soc. **47,** 635 (1964).
[36] Vest, R. W., and Tallan, N. M., J. Am. Ceram. Soc. **48,** 472 (1965).
[37] Anthony, A. M., Guillot, A., and Nicolau, P., Compt. Rend., Ser. A **262B,** 896 (1966).
[38] McClaine, L. A., and Coppel, C. P., J. Electrochem. Soc. **113,** 80 (1966).
[39] Etsell, T. H., and Flengers, S. N., Chem. Revs. **70,** 339 (1970).
[40] Subbarao, E. C., in Non-Stoichiometric Compounds, Ed. L. Mandelcorn (Academic Press, New York, 1964).
[41] Grain, C. F., J. Am. Ceram. Soc. **50,** 288 (1967).
[42] Viechnicki, D., and Stubican, U.S., J. Am. Chem. Soc. **48,** 292 (1965).
[43] Noguchi, T., Okubo, T., and Yonemochi, O., J. Am. Ceram. Soc. **52,** 178 (1969).
[44] Bayer, G., J. Am. Ceram. Soc. **53,** 294 (1970).
[45] Thornber, M. R., Bevan, D. J. M., and Graham, J., Acta Cryst. **24B,** 1183 (1968).
[46] Spiridonov, F. M., Popova, L. N., and Popilskii, R. Y., J. Solid State Chem. **2,** 430 (1970).
[47] Isupova, E. N., Glushkova, V. B., and Keler, E. V., Izv. Akad. Nauk SSSR Neorg Mater. **4,** 399 (1968).
[48] Collongues, R., Queyroux, F., Jorba, M. P. Y., and Gilles, J. C., Bull. Soc. Chim. France **1141** (1965).
[49] Rouanet, A., Compt. Rend. **267C,** 1581 (1968).
[50] Takahashi, T., and Suzuki, Y., Deuxiemes Jour. Int. des Piles a Combustible, Bruxelles, 378 (1967).
[51] Mazdiyasni, K. S., Lynch, C. T., and Smith, J. S., J. Am. Ceram. Soc. **50,** 532 (1967).
[52] Glushkova, V. B., and Koehler, E. K., Mat. Res. Bull. **2,** 503 (1967); see also, Sci. Ceram. **4,** 233 (1967), **CA, 70,** 60405r.
[53] Davtyan, I. A., Glushkova, V. B., and Keler, E. K., Izv. Akad Nauk SSSR Neorg Mater. **2,** 890 (1966).
[54] Strickler, D. W., and Carlson, W. G., J. Am. Ceram. Soc. **48,** 286 (1965).
[55] Casselton, R. E. W., Phys. stat. solidi (a) **1,** 787 (1970).
[56] Lefevre, J., and Collongues, R., Bull. Soc. Chim. France 1959 (1966).
[57] Ksendzov, Y. M., and Prokhvatilov, V. G., Zhur Fiz. Khim. **31,** 321 (1957).
[58] Keler, E. K., and Andreeva, A. B., Ognewpory **25,** 320 (1960); **CA, 51,** 15237d; **CA, 48,** 6798h.
[59] Shakhtin, D. M., Levintovich, E. V., Pivovar, T. L., and Eliseeva, G. G., Izv. Akad. Nauk SSSR Neorg. Mater. **4,** 1603 (1968).
[60] Gavrish, A. M., Susharevskii, B. Y., Krivoruchko, P. P., and Zoz, E. I., Izv. Akad. Nauk SSSR Neorg. Mater. **5,** 547 (1969).
[61] Ruh, R., Garret, H. J., Domagala, R. F., and Tallan, N. M., J. Am. Ceram. Soc. **51,** 23 (1968).
[62] Stansfield, O. M., J. Am. Ceram. Soc. **48,** 436 (1965).
[63] Grain, C. F., and Campbell, W. J., U.S. Bur. Mines Rept. Invest. 5982 (1962).
[64] Lang, S. M., Sci. Tech. Aerospace Rept. **2,** 2065 (1964).
[65] Filatov, S. K., and Frank-Kamenetskii, V. A., Soviet Phys.-Cryst. **14,** 696 (1970).
[66] Coughlin, J. P., and King, E. C., J. Am. Chem. Soc. **72,** 2262 (1950).
[67] Hart, J. L., and Chakladar, A. C. D., Mat. Res. Bull. **2,** 521 (1967).
[68] White, W. B., Mat. Res. Bull. **2,** 381 (1967).
[69] Adam, J., and Cox, B., J. Nucl. Energy **17,** 435 (1963).
[70] Mazdiyasni, K. S., and Brown, L. M., J. Am. Ceram. Soc. **53,** 43 (1970).

II.3. Niobium Oxides

Phase relations in the Nb-O system have been examined and reviewed over the past years by many workers [1–12]. In addition to the well-established monoxide, dioxide and pentoxide, several suboxides as well as a homologous series of oxides of the formula, $Nb_{3n+1}O_{8n-2}$ ($n=5$ to 8), are known. Niobium sesquioxide, Nb_2O_3, is not known, but the data of Nakayama et al. [13] seem to indicate the formation of this material as a hexagonal-type oxide.

Suboxides: The suboxides NbO_x (Nb_6O), NbO_y (Nb_4O) and NbO_z (Nb_2O) form only by the oxidation of niobium metal or by ageing niobium which is supersaturated with oxygen in definite ranges of temperature and oxygen pressure. NbO_x and NbO_z are tetragonal while NbO_y is orthorhombic [11]. Detailed physical properties of these suboxides are not known.

NbO: Niobium monoxide is easily made by the oxidation of the metal and has a narrow range of homogeneity ($0.982 \leqslant x \leqslant 1.008$ in NbO_x) [1, 11, 14–17]. It has a cubic rock salt structure with ~25 percent vacancies in the lattice which are ordered [1]. No phase transformations are known in this material; high temperature, high-pressure studies [18, 19] indicate no change in the vacancy concentration up to 77 kbar and at 1920 K. It appears that the nature of bonding in the ordered NbO structure is significantly different from that in the disordered vacancy structures of TiO and VO. Detailed resistivity studies by many workers [14–16, 20–22] indicate the metallic behavior of NbO in the range 2 to 900 K. The material becomes superconducting at ~1.5 K [20]. Solid solution formation and the solubility of other monoxides in NbO have been examined by Gel'd et al. [23].

NbO_2: Niobium dioxide has a distorted rutile structure with a narrow homogeneity range at room temperature [11, 12, 15, 24–29] and exhibits a first order transition at ~1070 K transforming to a (perfect) rutile phase [26–29]. Discontinuities in χ and ρ have been noted at T_t, but the material is paramagnetic with no magnetic ordering in the range 300 to 1200 K [30]. Reports of the electrical properties are conflicting: Janninck and Whitmore [31] and Roberson and Rapp [21] reported an apparent semiconductor-to-metal transition at T_t, but Sakata [27] finds semiconductor behavior throughout the range 300 to 1270 K with a ten-fold jump in σ at T_t. Metal-metal bonding in the low temperature phase of NbO_2 has been established [26, 27] and it may be argued [32, 33] that this oxide should exhibit a semiconductor-metal transition anologous to VO_2. The available data are all on polycrystalline samples and may not be reliable. Rao et al. [28] have studied the transitions in NbO_2 and its solid solutions with VO_2, $Nb_{1-x}V_xO_2$ ($0<x\leqslant 0.05$), and clearly established that the transitions are from semiconducting to metallic state; vibration mode softening and c-axis Nb-Nb pairing have been shown to be important factors in the mechanism of the transitions. Detailed studies on single crystal samples are, however, necessary to draw definitive conclusions.

Solid solutions of NbO_2 with TiO_2 [30, 34, 35], VO_2 [28, 29, 34, 36, 37], CrO_2 [34], and MoO_2 [34, 37] have been examined in the literature to elucidate the metal-metal bonding and the nature of the transition. It may be noted that in some of these solid solutions, there would be change in cation valencies.

Homologous series, $Nb_{3n+1}O_{8n-2}$ ($5\leqslant n\leqslant 8$): Studies by Norin and Magneli [38] indicate that in the composition range between NbO_2 and Nb_2O_5 there exist several nonstoichiometric oxides shown by Gatehouse and Wadsley [39] (and in many later papers) to belong to the general homologous series of the formula $Nb_{3n+1}O_{8n-2}$ ($n=9$ would be Nb_2O_5 if it formed, but H-Nb_2O_5 actually has a slightly different structure). In addition, oxides $Nb_{12}O_{29}$ ($NbO_{2.417}$) and $Nb_{47}O_{116}$ ($NbO_{2.464}$) have also been reported [40, 41]. All these oxides have structures similar to but different from, the basic high temperature (monoclinic) structure of H-Nb_2O_5 [42]. Physical properties of these systems have not been investigated in detail.

Nb_2O_5: Niobium pentoxide, Nb_2O_5, has a narrow homogeneity range [1, 43] and the stable phase is the high-temperature (H) form. The polymorphic behavior of this oxide has been examined by various workers over the past many years; however, a detailed picture is far from clear at the present stage and several metastable phases of Nb_2O_5 are being reported from time to time and several reports are contradictory in nature.

There are at present eight crystalline modifications of Nb_2O_5 known and many of them can be grown by vapor transport methods. Schäfer et al. [44] have reviewed various preparation methods of the Nb_2O_5 polymorphs while Wadsley and Andersson [42] elucidated the structural relationships involved and pointed out that many new modifications are feasible and may be discovered in future.

The low-temperature form, TT-Nb_2O_5, first reported by Frevel and Rinn [45]; is hexagonal and can be best prepared by the oxidation of NbO_2 in air at 590 K for 24 h [44]. Holtzberg et al. [46] and Shafer and Roy [47] obtained this (δ) phase by carefully heating the niobic acid hydroxide gel or amorphous Nb_2O_5 at 770 to 870 K or at low temperatures for prolonged periods of time. This metastable form has also been realized by vapor transport reactions with Nb_2O_5 [48] and by rapid-quenching of the melt [49]. The TT form transforms continuously into T-Nb_2O_5 on heating at 870 to 1073 K [50]; annealing at 1670 K results in the high temperature (H) polymorph [49].

The orthorhombic T-Nb_2O_5 has been obtained by Brauer [1], Holtzberg et al. [46] (γ-form) and Shafer and Roy [47] (III-form), by heating the hydroxide gels or amorphous Nb_2O_5 at 870 to 1073 K. It is also produced by the oxidation of Nb or Nb alloys below 1270 K [51] or NbO_2 at 870 to 1070 K in air [50]. Under hydrothermal conditions (170 atm, 600–650 K), amorphous niobic acid also changes to T-Nb_2O_5 [47]. Single crystals of the *T*-form can be obtained either by vapor transport or quenching the supercooled melt [52].

The T-form changes to the B-form on heating by an exothermic irreversible process and DTA scan indicates a T_t of 1090 K; heating to higher temperatures, however, leads to the formation of M and H forms of Nb_2O_5. However, Goldschmidt [53] concluded from his x-ray data that T→H conversion is time-dependent and that the T form transforms slowly to H modification even at room temperature.

The detailed crystal structure of the T-Nb_2O_5 is not known at present but it appears that TT and T modifications are closely related since TT→T process is continuous and TT may be a less ordered form of T-Nb_2O_5 and it is likely that substitution of F^- or $(OH)^-$ for O^{2-} is necessary for their stability [42]. On the other hand, these two phases may well be members of a family with complex compositions and large unit cells and not true polymorphs of Nb_2O_5 [54]. Schäfer and co-workers noticed the 'memory' effect in T-Nb_2O_5 [42]. Thus, the sample prepared by heating NbO_2 in air at 770 to 870 K is converted to the B-form sharply at 1090 K whereas the T-Nb_2O_5 obtained by reaction of NbO_2 with Cl_2 (9–10 h, 540 to 570 K and further heating at 770 K for 15 min in air) exhibited a slow T→B transition and not to completion even after heating for 165 h at 1120 K. On the other hand, T-Nb_2O_5 obtained by wet-precipitation-and-ignition methods transformed to a mixture of M and H forms after heating for 16 h at 1070 K without first going into the B-form. The detailed mechanism is not known but probably impurities play a significant role.

B-Nb_2O_5 is the densest of all the polymorphs of niobium pentoxide [55–57] and obtained as characteristic plate-like crystals having monoclinic symmetry by vapor transport methods [44]. Polycrystalline material can be obtained easily by the oxidation of NbO_2 in air (24 h heat treatment at 590 and at 1120 K) [44]. This polymorph is depicted as the high-pressure phase by Wadsley and Andersson [42] and thermal studies by Schäfer et al. [44] indicate it to be thermodynamically stable at low temperatures.

DTA studies indicate a B→H endothermic conversion at 1230 K but isothermal experiments in $NbOCl_3$ and Cl_2 atmospheres reveal that the transition is reversible and occurs at lower temperatures (T_f=1020 K; T_r=920 K) with $\Delta H \sim 2$ kcal/mol.

The tetragonal M-Nb_2O_5 has been first reported by Brauer [1] and can be obtained by heating either the amorphous or T form at 1170 to 1220 K for some hours or for shorter periods at higher temperatures [46, 58]. Single crystals have been grown by vapor transport [59] which indicate the true symmetry to be tetragonal rather than monoclinic [57]. This phase transforms to H-Nb_2O_5 continuously on heating at 1170 K.

Monoclinic N-Nb_2O_5 can be prepared by vapor transport and also by the thermal decomposition of NbO_2F [48, 60–62]. It has a needle-like habit and F^- ion appears to stabilize the structure. Transformation to H-Nb_2O_5 takes place slowly on heating to 1170 to 1270 K [44].

P-Nb_2O_5 has been obtained by Schäfer et al. [48] and Lavers et al. [56] by vapor transport in the range 1020–1120 K. Water vapor and chloride ions seem to have stabilizing effect on this phase [44]. This tetragonal modification has an idealized V_2O_5 structure and transforms to H-Nb_2O_5 on heating at 1120 K; the process is endothermic and irreversible [44].

Gruehn [63] has reported the formation of R-Nb_2O_5 by vapor transport. It has a monoclinic symmetry and is supposed to have a simple structure compared to all other polymorphs. Thermochemical behavior is not known at present.

The stable H-Nb_2O_5 is easy to obtain and all other forms of the niobium pentoxide transform to this polymorph on heating in air to ~1370 K. The same result is obtained on heating the amorphous forms of Nb_2O_5 or the oxidation of Nb, Nb alloys or NbO_2 or slow cooling of the molten Nb_2O_5 [64] or under hydrothermal conditions (170 atm, 1350

K) [47]. The detailed crystal structure of this monoclinic modification has been worked out by Gatehouse and Wadsley [39, 42].

Several metastable phases of Nb_2O_5 have been reported in the literature whose identity is not very well established. Reisman and Holtzberg [64] observed a high-temperature ϵ form which crystallizes without supercooling from the molten Nb_2O_5 at 1708 K. The ϵ form transforms on cooling irreversibly (without evolution of much heat) to the H-form at 1670 to 1470 K; ϵ-Nb_2O_5 melts at 1708 K whereas the equilibrium melting point of H-Nb_2O_5 is 1764 K. X-ray and DTA studies by Shafer and Roy [47] indicated the existence of a metastable H′ form of Nb_2O_5 obtained on heating the H-Nb_2O_5 above 1560 K; H→H′ is an endothermic and reversible transition. Recently, Jonejan and Wilkins [65] reported a high-temperature phase transition in Nb_2O_5 taking place at 1756 K; the true melting point of Nb_2O_5 obtained is 1780 K as evidenced by DTA and hot-stage microscopic data.

Schäfer and co-workers [44] reported the formation of several modifications of Nb_2O_5 under nonequilibrium conditions from the NbO_x phases (Ox I to Ox VI); the powder x-ray data are almost identical to the initial NbO_x phases from which they are obtained but differ from one another and from all other polymorphs of Nb_2O_5. Detailed structural information is lacking at present and it is not known whether they can be classified as the true polymorphs of Nb_2O_5. Ox I to Ox VI change to H-Nb_2O_5 above 1370 K.

Electrical properties of Nb_2O_5 have been examined by Greener and co-workers [66, 67]. The stoichiometric Nb_2O_5 is a semiconductor and the defect structure is interpreted to be due to the oxygen vacancies; highly reduced material appears to be degenerate. Dielectric properties have been reported by a few workers in the literature [68, 69].

Systems Nb_2O_5-PbO [70], $-B_2O_3$ [71], $-Ln_2O_3$ (Ln = Rare earth) [72], $-GeO_2$ [73], $-TiO_2$ [65], $-P_2O_5$ [74], $-V_2O_5$ [75], $-Ta_2O_5$ [76, 77], $-WO_3$ [78] have been examined in the literature.

Niobium oxides

Oxide and description of the study	Data	Remarks and inferences	References
Suboxides			
Crystal structures.	NbO_x (Nb_6O): forms at 570–620 K; tetragonal; $a=3.387$ Å; $c=3.27$ Å. NbO_y (Nb_4O): forms at 620–670 K; orthorhombic or tetragonal; details not known. NbO_z (Nb_2O): forms at 670–970 K; tetragonal; $a=6.645$ Å; $c=4.805$ Å.	These suboxides form only by oxidation of metal or by ageing of Nb that is supersaturated with oxygen in definite ranges of temperature and oxygen pressures. They are metallic in nature but the detailed structure and properties are not known.	[11, 12].
NbO			
Crystal structure and physical properties.	Narrow homogeneity range; cubic; space group, Fm3m; $Z=4$; $a=4.2101$ Å. Contains 25% cation and anion vacancies. TEC (°/K): 4.8×10^{-6} at ~297 K; κ (cm^2/dyn): $4.2\pm0.06\times10^{-13}$; C_v (erg/mol, deg at 297 K): 41.06×10^7; $\gamma_G=1.26$. Melting point = 2218 K. Pressure and temperature do not produce any change in the concentration of vacancies indicating that these are either greatly ordered or form an inherent part of the structure and are not true lattice defects in NbO.	No crystal structure transformations are known in this material. The low value of κ and the magnitude of γ_G indicate that NbO is metallic in nature. Banus and Reed [18] suggest that NbO can be considered as a simple cubic oxide (with $Z=3$ and Nb and O in four-fold coordination and not octahedral type) with no vacancies in the structure which would explain the results of pressure experiments.	[15–19, 79, 80].

Niobium oxides—Continued

Oxide and description of the study	Data	Remarks and inferences	References
Electrical and optical properties.	Metallic behavior in the range 2–900 K with low resistivity; ρ (77 K)$\sim 10^{-6}$ Ωcm; ρ (300 K)$\sim 10^{-5}$ Ωcm. Seebeck coefficient and Hall data not available. Exhibits superconductivity below 1.5 K. Plasma edge from reflectance data = 4.3 eV; IR frequency = 1080 ± 10 cm^{-1}.	Detailed band picture and vacancy ordering effects not known. Available superconductivity data are qualitative and need reinvestigation.	[14–16, 20–22, 81].
NbO_2			
Crystal structure, x-ray and DTA studies.	Rutile structure; space group, $I4_1/a$; $Z=32$; $a=13.690\pm0.001$ Å; $c=5.9871\pm0.0003$ Å. Superstructure and metal-metal bonding below T_t. $T_t \approx 1070$ K; thermal hysteresis $\sim 10°$; $\Delta H=$ 600 cal/mol. The T_t obtained by x-ray data is higher ($\sim 50°$) than the DTA value. Melting point = 2190 K.	The first order nature of the transition is established. Superstructure lines of the a sublattice of rutile structure and metal-metal bonding disappears above T_t.	[15, 24–29].
Magnetic and electrical properties.	Paramagnetic in the range 100–1300 K; $\chi_M \approx 20\times10^{-6}$ emu/mol; χ_M exhibits jump at T_t. Semiconductor behavior below T_t; $\rho \sim 10^5$ Ωcm (300 K; polycrystalline material); $\rho \sim 14$ Ωcm (300 K, single crystal). $E_a \approx 0.26$ eV (both samples). Drop in ρ by a factor of 10 at T_t. Temperature independent ρ observed by Janninck and Whitmore [31] above T_t while Sakata [27] noted semiconductor behavior with $E_a \sim$ 0.15 eV in the range 1100–1270 K.	Paramagnetic semiconducting characteristics are confirmed below T_t and above $T_t NbO_2$ appears to be metallic. There is also discrepancy in the absolute magnitude of ρ for polycrystalline and single crystal samples of NbO_2.	[21, 27, 28, 30, 31, 37].
Infrared studies.	Bands at 715 and 1080 cm^{-1} are noted and are correlated with the metal-oxygen vibrations.	—	[81].
Homologous series, $Nb_{3n+1}O_{8n-1}$			
Crystal structure.	All phases are monoclinic; $n=5$; $NbO_{2.37}$; $a=21.2$ Å; $b=3.82$ Å; $c=12.0$ Å; $\beta=132.2°$. $n=6$; $NbO_{2.42}$; $a=20.73$ Å; $b=3.835$ Å; $c=15.67$ Å; $\beta=112.93°$. $n=7$; $NbO_{2.46}$; $a=21.19$ Å; $b=3.822$ Å; $c=15.75$ Å; $\beta=124.51°$. $n=8$; $NbO_{2.48}$; $a=21.20$ Å; $b=3.824$ Å; $c=29.97$ Å; $\beta=95.07°$.	These homologous series have structures somewhat to the high-temperature structure of Nb_2O_5 even though $n=9$ actually corresponds to this oxide.	[11].

Oxide and description of the study	Data	Remarks and inferences	References
$NbO_{2.417}$($Nb_{12}O_{29}$)			
Crystal structure.	Appears to exist in orthorhombic and monoclinic forms. Orthorhombic form: space group. Amma; $Z=4$; $a=28.99$ Å; $b=3.825$ Å; $c=20.72$ Å. Physical properties not known.	—	[40].
$NbO_{2.464}$ ($Nb_{47}O_{116}$)			
Crystal structure.	Monoclinic: $a=57.74$ Å; $b=3.823$ Å; $c=21.18$ Å; $\beta=105.32°$. The oxide has been prepared using $NbCl_5/NbOCl_3$ at 1520 K and the structure is probably a combination of $Nb_{22}O_{54}$ and $Nb_{25}O_{62}$ of the homologous series. Physical properties are not known.	—	[41].
Nb_2O_5			
Crystal structures and transformations.	Eight modifications known. TT-Nb_2O_5: best prepared by the oxidation of NbO_2 in air at 590 K for 24 h; pseudohexagonal; $Z=0.5$; $a=3.607$ Å; $c=3.925$ Å: Transforms continuously to T-Nb_2O_5 on heating at 870–1073 K [50]; annealing at 1670 K results in H-Nb_2O_5 [49]. T-Nb_2O_5: best prepared by heating the amorphous oxide at 870–1073 K [46, 47] or oxidation of NbO_2 at 670 K for 4 to 5 h. Two forms are reported. Orthorhombic: $a=6.19$ Å; $b=3.65$ Å; $c=3.94$ Å; $Z=12$. Monoclinic: $a=7.13$ Å; $b=15.72$ Å; $c=10.75$ Å; $\beta=120.7°$; $Z=12$. Changes to B-Nb_2O_5; $T_t=1090$ K; exothermic and irreversible; heating to higher temperatures produces H-Nb_2O_5. TT and T modifications appear to be structurally related. B-Nb_2O_5: Best prepared by the oxidation of NbO_2 in air (24 h at 590 and at 1120 K) or by vapor transport. Monoclinic; space group, C2/c; $Z=4$; $a=12.73$ Å; $b=4.88$ Å; $c=5.56$ Å; $\beta=105.1°$; density = 5.29 g/cm³. Densest of all the modifications; depicted as the high-pressure form; thermal studies indicate it to be	The polymorphic behavior of Nb_2O_5 is complicated. Wadsley and Andersson [42] have been able to explain the stability and structure of the stable polymorphs using the principle of crystallographic shear and even predicted the existence of hitherto unknown forms: However, various metastable and nonequilibrium phases need explanation. Hydrothermal behavior, various impurity effects and 'memory' of Nb_2O_5 warrant careful and comprehensive investigation.	[39, 42, 44–49, 54–57, 59–63].

Oxide and description of the study	Data	Remarks and inferences	References
	the thermodynamically stable form at low temperatures. DTA studies show endothermic B→H transition at 1230 K; however, isothermal experiments in $NbOCl_3$ and Cl_2 atmospheres indicate the transition to be reversible and lower T_t with $\Delta H \sim 2$ kcal/mol. M-Nb_2O_5: Pure phase is difficult to obtain and partial transformation to H-form always occurs; prepared by heating oxide gels or amorphous form to 1170–1220 K or by vapor transport of Nb_2O_5 with $NbOCl_3$ or $NbOBr_3$ (T_1=1120–1170 K and T_2–T_1=100 K). Tetragonal; space group, I4/mmm; a=20.01 Å; c=3.84 Å. Transforms to H-Nb_2O_5 on heating at 1170 K; no thermal effects noticeable. N-Nb_2O_5: Best prepared by heating NbO_2F at 1270 K in vacuum for some hours; F^- ion appears to stabilize the structure. Monoclinic; space group, C2/m; a=28.51 Å; b=3.83 Å; c=17.48 Å; β=120.8°. Structures of M and N forms appear to be basically related [42]. N-Nb_2O_5 transforms to H-Nb_2O_5 slowly on heating at 1170–1270 K. P-Nb_2O_5: Prepared by vapor transport (Cl_2; T_1=1020 K; T_2–T_1=100 K). Cl^- ions and water vapor appear to have stabilizing effect. Tetragonal: space group, $I4_1/22$; Z=4; a=3.896 Å; c=25.43 Å. $P \rightarrow H$ at 1120 K; endothermic and irreversible. R-Nb_2O_5: Prepared by vapor transport but usually associated with other polymorphs. Monoclinic; space group, C2/m; a=12.79 Å; b=3.826 Å; c=3.983 Å; β=90.75°. Thermal behavior not known. H-Nb_2O_5: Easy to obtain; any other form heated in air at 1370 K produces this form; also under hydrothermal conditions. Monoclinic; space group, P2; Z=14; a=21.16 Å; b=3.822 Å; c=19.35		

Oxide and description of the study	Data	Remarks and inferences	References
	Å; $\beta = 119.83°$. Most stable form; structure based on the crystallographic shear has been worked out by Gatehouse and Wadsley [39, 42]. The melting points of Nb_2O_5 reported are inconclusive and the values quoted are 1758, 1764, and 1780 K [46, 65, 78].		
Electrical properties.	Semiconductor; $\sigma \sim 10^{-4}$ Ωcm at ~1000 K; $E_a = 1.65$ eV. Reduced Nb_2O_5 tends to behave as a degenerate semiconductor. Defect structure is interpreted to be due to anion vacancies.	—	[66, 67].
IR studies.	Bands are noted at 790 and 1010 cm^{-1} for H-Nb_2O_5 and are interpreted in terms of metal-oxygen vibrations.	—	[81].

References

[1] Brauer, G., Naturwiss. 28, 30 (1940); Z. Elektrochem. 46, 397 (1940); Z. anorg. allgem. Chem. 248, 1 (1941).
[2] Elliot, R. P., Trans. ASM. 52, 990 (1960).
[3] Brauer, G., Mueller, H., and Kuehner, G., J. Less-Comm. Metals 4, 533 (1962).
[4] Norman, N., J. Less-Comm. Metals 4, 52 (1962).
[5] Blackburn, P. E., J. Electrochem. Soc. 109, 1142 (1962).
[6] Kofstad, P., and Espevik, S., J. Electrochem. Soc. 112, 153 (1965).
[7] Taylor, A., and Doyle, N. J., J. Less-Comm. Metals 13, 313 (1967).
[8] Fromm, E., and Jehn, H., J. Less-Comm. Metals 15, 242 (1968)
[9] Schäfer, H., Bergner, D., and Gruehen, R., Z. anorg. allgem. Chem. 365, 31 (1969).
[10] Terao, N., Japan J. Appl. Phys. 2, 156 (1963).
[11] Niebuhr, J., J. Less Comm. Metals 11, 191 (1966).
[12] Chang, L. L. Y., and Phillips, B., J. Am. Ceram. Soc. 52, 527 (1969).
[13] Nakayama, T., Osaka, T., and Kitada, A., J. Less-Comm. Metals 19, 291 (1969).
[14] Pollard, E. R., Ph.D. Thesis, MIT, USA (1968).
[15] Subbarao, G. V., Ph.D. Thesis, Indian Institute of Technology, Kanpur, India, 1969.
[16] Rao, C. N. R., Wahnsiedler, W. E., and Honig, J. M., J. Solid State Chem. 2, 315 (1970).
[17] Taylor, A., and Doyle, N. J., J. Appl. Cryst. 4, 103 (1971).
[18] Banus, M. D., and Reed, T. B., in The Chemistry of Extended Defects in Non-metallic Solids, Eds. L. Eyring and M. O'Keeffe (North Holland Publ. Co., Amsterdam, 1970), p. 488.
[19] Taylor, A., and Doyle, N. J., in The Chemistry of Extended Defects in Non-metallic Solids, Eds. L. Eyring and M. O'Keeffe (North Holland Publ. Co., Amsterdam, 1970), p. 523.
[20] Meissner, W., Franz, H., and Westerhoff, H., Ann Phys. (Leipzig) 17, 593 (1933).
[21] Roberson, J. A., and Rapp, R. A., J. Phys. Chem. Solids 30, 1119 (1969).
[22] Chandrashekar, G. V., Moyo, J., and Honig, J. M., J. Solid State Chem. 2, 528 (1970).
[23] Gel'd, P. V., Shveikin, G. P., Alyamovskii, S. I., and Tskhai, V. A., Russ. J. Inorg. Chem. 12, 1053 (1967).
[24] Marinder, B.-O., Arkiv Kemi 19, 435 (1962).
[25] Rogers, D. B., Shannon, R. D., Sleight, A. W., and Gillson, J. L., Inorg. Chem. 8, 841 (1969).
[26] Sakata, T., Sakata, K., and Nishida, I., Phys. Stat. Solidi 20, K155 (1967).
[27] Sakata, K., J. Phys. Soc. Japan 26, 582 (1969); 26, 867 (1969); 26, 1067 (1969).
[28] Rao, C. N. R., Rama Rao, G., and Subba Rao, G. V., J. Solid State Chem. 6, 340 (1973).
[29] Rao, C. N. R., Natarajan, M., Subba Rao, G. V., and Loehman, R. E., J. Phys. Chem. Solids 32, 1147 (1971).
[30] Sakata, K., Nishida, I., Matsushima, M., and Sakata, T., J. Phys. Soc. Japan 27, 506 (1969).
[31] Janninck, R. F., and Whitmore, D. H., J. Phys. Chem. Solids 27, 1183 (1966).
[32] Adler, D., Solid State Phys. 21, 1 (1968).
[33] Rao, C. N. R., and Subba Rao, G. V., Phys. Stat. Solidi (a), 1, 597 (1970).
[34] Marinder, B.-O., Dorm, E., and Seleborg, M., Acta Chem. Scand. 16, 293 (1962).
[35] Rüdorff, W., and Luginsland, H. H., Z. anorg. allgem. Chem. 334, 125 (1964).
[36] Kristensen, I. K., J. Appl. Phys. 40, 4992 (1969).
[37] Rao, C. N. R., unpublished results (1971).
[38] Norin, R., and Magnéli, A., Naturwiss. 47, 354 (1960).
[39] Gatehouse, B. M., and Wadsley, A. D., Acta Cryst. 17, 1545 (1964).
[40] Norin, R., Acta Chem. Scand. 17, 1391 (1963).
[41] Gruehn, R., and Norin, R., Z. anorg. allgem. Chem. 367, 209 (1967).

[42] Wadsley, A. D., and Andersson, S., in Perspectives in Structural Chemistry, Vol. III, Eds. J. D. Dunitz and J. A. Ibers (John Wiley & Sons, New York, 1970), pp. 1–58.
[43] Blumenthal, R. N., Moser, J. B., and Whitmore, D. H., J. Am. Ceram. Soc. 48, 617 (1965).
[44] Schäfer, H., Gruehn, R., and Schulte, F., Angew. Chem. Internat. Edit. 5, 40 (1966).
[45] Frevel, L. K., and Rinn, H. W., Anal. Chem. 27, 1329 (1955).
[46] Holtzberg, F., Reisman, A., Berry, M., and Berkenblit, M., J. Am. Chem. Soc. 79, 2039 (1957).
[47] Shafer, M. W., and Roy, R., Z. Krist. 110, 241 (1958).
[48] Schäfer, H., Schulte, F., and Gruehn, R., Angew. Chem. Internat. Edit. 3, 511 (1964).
[49] Sarjeant, P. T., and Roy, R., J. Am. Ceram. Soc. 50, 500 (1967).
[50] Brendel, C., quoted in ref. [44].
[51] Nowotny, H., Benesovsky, F., Rudy, E., and Wittmann, A., Mh. Chem. 91, 975 (1960).
[52] Mertin, W., and Jagusch, W., quoted in ref. [44].
[53] Goldschmidt, H. J., J. Inst. Metals 87, 235 (1958/59).
[54] Jahnberg, L., and Andersson, S., Acta Chem. Scand. 21, 615 (1967).
[55] Laves, F., Moser, R., and Petter, W., Naturwiss. 51, 356 (1964).
[56] Laves, F., Petter, W., and Wulf, H., Naturwiss. 51, 633 (1964).
[57] Terao, N., Japan J. Appl. Phys. 4, 8 (1965).
[58] Schulte, F., Gruehn, R., and Görbing, M., quoted in ref. [44].
[59] Mertin, W., Andersson, S., and Gruehn, R., J. Solid State Chem. 1, 419 (1970).
[60] Andersson, S., and Åström, A., Acta Chem. Scand. 19, 2136 (1965).
[61] Lundberg, M., and Andersson, S., Acta Chem. Scand. 21, 615 (1967).
[62] Andersson, S., Z. anorg. allgem. Chem. 351, 106 (1967).
[63] Gruehn, R., J. Less-Comm. Metals 11, 119 (1966).
[64] Reisman, A., and Holtzberg, F., J. Am. Chem. Soc. 81, 3182 (1959).
[65] Jonejan, A., and Wilkins, A. L., J. Less-Comm. Metals 19, 185 (1969).
[66] Greener, E., Whitmore, D., and Fine, M., J. Chem. Phys. 34, 1017 (1961).
[67] Greener, E. H., and Hirthe, W. M., J. Electrochem. Soc. 109, 600 (1962).
[68] Robinson, M. L. A., and Roetschi, H., J. Phys. Chem. Solids 29, 1503 (1968).
[69] Emmenegger, F. P., and Robinson, M. L. A., J. Phys. Chem. Solids 29, 1673 (1968).
[70] Roth, R. S., J. Res. Nat. Bur. Stand. (U.S.), 62, 27 (1959).
[71] Levin, E. M., J. Res. Nat. Bur. Stand. (U.S.), 70A (Phys. and Chem.), No. 1, 11–16 (Jan.–Feb. 1966).
[72] Godina, N. A., Savchenko, E. P., and Keler, E. K., Russ. J. Inorg. Chem. 14, 1162 (1969).
[73] Levin, E. M., J. Res. Nat. Bur. Stand. (U.S.) 70A (Phys. and Chem.), No. 1, 5–10 (Jan.–Feb. 1966).
[74] Levin, E. M., and Roth, R. S., J. Solid State Chem. 2, 250 (1970).
[75] Waring, J. L., and Roth, R. S., J. Res. Nat. Bur. Stand. (U.S.), 69A (Phys. and Chem.), No. 2, 119–129 (Mar.–Apr. 1965).
[76] Holtzberg, F., and Reisman, A., J. Phys. Chem. 65, 1192 (1961).
[77] Mohanty, G. P., Fiegel, L. P., and Healy, J. H., J. Phys. Chem. 68, 208 (1964).
[78] Roth, R. S., and Waring, J. L., J. Res. Nat. Bur. Stand. (U.S.), 70A (Phys. and Chem.), No. 4, 281–303 (July–Aug. 1966).
[79] Taylor, A., and Doyle, W. J., J. Appl. Cryst. 4, 109 (1971).
[80] Gel'd, P. V., and Kusenko, F., Izv. Akad. Nauk SSSR, Otdel. Tekhn. Nauk Met. i Toplivo 2, 79 (1960).
[81] Alyamovskii, S. I., Shveikin, G. P., and Gel'd, P. V., Russ. J. Inorg. Chem. 12, 915 (1967).

II.4. Molybdenum Oxides

Phase studies on the Mo-O system have been carried out by various workers [1–6]. In addition to the well-known dioxide and trioxide, many mixed valence phases (between MoO_2 and MoO_3) have been reported [3–7]; of these, Mo_4O_{11} and Mo_9O_{26} seem to be stable [1, 5, 6] whereas $Mo_{17}O_{47}$, Mo_5O_{14} and Mo_8O_{23} seem to be metastable and can be stabilized by incorporation of other elements like Ti, V, and W [8]. These mixed valence oxides can not be considered to be truly nonstoichiometric, since they have narrow ranges of homogeneity; some of them have tunnel and layer structures. No oxide of molybdenum in the range Mo-MoO_2 is known and the reported existence of Mo_3O [2] is in doubt [1, 5, 6, 9].

MoO_2: Molybdenum dioxide, MoO_2, has a monoclinic structure [1, 7, 10–12] and exhibits metallic behavior in the range 4 to 300 K [12, 13]. No phase transitions are known in this material. Other properties are not known.

MoO_2 forms solid solutions with TiO_2 [14], NbO_2 [14] and VO_2 [15–17] which have rutile structures.

Mixed Valence Phases: Mo_4O_{11} has a monoclinic structure (stable below 890 K) and assumes an orthorhombic symmetry when synthesized in the range 890 to 950 K; both the forms are closely related [3, 7, 18] in structure and T_t appears to be ~900 K. Mo_4O_{11} appears to be metallic [3] with no significant change in ρ at T_t. $Mo_{17}O_{47}$ has an orthorhombic symmetry [3, 18] whereas Mo_5O_{14} is tetragonal [8]; Mo_8O_{23} is monoclinic [3, 7, 18–20]. Mo_9O_{26} is dimorphic and can assume a triclinic or monoclinic structure depending on the method of preparation [5, 9, 18, 19]. Phillips and Chang [5] report a phase transformation in Mo_9O_{26} at 1040 K; the low-temperature form is monoclinic, but the structure of the high-temperature form is not exactly known. $Mo_{17}O_{47}$ exhibits low resistivity and appears to be metallic [3]. Mo_4O_{11} and Mo_9O_{26} melt at high temperature (>1000 K) and decompose to lower oxides [5]. Detailed physical properties are not known for these mixed valence phases.

MoO_3: Molybdenum trioxide, MoO_3, has an orthorhombic symmetry and consists of a layered (or chain) structure [1, 5, 7, 21]. Detailed studies [5] indicate no phase transitions in this material up to the melting point (~1055 K). MoO_3 is a semiconductor [22].

Molybdenum bronzes are formed from MoO_3 and other metallic oxides; these interesting materials have been discussed in detail in the literature [23]

Oxide and description of the study	Data	Remarks and inferences	References
MoO_2			
Crystal structure and electrical properties.	Monoclinic; space group, $P2_1/c$; $Z=4$; $a=5.6109\pm0.0008$ Å; $b=4.8562\pm0.0006$ Å; $c=5.6285\pm0.0007$ Å; $\beta=120.95°$. No phase transitions are known. Metallic behavior; ρ (4.2 K) $\approx 5.4\times10^{-7}$ Ωcm; ρ (300 K) $\approx 8.8\times10^{-5}$ Ωcm.	The structure is closely related to that of rutile; the metallic properties have been interpreted in terms of a modified Goodenough's model.	[1, 7, 10–13].
Mixed Valence Phases			
Mo_4O_{11}			
Crystal structure and electrical properties.	Monoclinic (<900 K); $a=24.54$ Å; $b=5.439$ Å; $c=6.701$ Å; $\beta=94.28°$. Orthorhombic (>900 K); $a=24.49$ Å; $b=5.459$ Å; $c=6.752$ Å. $T_t\approx900$ K. Monoclinic and orthorhombic forms can be obtained at ordinary temperatures depending on the method of preparation. Both forms show metallic behavior; ρ (300 K) ~0.2 Ωcm; ρ does not show much change at T_t.	Both the modifications are closely related structurally and are built up of MoO_4 tetrahedra and distorted MoO_6 octahedra; the difference lies in the relative orientation of the substructures in nieghboring slabs, being parallel in the monoclinic and alternating in the orthorhombic form. Detailed data on the physical properties are lacking.	[3, 7, 18].
$Mo_{17}O_{47}$			
Crystal structure and electrical properties.	Orthorhombic; space group, Pba2; $Z=2$; $a=21.61$ Å; $b=19.63$ Å; $c=3.951$ Å. Metallic behavior; ρ (300 K) ~5×10^{-2} Ωcm. Detailed data are lacking.	This has a tunnel structure which may be considered as built up from MoO_6 octahedra and MoO_7 pentagonal bipyramids. Metal-metal bonding is noted and probably accounts for the low measured resistivity.	[3, 18].
Mo_5O_{14}			
Crystal structure.	Tetragonal; $a=11.50$ Å; $c=3.937$ Å. Metastable form and decomposes on prolonged heat treatment; Ti, V, and W seem to stabilize the phase.	The structure is related to that of $Mo_{17}O_{47}$. Detailed data are lacking.	[8].
Mo_8O_{23}			
Crystal structure.	Monoclinic; $a=16.88$ Å; $b=4.052$ Å; $c=13.39$ Å; $\beta=106.19°$. Properties not known.	The structure is that of distorted ReO_3-type in which recurrent dislocations of atoms occur along the shear planes.	[3, 7, 18–20].
Mo_9O_{26} ($Mo_{18}O_{52}$)			
Crystal structure and x-ray studies.	Dimorphic: Triclinic phase; $a=8.145$ Å; $b=11.89$ Å; $c=21.23$ Å; $\alpha=102.67°$; $\beta=67.82°$; $\gamma=$	The triclinic phase has a basic MoO_3 structure. According to Kihlborg [24], $Mo_{18}O_{52}$ is the	[5, 9, 18, 19].

Molybdenum oxides—Continued

Oxide and description of the study	Data	Remarks and inferences	References
	109.97°. Monoclinic phase; $a=16.74$ Å; $b=4.019$ Å; $c=14.53$ Å; $\beta=95.45°$. Both forms can be prepared at room temperature. Monoclinic phase shows a transition at 1040 K; the structure of the high-temperature phase is not known in detail. Physical properties are not known.	first member ($m=1$) of a homologous series, Mo_nO_{3n-m+1}. The existence of oxides $Mo_{12}O_{33}$ and $Mo_{26}O_{75}$ is suggested.	
MoO_3			
Crystal structure and properties.	Orthorhombic; space group, Pbnm; $Z=4$; $a=3.966$ Å; $b=13.88$ Å; $c=3.703$ Å. No phase transformations exist up to the melting point (1055 K). Semiconductor; ρ (450 K)$\sim 10^{10}$ Ωcm; ρ (900 K) $\sim 10^5$ Ωcm; $\ln\rho - 1/T$ plot shows a break at ~650 K; E_a (<650 K) ≈ 0.56 eV; E_a (>650 K) ≈ 1.83 eV.	It has a chain structure. The break in $\ln\rho - 1/T$ plot at 650 K may correspond to a change in the mechanism of conduction.	[1, 5, 7, 21, 22].

References

[1] Hägg, G., and Magnéli, A., Arkiv Kemi, Mineral Geol. 19A, 1 (1945).
[2] Schönberg, N., Acta Chem. Scand. 8, 221 (1954); 8, 617 (1954).
[3] Kihlborg, L., Acta Chem. Scand. 13, 954 (1959); Adv. Chem. Ser. 39, 3745 (1963).
[4] Rode, E. Ya., and Lysanova, G. V., Dokl. Akad. Nauk SSSR 145, 351 (1962).
[5] Phillips, B., and Chang, L. L. Y., Trans. AIME 233, 1433 (1965).
[6] Chang, L. L. Y., and Phillips, B., J. Am. Ceram. Soc. 52, 527 (1969).
[7] Magnéli, A., Andersson, G., Holmberg, B., and Kihlborg, L., Anal. Chem. 24, 1998 (1952).
[8] Kihlborg, L., Acta Chem. Scand. 23, 1834 (1969).
[9] Kihlborg, L., Acta Chem. Scand. 16, 2458 (1962).
[10] Magnéli, A., Arkiv Kemi, Mineral Geol. 24A, 11 (1946).
[11] Brandt, B. G., and Skapski, A. C., Acta Chem. Scand. 21, 661 (1967).
[12] Rogers, D. B., Shannon, R. D., Sleight, A. W., and Gillson, J. L., Inorg. Chem. 8, 841 (1969).
[13] Perloff, D. S., and Wold, A., Crystal Growth, Proc. Int. Conf. on Cryst. Growth, Ed. H. S. Peiser (Pergamon, London, 1967).
[14] Marinder, B.-O., Dorm, E., and Seleborg, M., Acta Chem. Scand. 16, 293 (1962).
[15] Marinder, B.-O., and Magnéli, A., Acta Chem. Scand. 11, 1635 (1957); 12, 1345 (1958).
[16] Israelson, M., and Kihlborg, L., Mat. Res. Bull. 5, 19 (1970).
[17] Rao, C. N. R., Natarajan, M., Subba Rao, G. V., and Loehman, R. E., J. Phys. Chem. Solids 32, 1147 (1971).
[18] Kihlborg, L., Arkiv Kemi 21, 471 (1963).
[19] Magnéli, A., Acta Chem. Scand. 2, 501 (1948).
[20] Kihlborg, L., Arkiv Kemi 21, 461 (1963).
[21] Kihlborg, L., Arkiv Kemi 21, 357 (1963).
[22] Deb, S. K., and Chopoorian, J. A., J. Appl. Phys. 37, 4818 (1966).
[23] Rao, C. N. R., and Subba Rao, G. V., Phys. Stat. Solidi (a) 1, 597 (1970).
[24] Kihlborg, L., Arkiv Kemi 21, 443 (1963).

II.5. Technitium Oxides

Studies by various workers [1–3] have shown that in the system Tc-O, TcO_2 is the only stable oxide at high temperatures. A covalent heptoxide, Tc_2O_7, is also known. TcO_2 has a monoclinic, MoO_2-type structure [1, 3] and according to Marinder and Magnéli [5], metal-metal bonds exist in this material. A different monoclinic cell was suggested by Zachariasen [6]; it has been pointed out [3] that TcO_2 may exhibit polymorphism like ReO_2.

Tc_2O_7 is orthorhombic and the structure consists of an arrangement of isolated Tc_2O_7 molecules with tetrahedral coordination of Tc atoms; the structure of Tc_2O_7 is more closely related to CrO_3, RuO_4 and OsO_4 than to Re_2O_7. Physical properties are not known at present.

Technitium oxides

Oxide and description of the study	Data	Remarks and inferences	References
TcO_2			
Crystal structure.	Monoclinic; space group, $P2_1/C$; $Z=4$; $a=5.55\pm0.01$ Å; $b=4.85\pm0.01$ Å; $c=5.62\pm0.01$ Å; $\beta=121.9\pm0.1°$.	Rutile based structure with metal-metal bonds.	[1, 3, 5].
Tc_2O_7			
Crystal structure.	Orthorhombic; space group, Pbca; $Z=4$; $a=13.756$ Å; $b=7.439$ Å; $c=5.617$ Å.	The structure consists of isolated Tc_2O_7 molecules.	[4].

References

[1] Muller, O., White, W. B., and Roy, R., J. Inorg. Nucl. Chem. **26**, 2075 (1964).

[2] Rulfs, C. L., Pacer, R. A., and Hirsch, R. F., J. Inorg. Nucl. Chem. **29**, 681 (1967).

[3] Rogers, D. B., Shannon, R. D., Sleight, A. W., and Gillson, J. L., Inorg. Chem. **8**, 841 (1969).

[4] Krebs, B., Angew. Chem. Int. Ed. (Engl.) **8**, 381 (1969); Z. anorg. allgem. Chem. **380**, 146 (1971).

[5] Marinder, B.-O., and Magnéli, A., Acta Chem. Scand. **11**, 1635 (1957).

[6] Zachariasen, W. H., ACA Program and Abstr. of Winter Meeting, F-4 (1951).

II.6. Ruthenium Oxides

Phase relations in the Ru-O system have been reported in the literature [1,2]. In the temperature range 1070 to 1770 K, RuO_2 is the only stable oxide (in air); RuO_3 and RuO_4 exist as vapor species. Attempts to prepare the stable nonstoichiometric oxide, $RuO_{2\pm x}$, have not been successful [2]. RuO_2 dissociates in air at ~1680 K to the metal.

Several workers have studied the crystal growth of RuO_2 by chemical transport [3–5] and other methods [6, 7]. RuO_2 has a tetragonal rutile structure [2, 3, 5–9] at room temperature and no phase transitions are known in the temperature range 4.2–1270 K [5, 8, 10–12]. It has a low and almost temperature independent magnetic susceptibility [6, 13]; the resistivity is very low and exhibits metallic behavior [3, 5–7, 11–14].

Fletcher and co-workers [13] have shown that the oxidation state of Ru in RuO_2 is more than 4. The de Hass-van Alphen effect [15], magnetoresistance [16] and Azbel-Kaner cyclotron resonance [17] studies on RuO_2 suggest that the simple band picture proposed by Rogers and co-workers [7] is inadequate to explain the observed properties. Ryden et al. [12] have found that electron-phonon and electron-electron interband scattering mechanism accounts quantitatively for the observed resistivity behavior of RuO_2 in the range 10 to 1000 K.

McDaniel and Schneider [2] report that RuO_2 and IrO_2 can form complete solid solutions of rutile structure in the entire composition range.

Ruthenium oxides

Oxide and description of the study	Data	Remarks and inferences	References
RuO_2			
Crystal structure and TEC.	$T=298$ K: Tetragonal; space group, $P4_2/mnm$; $Z=2$; $a=4.4910\pm0.0003$ Å; $c=3.1064\pm0.0002$ Å. TEC ($\times10^{-6}$/°C: $\|\|^c=-1.4$; $\|\|^a=+7.0$.	The c lattice parameter decreases with rise in T; slight anisotropy is evident.	[5, 10].
Magnetic and electrical properties.	$\chi_M=2.03\times10^{-4}$ cgs units at 298 K. ρ (4.2 K)~1.0×10^{-8} Ωcm; ρ (100 K)~1×10^{-6} Ωcm; ρ (298 K)~4.0×10^{-5} Ωcm. At 77 K, $R_H=-0.79$, $\mu_H=61$ cm²/V s; at 300 K, $R_H=-1.10$, $\mu_H=3.1$ cm²/V s. θ_D (calc.) $=900\pm5$ K. $1/\kappa=\beta/T+\alpha T^n$ (for $T<1.5\ T_m$) where $\beta=18.1$ cm K²/W, $\alpha=8.42\times10^{-4}$ cm K^{1-n}/W, $n=1.66$ and T_m is the temperature at which κ is a maximum. Lorentz ratio $=2.6\times10^{-8}$W Ω/K².	The metallic behavior of RuO_2 is evident; the Lorentz number is close to the theoretical value for typical metals.	[3, 6, 7, 11, 12, 18].

References

[1] Bell, W. E., and Tagami, M., J. Phys. Chem. 67, 2432 (1963).
[2] McDaniel, C. L., and Schneider, S. J., J. Res. Nat. Bur. Stand. (U.S.), 73A (Phys. and Chem.), No. 2, 213–219 (Mar.–Apr. 1969).
[3] Schafer, H., Schneidereit, G., and Gerhardt, W., Z. anorg. allgem. Chem. 319, 327 (1963).
[4] Schafer, H., Chemical Transport Reactions (Academic Press, New York, 1964), p. 48.
[5] Butler, S. R., and Gillson, J. L., Mat. Res. Bull. 6, 81 (1971).
[6] Cotton, F. A., and Mague, J. T., Inorg. Chem. 5, 317 (1966).
[7] Rogers, D. B., Shannon, R. D., Sleight, A. W., and Gillson, J. L., Inorg. Chem. 8, 841 (1969).
[8] Krishna Rao, K. V., and Iyenger, L., Acta Cryst. 25A, 302 (1969).
[9] Boman, C. E., Acta Chem. Scand. 24, 116 (1970).
[10] Hazony, Y., and Perkins, H. K., J. Appl. Phys. 41, 5130 (1970).
[11] Osburn, C. M., and Vest, R. W., Bull. Am. Ceram. Soc. 47, 354 (1968).
[12] Ryden, W. D., Lawson, A. W., and Sartain, C. C., Phys. Rev. B 1, 1494 (1970).
[13] Fletcher, J. M., Gardner, W. E., Greenfield, B. F., Holdoway, M. J., and Rand, M. H., J. Chem. Soc. A 653 (1968).
[14] Ryden, W. D., Lawson, A. W., and Sartain, C. C., Phys. Letters 26A, 209 (1968).
[15] Marcus, S. M., and Butler, S. R., Phys. Letters 26A, 518 (1968).
[16] Marcus, S. M., Phys. Letters 28A, 191 (1968).
[17] Slivka, R. T., and Langenberg, D. N., Phys. Letters 28A, 169 (1968).
[18] Millstein, J., J. Phys. Chem. Solids 31, 886 (1970).

II.7. Rhodium Oxides

In the Rh-O system, the only well-established oxides are Rh_2O_3 and RhO_2, even though there are numerous claims and counter claims regarding the existence of oxides such as Rh_2O and RhO [1–5]. Rh_2O_3 exhibits polymorphism; the low-temperature low-pressure form belongs to the corundum structure and the high-temperature low-pressure form has the orthorhombic perovskite structure [1, 5]. According to Wold and co-workers [1], the transition temperature is ~1020 K and is sluggish; T_t also depends on the starting materials used. The high-temperature low-pressure form can be prepared from Rh metal at 1270 K [1]. Shannon and Prewitt [6] have prepared a high-temperature high-pressure form of Rh_2O_3 (at 65 kbar pressure and 1470 K) which has an orthorhombic symmetry but closely related to the corundum structure. The high-temperature form of Wold et al., and the high-pressure form of Shannon and Prewitt appear to be closely related [6]. The latter material appears to be semiconducting at room temperature [6].

RhO_2 has the rutile structure [2–4]; it has a low resistivity and exhibits metallic behavior [3, 4]. Other Physical properties are not known.

Rhodium oxides

Oxide and description of the study	Data	Remarks and inferences	References
Rh_2O_3			
Crystal structures and electrical properties.	Low-temperature low-pressure form: Hexagonal (Corundum structure); space group, $R\bar{3}C$; $Z=6$; $a=5.108$ Å; $c=13.810$ Å. T_t is ~1020 K. High temperature form: Orthorhombic; space group, Pbca; $a=5.1477$ Å; $b=5.4425$ Å; $c=14.6977$ Å. High-temperature high-pressure form: Orthorhombic; space group, Pbna; $Z=4$; $a=5.1686\pm0.0003$ Å; $b=5.3814\pm0.0004$ Å; $c=7.2486\pm0.0004$ Å. ρ (300 K)~130 Ωcm; $E_a=0.16$ eV.	The low-temperature→high-temperature transformation is sluggish and depends on the starting materials employed; the high temperature form can be prepared directly from Rh metal at 1270 K. The orthorhombic structures are related to the corundum structure and may be described as containing layers of the corundum structure cut parallel to $(10\bar{1}1)$ and stacked together.	[1, 1a, 6, 7]. [6].
RhO_2			
Crystal structure and electrical properties.	Rutile structure; space group $P4_2/mnm$; $Z=2$; $a=4.4862\pm0.0005$ Å; $c=3.0884\pm0.0005$ Å. ρ (4.2 K)~2×10^{-5} Ωcm; ρ (300 K)~1×10^{-4} Ωcm. RhO_3 decomposes to RhO_2 at ~1120 K followed by decomposition to the metal and oxygen at ~1320 K.	Rutile structure characteristic of many transition metal dioxides. Typical metallic behavior.	[2–4].

References

[1] Wold, A., Arnott, R. J., and Croft, W. J., Inorg. Chem. 2, 972 (1963).
[1a] Biesterbos, J. W. M., and Horustia, J., J. Less-Common Metalt, 30, 121 (1973).
[2] Muller, O., and Roy, R., J. Less-Common Metals 16, 129 (1968).
[3] Shannon, R. D., Solid State Commun. 6, 139 (1968).
[4] Rogers, D. B., Shannon, R. D., Sleight, A. W., and Gillson, J. L., Inorg. Chem. 8, 841 (1969).
[5] Prewitt, C. T., Shannon, R. D., Rogers, D. B., and Sleight, A. W., Inorg. Chem. 8, 1985 (1969).
[6] Shannon, R. D., and Prewitt, C. T., J. Solid State Chem. 2, 134 (1970).
[7] Coey, J. M. D., Acta Cryst. 26B, 1876 (1970).

II.8. Palladium Oxide

Palladium monoxide is the only stable oxide known in the Pd-O system. Attempts to prepare Pd_3O_4 have not been successful [1]. PdO has a tetragonal structure [2–4]. Studies by Rogers et al. [4] on PdO single crystals indicate that the material is a *p*-type semiconductor. No phase transformations are known in this material; it decomposes in air at ~1070 K [5].

PdO forms solid solutions with CuO [6, 7], PbO [8] and rare-earth sesquioxides [5] and the phase relations have been described in detail.

Palladium oxide

Oxide and description of the study	Data	Remarks and inferences	References
PdO			
Crystal structure and properties.	Tetragonal; space group, $P4_2/mmc$; $Z=2$; $a=3.0434\pm0.0002$ Å; $c=5.3363\pm0.0004$ Å. Semiconductor (*p*-type); ρ (300 K)~10–1000 Ωcm; $E_a=0.04$–0.10 eV. Decomposes to the metal and oxygen in air at ~1070 K; the process of decomposition is reversible. No phase transitions are known.	The material is a *p*-type extrinsic semiconductor.	[2–5].

References

[1] Muller, O., and Roy, R., J. Less-Comm. Metals **16**, 129 (1968).
[2] Moore, W. J., Jr. and Pauling, L., J. Am. Chem. Soc. **63**, 1392 (1941).
[3] Wasor, J., Levy, H. A., and Peterson, S. W., Acta Cryst. **6**, 661 (1953).
[4] Rogers, D. B., Shannon, R. D., and Gillson, J. L., J. Solid State Chem. **3**, 314 (1971).
[5] McDaniel, C. L., and Schneider, S. J., J. Res. Nat. Bur. Stand. (U.S.), **72A** (Phys. and Chem.), No. 1, 27–37 (Jan.–Feb. 1968).
[6] Schmahl, N. G., and Minzyl, E., Z. Phys. Chem. (N.F.) **47**, 142 (1965).
[7] Schmahl, N. G., and Eikerling, G. F., Z. Phys. Chem. (N.F.) **62**, 268 (1968).
[8] Shaplygin, I. S., Bromberg, A. V., and Sokol, V. A., Russ. J. Inorg. Chem. (English Transl.) **15**, 1195 (1970).

II.9. Silver Oxides

Even though the literature contains many references [1–8] where silver oxides have been studied, it appears that only Ag_2O and AgO (and probably Ag_2O_3) are the only well-characterized oxides of silver. Silver sesquioxide, Ag_2O_3, is prepared at low temperature in aqueous solutions [8]; it appears to have cubic structure [9] and decomposes to AgO at higher temperatures.

Ag_2O: The stability range of Ag_2O is limited [8, 10–13] and decomposes to the metal above ~500 K. Ag_2O has a cubic structure [11] and exhibits semiconducting behavior [14, 15]. A new high pressure modification of Ag_2O has been described by Kabalkina et al. [16]; this appears to have a layered CdI_2 structure possesing metal-metal bonds. These authors report that it may be a degenerate semiconductor or a semiconductor with a low energy gap.

AgO: Silver monoxide, AgO, has a monoclinic structure [3, 17, 18]; the oxygen content seems to vary depending on the method of preparation [3], but no other crystalline modifications of AgO are known. The material is diamagnetic and has a very low room temperature resistivity (~10Ωcm), but ρ shows negative temperature coefficient in the range 230 to 290 K [1, 18]; these properties are explained as due to the existance of monovalent and trivalent Ag ions in AgO and confirmed by x-ray structure analysis [17].

Silver oxides

Oxide and description of the study	Data	Remarks and inferences	References
Ag_2O			
Crystal structure and x-ray studies.	Cubic; space group, Pn3m; $Z=2$; $a=4.720\pm0.004$ Å. TEC~2×10^{-6}/°C (not very accurate value). Decomposes above ~500 K at atmospheric pressure. High-pressure form (prepared at 115–125 kbar and 1670 ± 200 K): Hexagonal; $a=3.072\pm0.003$ Å; $c=4.941\pm0.004$ Å. The high pressure phase is denser by ~30%.	Ag_2O has the same structure as Cu_2O with considerable covalency; the high-pressure modification has a layer-structure probably with metal-metal bonding.	[11, 16].
Thermal properties (10–470 K).	Heat capacity data have been reported in the 10–500 K range. DTA studies have been carried out in the 300–470 K range.	Anomalies have been noted in the heat capacity curves around 30 and 420 K. The low temperature anomaly is difficult to understand in terms of particle size of surface area effects alone. The high temperature anomaly is probably associated with annealing of crystal defects or crystalization.	[19–21].
Electrical properties measured in oxygen atmospheres (300 and 450 bar)	Semiconductor; p-type behavior with $\rho \propto p_{O_2}^{-1/4}$. ρ (500 K)~10^3-10^4 Ωcm; ρ (620 K)~10^1-10^2 Ωcm; $E_a=0.64$ eV.	α data lacking; the conduction mechanism is interpreted as due to positive holes excited from traps (cation vacancies).	[14, 15].

Oxide and description of the study	Data	Remarks and inferences	References
AgO			
Crystal structure, magnetic and electrical properties.	Monoclinic; space group, $P2_1/c$; $Z=4$; $a=5.85\pm0.02$ Å; $b=3.47\pm0.08$ Å; $c=5.49\pm0.05$ Å; $\beta=107.5°$. Structure analysis indicates that Ag^+ and Ag^{3+} ions exist; two different Ag-O distances are encountered. Diamagnetic in the range 90–370 K; $\chi_M=-19.1\times10^{-6}$ emu; Unusually low room temperature resistivity ($\rho\sim10$ Ωcm); ρ decreases with rise in T in the range 230–290 K.	AgO and CuO are isomorphous; the unusual physical properties of AgO compared to CuO are explained as due to the coexistence of mono- and trivalent Ag. ρ-T behavior indicates either near degeneracy or a semiconductor with a low energy gap. Detailed studies on AgO are urgently needed.	[1, 3, 17, 18].

References

[1] Neiding, A. B., and Kazarnovskii, I. A., Dokl. Akad. Nauk SSSR 78, 713 (1951).
[2] Jones, P., and Thirsk, H. R., Trans. Faraday Soc. 50, 732 (1954).
[3] Graff, W. S., and Stadelmair, H. H., J. Electrochem. Soc. 105, 446 (1958).
[4] Vlach, J., and Stehlik, B., Collec. Czech. Chem. Commun. 25, 676 (1960).
[5] Amlie, R. F., and Rüetschi, P., J. Electrochem. Soc. 108, 813 (1961).
[6] Karpov, A. A., Borisova, T. I., and Veselovskii, V. I., Zh. Fiz. Khim. 36, 1426 (1962).
[7] Allen, J. A., Proc. Australian Conf. Electrochem., Sydney, Hobart, Australia, 72, (1963) Publ. 1965.
[8] Nagy, G. D., Moroz, W. J., and Casey, E. J., Proc. Am. Power Sources Conf. 19, 80 (1965).
[9] Stehlik, B., Weidenthaler, P., and Vlach, J., Chem. Listy 52, 2230 (1958).
[10] Garner, W. E., and Reeves, L. W., Trans. Faraday Soc. 50, 254 (1954).
[11] Suzuki, T., J. Phys. Soc. Japan 15, 2018 (1960).
[12] Weidenthaler, P., Collec. Czech. Chem. Commun. 28, 137 (1963).
[13] Otto, E. M., J. Electrochem. Soc. 113, 643 (1966).
[14] Cahan, B. D., Ockerman, J. B., Amlie, R. F., and Rüetschi, P., J. Electrochem. Soc. 107, 725 (1960).
[15] Talukdar, M. I., and Baker, E. H., Solid State Commun. 7, 309 (1969).
[16] Kabalkina, S. S., Popova, S. V., Serebryanaya, N. R., and Vereshchagin, L. F., Dokl. Akad. Nauk SSSR 152, 853 (1963).
[17] Scatturin, V., Bellon, P. L., and Zannetti, R., J. Inorg. Nucl. Chem. 8, 462 (1958).
[18] Scatturin, V., Bellon, P. L., and Salkind, A. J., J. Electrochem. Soc. 108, 819 (1961).
[19] Pitzer, K. S., and Smith, W. V., J. Am. Chem. Soc. 59, 2633 (1937).
[20] Kobayashi, K., Sci. Rep. Tohoku Univ. 35, 173 (1951).
[21] Pitzer, K. S., Gerkin, R. E., Gregor, L. V., and Rao, C. N. R., Pure and Applied Chem. (J.IUPAC) 2, 211 (1961).

II.10. Cadmium Oxides

Cadmium monoxide, CdO, is the well known oxide in the Cd-O system [1–4]. Hoffman et al. [5] reported the preparation and structure of the peroxide CdO_2, but detailed properties are not known.

CdO: CdO has the cubic rock salt structure and is diamagnetic [6]. No phase transitions are known in this oxide. The substance is usually nonstoichiometric (Cd excess) with pronounced cation interstitials or anion vacancies [2, 7–9], resulting in a free electron concentration of $\sim10^{19}$–10^{21} cm^{-3}. Such high electron concentration induces degenerate behavior; at high temperatures, CdO is either nondegenerate or degenerate n-type semiconductor depending on the history of the sample, i.e., sintering time and temperature, carrier concentration and oxygen pressure [1]. Donor impurities which contribute conduction electrons give rise to an impurity level a few tenths of an electron volt below the conduction band [10]. Detailed resistivity, Seebeck coefficient and Hall coefficient measurements [1, 2, 9–14] as well as optical [15, 16], NMR [17, 18] and Faraday rotation [19] studies indicate that depending on the carrier concentration, the impurity band may overlap with the conduction band in CdO giving rise to quasimetallic or metallic properties.

Oxide and description of the study	Data	Remarks and inferences	References
CdO			
Crystal structure and magnetic properties.	Cubic; space group, Fm3m; $Z=4$; $a=4.6949$ Å. Slight variation of a with the stoichiometry. Diamagnetic; $\chi=-48.74\times10^{-6}$ emu/g.	CdO exhibits pronounced nonstoichiometry which is attributed to either Cd interstitials or oxygen vacancies.	[3, 6, 7].
Electrical properties.	Degenerate semiconductor behavior; ρ (300 K)$\sim10^{-2}$–10^{-3} Ωcm; $n\sim10^{18}$–10^{21} cm^{-3} depending on the sample history but independent of temperature; α (300 K)~20 μV/°C; μ_H (81 K) $\sim$700–1100 cm^2/V s; $m^*=0.15$–0.45 m.	Nonstoichiometry gives rise to large number of charge carriers; n can be controlled by sample treatment. The impurity level belonging to the ionized donors merges into the conduction band giving rise to quasi-metallic behavior in some samples. Detailed conduction mechanism treated.	[1, 2, 9–14].
Optical properties.	Band gap = 2.3 eV; a possible indirect gap noted at $\sim$1.2 eV; m^* (optical) = 1.4 m. Plasma edge is $\sim$0.2–0.5 eV depending on n. $\epsilon_0=18.1$; $\epsilon_\infty=5.6$.	Free carrier absorption is noted in the optical spectra due to quasi-free electrons. The results are interpreted in terms of the band structure of CdO [20].	[15, 16, 19].
^{113}Cd NMR studies (1.4–300 K).	Results indicate that the nuclei interact strongly with the degenerate conduction electrons and the electrons are in the host lattice conduction band. $\tau\propto n^{-2/3}T^{-1}$; $k\propto n^{1/3}$.	—	[17, 18].
CdO_2			
Crystal structure	Cubic; space group, Pa3; $Z=4$; $a=5.313\pm0.003$ Å. Decomposes violently at $\sim$450–470 K to CdO and oxygen. Other properties not known.	—	[5].

References

[1] Hogarth, C. A., Proc. Phys. Soc. (Lond.) 64B, 691 (1951).
[2] Wright, R. W., and Bastin, J. A., Proc. Phys. Soc. (Lond.) 71, 109 (1958).
[3] van Houten, S., Nature (Lond.) 195, 484 (1962).
[4] Höschl, P., Konak, C., and Prosser, V., Mat. Res. Bull. 4, 87 (1969).
[5] Hoffman, C. W. W., Ropp, R. C., and Mooney, R. W., J. Am. Chem. Soc. 81, 3830 (1959).
[6] Mookherji, T., J. Electrochem. Soc. 117, 1201 (1970).
[7] Cimino, A., and Merezio, M., J. Phys. Chem. Solids 17, 57 (1960).
[8] Haul, R., and Just, D., J. Appl. Phys. 33, 487 (1962).
[9] Koffyberg, F. P., Phys. Letters 30A, 37 (1969).
[10] Lamb, E. F., and Tompkins, F. C., Trans. Faraday Soc. 58, 1424 (1962).
[11] Bastin, J. A., and Wright, R. W., Proc. Phys. Soc. (Lond.) 68A, 312 (1955).
[12] Konak, C., Höschl, P., Dillinger, J., and Prosser, V., Crystal Growth, Suppl. J. Phys. Chem. Solids 341 (1967).
[13] Wada, M., Japan J. Appl. Phys. 9, 327 (1970).
[14] Koffeyberg, F. P., J. Solid State Chem. 2, 176 (1970); Canad. J. Phys. 49, 435 (1971).
[15] Finkenrath, H., and von Ortenberg, M., Z. angew. Phys. 23, 323 (1967).
[16] Altwein, M., Finkenrath, H., Konak, C., Stuke, J., and Zimmerer, G., Phys. Stat. Solidi 29, 203 (1968).
[17] Look, D. C., Phys. Rev. 184, 705 (1969).
[18] Benedict, R. P., and Look, D. C., Phys. Rev. B 2, 4949 (1970).
[19] Zvara, M., Kocka, J., Konak, C., and Höschl, P., Phys. Stat. Solidi 42, K5 (1970).
[20] Maschke, K., and Rossler, U., Phys. Stat. Solidi 28, 577 (1968).

III. Oxides of 5*d* Transition Elements

III.1. Lanthanum Oxides

The common oxide of lanthanum is the sesquioxide, La_2O_3 [1]. Warf and Korst [2] have reported the monoxide, LaO, (probably a surface film), but the material has not been prepared in bulk form.

Rare-earth sesquioxides (of which La_2O_3 is the first member) generally exist in the cubic (C), hexagonal (A) or the monoclinic [1, 3] modifications; the C-form is a defect structure of fluorite type where the metal ion has the MO_6V_2 coordination, where V stands for a vacancy along the body diagonal. The A- and B-forms are essentially close-packed structures with MO_7 coordination. All the oxides have the C-type structure at low temperature. The sesquioxides of heavier rare earths (Dy to Lu) as well as Sc_2O_3 and Y_2O_3 retain the C structure even up to very high temperatures (~2300 K); however, sesquioxides from La to Nd revert to the A-type structure depending on the temperature and method of preparation of the sample etc. High-temperature, high-pressure transitions are exhibited by almost all the rare-earth sesquioxides and these have been discussed in detail in the literature [1, 3].

La_2O_3: The usual form of La_2O_3 that is encountered is the hexagonal (A) modification [1, 4]. Detailed studies by Foëx and co-workers [5, 6] indicate that the A-form transforms on heating to another hexagonal form (H) at 2310 K which is followed by an additional transformation at 2380 K to an unidentified structure (X) before melting (at 2573 K); A→H and H→X transformations are reversible. The A⇄H transition does not involve a change in the crystal symmetry, but discontinuities are noted in the *a* and *c* parameters as well as in the *c*/*a* ratio at T_t. The presence of the X-modification is indicated by the appearance of one or two characteristic lines in the x-ray diffraction patterns. The X-form appears to be denser than the H-form, but the detailed structure has not yet been established; preliminary data seem to indicate [7, 8] a cubic structure different from the C modification.

The C-form of La_2O_3 can be prepared by decomposing the precipitated hydroxide under vacuum and slow heating to 670 K [9]. DTA and resistivity studies indicate the C→A transition at ~870 K which is irreversible and apparently sluggish; moisture seems to affect the T_t considerably. According to Foex et al. [5, 6, 10], the A⇄H transition (marked by small thermal effects and lack of hysteresis) is of the displacive type [11] whereas the H⇄X transition (marked by strong thermal effects) belongs to the reconstructive type. During the course of the latter transition, the two corresponding modifications are usually observed to coexist over a remarkably extended range of temperatures; the energy barrier between the corresponding modifications is relatively high. No high pressure transitions are known in La_2O_3. Daire and Willer have recently reported the existence of the B-modification of La_2O_3 [12, 13]; thus, in this oxide it is possible to realize all the different modifications that are generally exhibited by the rare-earth oxides.

The magnetic behavior of La_2O_3 has been examined in the range 290 to 1070 K by Smol'kov and Dobrovol'skaya [14] who found that the substance is diamagnetic. Electrical properties have been examined in detail by various workers in the literature [9, 15–21]. La_2O_3 is a *p*-type semiconductor and shows considerable ionic conductivity at relatively low temperatures (<800 K). Impurities seem to play a significant role in determining the contribution to ionic conductivity [22]; pure electronic conduction exists at high temperatures.

La_2O_3 forms solid solutions with oxides of the type MO (M = Be [23], Mg [24], Ca [20, 25], Pb [26], and Pd [27]); M_2O_3 (M = B [28], Al [29, 30], Cr [29], Fe [29], Ga [29], Pr [31], and Y [29]); MO_2 (M = Ti [29, 32], Zr [29, 32–35], Hf [36], Ce [18, 29], and Sn [29]); M_2O_5 (M = Pa [37]) and MO_3 (M = W [38], and U [39]). The crystal structures and electrical properties of these solid solutions have been examined in detail in the literature with particular reference to ionic conduction.

Oxide and description of the study	Data	Remarks and inferences	References
La_2O_3			
Crystal structure and high temperature x-ray studies.	*C-type*: Cubic; space group, Ia3; $Z=16$; $a=11.39\pm0.03$ Å. C-form is metastable; $C\rightarrow A$ transition at ~870 K; energy of activation ~20 Kcal/mol. *A-type*: Hexagonal; space group, $P\bar{3}m1$; $Z=1$; at $T=293$ K, $a=3.937$ Å; $c=6.13$ Å; at $T=2213$ K, $a=4.028$ Å; $c=6.385$ Å. $A\rightarrow H$ transition at 2310 K. *H-type*: Hexagonal; at 2393 K, $a=4.063$ Å; $c=6.43$ Å. $H\rightarrow X$ transition at (or above) 2380 K. *X-type*: Most probably cubic; detailed structure not known. Melting point ~2570 K. *B-type*: Monoclinic; space group, C2/m; $Z=6$; $a=14.60$ Å; $b=3.717$ Å; $c=9.275$ Å; $\beta=99.77°$.	Depending on the method of preparation of the sample, different types of polymorphs of La_2O_3 can be realized. $C\rightarrow A$ transition is irreversible; $A\rightarrow H$ and $H\rightarrow X$ transitions are reversible but differ in the mechanism of the process.	[1, 4–9, 12, 13].
Magnetic and electrical properties.	Diamagnetic (range 290–1070 K); $\chi=-0.23\times10^{-6}$ emu/g. Semiconductor; ρ (700 K) ~10^5–10^6 Ωcm; E_a (C-form) ~1.1 eV; E_a (A-form) ~1.2 eV. $C\rightarrow A$ transition is shown as a change in the slope of $\ln\rho-1/T$ plot; moisture seems to affect T_t considerably. p-type behavior; $\rho\propto p_{O_2}^{-1/4}$; seems to show p- to n-transition at low p_{O_2} and high temperature. Considerable ionic conductivity at low enough temperatures and probably controlled mostly by impurities.	The magnetic behavior is understandable because there are no $4f$ electrons to contribute to paramagnetism. Electrical data are lacking especially at high temperatures where crystal structure transitions occur. The conductivity behavior of highly pure and single crystalline material is urgently needed to elucidate the detailed mechanism of conduction and the contribution of the ionic conductivity.	[9, 14–21].
Infrared studies.	Bands are noted in the range 280–430 cm^{-1} and are ascribed to the metal-oxygen vibrations.	—	[40].
Heat capacity studies (5–1800 K).	C_p (300 K) $=25.92\pm0.08$ cal/mol, K. There are no anomalies in the measured temperature range.	—	[41].

References

[1] Brauer, G., Progr. in the Science and Technology of Rare Earths Ed. L. Eyring (Pergamon, Oxford) 1, 152 (1964); 2, 312 (1966); 3, 434 (1968).

[2] Warf, J., and Korst, W., U.S. At. Energy Comm. NP–6078, 1956.

[3] Eyring, L., and Holmberg, B., in Non-stoichiometric Compounds (Adv. in Chem. Series) 39, 46 (1963).

[4] Brauer, G., and Siegert, A., Z. anorg. allgem. Chem. 371, 263 (1969).

[5] Foëx, M., Z. anorg. allgem. Chem. 337, 313 (1965).
[6] Foëx, M., and Traverse, J.-P., Bull. Soc. Franc. Mineral Crist. 89, 184 (1966); Compt. Rend. (Paris) 262C, 743 (1966).
[7] Foëx, M., and Pierre, J., Rev. Inst. Hautes Temp. Refract. 3, 429 (1966).
[8] Foëx, M., Sci. Ceram. 4, 217 (1967), Publ. 1968; Chem. Abstr. 70, 60406s (1969).
[9] Mehrotra, P. N., Chandrashekar, G. V., Rao, C. N. R., Subbarao, E. C., Trans. Faraday Soc. 62, 3586 (1966).
[10] Foëx, M., and Traverse, J.-P., Compt. Rend. (Paris) 262C, 636 (1966).
[11] Buerger, M. J., in Phase Transformations in Solids Ed. R. Smoluchowski (John Wiley, New York, 1951).
[12] Daire, M., and Willer, B., Compt. Rend. (Paris) 266C, 548 (1968).
[13] Willer, B., and Daire, M., Bull. Soc. Franc. Mineral Crist. 92, 33 (1969).
[14] Smol'kov, N. A., and Dobrovol'skaya, N. V., Izv. Akad. Nauk SSSR, Neorg. Mater. 1, 1564 (1965).
[15] Foëx, M., Compt. Rend. (Paris) 220, 359 (1945).
[16] Rudolph, J., Z. Naturforsch. 14a, 727 (1959).
[17] Noddack, W., and Walch, H., Z. Elektrochem. 63, 269 (1959); Z. Phys., Chem. (Leipzig) 211, 194 (1959).
[18] Neuimin, A. D., and Pal'guev, S. F., Tr. Inst. Elektrokhim., Akad. Nauk SSSR Ural'sk. Filial 133 (1963).
[19] Pal'guev, S. F., and Vol'chenkova, Z. S., in Electrochemistry of Molten and Solid Electrolytes Ed. A. N. Baraloshkin (Consultants Bureau, New York, 1968), Vol. 6.
[20] Etsell, T. H., and Flengas, S. N., J. Electrochem. Soc. 116, 771 (1969).
[21] Subba Rao, G. V., Ramdas, S., Mehrotra, P. N., and Rao, C. N. R., J. Solid State Chem. 2, 377 (1970).
[22] Etsell, T. H., and Flengas, S. N., Chem. Rev. 70, 339 (1970).
[23] Kuo, C.-K., and Yen, T.-S., Chem. Abstr. 63, 10743e (1965).
[24] Tresvyatskii, S. G., and Lopato, L. M., Vpor. Teorii i Prim. Redkozem. Metal. Akad. Nauk SSSR 155 (1964).
[25] Barry, T. L., Nucl. Sci. Abstr. 20, 36784 (1966).
[26] Cassedanne, J., Anais Acad. Brasil. Cienc. 36, 413 (1964).
[27] McDaniel, C. L., and Schneider, S. J., J. Res. Nat. Bur. Stand. (U.S.), 72A (Phys. and Chem.), No. 1, 27–37 (Jan.–Feb. 1968).
[28] Levin, E. M., Phys. Chem. Glasses 7, 90 (1966).
[29] Andreeva, A. B., and Keler, E. K., Zh. Prikl. Khim. 39, 489 (1966).
[30] Bonder, I. A., and Toropov, N. A., Izv. Akad. Nauk SSSR, Ser. Khim. 212 (1966).
[31] Brauer, G., and Pfeiffer, B., Paper presented in Fifth Rare Earth Conference', Chem. Session C, 1965.
[32] Collongues, M. R., Queyroux, F., Perez, M., Zorba, Y., and Gilles, J.-C., Bull. Soc. Chim. France 4, 1141 (1965).
[33] Lin, T.-H., and Yu, H.-C., Kuei Suan Yen Hsueh Pao 3, 159 (1964).
[34] Fehrenbacher, L. L., Jacobson, L. A., and Lynch, C. T., Proc. Conf. Rare Earth Res., 4th, Phoenix, Arizona, 1964, p. 687 (Publ. 1965).
[35] Strickler, D. W., and Carlson, W. G., J. Am. Ceram. Soc. 48, 286 (1965).
[36] Komissarova, L. N., Wang, K. S., Spitsyn, V. I., and Simanov, Yu. P., Russ. J. Inorg. Chem. (English Transl.) 9, 385 (1964).
[37] Keller, C., J. Inorg. Nucl. Chem. 27, 797 (1965).
[38] Tyushevskaya, G. I., Afonskii, N. S., and Spitsyn, V. I., Dokl. Akad. Nauk. SSSR 170, 859 (1966).
[39] Koshcheev, G. G., and Kovba, L. M., Izv. Akad. Nauk SSSR, Neorg. Mater. 2, 1254 (1966).
[40] Subba Rao, G. V., Rao, C. N. R., and Ferraro, J. R., Appl. Spec. 24, 436 (1970) and references therein.
[41] Holley, C. E., Jr., Huber, E. J., Jr. and Baker, F. B., Progr. in the Science and Technology of Rare Earths, Ed. L. Eyring, (Pergamon, Oxford) 3, 343 (1968) and references therein.

III.2. Hafnium Oxides

Phase studies on the Hf-O system [1–3] have shown that the dioxide, HfO_2, is the only stable oxide. HfO_2 exhibits polymorphism and has been investigated in detail by many workers.

The stable room temperature modification of HfO_2 is monoclinic [4, 5] which transforms to the tetragonal structure reversibly at ~1890 K [6, 7] with appreciable thermal hysteresis [8]. A reversible tetragonal-cubic inversion in HfO_2 has been reported at ~2970 K, which is close to the melting point [7]. Even though the detailed mechanism of the monoclinic-tetragonal transition in HfO_2 is not known, comparison with the analogous transition in ZrO_2 suggests the first order, diffusionless and athermal nature of the transformation in this oxide [5, 6, 8, 9].

A high pressure orthorhombic modification of HfO_2 has been described by Bocquillon et al. [10]; this is obtained by heating the monoclinic HfO_2 at ~1870 K under a minimum pressure of ~15 kbar; this metastable phase reverts to the monoclinic form on prolonged heating at ~570 K.

The tetragonal or cubic modification of HfO_2 cannot be quenched nor can it be stabilized at room temperature [7, 10] and efforts to obtain these forms by precipitating HfO_2 in finely divided form have been unsuccessful [9]. Submicron HfO_2 prepared by the hydrolytic decomposition of alkoxides [9] is amorphous and transforms directly to the monoclinic form at ~600 K. However, the cubic form (and not the tetragonal form) seems to be stabilized in thin films of HfO_2 and recently El-Shanshoury et al. [11] have discussed their polymorphic behavior.

Electrical properties of HfO_2 have been examined in detail by Tallan, Tripp, and Vest [12]. The material is a p-type semiconductor and σ is essentially electronic in the range 1300–1800 K (p_{O_2} from 10^{-18} to 1 atm). At low oxygen partial pressures, a small contribution due to the ionic conductivity has been noticed [12–14]. Measurements on polycrystalline HfO_2 by Tallan et al. [12] did not show a discontinuity in the $\ln\sigma - 1/T$ plot at the monoclinic-tetragonal phase transition.

HfO_2 forms a complete series of solid solutions with ZrO_2 (8, 15–17] and generally, the monoclinic-tetragonal transition temperature is decreased with increasing concentration of ZrO_2. A decrease in T_t is also observed in the solid solutions of HfO_2 with rare-earth sesquioxides [18]. Systems HfO_2-MO (M = Mg [19], Ca [19–22]), and HfO_2–M_2O_3 (M = Sc [23, 24], Y [20, 25–27], La [25, 28], Nd [25, 29], Sm [30], and Gd [31]) have been investigated in the literature.

Oxide and description of the study	Data	Remarks and inferences	References
HfO_2			
Crystal structure and x-ray studies.	$T=298$ K: Monoclinic; space group, $P2_1/c$; $Z=4$; $a=5.1156\pm0.0005$ Å; $b=5.1722\pm0.0005$ Å; $c=5.2948\pm0.0005$ Å; $\beta=99.02\pm0.08$ Å. TEC (470–670 K): [100], 5.9×10^{-6}; [001], 11.9×10^{-6}. TEC slightly increases with temperature up to 1470 K. Monoclinic→tetragonal transition at 1890 K; thermal hysteresis, 30 K. The transition appears to be endothermic associated with a volume contraction, but detailed data are not available. Boganov et al. [7] report the T_t to be ~2170–2270 K for this transition. At 2770 K, $a=5.21$ Å, $c=5.35$ Å; this tetragonal phase is stable up to ~2970 K and then transforms to cubic fcc modification with $a=5.300$ Å. The tetragonal-cubic inversion is reversible; however detailed data are lacking. *High*-pressure form: obtained by heating at 1870 K under 60 kbar pressure and quenching; orthorhombic; $a=5.008\pm0.006$ Å; $b=5.062\pm0.006$ Å; $c=5.223\pm0.006$ Å. This metastable phase reverts to the monoclinic form on prolonged heating at 570 K. Amorphous HfO_2 obtained by the thermal decomposition of the metal alkoxide goes to the monoclinic variety on heating at ~600 K; the intermediate cubic and tetragonal forms are not realizable, neither they can be quenched to room temperature from the respective temperature ranges of existence. Melting point of HfO_2 is 3070 K.	In many respects, HfO_2 resembles ZrO_2 *even though* there are subtle differences in behavior. The sequence (and the mechanism)of the transformations from the low symmetry to the high symmetry in the crystal structure are the same in HfO_2 and ZrO_2 except that the T_t for HfO_2 are higher and the thermal hysteresis values are lower. The high temperature modifications of HfO_2 cannot be quenched nor can they be stabilized at room temperature by solid solution formation.	[4–8, 10, 32].
Electrical properties.	*p*-type semiconductor in the range 1270–1770 K; σ (1570 K)~10^{-3} Ω^{-1} cm^{-1}; E_a is 0.7 eV (<1570 K) and 0.2 eV (>1570 K); $\sigma\propto p_{O_2}{}^{1/6}$ ($p_{O_2}>10^{-6}$ atm); $\mu_D=0.3$–1.6×10^{-3} cm^2/V s. At low p_{O_2} ($<10^{-8}$ atm) small contribution due to ionic conductivity seems to be present. The defect structure is interpreted in terms of holes and fully ionized cation vacancies.	The electrical behavior is as expected and similar to ZrO_2 which also behaves as an extrinsic *p*-type semiconductor. Apparently, no discontinuity in the $\ln\sigma-1/T$ plot has been noticed at the monoclinic-tetragonal transition in HfO_2.	[12].

References

[1] Rudy, E., and Stecher, P., J. Less-Comm. Metals 5, 78 (1963).
[2] Domagala, R. F., and Ruh, R., Trans. Am. Soc. Met. 58, 164 (1965).
[3] Karnilov, I. I., Glazova, V. V., and Ruda, I. G., Izv. Akad. Nauk SSSR, Neorg. Mater. 4, 2106 (1968).
[4] Adam, J., and Rogers, M. D., Acta Cryst. 12, 951 (1959).
[5] Ruh, R., and Corfield, P. W. R., J. Am. Ceram. Soc. 53, 126 (1970).
[6] Wolten, G. M., J. Am. Ceram. Soc. 46, 418 (1963).
[7] Boganov, A. G., Rudenko, V. S., and Makarov, L. P., Dokl. Akad. Nauk SSSR 160, 1065 (1965).
[8] Ruh, R., Garret, H. J., Domagala, R. F., and Tallan, N. M., J. Am. Ceram. Soc. 51, 23 (1968).
[9] Mazdiyasni, K. S., and Brown, L. M., J. Am. Ceram. Soc. 53, 43 (1970).
[10] Bocquillon, G., Susse, C., and Vodar, B., Rev. Int. Hautes, Temp. Refract. 5, 247 (1968).
[11] El-Shanshoury, I. A., Rudenko, V. A., and Ibrahim, I. A., J. Am. Ceram. Soc. 53, 264 (1970).
[12] Tallan, N. M., Tripp, W. C., and Vest, R. W., J. Am. Ceram. Soc. 50, 279 (1967).
[13] Robert, G., Deportes, C., and Besson, J., J. Chim. Phys. 64, 1275 (1967).
[14] Etsell, T. H., and Flengas, S. N., Chem. Rev. 70, 339 (1970).
[15] Mazdiyasni, K. S., Lynch, C. T., and Smith, J. S., J. Am. Ceram. Soc. 48, 372 (1965).
[16] Stansfield, O. M., J. Am. Ceram. Soc. 48, 436 (1965).
[17] Gavrish, A. M., Sukharevskii, B. Ya., Krivornchko, P. P., and Zoz, E. I., Ivz. Akad. Nauk SSSR, Neorg. Mater. 5, 547 (1969).
[18] Koehler, E. K., and Glushkova, V. B., Sci. Ceramics 4, 233 (1967, publ. 1968).
[19] Strekalovskii, V. N., Volchenkova, Z. S., and Pal'guev, S. F., Izv. Akad. Nauk SSSR, Neorg. Mater. 2, 1230 (1966).
[20] Volchenkova, Z. S., and Pal'guev, S. F., Trans. Inst. Elektrokhim Akad. Nauk SSSR, Ural. Filial 5, 133 (1964).
[21] Johansen, H. A., and Cleary, J. G., J. Electrochem. Soc. 111, 100 (1964).
[22] Delamarre, C., Silicates Ind. 32, 345 (1967).
[23] Komissarova, L. N., and Spiridinov, F. M., Dokl. Akad. Nauk SSSR 182, 334 (1968).
[24] Kalinovskaya, C. A., Spiridinov, F. M., and Komissarova, L. N., J. Less-Comm. Metals 17, 151 (1969).
[25] Komissarova, L. N., Wang, C. S., and Spitsyn, V. I., Izv. Akad. Nauk SSSR, Ser. Khim. 1, 3 (1965).
[26] Besson, J., Deportes, C., and Robert, C., Compt. Rend. (Paris) 262, 527 (1966).
[27] Duclot, M., Vicat, J., and Deportes, C., J. Solid State Chem. 2, 236 (1970).
[28] Komissarova, L. N., Wang, C. S., Spitsyn, V. I., and Simanov, Yu. P., Russ. J. Inorg. Chem. 9, 385 (1964).
[29] Komissarova, L. N., Spitsyn, V. I., and Wang, C. S., Dokl. Akad. Nauk SSSR 150, 816 (1963).
[30] Isupova, E. N., Glushkova, V. B., and Keler, E. V., Izv. Akad. Nauk SSSR, Neorg. Mater. 4, 399 (1968).
[31] Spiridinov, F. M., Stepanov, J. A., Komissarova, L. N., and Spitsyn, V. I., J. Less-Comm. Metals 14, 435 (1968).
[32] Filatov, S. K., and Frank-Kamenetskii, V. A., Sov. Phys.-Crystallogr. (English Transl.) 14, 696 (1970).

III.3. Tantalum Oxides

The Ta-O system has been investigated by many workers [1–7] and the stability and phase relationships of the various oxides have been reviewed and discussed by Steeb and Renner [8], Niebuhr [9], and Chang and Phillips [10]. In addition to the suboxides, TaO_x (Ta_6O), TaO_y (Ta_4O) and TaO_z (Ta_2O), the monoxide TaO (whose existence is not proved beyond doubt), dioxide, TaO_2 and the pentoxide, Ta_2O_5 are known; however, Ta_2O_5 is the only oxide which is well-characterized and extensively investigated in recent years.

Suboxides: The suboxides form only by the oxidation of tantalum metal or tantalum compounds. Ta_6O (tetragonal) forms at ~570 K; Ta_4O (orthorhombic) forms below 770 K and Ta_2O (tetragonal) forms between 620 to 1470 K. A complex suboxide of unknown structure is formed above 1770 K. Electron diffraction studies of monocrystalline samples above 1770 K. Electron diffraction studies of monocrystalline samples reveal superlattices [8, 9]. These suboxides appear to be metallic, but detailed data are lacking.

Monoxide, TaO: Lagergren and Magnéli [1] and Schönberg [3] reported the existence of tantalum monoxide with a narrow homogeneity range; it has a cubic rock salt structure with a variable lattice parameter. Physical properties are not known. The existence of this monoxide has not been proved beyond doubt and systematic investigations are called for.

TaO_2: Rutile type TaO_2 is known to be a stable oxide [1, 3, 11], but detailed data on the physical properties are lacking. TaO_2 appears to form solid solutions with TiO_2 [3, 12], although there are changes in the cation valencies.

Ta_2O_5: Tantalum pentoxide, Ta_2O_5, is a stable oxide with a very narrow homogeneity range [13] and has been well-investigated by various workers. The exact relationships of the various polymorphs of Ta_2O_5 are not clearly understood because of the complexity of the structures of the phases, sluggish nature of the transitions and the existence of various metastable phases that can be stabilized by impurities.

It is fairly well established that Ta_2O_5 exists in two polymorphic forms, β and α, with a reversible phase transition at ~1630 K [1, 14]; the transition between them is sluggish and the low temperature β form can persist as a metastable phase in the stability field of the α form and can be melted at ~2060 K. The high temperature (α) form melts at ~2160 K [14, 15].

The proper method of indexing the powder pattern

of the β form has puzzled crystallographers for a long time; the more intense diffraction lines can be indexed on the basis of a simple orthorhombic subcell with $a=6.20$, $b=3.66$, and $c=3.89$ Å. However, numerous weak lines which also appear in the pattern have not been interpreted unambiguously mainly because the position of these super-structure lines is strongly dependent upon both the nature of the heat treatment and the amount of impurities [16, 17]. Consequently, different workers have suggested different lattice parameters and symmetries to explain the x-ray pattern of the β form of Ta_2O_5 [7, 18–25]. Systematic examination of the polymorphic behavior of Ta_2O_5 by Roth and co-workers [15, 16, 26–28] has contributed significantly to the understanding of the structure of the low-temperature phase. These workers found that many metallic oxides, especially WO_3, can stabilize the β-form and that this pure phase exists in two slightly different modifications with b-axis multiplicities of 11 and 14 at low temperatures and at ~1580 K respectively. At intermediate temperatures, an infinite number of at least partially ordered sequences of these two modifications exist in equilibrium. The addition of WO_3 (or other impurities) causes the stabilization of an infinite number of phases similar in structure to the low-temperature form of Ta_2O_5.

The structure of the high-temperature (α) form of Ta_2O_5 has been a subject of intensive study and and tetragonal, hexagonal, orthorhombic, monoclinic, and triclinic symmetries have been suggested by various workers [1, 14, 20, 22, 29]. Detailed studies have, however, indicated [15, 29] that the α form actually undergoes several unquenchable phase transitions upon cooling from high temperatures. The true high-temperature form is postulated to be tetragonal in its field of stability and several metastable phases occur in the stability field of the low-temperature polymorph. Ta_2O_5 when quenched from above 1630 K (T_t) is triclinic and transforms to a monoclinic form on heating to ~590 K and this in turn reverts to the tetragonal form at ~1220 K. Sarjeant and Roy [30] reported a metastable high-temperature hexagonal form of Ta_2O_5 obtainable by rapid quenching techniques; this δ form reverts to the β form on annealing at ~1470 K. Impurities like titanium lower the T_t of the $\beta \rightarrow \alpha$ transition and Sc^{3+} in low concentrations appears to stabilize the high-temperature tetragonal phase [16, 28]; the crystal structure consists of α-UO_3-type blocks in which Ta atom is surrounded by a pentagonal bipyramid of oxygen atoms. These blocks are infinite in two directions and are separated from similar blocks along a third direction by shear planes and in the vicinity of these shear planes, the Ta atoms are surrounded by distorted octahedral coordination polyhedra.

Semiconducting behavior of Ta_2O_5 has been examined by Kofstad [13] who finds that the material is p- or n-type depending on the p_{O2}. Differences in the dielectric behavior of the polymorphs of Ta_2O_5 have been reported by Pavlovic [31]. Systems K_2O-Ta_2O_5 [32] and Nb_2O_5-Ta_2O_5 [33, 34] have been investigated in the literature.

Tantalum oxides

Oxide and description of the study	Data	Remarks and inferences	References
Suboxides			
Crystal structure.	Ta_6O: Tetragonal; $a=3.36$ Å; $c=3.25$ Å. Ta_4O: Orthorhombic; $a=3.61$ Å; $b=3.27$ Å; $c=3.20$ Å. Ta_2O: Tetragonal; $a=6.63$ Å; $c=4.75$ Å. Detailed data on the physical properties are lacking.	These oxides are formed from Ta by the oxidation at various temperatures; some reveal superstructure in electron diffraction patterns.	[1, 2, 3, 5, 9, 10].
TaO			
Crystal structure.	Cubic; space group, Fm3m; $Z=4$; $a=4.422$–4.429 Å. Formed in the range 870–1770 K; physical properties not known in detail.	—	[1, 3].

Oxide and description of the study	Data	Remarks and inferences	References
TaO_2			
Crystal structure.	Tetragonal; space group, $P4_2/mnm$; $Z=2$; $a=4.709$ Å; $c=3.065$ Å. Physical properties are not known in detail.	—	[1, 3].
Ta_2O_5			
Crystal structures and x-ray studies.	Low-temperature (β) form: Subcell: orthorhombic; $Z=1$; $a=6.20$ Å; $b=3.66$ Å; $c=3.89$ Å. True-cell: orthorhombic; $Z=11$; $a=6.198$ Å; $b=40.29$ Å; $c=3.888$ Å; b-axis multiplicity = 11. β-form at a given temperature consists of an infinite number of partially ordered sequences of two simple modifications with multiplicities 11 and 14 and these sequences are affected both by heat treatments and by impurities thus explaining considerable ambiguity encountered by various workers in the interpretation of the powder patterns. $T_t \sim 1630$ K; sluggish but completely reversible transition. High-temperature (α) form: tetragonal; space group; $I4_1/amd$; $Z=6$; $a=3.81$ Å; $c=36.09$ Å. This phase is unquenchable in pure Ta_2O_5; however, Sc^{3+} appears to stabilize this form. The structure consists of α-UO_3 type blocks in two directions and separated in the third direction by shear planes. Sc^{3+} doping seems to introduce random shear planes (Wadsley defects) which stabilize the structure. Ta_2O_5 quenched from temperatures above T_t is triclinic: $a=3.801$ Å; $b=3.785$ Å; $c=35.74$ Å; $\alpha=90.91°$; $\beta=90.19°$; $\gamma \simeq 90°$. This triclinic phase transforms to monoclinic phase on heating to ~ 590 K; $a_{mono} = \sqrt{2}\, a_{tric}$; $b_{mono} = \sqrt{2}\, b_{tric}$; $c_{mono} \approx c_{tric}$. Monoclinic phase reverts to the tetragonal phase on heating to ~ 1220 K. Rapid quenching of Ta_2O_5 from high temperatures appears to produce a hexagonal modification; $a=3.874$ Å; $c=$	Systematic examination of the detailed phase relationships by Roth and coworkers has revealed a proper understanding of the structures of Ta_2O_5 modifications and cleared the ambiguities of the earlier workers.	[15, 16, 26–28].

Oxide and description of the study	Data	Remarks and inferences	References
	3.62 Å. This δ form reverts to the β form on annealing at ~1470 K. Melting point≃2160±20 K.		
Electrical properties.	Semiconductor in the range 1000–1670 K. σ (1000 K)~10^{-5} Ω^{-1} cm^{-1}; E_a=1.79 eV; α (1300 K; p_{O_2}~1 atm)~1 mV/K. p-type behaviour at p_{O_2}~1 atm and n-type at lower p_{O_2}. p to n transition takes place at lower p_{O_2} with decreasing T.	The defect structure is interpreted in terms of oxygen interstitials (p-type) and oxygen vacancies (n-type). No change in the slope of $\ln\sigma$-$1/T$ plot noticed at T_t; the reason is not clearly understood.	[13].
Infrared spectra.	Bands are noted at 720 and 860 cm^{-1} for α-Ta_2O_5 and interpreted in terms of the metal-oxygen vibrations.	—	[34].

References

[1] Lagergren, S., and Magnéli, A., Acta Chem. Scand. 6, 444 (1952).
[2] Wasilewski, R. J., J. Am. Chem. Soc. 75, 1001 (1953).
[3] Schönberg, N., Acta Chem. Scand. 8, 240 (1954).
[4] Pawel, R. E., Cathcart, J. V., and Campbell, J. J., Acta Met. 10, 149 (1962).
[5] Norman, N., J. Less-Comm. Metals 4, 52 (1962).
[6] Kofstad, P., J. Inst. Metals 90, 253 (1962); 91, 209 (1963).
[7] Terao, N., Japan J. Appl. Phys. 6, 21 (1967).
[8] Steeb, S., and Renner, J., J. Less-Comm. Metals 10, 246 (1966).
[9] Niebuhr, J., J. Less-Comm. Metals 10, 312 (1966).
[10] Chang, L. L. Y., and Phillips, B., J. Am. Ceram. Soc. 52, 527 (1969).
[11] Rogers, D. B., Shannon, R. D., Sleight, A. W., and Gillson, J. L., Inorg. Chem. 8, 841 (1969).
[12] Rüdorff, W., and Luginsland, H. H., Z. anorg. allgem. Chem. 334, 125 (1964).
[13] Kofstad, P., J. Electrochem. Soc. 109, 776 (1962).
[14] Reisman, A., Holtzberg, F., Berkenblit, M., and Berry, M., J. Am. Chem. Soc. 78, 4514 (1956).
[15] Waring, J. L., and Roth, R. S., J. Res. Nat. Bur. Stand. (U.S.), 72A (Phys. and Chem.) No. 2, 175–186 (Mar.–Apr. 1968).
[16] Roth, R. S., Waring, J. L., and Brower, W. S., Jr., J. Res. Nat. Bur. Stand. (U.S.), 74A (Phys. and Chem.), No. 4, 485–493 (July–Aug. 1970).
[17] Jahnberg, J., and Andersson, S., Acta Chem. Scand. 21, 615 (1967).
[18] Frevel, L., and Rim, H., Anal. Chem. 27, 1329 (1955).
[19] Simanov, Yu. P., Lapitskii, A. V., and Artamanova, E. P., Vetn. Mosk. Univ. 9, Ser. Fiz. Mat. i Estestven Nauk (6), 109 (1954).
[20] Zaslavskii, A. I., Zvinshuk, R. A., and Tutov, A. G., Dokl. Akad. Nauk SSSR 104, 409 (1955).
[21] Lapitskii, A. V., Simanov, Yu. P., Semenen, K. N., and Yarembash, E. I., Vetn. Mosk. Univ. 9, Ser. Fiz. Mat. i Estestven Nauk, (2), 85 (1959).
[22] Harvey, J., and Wilman, H., Acta Cryst. 14, 1278 (1961).
[23] Lehovec, K., J. Less-Comm. Metals 7, 397 (1964).
[24] Turnock, A. C., J. Am. Ceram. Soc. 48, 258 (1965); 49, 382 (1966).
[25] Wolten, G. M., and Chase, A. B., Z. Krist. 129, 365 (1969).
[26] Roth, R. S., and Stephenson, N. C., in The Chemistry of Extended Defects in non-Metallic Solids, Eds. L. Eyring and M. O'Keeffe, (North Holland Publ. Co., Amsterdam, 1970).
[27] Roth, R. S., Waring, J. L., and Parker, H. S., J. Solid State Chem. 2, 445 (1970).
[28] Stephenson, N. C., and Roth, R. S., J. Solid State Chem. 3, 145 (1971).
[29] Laves, F., and Petter, W., Helv. Phys. Acta 37, 617 (1964).
[30] Sarjeant, P. T., and Roy, R., J. Am. Ceram. Soc. 50, 500 (1967).
[31] Pavlovic, A. S., J. Chem. Phys. 40, 951 (1964).
[32] Holtzberg, F., and Reisman, A., J. Phys. Chem. 65, 1192 (1961).
[33] Mohanty, G. P., Fiegel, L. J., and Healy, J. H., J. Phys. Chem. 68, 208 (1964).
[34] Alyamovskii, S. I., Shveikin, G. P., and Gel'd, P. V., Russ. J. Inorg. Chem. 12, 915 (1967).

III.4. Tungsten Oxides

Tungsten dioxide and trioxide are the well-known oxides in the W-O system [1–3]. Two mixed valence phases, $W_{18}O_{49}$ ($WO_{2.72}$) and $W_{20}O_{58}$ ($WO_{2.90}$) also exist [1, 4–7] in the range WO_2-WO_3 and substoichiometric phases of WO_3, viz., $WO_{2.96}$ ($W_{50}O_{148}$) and $WO_{2.98}$ ($W_{40}O_{119}$) have been characterized in the literature [8]. Even though earlier workers [9, 10] have claimed the existence of an oxide W_3O, recent studies [7, 11] indicate that the oxide is not a stable phase.

WO_2: The range of homogeneity of WO_2 appears to be small (1.94–2.025) [12] and the material is stable up to 1800 K after which it decomposes. It has a monoclinic structure [2, 5, 13, 14] and exhibits metallic behavior [13]; no phase transitions are known in WO_2.

WO_2 forms solid solutions with TiO_2 [15] and VO_2 [14, 16] giving rise to rutile based structures

$W_{18}O_{49}$: This oxide is monoclinic [4, 5] and is stable above 860 K; below this temperature, it decomposes to WO_2 and $W_{20}O_{58}$. $W_{18}O_{49}$ is the most refractory oxide (stable up to 1970 K) of the W-O system [7]. Physical properties of this oxide are not known.

$W_{20}O_{58}$: This monoclinic oxide seems to have a narrow range of homogeneity [4, 5, 17, 18] and decomposes below 760 K to WO_2 and WO_3 [7]. Measurements of resistivity and Seebeck coefficient indicate metallic behavior [18].

Substoichiometric phases: $W_{50}O_{148}$ and $W_{40}O_{119}$ are monoclinic and according to Gebert and Ackerman [8], a high-temperature polymorph of $W_{50}O_{148}$ exists. Detailed data are lacking.

WO_3: Tungsten trioxide is a stable phase and is usually associated with slight nonstoichiometry [1, 7, 18]; it is polymorphic and not less than five distinct crystallographic modifications are known (fig. III.1). The phase transitions among the various forms of WO_3 have been examined using a variety of techniques.

At room temperature, WO_3 is monoclinic [1, 5, 7, 12, 19–22] and this phase is stable in the range 290 to 583 K [23]. On cooling to 290 K, the room temperature polymorph transforms to a triclinic form; this reversible change is associated with some thermal hysteresis (3–13° depending on the sample), ΔH and ΔS and discontinuities in ρ, α, R_H, and μ_H [18, 23–25]. Roth and Waring [26] noted that the monoclinic WO_3 can be partially transformed to the triclinic phase by grinding. The latter phase is stable in the range 233 to 290 K. On cooling to 233 K, the triclinic phase of pure WO_3 changes to a monoclinic phase with observable temperature hysteresis, TEC, ΔH and ΔS changes, discontinuities in ρ, α, R_H, and μ_H [18, 23–25, 27–29] and changes in the domain structure [29]. This monoclinic form seems to be stable in the range 77 to 233 K and has been found to be ferroelectric [28, 30, 31]. Roth and Waring [26] obtained this phase at room temperature by quenching a soid solution of 2 percent Nb_2O_5 in WO_3 from 1500 to 1660 K; however, this solid solution does not exhibit ferroelectricity whereas specimens of sintered WO_3 containing 2–4 percent Ta_2O_5 have been reported to be ferroelectric at room temperature [32]. Nonstoichiometry in WO_3, by way of removal of oxygen from the lattice, apparently decreases the T_t of the two low-temperature transitions and brings about changes in the electrical properties [18].

The room-temperature monoclinic modification of WO_3 transforms to an orthorhombic structure reversibly at ~580 K [24, 33–37]; DTA peak [31] and resistivity discontinuity have been noted at this temperature [24]. Roth and Waring [26] obtained the orthorhombic form at room temperature on heating the stabilized monoclinic WO_3 (containing 2% Nb_2O_5) to ~1170 K and rapid cooling. The orthorhombic→tetragonal transition in WO_3 is well established and investigated by many workers [26, 33, 34, 36, 38–41]; x-ray diffraction, DTA and resistivity measurements indicate the T_t to be 1010 K (accompanied by thermal hysteresis). The tetragonal phase is related to the ReO_3 structure and doping with Nb lowers the T_t considerably [26]; according to Roth and Waring [26], the (Nb) stabilized monoclinic phase of WO_3 transforms to the tetragonal modification (without going through the triclinic, monoclinic and orthorhombic structures as in the case of pure WO_3) at ~1010 K and this monoclinic→tetragonal transition has been found to be reversible below 1025 K.

DTA [35, 38], heat capacity and resistivity [39] studies indicate transitions at ~1170 and ~1500 K in pure WO_3, but no structural changes have been observed (fig. III.1) [26, 35, 38]; the high temperature phases remain tetragonal. A transformation from tetragonal to cubic structure of the ideal ReO_3 type (which seems quite logical) has not been observed in pure WO_3 below the melting point (1700 K). Attempts to prepare the cubic phase by doping have not been successful.

WO_3 is diamagnetic [18, 42] in the range 77 to 292

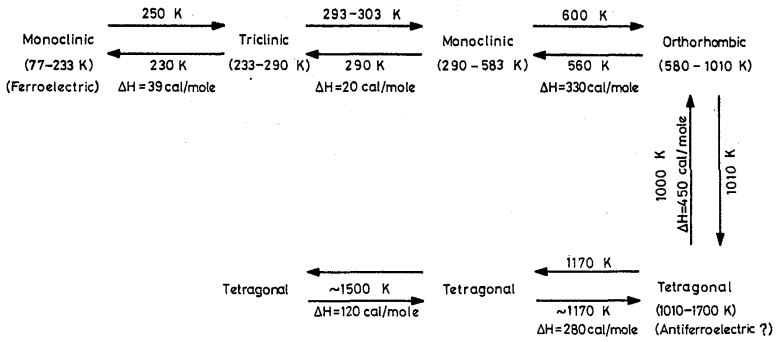

FIGURE III.1. *Phase relations in* WO_3.

K; feeable paramagnetism has been noted at ~1.3 K in the oxygen deficient WO_3 [18]. It is semiconducting at low temperatures, but exhibits semimetallic behavior at higher temperatures. As mentioned earlier, electrical characteristics show anomalous behavior at the transition points. The mechanism of electrical conduction in stoichiometric and oxygen deficient WO_3 has been investigated in detail by Sienko and co-workers [18, 24, 25].

WO_3 in combination with other metal oxides form very interesting mixed oxides called 'tungsten bronzes.' The physical properties of these bronzes have been examined in great detail and discussed in the literature [43–46].

Tungsten oxides

Oxide and description of the study	Data	Remarks and inferences	References
WO_2			
Crystal structure and electrical properties.	Monoclinic; space group, $P2_1/c$; $Z=4$; $a=5.5607\pm0.0005$ Å; $b=4.9006\pm0.0005$ Å; $c=5.6631\pm0.0005$ Å; $\beta=120.44°$. Metallic behavior; ρ (4.2 K) $=2.0\times10^{-4}$ Ωcm; ρ (300 K) $=2.9\times10^{-3}$ Ωcm.	The structure is that of a distorted rutile; metal-metal bonding seems to exist and the electrical properties are consistent with this assumption.	[2, 5, 13, 14].
$W_{18}O_{49}$			
Crystal structure.	Monoclinic; $a=18.28$ Å; $b=3.775$ Å; $c=13.98$ Å; $\beta=115.14°$. Decomposes below 860 K but stable up to 1970 K. Detailed data are lacking.	—	[4, 5, 7].
$W_{20}O_{58}$			
Crystal structure and electrical properties.	Monoclinic; $a=16.74$ Å; $b=4.019$ Å; $c=14.53$ Å; $\beta=95.45°$. Decomposes below 760 K but stable up to 1820 K. Metallic behavior; ρ (80 K) ~ 5×10^{-4} Ωcm; ρ-T plot exhibits a maximum at 270 K. α (90 K) ~ −15 μV/°C; α (240–320 K) ~ −30 μV/°C. $n\approx4\times10^{21}$/cm³.	The structure appears to be related to WO_2 and metal-metal bonding seems to be present. ρ anomaly at ~270 K is not explainable at present.	[4, 5, 7, 17, 18].

Tungsten oxides—Continued

Oxide and description of the study	Data	Remarks and inferences	References
$W_{50}O_{148}$ ($WO_{2.96}$)			
Crystal structure	Monoclinic; space group, P2/c; $a=11.90\pm0.02$ Å; $b=3.826\pm0.012$ Å; $c=59.64\pm0.06$ Å; $\beta=98.4°$. A high-temperature polymorph with a unit cell having the formula $W_{25}O_{74}$ is found to be stable at ~1520 K. Detailed data are lacking.	The structure appears to be related to that of WO_3.	[8].
$W_{40}O_{119}$ ($WO_{2.98}$)			
Crystal structure	Monoclinic; space group, $P2_1/m$; $Z=4$; $a=7.354\pm0.005$ Å; $b=7.569\pm0.005$ Å; $c=3.854\pm0.005$ Å; $\beta=90.6°$. Detailed properties not known.	—	[8].
WO_3			
Crystal structure and x-ray studies.	Range 77–233 K: Monoclinic; $a=5.27$ Å; $b=5.16$ Å; $c=7.67$ Å; $\beta=91.72°$. This phase can be stabilized at room temperature by quenching a solid solution of 2% Nb_2O_5 in WO_3 from 1500–1660 K. Monoclinic to triclinic transition at 251 K (heating); hysteresis ~15°. The stabilized solid solution transforms to a tetragonal form at ~1010 K; transition reversible if the sample is heated below 1015 K and if heated to ~1170 K, tetragonal phase transforms irreversibly to an orthorhombic modification. Range 233–290 K: Triclinic; $a=7.30$ Å; $b=7.52$ Å; $c=7.69$ Å; $\alpha=88.83°$; $\beta=90.92°$; $\gamma=90.93°$. Triclinic phase not encountered in the solid solutions of WO_3 with Nb_2O_5 at any temperature. Triclinic to monoclinic transition at ~293–303 K (heating); hysteresis, ~3–13°. Reverse transition (mono.→tric.) noted on grinding the specimen at room temperature. Removal of oxygen from the lattice of pure WO_3 reduces the T_t of the two low-temperature transitions. Range 290–583 K: Monoclinic; space group, $P2_1/n$; $Z=8$; $a=7.306\pm0.001$ Å; $b=7.540\pm0.001$ Å; $c=7.692\pm0.001$ Å;	WO_3 is the only oxide which shows a wide variety of crystallographic transitions in the easily attainable ranges of temperatures; many of the transitions are of first order. Surprisingly, the tetragonal→cubic transition has not been noticed either in the pure or doped or nonstoichiometric samples; neither it has been possible to stabilize the cubic phase at any temperature. The effect of nonstoichiometry is pronounced in the case of low-temperature transitions. Data is lacking for the high-temperature transitions and also the effect of pressure on the transitions.	[1, 5, 7, 12, 19–22, 26, 27–29, 33–41].

Oxide and description of the study	Data	Remarks and inferences	References
	$\beta = 90.881 \perp 0.005°$. Solid solution with Nb_2O_5 retains the monoclinic structure but slightly changes the lattice parameters. Monoclinic to orthorhombic transition at ~600 K (heating); thermal hysteresis ~40–50°. Range 580–1010 K: Orthorhombic; the lattice parameters remain the same as in the monoclinic phase (except for the effect of thermal expansion) and β approaches 90° at $\approx T_t$. According to Rosen et al. [35], the b parameter shows an anomaly at T_t in WO_3. The orthorhombic form can be stabilized at room temperature by heating the 2% Nb_2O_5 solid solution to 1170 K and rapid cooling. Orthorhombic to tetragonal transition at ~1010 K; hysteresis ~10°. The solid solution (of 2% Nb_2O_5) transforms to tetragonal form at a lower temperature. Range 1010–1700 K: Tetragonal; space group, P4/nmm; $Z=2$; $a=5.25$ Å; $c=3.91$ Å. A transition takes place at ~1170 K in WO_3 but x-ray studies do not indicate any change in the crystal symmetry. Roth and Waring [26] point out that it is possible that the tetragonal unit cell has a doubled c axis below 1170 K and only above this temperature does the powder pattern yields the correct unit cell. Melting point of WO_3 is 1700 K and it melts under its own equilibrium oxygen partial pressure [12, 41, 47].		
Magnetic properties.	Diamagnetic in the range 77–300 K; χ_M (=300 K) = $-21.0 \pm 1.7 \times 10^{-6}$. Below 77 K, oxygen deficient WO_3 shows decrease in χ_M eventually switching to a feeble paramagnetism ($\chi_M = 10 \times 10^{-6}$ cgs u.) at 1.28 Å.	Both stoichiometric and nonstoichiometric samples exhibit similar magnetic behavior.	[18, 42].

Tungsten oxides—Continued

Oxide and description of the study	Data	Remarks and inferences	References
Electrical properties.	Semiconductor behavior; ρ (200 K) $\sim 10^3$ Ωcm; ρ (400 K) ~ 5 Ωcm; α (300 K) ~ -0.5 mV/°C; μ_H (400 K) ~ 10 cm²/V s. Discontinuities in ρ, α and μ_H are encountered near the transition temperatures of the various phases encountered with the associated hysteresis. In the range 400–900 K, ρ is very small ($\sim$0.1–0.5 Ωcm) and shows slight increase with rise in temperature (quasi-metallic behavior). Sawada [31] has reported a resistivity anomaly at $\sim$1500 K in WO_3; this may correspond to a change in the mechanism of conduction or to a new modification. Details are not known. The mechanism of electrical conduction in the range 100–500 K is interpreted in terms of various polaron theories.	The electrical properties show complex behavior; the actual values of ρ, α and μ_H vary from sample to sample and depend on the method of preparation, stoichiometry etc. However, the qualitative features are reproducible and ρ-T behavior provides a good tool for indicating the phase transitions. Electrical data on the doped WO_3 (where various high- and low-temperature phases have been stabilized) are lacking.	[18, 23–25, 31, 48].
Optical and dielectric properties.	Absorption edge is at 2.7 eV. Removal of oxygen from the lattice causes an increase in absorption at all wave lengths. Absorption edge shows an anomalous shift at the $\sim$250 K transition. In the range 270–970 K, absorption edge shows a red shift ($\sim 10^{-4}$ eV/K); near 1010 K transition, a sudden red shift is noted for a polarized light. The static dielectric constant at room temperature is $\sim 10^3$–10^4 (at 1 MHz) and decreases to $\sim 10^2$ [50] at $\sim$250 K. According to Matthias and Wood [28, 30], the low-temperature monoclinic phase (in the range 77–233 K) is ferroelectric. On the basis of structural studies, Kehl et al. [38] concluded that the high-temperature tetragonal may be antiferroelectric. Levine et al. [32] reported that WO_3 containing 2–4% Ta_2O_5 exhibits ferroelectricity at room temperature whereas Roth and Waring [26] do not find this behavior in the 2% Nb_2O_5 doped sample.	Accurate dielectric constant data and the study of ferroelectric and antiferroelectric properties could not be carried out because of the high conductivity effects in pure WO_3.	[18, 28, 30, 38, 49, 50].

Oxide and description of the study	Data	Remarks and inferences	References
DTA studies.	All the crystallographic transitions are associated with DTA anomalies; in addition, transitions are also indicated at ~1170 and ~1500 K (fig. III.1). Hysteresis is noted in all cases. ΔH (cal/mol): Monocl. (low-temperature) →triclinic, 39; tricl.→monocl., 20; monocl.→orthorh., 330; orthorh. →tetra., 450; tetra.→tetra., 280; 1500 K transition, 120. Removal of oxygen from the lattice decreases T_t as well as the ΔH of the two low-temperature transitions. Data are not available for other transitions.	The nature of the high-temperature transitions is not known in detail; the transitions seem to be first order.	[18, 31].

References

[1] Hägg, G., and Magnéli, A., Arkiv Kemi Mineral. Geol. 19A, No. 2 (1944).
[2] Magnéli, A., Arkiv Kemi Mineral. Geol. 24A, No. 2 (1946).
[3] H., Braekken, Z. Krist. 78, 484 (1931).
[4] Magnéli, A., Arkiv Kemi 1, 223 (1949); 1, 513 (1950).
[5] Magnéli, A., Andersson, G., Blomberg, B., and Kihlborg, L., Anal. Chem. 24, 1998 (1952).
[6] Glemser, O., and Sauer, H., Z. anorg. allgem. Chem. 252, 144 (1943).
[7] Phillips, B., and Chang, L. L. Y., Trans. AIME 230, 1203 (1964).
[8] Gebart, E., and Ackermann, R. J., Inorg. Chem. 5, 136 (1966).
[9] Neuberger, M. C., Z. Krist. 85, 232 (1933).
[10] Hägg, G., and Schönberg, N., Acta Cryst. 7, 351 (1954).
[11] St. Pierre, G. R., Ebihara, W. T., Pool, M. J., and Speiser, R., Trans. AIME 224, 259 (1962).
[12] Chang, L. L. Y., and Phillips, B., J. Am. Ceram. Soc. 52, 527 (1969).
[13] Rogers, D. B., Shannon, R. D., Sleight, A. W., and Gillson, J. L., Inorg. Chem. 8, 841 (1969).
[14] Israelsson, M., and Kihlborg, L., Mat. Res. Bull. 5, 19 (1970).
[15] Chang, L. L. Y., Scroger, M. G., and Phillips, B., J. Less-Comm. Metals 12, 51 (1967).
[16] Nygren, M., and Israelsson, M., Mat. Res. Bull. 4, 881 (1969).
[17] Magnéli, A., Nature (Lond.) 165, 356 (1950).
[18] Berak, J. M., and Sienko, M. J., J. Solid State Chem. 2, 109 (1970).
[19] Andersson, G., Acta Chem. Scand. 7, 154 (1953).
[20] Tanisaki, S., J. Phys. Soc. Japan 15, 573 (1960).
[21] Loopstra, B. O., and Boldrini, P., Acta Cryst. 21, 158 (1966).
[22] Loopstra, B. O., and Rietveld, H. M., Acta Cryst. 25B, 1420 (1969).
[23] Tanisaki, S., J. Phys. Soc. Japan 15, 566 (1960).
[24] Crowder, B. L., and Sienko, M. J., J. Chem. Phys. 38, 1576 (1963).
[25] Crowder, B. L., and Sienko, M. J., Inorg. Chem. 4, 73 (1965).
[26] Roth, R. S., and Waring, J. L., J. Res. Nat. Bur. Stand. (U.S.), 70A (Phys. and Chem.), No. 4, 281–303 (July–Aug. 1966).
[27] Foëx, M., Compt. Rend. (Paris) 220, 917 (1945); 228, 1335 (1949).
[28] Matthias, B. T., and Wood, E. A., Phys. Rev. 84, 1255 (1951).
[29] Hirakawa, K., J. Phys. Soc. Japan 7, 331 (1952).
[30] Matthias, B. T., Phys. Rev. 76, 430 (1949).
[31] Sawada, S., J. Phys. Soc. Japan 11, 1237 (1956).
[32] Levine, S., Corwin, R., and Blood, H. L., Bull. Am. Phys. Soc. Ser. II, 1, 255 (1956).
[33] Wyart, J., and Foëx, M., Compt. Rend. (Paris) 232, 2459 (1951).
[34] Ueda, R., and Ichinokawa, T., Phys. Rev. 82, 563 (1951).
[35] Rosen, C., Banks, E., and Post, B., Acta Cryst. 9, 475 (1956).
[36] Perri, J. A., Banks, E., and Post, B., J. Appl. Phys. 28, 1272 (1957).
[37] Gado, P., Magy Fiz. Folyoirat 10, 347 (1962).
[38] Kehl, W. L., Hay, R. G., and Wahl, D., J. Appl. Phys. 23, 212 (1952).
[39] Sawada, S., Phys. Rev. 91, 1010 (1953).
[40] Fiegel, L. J., Mohanty, G. P., and Healy, H., J. Chem. and Engg. Data 9, 365 (1964).
[41] Chang, L. L. Y., Schroger, M. G., and Phillips, B., J. Am. Ceram. Soc. 49, 385 (1966).
[42] Sienko, M. J., and Banerjee, B., J. Am. Chem. Soc. 83, 4149 (1961).
[43] Sienko, M. J., in Non-stoichiometric Compounds, Adv. Chem. Ser. 39, 224 (1963).
[44] Wadsley, A. D., in Non-stoichiometric Compounds, Ed. L. Mandelcorn, (Academic Press, New York, 1964).
[45] Dickens, P. G., and Whittingham, M. S., Quart. Rev. (Lond.) 22, 30 (1968).
[46] Rao, C. N. R., and Subba Rao, G. V., Phys. stat. Solidi (a) 1, 597 (1970).
[47] Levin, E. M., J. Am. Ceram. Soc. 48, 491 (1965).
[48] Sawada, S., and Danielson, G. C., Phys. Rev. 113, 803 (1959).
[49] Iwai, T., J. Phys. Soc. Japan 15, 1596 (1960).
[50] Hirakawa, K., and Ueda, I., Mem. Fac. Sci. Kyusyu Univ. B1, 112 (1954).

III.5. Rhenium Oxides

In the Re-O system, ReO_2, ReO_3, and Re_2O_7 are the oxides that are well characterized and examined in detail. A tetragonal Re_2O_5 has been reported by Trabalat et al. [1]. The di- and sesquioxides are stable ionic compounds whereas Re_2O_7 is mostly covalent and has a low melting point (~490 K).

ReO_2 is polymorphous and when synthesized below 570 K, the structural modification (α) is that of monoclinic MoO_2 type [2, 3]; above ~570 K, this oxide transforms irreversibly to an orthorhombic form (β) with a structure characterized by zig-zag chains of Re atoms propagating along the c axis of the unit cell. It is also possible to directly synthesize the high temperature form [2, 3] and the material is stable in the range 570 to 1320 K. Magnetic susceptibility studies [4] indicate that both the forms of ReO_2 are Pauli paramagnetic. Resistivity data indicate that β-ReO_2 is metallic [3] and most probably the low temperature modification also is metallic. Monoclinic ReO_2 forms rutile type solid solutions with VO_2 and MoO_2 [5].

Re_2O_5 is prepared by precipitation from aqueous solutions [1] and has a tetragonal structure. It appears to be stable up to 470 K, but decomposes to Re_2O_7 and ReO_2 in vacuum at $\leqslant$520 K. Detailed properties are not known at present.

ReO_3 is cubic and no phase transformations are known in the range 1 to 300 K [2, 6–8]; the material disproportionates to ReO_2 and Re_2O_7 in the neighborhood of 670 K. ReO_3 has a red metallic luster and magnetic susceptibility [6, 8], electrical [6, 8], optical [9], NMR [10], magneto-thermal oscillation [11], and de Hass-van Alphen effect [12] studies confirm the typical metallic behavior of ReO_3.

The simple cubic structure of ReO_3 is important from the view point of understanding the structures of perovskites (see fig. III.2) [13]. Goodenough [13–15] has explained the metallic behavior of ReO_3 by constructing a one-electron energy band diagram. Recent band structure calculations on ReO_3 have proved that the essential features of the Goodenough's model are correct [16, 17].

Re_2O_7 is orthorhombic at room temperature [18–20]. It is yellow in color and is supposed to have a polymeric structure in the solid state; in the liquid and vapor states, monomeric species have been identified [19, 21]. Infrared and Raman spectra of this material have been studied in detail [21, 22] but other properties are not known.

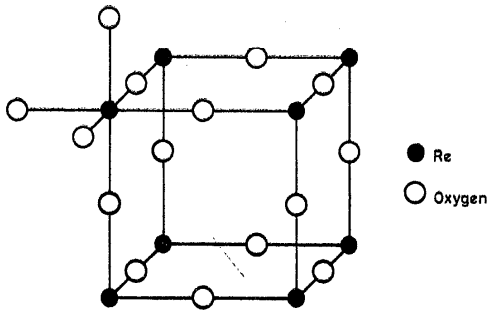

FIGURE III.2. *Cubic* ReO_3 *structure.*
Each metal atom is at the center of an octahedran of oxygen atoms. This structure is closely related to the perovskite structure which is obtained by insertion of a large cation in the center of the cube shown.

Rhenium oxides

Oxide and description of the study	Data	Remarks and inferences	References
ReO_2			
Crystal structure and x-ray studies.	Low-temperature for ($T<570$ K): Monoclinic: space group, $P2_1/c$; $Z=4$; $a=5.562$ Å; $b=4.838$ Å; $c=5.561$ Å; $\beta=120.87°$. High temperature form ($T>570$ K): orthorhombic; space group, Pbcn; $Z=4$; $a=4.810$ Å; $b=5.643$ Å; $c=4.601$ Å.	The low temperature form is closely related to rutile structure.	[2, 23].

Oxide and description of the study	Data	Remarks and inferences	References
Electrical properties.	β-ReO_2: ρ (4.2 K) $\approx 1.2\times10^{-5}$ Ωcm; ρ (300 K) $\approx 1.0\times10^{-4}$ Ωcm.	Metallic behavior is indicated; data for α-ReO_2 are not available.	[3].
Re_2O_5			
Crystal structure.	Tetragonal; $Z=4$; $a=5.80$ Å; $c=12.87$ Å.	The substance has been obtained from aqueous solutions; exact purity and characterization doubtful; other properties not known.	[1].
ReO_3			
Crystal structure.	Cubic, space group, Pm3m; $Z=1$; $a=3.7474\pm0.0003$ Å.	This simple cubic structure is closely related to the perovskite structure since the latter is obtained by insertion of a large cation in the center of the cube of the ReO_3 structure (fig. 1).	[8].
Magnetic and electrical properties.	χ_M (300 K) $=74.5\times10^{-6}$ emu. ρ (100 K) $\approx 6\times10^{-7}$ Ωcm; ρ (300 K) $\approx 1\times10^{-5}$ Ωcm.	Weak paramagnetism is indicated contrary to the earlier data [6].	[6, 8].
Optical and NMR studies.	Absolute reflection measurements on ReO_3 give plasma edge at 2.1 eV; interband transitions dominate the optical spectrum above the plasma edge. m^* (calc.)$\sim$ 0.86 m_0. $k=-(0.25\pm0.02)\%$.	The data confirm the metallic behavior of ReO_3 in which the conduction bands are predominantly d like.	[9, 10].
Band structure of ReO_3.	LCAO, APW, and Slater-Kostiner methods give a band structure in essential agreement with the band diagram proposed by Goodenough [13–15] and in reasonable agreement with the optical and Fermi surface data. The conduction bands are predominantly d like.	Honig et al. [17] point out that the band structure scheme will also be useful in the characterization of the band structure for perovskites which have a closely related structure.	[16, 17].
Re_2O_7	$T=300$ K: Orthorhombic; space group $P2_12_12_1$; $Z=8$; $a=12.508$ Å; $b=15.196$ Å; $c=5.448$ Å.	The structure consists of strongly distorted ReO_6 octahedra and fairly regular ReO_4 tetrahedra which are connected through corners to form polymeric double layers in the ac plane. The double layers have only van der Waals contacts to neighboring ones. Re_2O_7 is one of the few known examples where metal atoms of the same oxidation state occur with the coordination numbers 4 and 6 in the same structure. In its structure and bond	[20].

Rhenium oxides—Continued

Oxide and description of the study	Data	Remarks and inferences	References
		properties, Re_2O_7 represents an intermediate between the polymeric oxides MoO_3 and WO_3 and the more covalently bonded OsO_4, which forms a molecular structure.	
IR of Re_2O_7.	Several bands in the region 400–1010 cm^{-1} are noted and assigned to various stretching and bending vibrations.	—	[21].

References

[1] Tribalat, S., Dalafosse, D., and Piolet, C., Compt. Rend. (Paris) 261, 1008 (1965).
[2] Magnéli, A., Acta Cryst. 9, 1038 (1956); Acta Chem. Scand. 11, 28 (1957).
[3] Rogers, D. B., Shannon, R. D., Sleight, A. W., and Gillson, J. L., Inorg. Chem. 8, 841 (1969).
[4] Gibart, P., Bull. Soc. Chim. France 444 (1967).
[5] Marinder, B.-O., and Magnéli, A., Acta Chem. Scand. 11, 1635 (1957).
[6] Ferretti, A., Rogers, D. B., and Goodenough, J. B., J. Phys. Chem. Solids 26, 2007 (1965).
[7] Gukova, Yu. Ya., and Emolaev, M. I., Russian J. Inorg. Chem. (English Transl.) 13, 777 (1968).
[8] Quinn, R. K., and Neiswander, P. G., Mat. Res. Bull. 5, 329 (1970).
[9] Narath, A., and Barham, D. C., Phys. Rev. 176, 479 (1968).
[10] Feinleib, J., Scouler, W. J., and Ferretti, A., Phys. Rev. 165, 765 (1968).
[11] Graebner, J. E., and Greiner, E. S., Phys. Rev. 185, 992 (1969).
[12] Marcus, S. M., Phys. Letters 27A, 584 (1968).
[13] Rao, C. N. R., and Subba Rao, G. V., Phys. Stat. Solidi (a) 1, 597 (1970).
[14] Goodenough, J. B., J. Appl. Phys. 37, 1415 (1966).
[15] Goodenough, J. B., Czech. J. Phys. 17B, 304 (1967).
[16] Mattheis, L. F., Phys. Rev. 181, 987 (1969).
[17] Honig, J. M., Dimmock, J. O., and Kleiner, W. H., J. Chem. Phys. 50, 5232 (1969).
[18] Wilhelmi, K.-A., Acta Chem. Scand. 8, 693 (1954).
[19] Krebs, B., and Muller, A., Z. Naturforsch. 23b, 415 (1968).
[20] Krebs, B., Muller, A., and Beyer, H. H., Inorg. Chem. 8, 436 (1969).
[21] Ulbricht, K., and Kriegsmann, H., Z. Chem. 7, 244 (1967).
[22] Beattie, I. R., and Ozin, G. A., J. Chem. Soc. (Lond.) A2615 (1969).
[23] Magnéli, A., Andersson, G., Blomberg, B., and Kihlborg, L., Anal. Chem. 24, 1998 (1952).

III.6. Osmium Oxides

The dioxide, OsO_2 and the tetroxide, OsO_4, have been studied exhaustively. OsO_2 forms lustrous yellowish brown crystals which decompose at $T>770$ K. OsO_4 is a covalent solid and soluble in nonpolar solvents; the crystals are colorless with a low melting point ($\sim$310 K) and high vapor pressure.

OsO_2 has a tetragonal rutile structure [1–4] and exhibits slight temperature dependent magnetic susceptibility [3]. It has a very low room-temperature resistivity, positive temperature coefficient of resistivity and low negative Seebeck coefficient [1, 3] indicative of metallic behavior. No phase transitions are known in OsO_2 in the temperature range 77 to 500 K.

Thiele and Woditsch [2] report two forms (black and brown) of OsO_2; both have tetragonal symmetry, but the lattice parameters and χ values differ significantly. The lattice parameters of the brown form are identical with the data reported by other workers on single crystal OsO_2 [3, 4]. It is possible that the black form of OsO_2 reported by Thiele and Woditsche is slightly nonstoichiometric or impure.

OsO_4 at room temperature is a solid and has a monoclinic symmetry [5]. It is a covalent compound (mp, 310 K; bp, 374 K) and is soluble in polar solvents. The molecule is tetrahedral in vapor state. Infrared and Raman studies of OsO_4 is nonaqueous solvents have been carried out by various workers [6, 7]; other physical properties are not known.

Oxide and description of the study	Data	Remarks and inferences	References
OsO_2			
Crystal structure.	$T=300$ K: Tetragonal; space group, $P4_2/mnm$; $Z=2$; $a=4.5000\pm0.0003$ Å; $c=3.1830\pm0.0009$ Å.	Recent single crystal study; the values are in agreement with the data of earlier workers.	[4].
Magnetic properties.	χ_M ($\times10^{-6}$ emu) is 311, 220, and 204 at 90, 195, and 291 K respectively. Greedon et al. [1] report a temperature independent susceptibility (77–500 K) of $\chi_M\approx120\times10^{-6}$ emu.	The values of Thiele and Woditsch [2] have been corrected for the diamagnetic contribution. These authors argue for the presence of a magnetic ground state for Os^{4+} in OsO_2.	[2].
Electrical properties.	ρ (4.2 K) $=3.2\times10^{-7}$ Ωcm; ρ (300 K) $=6.0\times10^{-5}$ Ωcm. α ($\sim$300 K) ~1 μV/K (negative); no Hall voltage could be measured.	The data indicate the typical metallic nature of OsO_2; estimated carrier concentrations are $\sim10^{22}$–10^{23}/cm³. μ (calc.) $\sim$1.5–15 cm²/V s; $m^*\approx8\ m_0$. The model proposed by Goodenough [8] and Rogers et al. [3] seem to explain the observed behavior.	[1, 3].
OsO_4			
Crystal structure	$T=300$ K: Monoclinic; space group, $C2/c$; $Z=4$; $a=9.379\pm0.005$ Å; $b=4.515\pm0.002$ Å; $c=8.632\pm0.003$ Å; $\beta=116\pm0.05°$.	The structure can be described as cubic closest packing of oxygen atoms, with osmium in tetrahedral holes. The intermolecular O–O distances exceed 2.98 Å and are consistent with weak intermolecular forces indicated by the high vapor pressure and low melting point.	[5].
Infrared studies on solid OsO_4.	Bands at 965 and 959.5 cm^{-1} are noted.	IR of OsO_4 in CCl_4 solution and Raman studies are also consistent with the behavior in the solid state.	[6, 7].

References

[1] Greedon, J. E., Willson, D. B., and Haas, T. E., Inorg. Chem. 7, 2461 (1968).
[2] Thiele, G., and Woditsch, P., J. Less-Comm. Metals 17, 459 (1969).
[3] Rogers, D. B., Shannon, R. D., Sleight, A. W., and Gillson, J. L., Inorg. Chem. 8, 841 (1969).
[4] Boman, C.-E., Acta Chem. Scand. 24, 123 (1970).
[5] Ueki, T., Zalkin, A., and Templeton, D. H., Acta Cryst. 19, 157 (1965).
[6] Krebs, B., and Muller, A., Z. Chem. 7, 243 (1967).
[7] McDowell, R. S., and Goldblatt, M., Inorg. Chem. 10, 625 (1971) and references cited therein.
[8] Goodenough, J. B., Bull. Soc. Chim. France 4, 1200 (1965).

III.7. Iridium Oxides

The phase study of the Ir-O system by Cordfunke and Meyer [1] and McDaniel and Schneider [2, 3] indicate that IrO_2 is the only condensed oxide phase stable in an air environment. IrO_2 has a tetragonal rutile structure and no phase transformations are known in the range 4.2 to 1000 K [4–8].

Magnetic properties of IrO_2 have not yet been investigated. Electrical resistivity studies [5–8] confirm the metallic nature of the material; as pointed out by Butler and Gillson [8], the simple one-band model of Rogers and co-workers [7] may not explain the observed behavior. Ryden et al. [6] have found that electron-phonon and electron-electron interband scattering mechanism accounts for the observed temperature dependence of resistivity.

IrO_2 forms complete solid solutions with RuO_2 and to a limited extent with TiO_2 and SnO_2 [2, 3]; these have the rutile structure.

Iridium oxides

Oxide and description of the study	Data	Remarks and inferences	References
IrO_2			
Crystal structure and electrical properties.	$T=298$ K: Tetragonal; space group, $P4_2/mnm$; $Z=2$; $a=4.4980\pm0.0003$ Å; $c=3.1543\pm0.0002$ Å. TEC ($\times10^{-6}$/°C): $\|\|^c$: 1.7; $\|\|^a$: 3.8. ρ (4.2 K)$\sim1.5\times10^{-8}$ Ωcm; ρ (298 K)$\sim3.0\times10^{-5}$ Ωcm. R_H (77 K)≈ -3.12; μ_H (77 K)$=130$ cm²/V s; R_H (300 K)≈ -2.60; μ_H (300 K)$=7.5$ cm²/V s.	TEC is positive in IrO_2; anisotropy is evident. The compound is metallic and most probably Pauli paramagnetic.	[2–8].

References

[1] Cordfunke, E. H. P., and Meyer, G., Rec. Trav. Chim. 81, 495 (1962); 81, 670 (1962).
[2] McDaniel, C. L., and Schneider, S. J., J. Res. Nat. Bur. Stand. (U.S.), 71A (Phys. and Chem.), No. 2, 119–123 (Mar.–Apr. 1967).
[3] McDaniel, C. L., and Schneider, S. J., J. Res. Nat. Bur. Stand. (U.S.), 73A (Phys. and Chem.), No. 2, 213–219 (Mar.–Apr. 1969).
[4] Hazony, Y., and Perkins, H. K., J. Appl. Phys. 41, 5130 (1970).
[5] Ryden, W. D., Lawson, A. W., and Sartain, C. C., Phys. Letters 26A, 209 (1968).
[6] Ryden, W. D., Lawson, A. W., and Sartain, C. C., Phys. Rev. B1, 1494 (1970).
[7] Rogers, D. B., Shannon, R. D., Sleight, A. W., and Gillson, J. L., Inorg. Chem. 8, 841 (1969).
[8] Butler, S. R., and Gillson, J. L., Mat. Res. Bull. 6, 81 (1971).

III.8. Platinum Oxides

Although the literature on the Pt-O system is extensive due to the catalytic and electrochemical applications of the platinum oxides, many of them are poorly characterized. Recent careful study by Muller and Roy [1] has revealed the existence of α-PtO_2, β-PtO_2, and Pt_3O_4 as the stable oxides in the Pt-O system. Contrary to earlier reports [2–6], the existence of PtO and Pt_3O_8 are doubtful.

Pt_3O_4 is cubic [1]. α-PtO_2 has a chain structure and is hexagonal; β-PtO_2 is orthorhombic and has a distorted rutile structure [1, 7, 8]. α-PtO_2 transforms

to β-form either by heating to 970 K at 3 kbar pressure in the presence of $KClO_3$ or by heating to 1370 K at 65 kbar pressure [7]. DTA, TGA, and high temperature x-ray studies show that β-PtO_2 decomposes to the platinum metal and oxygen at ~860 to 920 K [7, 8].

β-PtO_2 appears to be a semiconductor [7, 9]. The physical properties of α-PtO_2 and Pt_3O_4 are not known. Muller and Roy [10] have found that solid solutions of the form $Cu_{1-x}Pt_xO$ possessing the tetragonal structure can easily be formed. The extrapolated lattice parameters for the hypothetical 'PtO' do not quite agree with the values reported by Moore and Pauling [2].

Platinum oxides

Oxide and description of the study	Data	Remarks and inferences	References
Pt_3O_4			
Crystal structure.	Cubic; space group, $Pm3m$; $Z=2$; $a=5.585$ Å.	—	[1].
α-PtO_2			
Crystal structure.	Hexagonal; space group, $C6/mmm$; $Z=1$; $a=3.10$ Å; $c=4.29$–4.41 Å.	Samples are poorly crystallized; Pt-O-O-Pt-O-O chain structure in the c direction.	[1].
β-PtO_2			
Crystal structure and electrical resistivity.	Orthorhombic; space group, Pnnm; $Z=2$; $a=4.487\pm0.0005$ Å; $b=4.536\pm0.0005$ Å; $c=3.137\pm0.0005$ Å. ρ (300 K) $\approx 10^6$ Ωcm; $E_a=0.2$ eV. Decomposes in air at ~860–920 K.	Distortion from the rutile structure is small; semiconductor behavior (in the range 4.2–300 K).	[1, 7, 9].

References

[1] Muller, O., and Roy, R., J. Less-Common Metals 16, 129 (1968).
[2] Moore, W. J., Jr. and Pauling, L., J. Am. Chem. Soc. 63, 1392 (1941).
[3] Suzuki, T., Z. Naturforsch. 12a, 497 (1957).
[4] Every, R. L., J. Electrochem. Soc. 112, 524 (1965).
[5] Fryburg, G. C., J. Chem. Phys. 42, 4051 (1965).
[6] Shishakov, N. A., Andreeva, V. V., and Andruschenko, N. K., Stroenie i Mekhanism Obrazovaniya Okisnykh Plenok na Metallakh, Akad. Nauk. SSSR, Moscow, 1959, Chap. 6.
[7] Shannon, R. D., Solid State Commun. 6, 139 (1968); 7, 257 (1969).
[8] Schneider, S. J., and McDaniel, C. L., J. Am. Ceram. Soc. 52, 519 (1969).
[9] Rogers, D. B., Shannon, R. D., Sleight, A. W., and Gillson, J. L., Inorg. Chem. 8, 841 (1969).
[10] Muller, O., and Roy, R., J. Less-Common Metals 19, 209 (1969).

III.9. Gold Oxides

Although Shishakov [1] earlier reported the formation of hexagonal Au_3O_2 on the surface of heated gold metal at 770 K, recent studies by Muller and Roy [2] indicate Au_2O_3 to be the only crystalline oxide phase in the Au-O system. Attempted preparation of Au_2O has not been successful [3].

Au_2O_3 is cubic ($a=4.832$ Å; space group, $P\bar{4}3m$) [2, 4]. The physical properties are not known in detail. The infrared bands of Au_2O_3 have been reported in the range 515–660 cm^{-1}.

References

[1] Shishakov, N. A., Kristallografiya 2, 686 (1957).
[2] Muller, O., and Roy, R., Am. Ceram. Soc. Bull. 46, 881 (1967).
[3] Suzuki, T., J. Phys. Soc. Japan 15, 2018 (1960).
[4] Schwarzmann, E., and Gramann, G., Z. Naturforsch. 25b, 1308 (1970).

III.10. Mercury Oxides

HgO is the well known oxide in the Hg-O system [1–3]. Vannerberg [4] reported the formation of two different forms (α- and β-) of the mercury peroxide, HgO_2; α-HgO_2 has a rhombohedral structure whereas β-form is orthorhombic.

HgO: HgO exists in the red and yellow forms but these are not polymorphs; they differ in the particle size and give identical x-ray patterns [2]. The stable form is orthorhombic [1–3, 5, 6] and has a structure with zig-zag -Hg-O-Hg- chains (Hg-O = 2.03 Å); there is only weak bonding between the chains. Laruelle [5] has described a rhombohedral form of HgO obtained by precipitation from aqueous solutions; it transforms irreversibly to the orthorhombic form at ~470 K and at this temperature, the transformation is a slow process. HgO is diamagnetic [7] and the diamagnetic susceptibility is almost the same for both the yellow and red forms. HgO decomposes at high temperatures to the metal; other properties are not known.

Mercury oxides

Oxide and description of the study	Data	Remarks and inferences	References
HgO			
Crystal structure and properties.	Orthorhombic; space group, Pnma; $Z=4$; $a=6.6129\pm0.0009$ Å; $b=5.5208\pm0.0007$ Å; $c=3.5219\pm0.0005$ Å. A rhombohedral form can be precipitated from solution and it transforms irreversibly to the orthorhombic modification at ~470 K; detailed structure not known. The red and yellow colors of HgO seem to be due to the particle size effect. HgO is diamagnetic; χ (red form) = -0.221×10^{-6} emu/g; χ (yellow form) = -0.216×10^{-6} emu/g. χ increases in the range 298–573 K. χ-T plot shows peaks at 323 (red form) and 387 K (yellow form); the reason is not clear.	HgO has a zig-zag structure associated with considerable covalency in the Hg-O bond. Detailed properties are not known.	[1–3, 5].
Infrared and Raman spectral studies.	Low frequency band is at 67 cm^{-1}; Raman bands at 331 and 550 cm^{-1}. The data are interpreted in terms of the chain structure of HgO.	—	[8, 9].
HgO_2			
Crystal structure.	α-form: rhombohedral; $a=4.74$ Å; $\alpha\approx90°$. β-from: orthorhombic; space group, Pbca; $Z=4$; $a=6.080$ Å; $b=6.010$ Å; $c=4.800$ Å. Detailed data on the properties are lacking.	—	[4].

References

[1] Zachariasen, W., Z. Physik. Chem. **128**, 421 (1927).
[2] Roth, W. L., Acta Cryst. **9**, 277 (1956).
[3] Aurivillius, K., Acta Chem. Scand. **10**, 852 (1956); **18**, 1305 (1964).
[4] Vennerberg, N. G., Arkiv för Kemi **13**, 515 (1959).
[5] Laruelle, P., Compt. Rend. (Paris) **241**, 802 (1955).
[6] Rooymans, C. J. M., Philips Res. Rep. Suppl. **1**, 1 (1968).
[7] Mikhail, H., Hanafy, Z., and Salem, T. M., J. Chem. Phys. **35**, 1185 (1961).
[8] Edmond, D., and Armand, H., J. Chim. Phys. Physicochim. Biol. **65**, 1030 (1968).
[9] Cooney, R. P. J., and Hall, J. R., Austr. J. Chem. **22**, 331 (1969).

IV. Some Recent Studies

Titanium Oxides

Rao and co-workers [1] have recently found that pressure has no effect on the Ti_2O_3 transition; this is consistent with the band-crossing mechanism wherein the a^T and e^T bands cross as the c/a ratio increases.

The very recent study of Marezio et al. [2] published in 1973 on the three phases of Ti_4O_7 has clearly established the structural aspects of the transitions. The room temperature phase is metallic with an average valence of 3.5 for Ti. In the low-temperature insulating nonmagnetic state, there is a separation into strings of Ti^{3+} and Ti^{4+} with the 3+ sites forming metal-metal bonds. In the intermediate phase, there is no evidence for charge separation or long range order of bonds.

The atomic vacancies in TiO have been discussed by Goodenough [3].

ESR studies on Ti_3O_5 have been reported by Schlenker et al. [5].

References

[1] Viswanathan, B., Devi, S. U., and Rao, C. N. R., Pramana 1, 48 (1973).
[2] Marezio, M., et al., J. Solid State Chem. 6, 213 (1973); Phys. Rev. Letters 28, 1390 (1973).
[3] Goodenough, J. B., Phys. Rev. 135, 2764 (1972).
[4] Honig, J. M., Wahnsiedler, W. E., and Dimmock, J. O., J. Solid State Chem. 5, 452 (1972).
[5] Schlenker, C., Buder, R., Schlenker, M., Houlihan, J. F., and Mulay, L. N., Phys. Stat. Solidii (b) 54, 247 (1972).

Vanadium Oxides

Recent studies of Honig and co-workers [1] on $V_{0.99}$ $Cr_{0.01}$ $O_{1.5}$ in the 200 to 900 K range indicate that the electrical anomaly is extrinsic and is caused by the coexistence of phases over a wide temperature range. If this be the case, much of the earlier arguments based on the I-M transition will be invalid.

Caruthers et al. [2] have recently calculated the band structure of VO_2.

The influence of atomic vacancies on the band structure of VO has been discussed by Goodenough [3].

For a recent ESCA study on V_2O_3, see [4].

For recent data on V_2O_5 and V_n O_{2n-1}, see [5].

Heat capacity studies on V_n O_{2n-1} are given in [6].

Recent single crystal studies on V_6O_{13} [7] confirm a negative volume change (−0.5%), a positive enthalpy change (+400 cal/mol) and a semiconductor-metal transition at 150 K. There is no change in the crystal system.

Marezio et al. [8] have studied some structural aspects of V_{1-x} Cr_x O_2 in detail.

References

[1] Honig, J. M., Chandrasekhar, G. V., and Sinha, A. P. B., Phys. Rev. Letts. 32, 13 (1974).
[2] Caruthers, E., Kleinman, L., and Zhang, H. I., Phys. Rev. B7, 3753 (1973).
[3] Goodenough, J. B., Phys. Rev. B5, 2764 (1972).
[4] Honig, J. M., Van Zandt, L. L., Board, R. D., and Weaver, H. E., Phys. Rev. B6, 1323 (1972).
[5] Kachi, S., Kosuge, K., and Okinaka, H., J. Solid State Chem. 6, 258 (1973).
[6] McWhan, D. B., Remeika, J. P., Maita, J. P., Kinaka, H. O., Kosuge, K., and Kachi, S., Phys. Rev. B7, 326 (1973).
[7] Saeki, J., Kimizuka, N., Ishii, M., Kawada, I., Nakamo, M., Ichinose, A., and Nakahira, M., J. Cryst. Growth 18, 101 (1973).
[8] Marezio, M., McWhan, D. B., Remeika, J. P., and Dernier, D. P., Phys. Rev. B5, 2541 (1972).
[9] Tewari, S., Solid State Commun. 11, 1139 (1972).

Nickel Oxides

Recent measurements [1] on highly pure NiO crystals gave the hole mobility, $\mu_d/ = 20$–50 cm²/Vs at 300 K; $m_p^* = 1.5\, m_0$; and $\alpha_F^* = 1.6$.

Reference

[1] Spear, W. E., and Tannhanser, D. S., Phys. Rev. B7, 831 (1973).

Niobium Oxides

Recently, measurements of electrical properties of NbO in high magnetic fields have been reported by Honig et al. [1] who have interpreted the results in terms of a nearly free electron model in which holes and electrons contribute jointly to conduction process; magnetoresistance anomalies have also been examined by these workers.

Reference

[1] Honig, J. M., Wahnsiedler, W. E., and Ekland, P. C., J. Solid State Chem. 6, 230 (1973).

☆ U.S. GOVERNMENT PRINTING OFFICE : 1974 O—522–205